HEAVY MINERAL PROVENANCE AND THE GENESIS OF STANNIFEROUS PLACERS IN NORTHEASTERN TASMANIA

by

Wai Sku

Wyss W.-S. Yim

B.Sc. Hons., Dip. Min. Tech., M.Phil., D.I.C.

in the Faculty of Science, Department of Geology

submitted in partial fulfilment of the requirements

for the degree of

Doctor of Philosophy

University of Tasmania

December, 1990

To Justin, Mark and Fiona

STATEMENT OF AUTHOR

This thesis contains no material which has been accepted for the award of any other higher degree or graduate diploma in any tertiary institution and that, to the best of my knowledge and belief, this thesis contains no material previously published or written by another person, except when due reference is made in the text of the thesis.

W. S. Yim

Wyss W.-S. Yim

Heavy minerals - "The portion of density greater than 2.8 ..... which are of the greatest interest, beauty, and value from a stratigraphic point of view" (Boswell 1916, p. 106).

ABSTRACT

A heavy mineral provenance study of stanniferous placers in northeastern Tasmania reveals that the placers were formed during 'long' periods of geologic time by episodic recycling dating back at least to the Permian. With the aid of heavy mineral species demonstrably deriving from granitic and basaltic source rocks, it is possible to identify placer formation events. Deep leads such as Briseis and Pioneer were stratigraphically confined between the Middle Eocene (ca. 47 Ma) and Middle Miocene (ca. 16 Ma) episodes of basaltic volcanic activity. This is supported by both fission track dating and electron spin resonance (ESR) studies of alluvial zircons. The latter is a rapid semi-quantitative technique for the age estimation of the host rocks of zircon.

In addition to deep leads comparatively shallow leads are also present filling bedrock channels or covering erosion surfaces cut across the rock basement. Because the erosion surfaces represent episodes of sufficient duration to cause heavy mineral enrichment, they are useful for the stratigraphic correlation of placer sequences. Quaternary placers are represented in the form of fluvial terrace deposits along the lower Ringarooma valley.

Bedrock tin mineralization is widespread in northeastern Tasmania and it is unnecessary to explain the placers by invoking long transport distances for cassiterite. The presence of large cassiterite nuggets and composite grains in most alluvial workings is consistent with local derivation involving short transport distances. This is also supported by geochemically distinctive trace element patterns in Mount Cameron and Blue Tier cassiterites. The former are enriched in niobium, tantalum, and zirconium, but depleted in tungsten in comparison to the latter. The selective removal of light minerals by winnowing through episodic

recycling is considered to have been mainly responsible for the genesis of the placers in northeastern Tasmania.

Major geomorphological evolution events have been identified in the study area. During the Middle Miocene, basaltic flows along the middle Ringarooma valley caused drainage diversion. The northwesterly flowing streams of the Blue Tier which were formerly connected to a proto-Boobyalla River system were diverted eastwards by these basalts into the South Mount Cameron Basin. An outlet of this basin into the Great Mussel Roe River existed before downcutting and/or capture shifted the river course towards the Great Northern Plains to form the Ringarooma River course of today. At least from the Middle Eocene until the Middle Miocene, the catchment area of the proto-Boobyalla River extended well into the Blue Tier prior to diversion by the younger basaltic flows.

A wide range of factors helps to determine the age of placer deposits. In the present study stratigraphic control of placers was achieved through an examination of heavy mineral provenance; volcanic and duricrust formation events, and sedimentologic, palaeo-oceanographic and palaeo-botanic evidence.

ACKNOWLEDGEMENTS

This work would not have been possible without the cooperation of tin miners operating in northeastern Tasmania between 1978 and 1980 when the field work was undertaken. I am particularly grateful to Drs J. C. van Moort (my supervisor), M. R. Banks and the late Dr R. J. Ford for their guidance and encouragement. Special thanks are due to D. J. Jennings, H. K. Wellington, Dr M.P. McClenaghan and S.M. Forsyth, Tasmania Department of Mines; A. W. Fleming, S. Everett and R. Munro, all formerly of Amdex Mining Limited; Dr F. L. Sutherland, Australian Museum; Professor A. J. W. Gleadow, formerly University of Melbourne, and Professor E. A. Colhoun, formerly University of Tasmania. Technical assistance was provided by W. Jablonski, P. Robinson and S. H. Stevens at the University of Tasmania, and, by H.K. Kwan, T.B. Wong and Lisa Nam at the University of Hong Kong.

The Tasmania Museum and Art Gallery (Hobart) and the Queen Victoria Museum and Art Gallery (Launceston) kindly provided access to their mineral collections. Elf Aquitaine Triako Mines Limited and Australian Anglo-American Prospecting Proprietary Limited made available reports and borehole samples.

Financial support was received from the Hui Oi Chow Trust and the Committee on Conference and Research Grants, University of Hong Kong; Amdex Mining Limited, and Carl Zeiss (Far East) Company Limited. Part of this work was carried out while I was on study leave from the University of Hong Kong.

CONTENTS

LIST OF FIGURES

LIST OF TABLES

LIST OF PLATES

PART 1 INTRODUCTION

CHAPTER 1 INTRODUCTION

1.1 The problem of tin placers

According to Bates & Jackson (1984) a placer is defined as a surficial mineral deposits formed by the mechanical concentration of mineral particles from weathered debris. Generally speaking, the two main pre-requisites for a mineral to form placer deposits are the resistance to chemical alteration and the high specific gravity. Placers are probably one of the earliest type of mineral deposits to have been utilized by man. However, as a subject of geological research, they have been much neglected. In the case of tin placer deposits, Batchelor (1983) pointed out that they were rarely treated as serious topics within classical tin geology, even though Denyer (1972) estimated that 80 % of the world production was derived from them.

The lack of understanding of tin placers may be illustrated by examining the inferred distance of transport of cassiterite from the source rock. According to a general review by Emery & Noakes (1968), the median distance of transport from bedrock source for economic tin placer deposits is only 8 km. Other, undiscovered bedrock mineralization sources were possibly contributing en route and the dispersion could be even shorter.

The following factors are considered important in determining the distance of transport:

(1) The grain size of cassiterite grains in the source rock. In fluvial regimes, coarse cassiterite would not travel as far as fine cassiterite.

(2) The hydrologic regime of the stream, particularly its gradient and discharge. A steep gradient stream with high discharge would be expected to transport cassiterite further away from the source than a low gradient stream with low discharge.

(3) The affect of geological history on landscape evolution termed 'evolutionary geomorphology' by Ollier (1979). Ancient placers would be expected to occur further from the source rock than young placers because of the greater likelihood of reworking. The tectonic, climatic and vegetational changes which controlled placer development may be episodic.

Without careful consideration of the above factors, distance of transport figures are of very little value. Furthermore there is a practical problem of sampling in studying placers. Large sampling errors are possible because of the segregation of tin in placer sequences.

Sutherland (1985) considered that the global distribution of placer deposits was largely a product of variation, both at present and in the recent geological past, in geomorphological processes acting at the Earth's surface, given suitable primary mineral sources. Global changes in climate and accompanying changes in the surface processes particularly during the Quaternary were thought to be especially important in placer formation. However, Tertiary and earlier events may also have played a part and their role remains to be investigated.

In northeastern Tasmania, placer tin ore was discovered before 1870. Mining commenced in 1874 (Nye 1925) and continued until the crash in international tin metal price in 1984. In spite of the effort of numerous mining companies carrying out intensive drilling programmes for tin placer exploration, returns for the investment made have been poor with few exceptions. It seems that if our understanding of the placers is to improve, advances will be needed in two main areas. Firstly, an improvement in the understanding of the stratigraphic control of the placers; and secondly, an improvement in investigation techniques. <u>This study is aimed at the former which is important in mineral exploration strategy as well as providing a better assessment of mineral reserves</u>.

1.2 Previous work

A general review of placer deposits was given by Hails (1976). Comprehensive reviews of tin placer genesis with special reference to southeast Asia were given by Batchelor (1973) and (1983). In this section, no attempt is made to review all the aspects of tin placer geology, and attention is focussed mainly on the stratigraphic control of placer deposits.

Four aspects were recognised by Aleva (1985) in the generation of tin placers in Indonesia. They include:

(1) The source rock containing the primary or secondary cassiterite.

(2) The liberation of the cassiterite from the source rock without excessive comminution of the cassiterite grains.

(3) The mechanical concentration of the now detrital cassiterite grains.

(4) The protection of at least part of the unconsolidated cassiterite concentration against attack by mechanical erosion.

An important factor in placer genesis requiring consideration is the stratigraphic control of the above aspects or in other words, the time scale of events. For example, the age and duration of exposure of the mineralized bedrock, and, the palaeoenvironmental and sedimentological changes which have taken place. Furthermore, because of the stability of cassiterite to chemical weathering, deep weathering of granite under a humid tropical climate would be favourable for cassiterite release. 'Long' periods of geologic time with climatic conditions suitable for deep weathering are thus helpful to placer formation. During the Quaternary Period, the 'short' duration of glacial and interglacial episodes may be insufficient to lead to the development of giant tin placers. It follows that tin placers occurring at or near the ground surface need not be Quaternary in age but may be relics. The failure to recognise their true age may be explained by inadequacies in our investigation technique.

Very few studies have previously been carried out on the stratigraphic control of tin placers. From evidence quoted by Batchelor (1979), Camm & Hosking (1985), and, Aleva (1985), the placers studied by these workers are predominantly palaeo-placers at least part of which are Tertiary. Batchelor (1979) concluded that the tin placers within the Older Sedimentary Cover of western Malaysia and Indonesia were Late Pliocene to Early Pleistocene (Fig. 1.1). In a conceptual diagram with the phases of destruction of primary tin deposits in Cornwall and the location and order of development of tin placers by Camm & Hosking (1985) (Fig. 1.2), placer deposits ranging from pre-Miocene to Holocene in age were indicated. Aleva (1985) suggested that the history of the Indonesian fluvial placers may well extend back to Miocene and Pliocene times but the upper limit is very young and may be within the limit of radiocarbon dating. In conclusion, he pointed out that future research on placers in the southeast Asian tin belt should direct special attention to the quantitative timing of events controlling concentration.

Major advances in palaeo-oceanography and seismic stratigraphy have been made in recent years through the Deep Sea Drilling Project (DSDP) and the offshore exploration for oil and gas. As a result of these advances, it is now possible to correlate between offshore and onshore sedimentary sequences and to identify palaeoenvironmental changes during the Cainozoic Era in different parts of the world. In palaeo-oceanography, oxygen-isotope analysis of deep sea cores by Shackleton & Opdyke (1973), Shackleton (1977) and others provided information on past ice volumes and sea-surface temperatures. On the other hand, investigation on seismic stratigraphy by Vail et al. (1977) and Haq et al. (1987) permitted recognition of global cycles of relative sea level changes for the entire Phanerozoic time scale. It is therefore

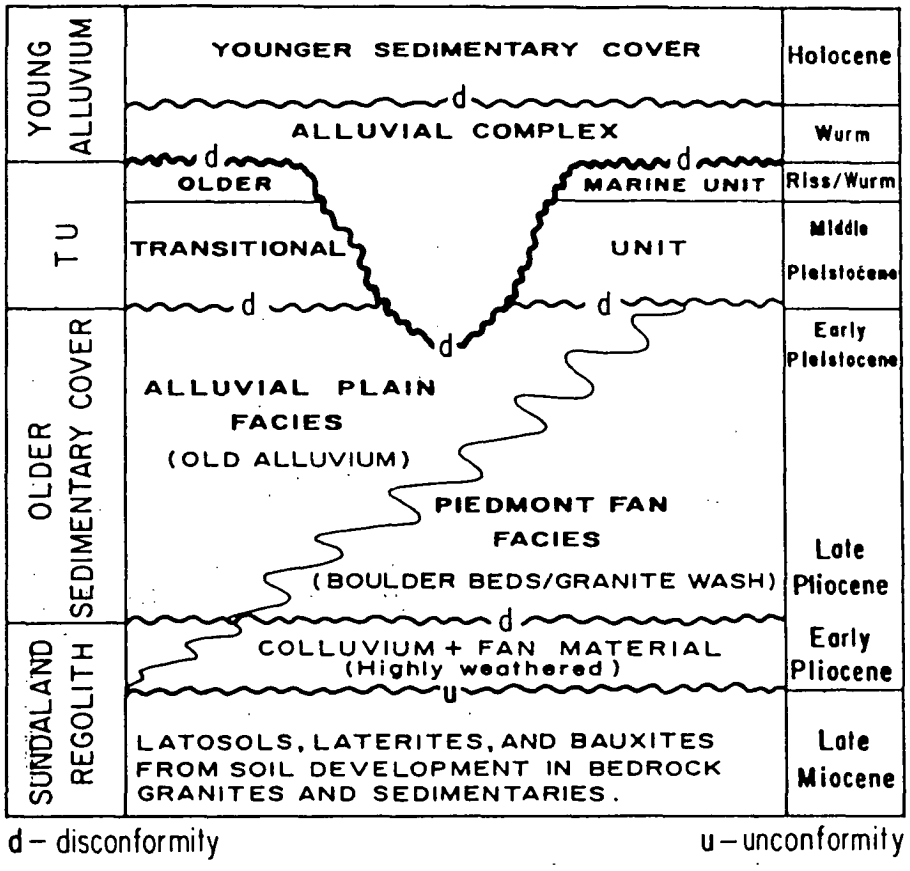

Fig. 1.1 Regional Cainozoic stratigraphic relationships in Sundaland, Southeast Asia. From Batchelor (1979).

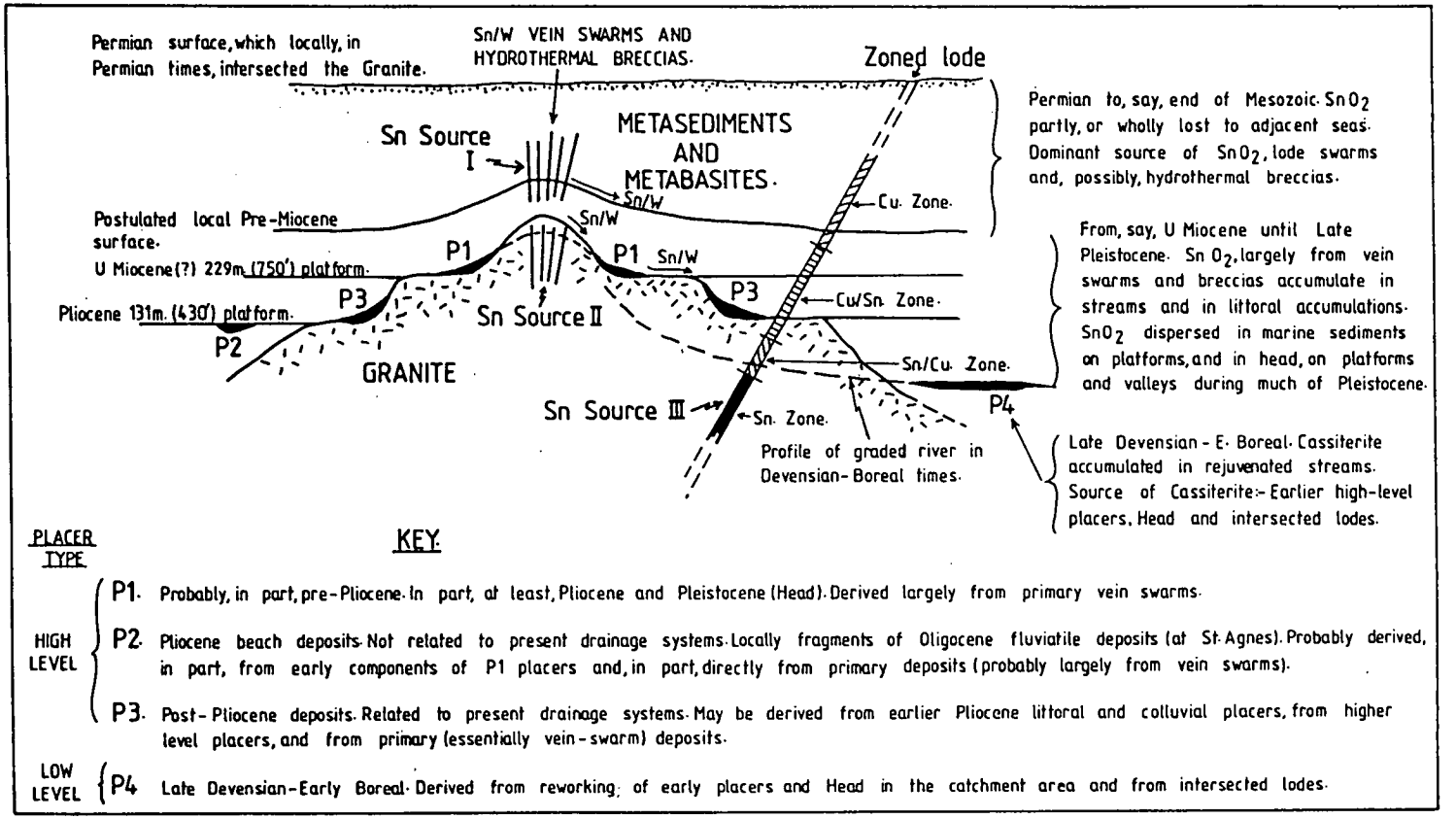

Fig. 1.2 Conceptual diagram indicating the phases of destruction of the major types of primary tin deposits in Cornwall, and, the location and order of development of the tin placers. From Camm & Hosking (1985).

particularly relevant to determine how tin placer deposits would fit into the stratigraphy obtained through these advances.

1.3 Objectives

The main objective of the present research is to investigate the provenance and genesis of tin placers in a major alluvial tin field. The occurrence of cassiterite and other heavy minerals was studied to test existing hypotheses. Mineralogical and sedimentological investigations have been made to permit identification of the source of the heavy minerals, and of events in landscape evolution important in the concentration of the placers. Where possible placers were dated to provide stratigraphic control on placer formation.

1.4 Choice of area

The area was chosen to satisfy the following four requirements:

(1) A major alluvial tin field with extensive bedrock mineralization.

(2) A diverse heavy mineral assemblage derived from multiple source rocks.

(3) Availability of good exposures, exploratory boreholes and/or documentary record.

(4) The presence of datable stratigraphic markers in the placer sequence.

All these requirements with the possible exception of (3) are met by the alluvial tin field of northeastern Tasmania. A number of old mines have ceased to operate and no outcrops are available. Unlike many tin belts in the world, eastern Australia (including northeastern Tasmania) is characterised by widespread basaltic volcanism during the Cainozoic Era. Numerous potassium-argon (K-Ar) determinations were made by McDougall & Wilkinson (1967), Wellman & McDougall (1974) and (1974a), Wellman (1974) and Sutherland & Wellman (1986). Furthermore, high to moderate pressure inclusions in alkali basaltic volcanic rocks have included the 'zircospilic' association of heavy minerals (Hollis 1984)

comprising zircon (zi), corundum (co), spinel (sp) and ilmenite (il). Therefore both the second and fourth requirements are satisfied.

1.5 Layout of thesis

This thesis is in four parts:

(1) Part one, consisting of chapters one and two, provides an introduction to the thesis and background information on the study area respectively.

(2) Part two divided into three chapters is concerned with the provenance and distribution of heavy minerals. Chapter three is on the field and laboratory procedures; chapter four is on the provenance of the heavy minerals, and, chapter five is on the follow-up studies of heavy mineral provenance.

(3) Part three is divided into three chapters on stratigraphic control, classification and genesis of stanniferous placers respectively.

(4) Part four is divided into two chapters on further discussion, and, conclusions and recommendations.

CHAPTER 2 THE STUDY AREA

2.1 Location

Tasmania is an island and the southernmost state of Australia (Fig. 2.1). It is separated from the mainland by Bass Strait and is located between latitudes 39 and 43 degrees south. The study area shown in Fig. 2.2 covers an area of approximately 250 sq. km in the northeastern part of Tasmania. It is bounded to the south by Mount Victoria including the Blue Tier and Mount Cameron Massifs.

2.2 Climate

Tasmania is under the influence of the prevailing westerly winds which are relatively cool and moist. Because there is no point lying more than 115 km from the sea, it has a temperate maritime climate (Anon. 1981). The average annual rainfall is the highest of any Australian State, reaching a maximum of 3600 mm in the west down to 500 mm in rain shadow zones in the east. In the area of study, the annual rainfall is between 900 and 1800 mm (Noble in Caine 1983) (Fig. 2.3). Summer and winter temperatures are cool and mild respectively. There is no permanent snow and seasonal temperature changes are relatively small.

The high ground of northeastern Tasmania has a cool and humid climate (Gentilli 1977). At 1200 m, the approximate elevation of the treeline (Caine 1983), there is a high frost frequency. The Blue Tier-Mount Victoria area was found by Caine (1983) to show a variability in precipitation strongly positively correlated with elevation (Fig. 2.3). Precipitation increased with elevation at a mean rate of about 117 mm /100 m.

2.3 Relief and drainage

In spite of the separation of Tasmania from the mainland by Bass Strait, its physiography forms an extension of the Eastern Australian Highland. The rugged hills and mountains provide marked contrast to the coastal region in the study area (Fig. 2.2). Three physiographic units

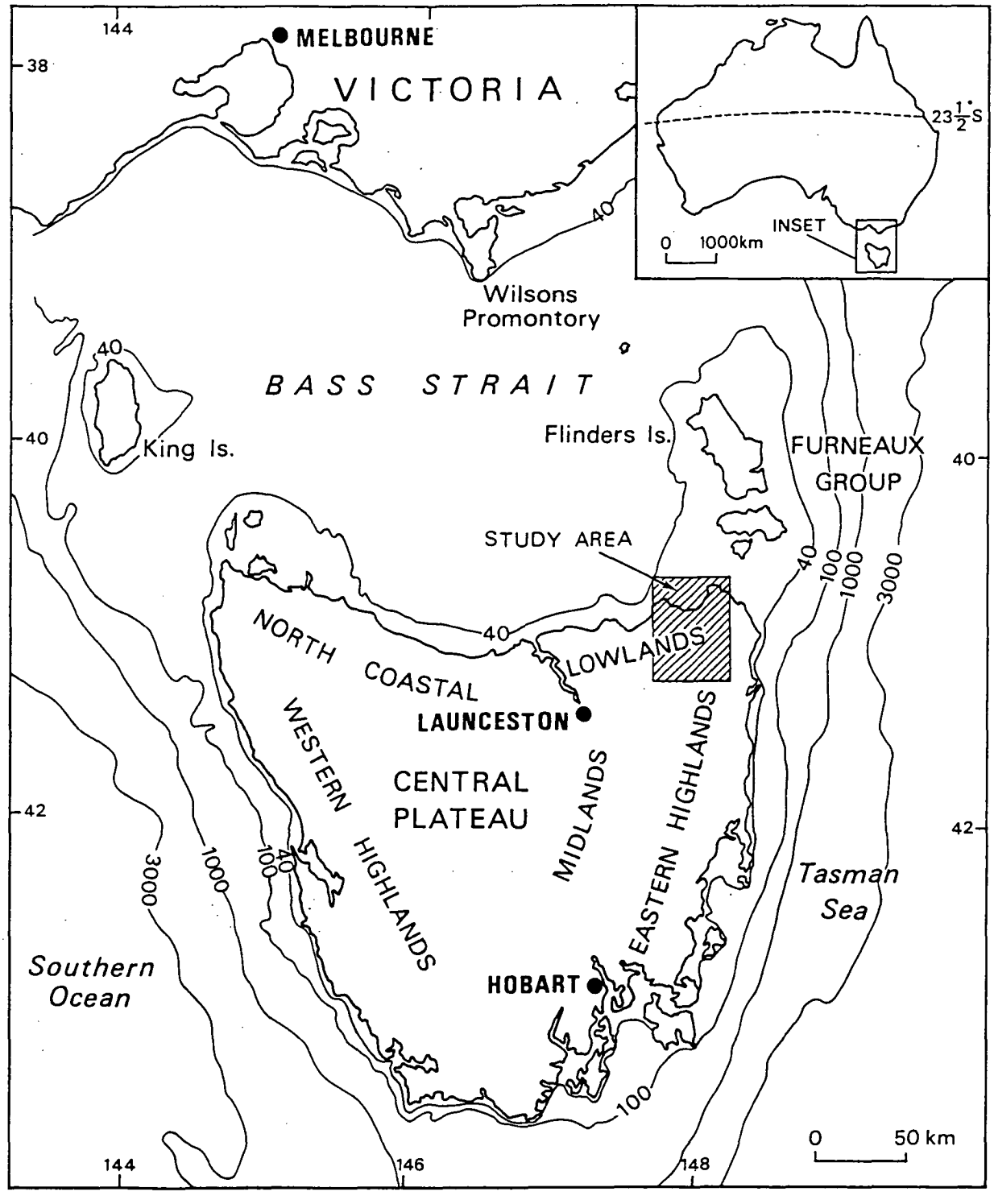

Fig. 2.1 Geographic position of the study area.

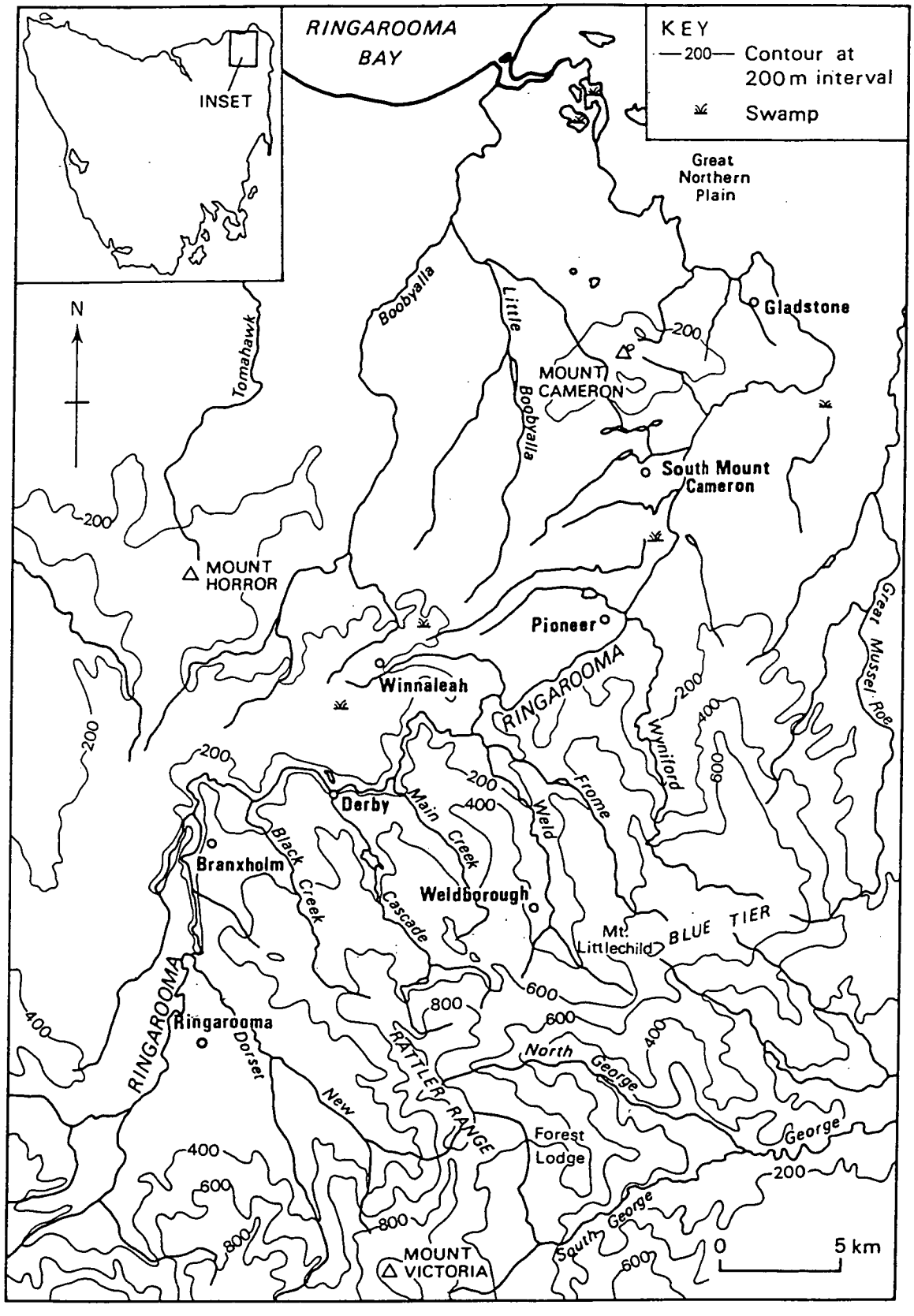

Fig. 2.2 Simplified relief and drainage map of the study area.

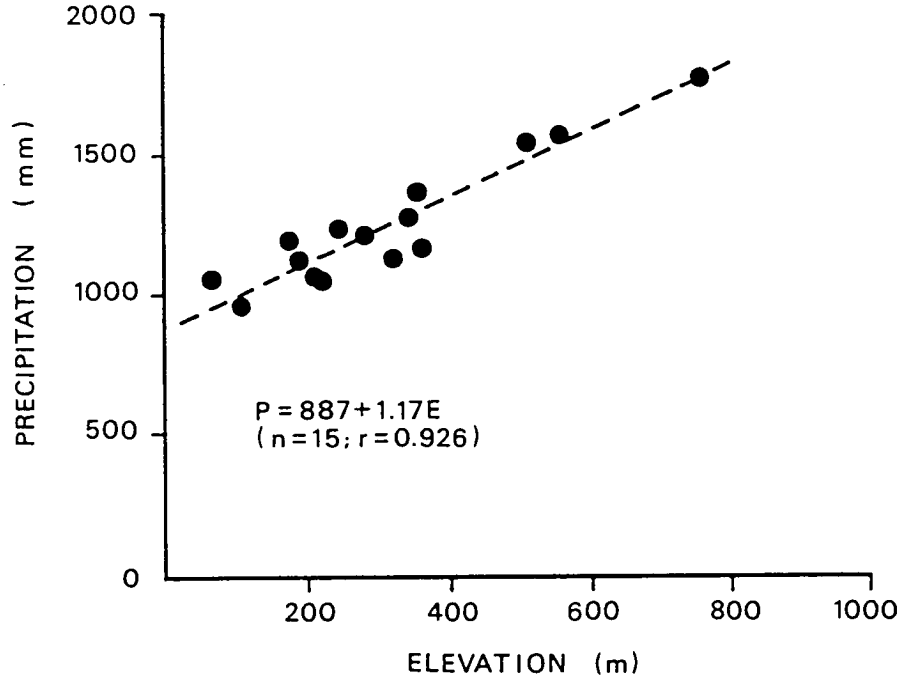

Fig. 2.3 Relationship between precipitation and elevation in the Blue Tier/Mount Victoria area of northeastern Tasmania. From Caine (1983).

falling within the area of the 1 : 50 000 Boobyalla and Ringarooma geological map sheets were recognised by Baillie & Turner in McClenaghan et al. (1982) including:

(1) Highland areas rising to a maximum elevation of nearly 900 m, including the Blue Tier and Mount Cameron Massifs, and Mount Horror.

(2) Coastal areas predominantly of flat plains rising to an elevation of about 40 m occurring north of the Mount Cameron Massif.

(3) An intervening dissected area of older bedrock separated by areas of dissected Tertiary sediments and basalt, which is well developed along the Ringarooma valley between Ringarooma and Derby (Fig. 2.3).

In a study of the alpine geomorphology of northeastern Tasmania, a model consisting of three zones was identified by Caine (1983). In order from lowest to highest, they are a forest zone up to about 800 m in elevation, a solifluction zone up to between 900 and 1200 m, and, a blockfield zone at 900 m and above. Only a relatively small part of the study area exceeded the elevation of 800 m and the blockfield zone occurs only on Mount Victoria where the rock type is dolerite.

The study area falls into the present day catchment area of the Boobyalla, Ringarooma and Great Mussel Roe river systems. A comparison between the maximum elevation, length, average gradient and catchment area of these rivers is shown in Table 2.1, and a map of drainage catchments in northeastern Tasmania after Jordan (1975) is shown in Fig. 2.4. It can be seen that the Ringarooma River is both the longest and largest catchment in the region at present. The main watershed of the river extends from Mount Michael to Mount Littlechild to Mount Victoria and Mount Maurice. Downstream, the river course changes in direction abruptly near Branxholm and between South Mount Cameron and Gladstone (Fig. 2.3). This is best explained by river capture involving both the Boobyalla and Great Mussel Roe river systems in the past.

River	Maximum elevation (m)	Length of main course (km)	Average gradient	Catchment area* (km^2)
Boobyalla	320	39.1	1:122	263
Great Mussel Roe	700	50.6	1: 73	383
Ringarooma	1020	104.3	1:102	937

* - From Jordan (1975).

Table 2.1 Comparison between maximum elevation, length, average gradient, and catchment area of the present day Boobyalla, Great Mussel Roe and Ringarooma Rivers.

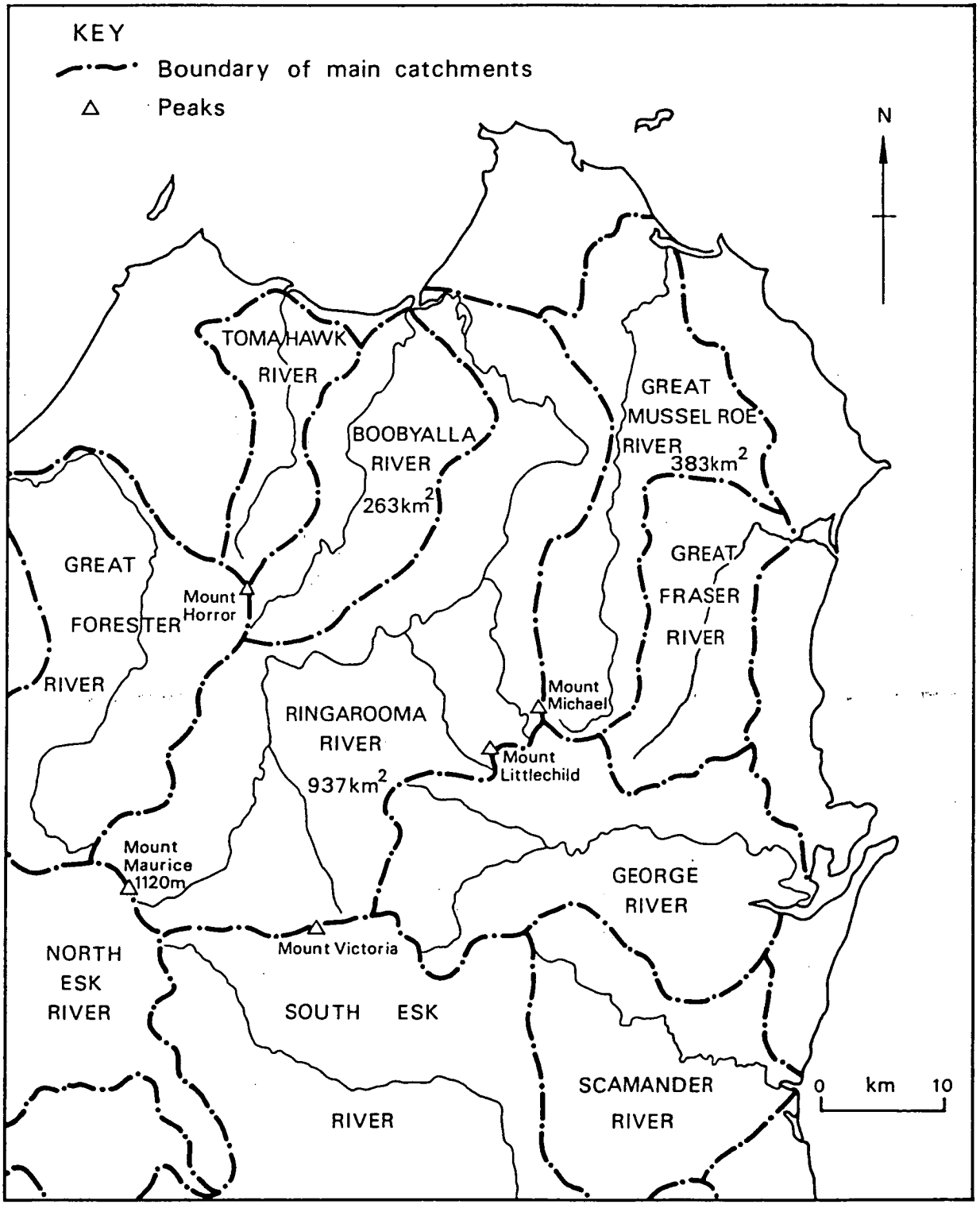

Fig. 2.4 River catchment map of northeastern Tasmania. After Jordan (1975).

The longitudinal profile of the present Ringarooma River shows three main terrace levels separated from each other by relatively fast-flowing gorge-like valley sections. Immediately upstream of Branxholm (Fig. 2.3), the terrace maintains an elevation of about 250 m. Between South Mount Cameron and Pioneer, encompassing the area referred to by Brown (1982) as the Tertiary basin south of Mount Cameron (throughout the thesis as the South Mount Cameron Basin), the terrace has an elevation close to 100 m. Both these terrace levels fall within the 'lower coastal' planation surface of Davies (1959). Downstream of Gladstone, the lowest terrace probably representing a succession of terraces including the Great Northern Plain, varies in elevation from 20 to 60 m. The occurrence of three main terrace levels and the intervening areas separating them suggest a complex history in landscape evolution. Antiquity in the landscape is indicated by the widespread occurrence of residual landforms in the Mount Cameron and Blue Tier Massifs.

2.4 Vegetation and soils

Figure 2.5 shows the distribution of vegetation in northeastern Tasmania after Kirkpatrick & Dickinson (1984). Two main types of low altitude forest occur, one characterised by high rainfall and the other by low rainfall. Rainforest is restricted to the higher and wetter parts of the Blue Tier Massif while Eucalyptus obliqua forest is common at elevations between 100 and 400 m. Typically the rain forest is either closed or open, more than 8 m tall and dominated singly and in various combinations by species of Nothofagus, Athrotaxis, Atherosperma, Lagarostrobos, Phyllocladus, Eucryphia and Anodopetalum with Eucalyptus species absent, or present with less than 10 % protective foilage cover. Where the annual precipitation exceeds 1500 mm, Nothofagus cunninghamii is common within the Eucalyptus rain forest (Caine 1983). Sclerophyll forest and heath are predominant in lowland areas below 100 m elevation.

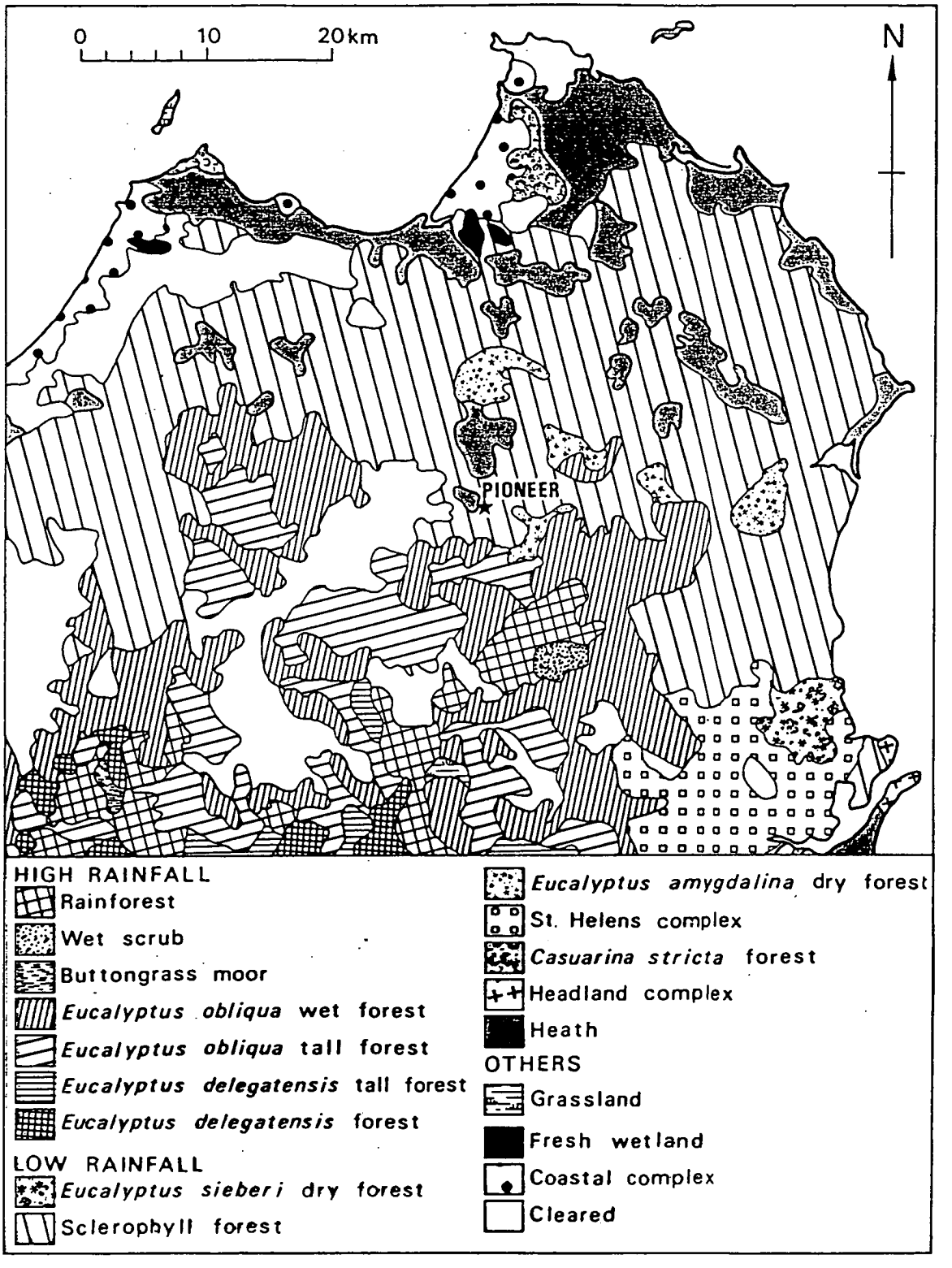

Fig. 2.5 Present day vegetation map of northeastern Tasmania. After Kirkpatrick & Dickinson (1984).

Duricrust is a general term for a hard crust at or near the ground surface. They may form in a variety of ways and there is no certainty that they are solely of pedogenic origin. Varieties of duricrust including ferricrete and silcrete (grey-billy) occur in the study area and are of special interest because of their possible value as stratigraphic markers. However, the palaeoenvironmental significance particularly of silcrete occurrence is unclear and there is little agreement between researchers in the literature (see Langford Smith 1978). Both ferricrete and silcrete have been mapped in the 1 : 50 000 Boobyalla, Ringarooma and Blue Tier geological map sheets of the Tasmania Department of Mines. Brown et al. in McClenaghan (1982) considered that the formation of ferricrete was due to iron enrichment and cementation of Tertiary sediments during the weathering and removal of the overlying basaltic rock formerly covering the area. Plate 2.1 shows the occurrence of ferricrete at the Tertiary sediment-basalt interface in a road cutting near Branxholm. Small outcrops of silcrete, often forming small isolated ellipsoidal hills, low ridges or flat pavement outcrops (Brown et al. in McClenaghan et al. 1982) are widespread in parts of the study area. They are particularly common south of Mount Cameron where they have been exposed probably with the assistance of alluvial tin mining operations. Typically they are nodular in form not usually exceeding 5 m long and 1 m thick consisting of lenses of silicified sands and gravels (Plate 2.2). Silcrete may occur in close association with granitic rocks in some areas but in other areas, it may form horizons within or above Tertiary sedimentary sequences.

2.5 General geology

A detailed account on the geology and mineral resources of Tasmania is presented by Burrett & Martin (1989). In this section, only the geological setting of the study area is examined. For convenience, the

Plate 2.1 Road-cut exposure near Branxholm showing the Tertiary basalt-sediment interface. The basalt probably of Middle Miocene age is lateritized.

Plate 2.2 Exposure of silcrete in an abandoned alluvial tin working at ABC Creek. The silcrete is nodular in form and consists of silicified sands and gravels. A small silcrete nodule isolated from the main mass can also be seen.

pre-Cainozoic and the Cainozoic geology are dealt with separately in two sub-sections. Fig. 2.6 shows a simplified geological map of the Blue Tier Batholith based on Groves et al. (1977). More attention is given to the Cainozic geology because of the greater relevance to placer deposits.

2.5.1 Pre-Cainozoic

The oldest rock type in the area is the Mathinna Beds of Early Ordovician (Banks & Smith 1968) to Devonian (Rickards & Banks 1979) age. According to Turner in McClenaghan et al. (1982), a possible thickness of 350 m is present in the area and the sequence consists of alternating beds of poorly sorted siltstone and mudstone with textures and sedimentary structures indicative of deposition from turbidity currents (Williams 1959). Prior to granite emplacement the Mathinna Beds were folded and cleaved, and underwent low grade metamorphism.

Both the Blue Tier and Scottsdale Batholiths are composite granite bodies emplaced into the Mathinna Beds at a high level in the crust. Gravity surveys by Leaman & Symmonds (1975) indicated that the two batholiths are connected at shallow depth. A cogenetic origin is consistent with K-Ar and Rb-Sr age determinations (McDougall & Leggo 1965) with ages of around 370 Ma. Similar Rb-Sr ages were obtained by Cocker (1982) for the Poimena, Mount Paris and Anchor granites.

McClenaghan et al. (1982) found that a (Ti/10)-Rb-Sr triangular diagram (Fig. 2.7) provided a convenient division of the granitic rocks of the Blue Tier Batholith into granodiorite, adamellite and alkali granite suites. They concluded that the Mathinna Beds were unlikely to be a source rock for any of the granitic rocks, while the granodiorite suite may have derived from igneous source rocks and the adamellite and alkali granite suites from sedimentary rocks. Minor granitic intrusions occur mainly in the form of dykes including quartz-feldspar-porphyry which may be garnetiferous, pegmatite and aplite. Chemical and isotopic

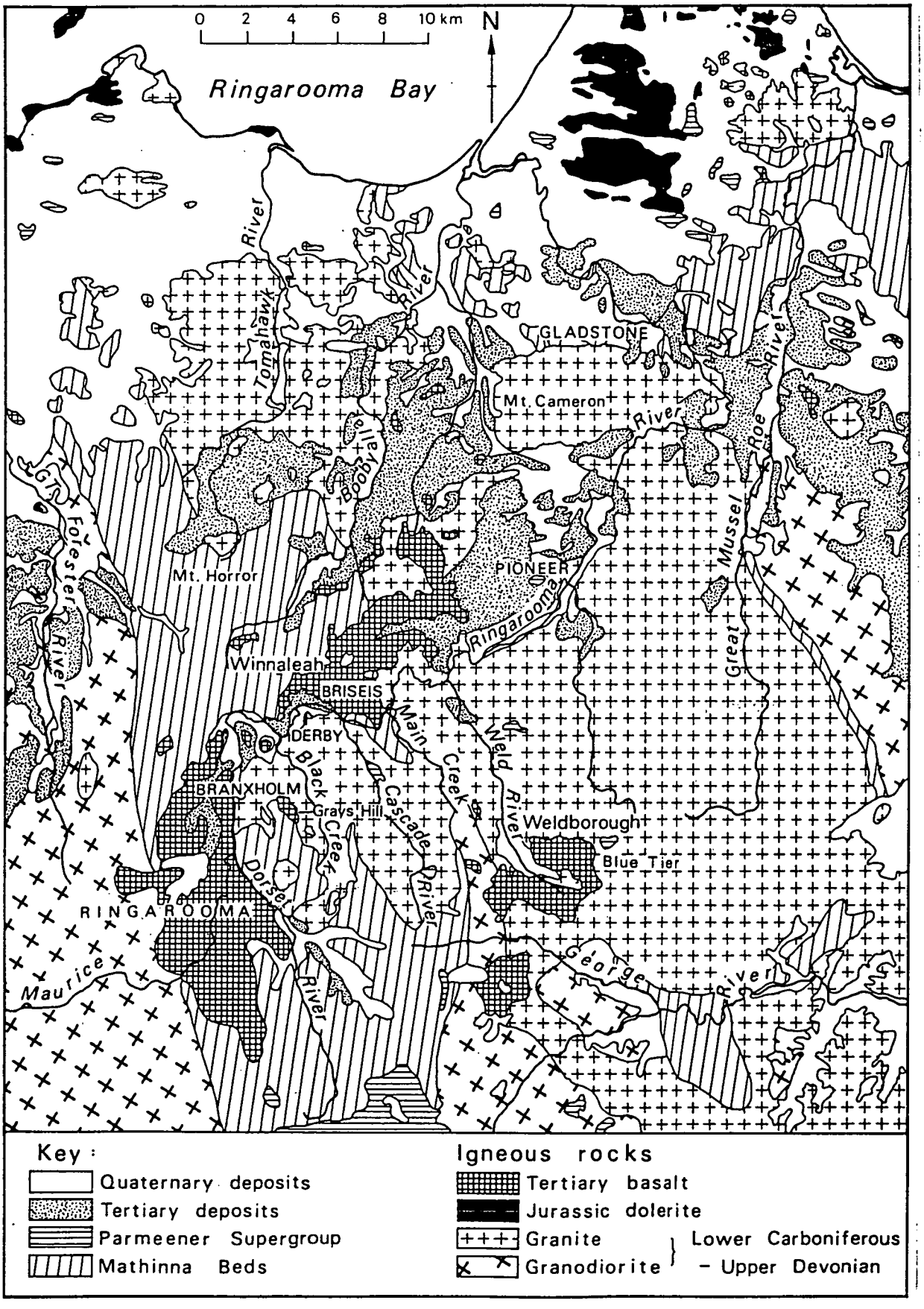

Fig. 2.6 Simplified bedrock geological map of the study area. Based on McClenaghan & Baillie (1975) and Groves et al. (1977).

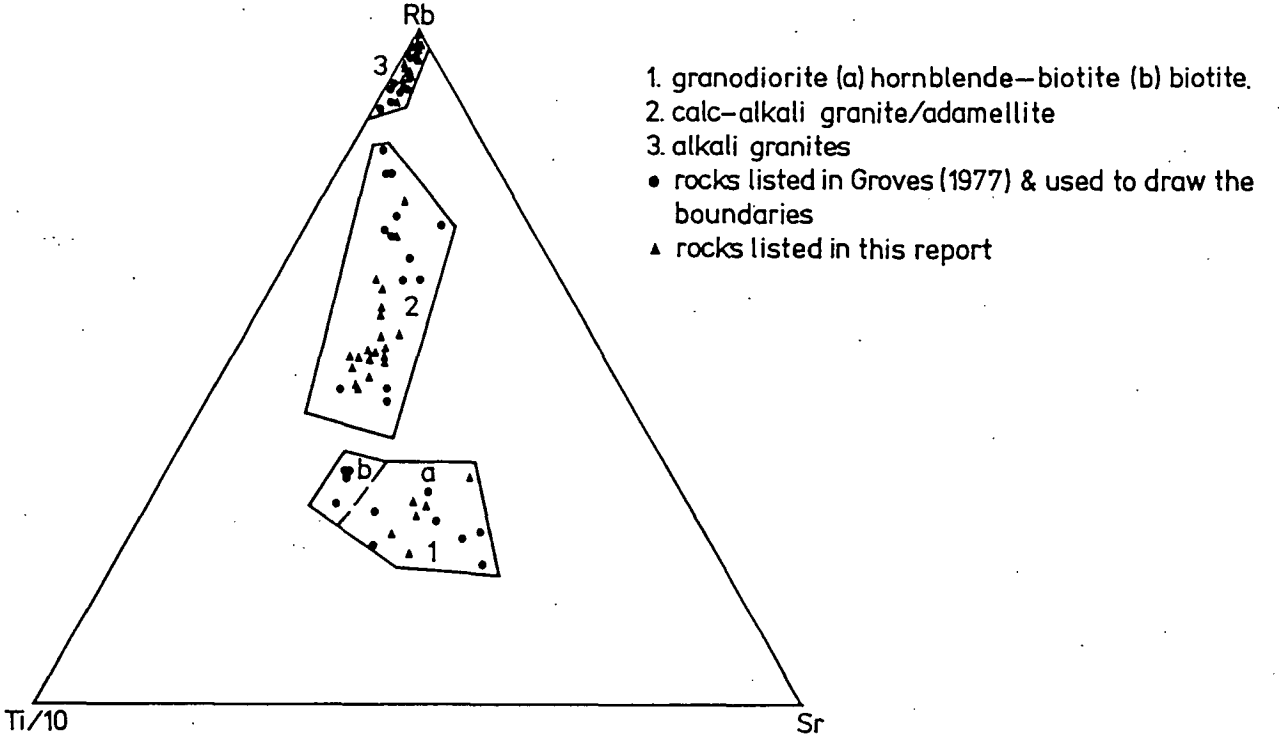

Fig. 2.7 Ti/10-Rb-Sr diagram of rocks from the Blue Tier Batholith. From McClenaghan et al. (1982).

data obtained by Higgins et al. (1985) from three major plutons of the Blue Tier Batholith support a model in which each granite type is formed from separate melts derived from partial melting.

On the 1 : 50 000 Ringarooma geological map sheet, a poorly sorted conglomerate with subrounded quartz pebbles of 60 mm length set in a quartz-rich matrix together with a quartz-rich sandstone are shown on the east side of Mount Littlechild (McClenaghan in McClenaghan et al. 1982). These unfossiliferous rocks may belong to the Parmeener Supergroup of Banks (1973) which is of Permo-Triassic age. Northeastern Tasmania was a highland area during deposition of the Lower Marine Sequence (Clarke et al. 1976) and the palaeotopography had northerly to northwesterly trends thought by Turner (1980) to reflect Devonian structure. This Supergroup rests unconformably on Late Devonian to Early Carboniferous granitic rocks of the Blue Tier Batholith. Such a stratigraphic relationship implies that the granitic rocks were exposed subaerially prior to the deposition of the Parmeener Supergroup. Near the Great Northern Plain, pebbly siltstone and sandstone, medium to coarse sandstone, quartz grits and lithic sandstone containing Eurydesma was assigned to the lower parts of the Lower Parmeener Supergroup (Baillie in McClenaghan et al. 1982). Based on the occurrence of sparse marine fossils and dropstones, the rock types were interpreted as glacial-marine deposits.

Late Devonian to Cretaceous dolerite dykes, Jurassic dolerite and Cretaceous appinites also occur within the study area. On the basis of chemical dissimilarity from the Tertiary basalts and intrusive relationship with all granitic types, McClenaghan in McClenaghan et al. (1982) suggested that the dolerite dykes near the top of the Blue Tier Massif must be post-Late Devonian but pre-Tertiary in age. Although not dated radiometrically in northeastern Tasmania, Jurassic dolerite intruded rocks of the Lower Parmeener Supergroup with both concordant

and transgressive contacts. A petrological summary of the appinitic rocks occurring in the Cape Portland area was presented by Jennings & Sutherland (1969). K-Ar and Rb-Sr dating of these rocks gave ages ranging from 91 to 103 Ma (Baillie in McClenaghan et al. 1982).

Faulting pre-dated and closely followed the Jurassic dolerite intrusion (Solomon 1962) and probably persisted as the predominant north-north-west trending faults until the Holocene. These faults were involved in the development of the Boobyalla Sub-basin (Moore et al. 1984) and may be traced into the Bass Basin (Robinson 1974). Other major fault trends found are in the northeasterly and northerly directions (Williams 1978).

2.5.2 Cainozoic

A review of the Cainozoic geology of Tasmania was given by Gill (1962). In mapping the non-marine Tertiary sediments of the study area, Brown et al. in McClenaghan et al. (1982) found difficulties in poor exposures, lack of datable material, lack of lithological marker beds, and finally, occurrence of lag deposits of uncertain age in areas marginal to those of known age. Only the last reason is considered to be valid in the present study. Good exposures of Tertiary and Quaternary sediments may be found in alluvial tin workings particularly when the tin mines are in operation. The main drawback is in the age identification of these deposits because sedimentological characteristics alone are inadequate due mainly to the discontinuity of exposures.

The widespread occurrence of Tertiary basalts in the study area has provided both datable material (Brown 1977; Sutherland & Wellman 1986) and lithological markers. Older and younger basalts have been identified on the basis of physiographic evidence by Nye (1925), Nye & Blake (1938) and Edwards (1939). The latter occurring along the middle Ringarooma valley near Winnaleah differ from the former at Weldborough Pass and

Grays Hill in their lower elevation and their comparatively fresh appearance. Subsequently, K-Ar dating of the older and younger basalts gave ages of about 47 Ma (Sutherland & Wellman 1986) and 16 Ma (Brown 1977) respectively. A convenient lithological marker is therefore provided by the base of the younger basalts. For example, this was used by Spry (1962) to separate Tertiary deposits in Tasmania into pre-basaltic and post-basaltic types.

Plant remains from the study area including pollen and spores (Harris 1965, 1965a, 1968; Macphail in Morrison 1980; Forsyth 1982; Hill & Macphail 1983) and leaves (Hill 1983; Bigwood & Hill 1985) are also useful in providing age indications for the Tertiary deposits. Palynological analysis by Harris (1965) on 17 samples from northeastern Tasmania suggested an Early Miocene age for the assemblage found. Further samples from the region indicated either an Early Miocene or Late Oligocene age (Harris 1965a). An older Oligocene age for the flora occurring at the Pioneer Tin Mine was favoured by Hill (1983) and Hill & Macphail (1983). More recently, leaves belonging to the family Araucariaceae with a probable Middle to Late Eocene age were found at the Hasties Tin Mine (Bigwood & Hill 1985). Because all these deposits occur beneath the younger basalts which were K-Ar dated at about 16 Ma (Brown 1977), the pre-Middle Miocene ages are in good agreement. A more extensive former cover of younger basalts overlying Tertiary sediments must have existed at Pioneer (Morrison 1980).

Tertiary sub-basaltic sediments containing economic values of tin were visualized by Jennings (1975) as segments of shallow alluvial cones formed at the break in stream gradient near the foot of the Blue Tier and Mount Cameron Massifs. A sedimentological study on the deposits at the Pioneer Tin Mine by Morrison (1980) identified a fining upward sequence of pre-Middle Miocene alluvial deposits divisible into two parts comprising:

(1) A tin-bearing lower sequence up to 6 m in thickness consisting of stratified gravels, trough cross-bedded gravels, and lenticular bodies of peat and associated clay. The main type of deposit represented is a high energy river channel facies.

(2) A tin-depleted upper sequence between 30 and 40 m in thickness consisting of trough cross-bedded sands and gravels, and large bodies of kaolinitic clay. The main type of deposit represented is a low energy floodplain facies.

Very few studies have been made on the Cainozoic volcanic activity and geomorphology of the study area. Most of the previous work carried out was in connection with alluvial tin exploration, and the emphasis on other geological aspects was small. An exception to this is the geological mapping of the Tertiary basaltic rocks by McClenaghan et al. (1982). At Weldborough Pass, the base of the volcanics ranges from 500 to 800 m with 150 m of agglomerate and tuff underlying 230 m of lavas. Eruptive centres were thought by Sutherland & Wellman (1986) to be at Weldborough Pass, 2 km southwest of Forest Lodge and possibly under Mount Littlechild (Fig. 2.3). Basalts with similar petrology and elevation at Grays Hill (Fig. 2.6) northwest of Mount Paris resembled a plug in morphology (Brown & McClenaghan in McClenaghan et al. 1982). In the Winnaleah area, at least two superimposed flows have been identified by Brown in McClenaghan et al. (1982), the lower part of olivine nephelinite with xenoliths and megacrysts, and the upper part of alkali olivine basalt. As in parts of Tasmania studied by Sutherland (1969), the flows are valley-fill extruded here through numerous small necks and fissures in granitic rocks and Mathinna Beds respectively.

Along the Ringarooma valley, the flows extend 40 km with a maximum basal elevation of 300 m in the south to 160 m in the north. Marshall (1968) concluded that the basaltic extrusions were probably related to activity of the noth-north-west trending fault lines. Ferricrete

horizons at the Tertiary sediment-basalt interface (Brown in McClenaghan et al. 1982) were considered to be due to iron enrichment and cementation of Tertiary sediments during weathering and removal of the overlying basaltic rocks. Based on this, ferricrete cappings above Tertiary sediments on flat-topped hills may be used to indicate the former extent of the younger basaltic flows.

Evidence of former higher sea level stands are present in northeastern Tasmania. Marine limestone of Miocene age was identified in a small area of Cape Portland to the north of the study area by Quilty in Jennings & Sutherland (1969) and Quilty (1972). The abundance of ostracod and rarity of foraminifera in the limestone are indicative of a lagoonal or shallow water origin. In a review of the geological development of the southern shores and islands of Bass Strait, Sutherland (1973) found that the Miocene marine transgression was impeded in troughs containing the older basaltic flows while aquagene volcanic sequences occur where lavas flowed into the sea. Volcanism continued during the regression of the Miocene high seas and dissection of its deposits, but since the Middle Pliocene, the Tasmanian margin of the Bass Strait appears to have remained tectonically and volcanically relatively inactive. Significant Late Cainozoic movements was ruled out in Tasmania by Sutherland (1971).

Baillie in McClenaghan et al. (1982) identified fluviatile, aeolian, slope and marine deposits (Table 2.2) through field mapping of superficial deposits in the study area. A similar but more detailed stratigraphical sequence for the region north of Mount Cameron was given in a geomorphological and groundwater hydrological study by Bowden (1981) (Table 2.3). However, the interglacial ages for the pre-last glacial deposits was tentatively determined by Bowden (1981) using the degree of surface solution of sponge spicules thought to be of marine origin. Since sponge spicules may also have a freshwater origin and a

Series	Holocene	Pleistocene	
		Last Glacial	Last Interglacial
Soils	Minor leaching, peat formation	Strong podsol, groundwater podsol development	?Palaeosol at Sheepwash Creek
Marine and related deposits	Beach sands, gravels		Sand, clay, minor peat and gravel
Aeolian	Dune sand	Lunette formation Dune sand: sheets and longitudinal dunes	
Talus and slope deposits		Talus, slope deposits	
Fluviatile/ Alluvial	Alluvium and related deposits		

Table 2.2 Classification of Quaternary deposits in the study area. From Baillie in McClenaghan et al. (1982).

Age	Formation	Landform and Origin	Extent
Holocene	Bowlers Lagoon Sand	Transverse calcareous sand dunes	Coastal margins of Anderson and Ringarooma Bays
	Waterhouse Sand	Parabolic sand dunes	Coastal margins of Anderson and Ringarooma Bays Musselroe Point
	Barnbougle Sand	Marine sand plains and beach ridges	All depositional coasts of northeastern Tasmania
Last Glacial	Forester Gravel	Fluvial terraces	Great Forester River
	Rushy Lagoon Sand	Terrestrial lunettes (? Holocene in part)	Widespread northeastern Tasmania
	Ainslie Sand	Terrestrial longitudinal sand dunes	Widespread northeastern Tasmania
	Croppies Marl	Inland lake deposits	5 km east of Croppies Point
Last Interglacial? (Isotope Stage 5)	Stumpys Bay Sand	Marine plains and beach ridges	Broad, coastal sand embayments: to +32 m
Second Last Interglacial? (Isotope Stage 7?)		Marine sands	Rockbank: to +49 m
Third Last Interglacial? (Isotope Stage 9?)		Marine sands	Rockbank: to +71 m
Older than Third Last Interglacial		Possibly marine sands	Star Hill Mine: to ~ 90 m
Middle Tertiary		Marine sands and freshwater peats	Bore 6 km SE of Cape Portland
Tertiary		Alluvial gravels	Widespread northeastern Tasmania

Table 2.3 Stratigraphic sequence of coastal northeastern Tasmania. From Bowden (1981).

Miocene age cannot be entirely ruled out, post-depositional recycling of freshwater and marine types are possible. Evidence for recycling of derived Upper Miocene foraminiferal faunas in dune deposits on Flinders Island was noted previously by Sutherland & Kershaw (1971). The presence of emergent Quaternary shorelines (Bowden 1978 and 1981; van de Geer et. al. 1979; Bowden & Colhoun 1984; Colhoun 1989) through tectonism is a problem requiring further investigation to resolve.

In Tasmania, the existence of frost and solifluction processes above 450 m and the occasional occurrence of the former down to 300 m during the Last Glaciation was suggested by Davies (1967). Therefore, the flat slopes of highland areas near Mount Maurice and Mount Victoria may have been sites of snow field accumulation. The thawing of snow fields during spring resulted in increased stream discharge, and may be responsible for the formation of fluvial terraces along the Ringarooma River. However, no dating has so far been carried out to confirm their Quaternary age. A study by Macphail (1975) on Late Pleistocene vegetation patterns in Tasmania showed markedly lower temperatures and eastern Tasmania may have experienced 'glacial-arid' climates.

Along the coastal area, sand drift traversed eastward under the persistent prevailing winds throughout the Pleistocene Epoch (Sprigg 1979). Estuarine sediments containing foraminifera and mollusca from Mussel Roe Bay were considered by Baillie et al. (1985) to be older than the aeolian sands which belonged to the Last Glaciation. The deposits were formed during the Last Interglacial Stage about 125 000 years BP.

2.6 Geology of stanniferous placers

This section is divided into three parts. Because the formation of stanniferous placers is dependent on the nature of bedrock tin mineralization, primary tin deposits are dealt with in the first part. Eluvial and alluvial placers are covered respectively in the second and third parts. Eluvial placers (kulit) are defined as residual deposits

formed essentially in situ without major lateral transport or sorting. Alluvial placers are defined as bedded deposits where mineral concentration has been effected by streams. These included fluvial lag gravel deposits overlying bedrock in valleys (kaksa) and alluvial concentrations interbedded in the sedimentary fill of the valley (mintjan). Explanation for a list of common mining terms used in connection with placers after Nye (1925) and Raeburn & Milner (1927) is given in Table 2.4.

2.6.1 Primary tin deposits

According to the classification of Hall & Solomon (1962), primary tin in the Blue Tier belonged to the type of deposits within magmatic rocks. Tin mineralization was considered by Gee & Groves (1971) to be connected with the youngest igneous bodies, consisting of biotite-muscovite granite and adamellite which were intruded into barren hornblende and biotite granodiorite. The tin-bearing granites formed sheet-like masses up to 300 m thick. Tin mineralization post-dated that for gold which is also present in the study area, with the latter probably related to the earlier granodiorite intrusion (Klominsky & Groves 1970). Primary tin accounted for less than 10 % of production from the Blue Tier district (Ingram 1977); the remainder came from rich alluvial and eluvial deposits derived particularly from the erosion of the Blue Tier Batholith.

Groves & Taylor (1973) carried out a study on the greisenization and mineralization of the Anchor tin mine in the Blue Tier district. The tin deposits are found to be associated with irregular, sheet-like bodies of greisenized granite and greisen located in the apical region of a sill-like intrusion of biotite-muscovite granite and adamellite. The zone of mineralization and greisenization is north-northeast trending and is restricted to a flat-lying part of the upper contact of this granite, which is about 152 m wide, over 600 m long, and occurs

Mining term	Definition
Bottom	the floor of the lead or ancient valley; same meaning as bedrock
Drift	clays, sands and grits which filled the ancient valley
False bottom	a stratum of barren alluvium, usually of fine grade separating two layers of pay-dirt
Gutter	the deepest portion of the lead representing the ancient stream course before its valley began to be filled with sediments
Lead	the valley of an ancient stream filled up with lower Tertiary sediments
Overburden	barren material overlying a deposit
Pay-dirt	mineral-bearing alluvium or eluvium
Pug	stiff clay
Shingle	rounded pebbles which in the study area is made up of Mathinna Beds
Wash	river gravels occurring at the base of drifts or along present streams

Table 2.4 Summary of selected mining terms used in connection with placer deposits. After Nye (1925) and Raeburn & Milner (1927).

within the upper 36 m of the sill. Because of the flat-lying disposition of the ore body, the dispersion of cassiterite during erosion is unfavourable.

A study of iron and titanium oxide minerals in granitoids from the Scottsdale and Blue Tier Batholiths was carried out by Calcraft (1980). The identification of magnesium-poor manganese-rich ilmenite is consistent with the ilmenite-series of Ishihara (1977) which is associated with greisen-type tin and tungsten deposits.

Tin lode deposits are well known in a number of localities in the study area. These included Mount Paris, Emu Hill, Masher Hill, Australia Hill, Poimena and the Fly-by-night Tin Mine near Gladstone. Description of these localities are available in the geological survey bulletins of the Tasmania Department of Mines for the Blue Tier Tin Field (Reid & Henderson 1928; Thomas 1953) and the Gladstone mineral district (Twelvetrees 1916). The small tin reserves at these localities is reflected by the lack of interest by mining companies even during periods of high tin metal prices. Furthermore, based on the hard rock reserves and the production figures from alluvial mining, it is estimated in the present study that over 90 % of the primary tin from northeastern Tasmania has already been released into placers.

2.6.2 Eluvial placers

Although eluvial placers are formed in situ, they may grade into alluvial placers through lateral transport and sorting. Therefore, it is difficult to recognise eluvial placers unless undisturbed exposures are available for examination. In past literature on the study of tin placers in northeastern Tasmania, there has been an absence of reference to the recognition of eluvial deposits. For example, a review on tin in northeastern Tasmania by Jennings (1980) recognised only lode and alluvial deposits. Explanation for this lack of recognition are:

(1) The low economic potential of eluvial deposits including inferior ore grade and reserves in comparison to alluvial deposits.

(2) Eluvial deposits have already been exhausted because of their thin overburden.

(3) The unfavourable geomorphological history such as a dominance of erosional activity on slopes with steep gradient, and, unfavourable palaeoenvironmental conditions for deep weathering and elutriation of the residual soil.

(4) The gradational change from eluvial to alluvial placers, and their close association with each other makes it difficult to draw a clear-cut separation line between them.

(5) The difficulty in distinguishing between disturbed samples of eluvial and alluvial deposits.

Eluvial placers are likely to have been relatively widespread on the Blue Tier Massif near Mount Paris and other areas with primary tin deposits and gentle slope gradients. However, eluvial placers are rarely exposed there partly because of their removal by mining and their marginal economic interest.

An example of an eluvial deposit is shown in Plate 2.3. In this deposit, cassiterite is present in the form of subrounded nuggets and the deposits resemble colluvium.

2.6.3 Alluvial placers

Alluvial placers in northeastern Tasmania are often referred to by the mining term 'lead' or 'deep lead' (Table 2.4). A lead may occur on the surface as an abandoned channel while a deep lead is covered or buried. In spite of a literature search, no information on the separation depth between the two types has been found. Both terms have been used to refer to the valley of an ancient stream which may be cut in bedrock or older sediments (e.g. Nye 1925). Economic ore minerals need not be present within leads but Nye (1925) used the term 'lead'

Plate 2.3 An eluvial placer section showing strong colluvial tendencies in the Blackberries Tin Mine on the Wyniford Lead. Cassiterite is present as subrounded nuggets and the deposits resemble colluvium in appearance.

Plate 2.4 An alluvial placer section in the Endurance Lead. A seam of cassiterite occurs at the base of an erosional channel cut in kaolinitic clay.

specifically in connection with a valley filled with sediments of Early Tertiary age in the study area. This age identification was based on wood and plant remains present which may be correlated with similar occurrences throughout Tasmania.

An example of an alluvial deposit is shown in Plate 2.4. In this deposit, cassiterite was deposited clearly by alluvial means at the base of an erosional channel in kaolinitic clay.

Figure 2.8 shows the inferred position of leads in the study area recognised by previous workers. Early work on the Ringarooma Lead was carried out by Twelvetrees (1900). Nye (1925) identified the Ringarooma lead system which followed a similar course to the present Ringarooma River but is mostly concealed by Tertiary basalts of Middle Miocene age (Brown 1977). Numerous northwesterly tributary leads originating from the Blue Tier Massif joined up with the main lead between Branxholm and Pioneer but to the north of Pioneer, the main lead swings from northeasterly to northerly and continues in the general direction of the Little Boobyalla River. A geophysical survey by Sedmik (1964) detected a north flowing channel system in the unweathered bedrock surface more than about 90 m below ground surface in many places. However, the actual depth of these leads probably is much smaller because a thick weathered zone is expected. Based on field mapping, geophysical and borehole data, Brown (1982) concluded that the original lead ended in a land-locked basin south of Mount Cameron. The infilling of the river system occurred during the mid-Tertiary prior to burial by Middle Miocene basaltic flows. On the other hand, in an exploration potential map compiled by Fleming (1979) the leads of South Mount Cameron shows a westerly direction (Fig. 2.8). With the exception of Brown (1982), all previous workers were in favour of an exit into Bass Strait for the Ringarooma Lead. King (1963) differed from the other workers in that he also identified the Mussel Roe Lead.

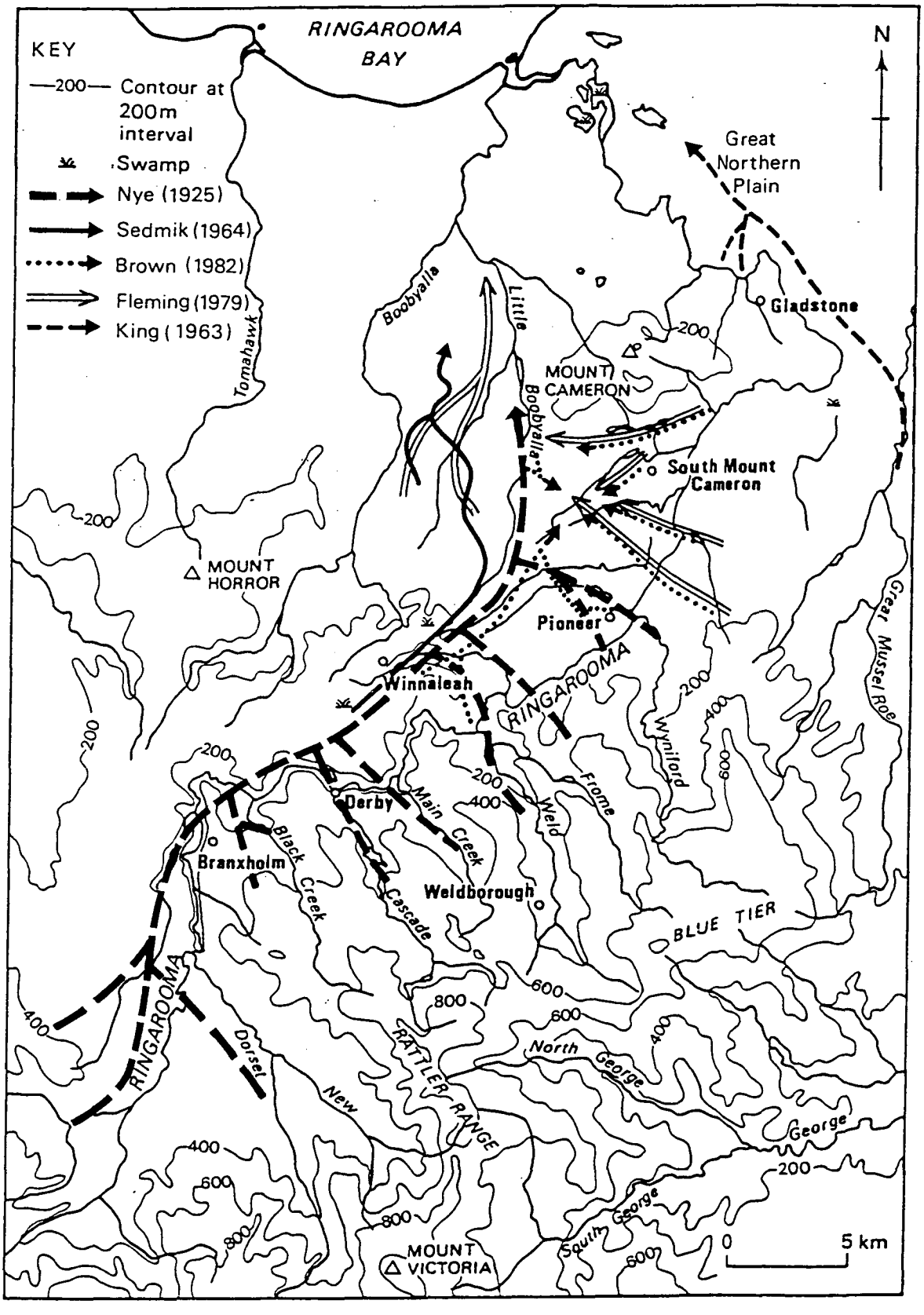

Fig. 2.8 Map of the study area showing inferred position of leads after Nye (1925), Sedmik (1964), Brown (1982), Fleming (1979) and King (1963).

A review of the alluvial tin deposits of the study area was given by King (1963). The best known deep lead mine is the Briseis at Derby (Plate 2.5). It was the second most productive tin mine in Australia, and yielded 21 120 tonnes of metallic tin during the period 1876 to 1960 (Ingram 1977). Fig. 2.9 shows the sediment section exposed at the mine after Nye (1925) who also proposed that the source was from the Cascade Lead. In part, the mine was sub-basaltic with basalt flows totalling 60 m in thickness overlying a 95 m cover of fluvial sediments. About half of the cassiterite recovered was estimated by Ingram (1977) to occur within 10 m of the basal alluvium at an average ore grade of 0.59 kg/m^3 of 70 % cassiterite. The remaining ore reserves was estimated by Braithwaite (1964) to be not more than 2000 tons (2032 tonnes) of metallic tin.

The only deep lead mine operating during the present study was the Pioneer Tin Mine (Plate 2.6). In a sedimentological study of this mine by Morrison (1980), eight sedimentary facies were identified. They are in order from the base upwards:

(1) Massive to crudely stratified, clast-supported imbricated gravels up to 5 m in thickness with near horizontal stratification and a maximum clast diameter of 0.4 m. This facies occupies topographically the highest part of the tin-bearing sequence.

(2) Sheets of gravel up to 1.5 m in thickness dipping at 3 to 10 degrees in a northeasterly direction.

(3) Near horizontal beds of gravel about 1 m thick containing abundant well-rounded vein quartz under 30 mm in diameter referred to by miner's as bird's eye wash.

(4) Thin 0.1 to 0.2 m sheets of gravel dipping at 10 to 20 degrees with climbing ripple lamination, soft sediment folding and tension cracking.

(5) Large scale trough cross-bedded basal drifts with granite boulders.

Plate 2.5 The old Briseis Tin Mine, an example of a deep lead. The pit exposure is now mostly underwater but three basaltic flows probably all of Middle Miocene age overlying a fining upwards sequence of Tertiary alluvial sediments are present (see Fig. 2.9).

Plate 2.6 Pit exposure of the Pioneer Tin Mine during 1980. The deep lead sequence from top to bottom consisted of organic-rich sediment, bleached sandy clays, and tin-bearing yellowish-brown pebble bed overlying decomposed granite.

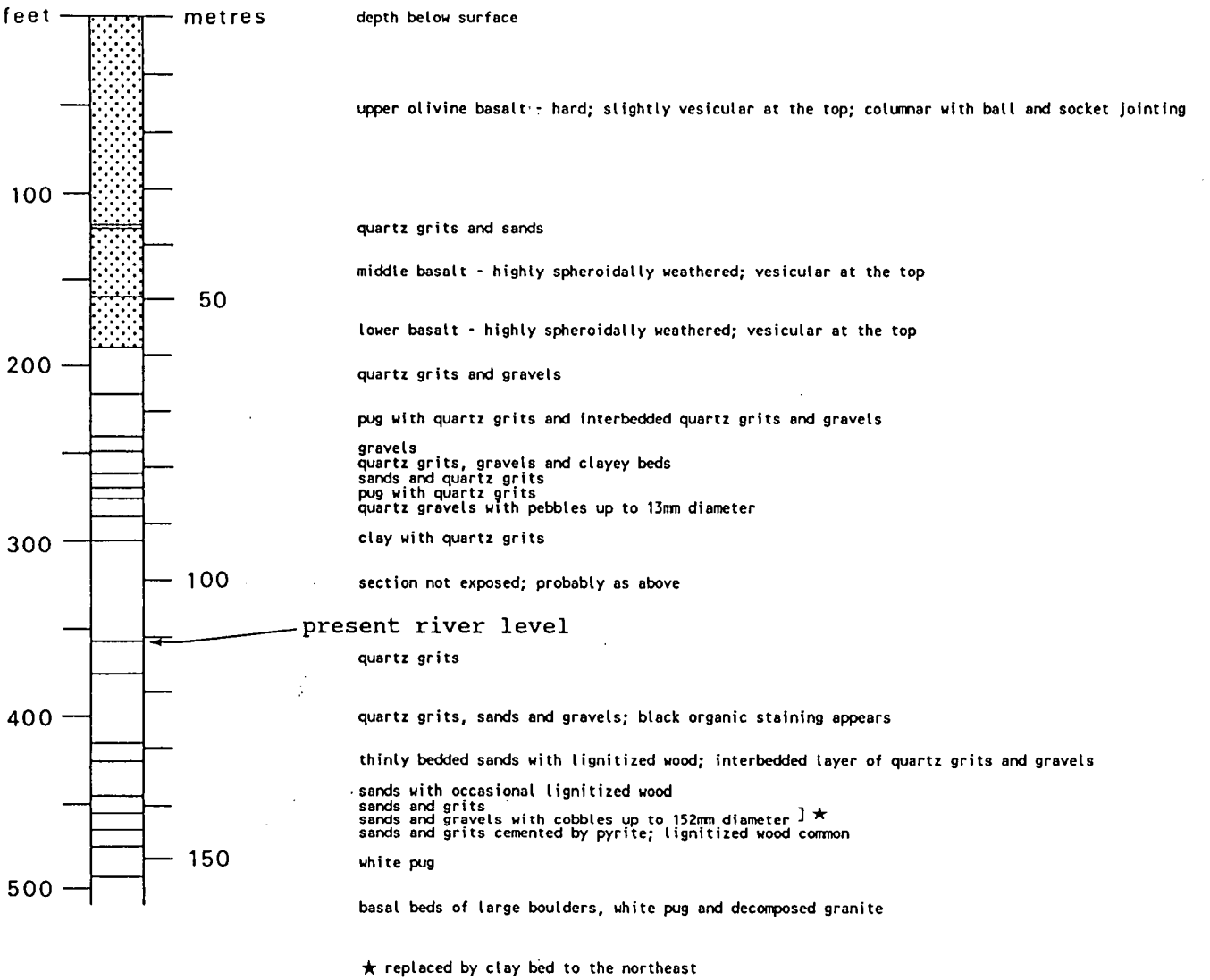

Fig. 2.9 Sediment section exposed at the Briseis Tin Mine. After Nye (1925) with minor modifications.

(6) Large scale festoon cross-beds of granules up to 1 m in thickness showing an erosional contact with the underlying sediment.

(7) Tabular cross-bedded sands 0.2 to 0.3 m in thickness dipping at angles of 18 to 30 degrees in a easterly direction.

(8) Lenticular bodies of peat and associated sandy clay.

The concentration of heavy minerals was interpreted by Morrison (1980) as having taken place in longitudinal and transverse bars, and channel facies. Furthermore, the bulk of the heavy mineral deposition had occurred during the initial stages of waning flow after flooding. Gravel fabrics and trough cross-beds confirmed transportation by unidirectional currents, which locally flowed from the east, southeast and south. The deposits were suggested by Nye (1925) to have formed by the confluence of the Wyniford and Gladstone Leads.

'Deep leads' and 'leads' occurring near the present course of the Ringarooma River between Branxholm and South Mount Cameron are situated at the break of stream gradient on the northwestern margin of the Blue Tier Massif. This led Jennings (1975) to visualize them as segments of shallow alluvial cones. On the Blue Tier Massif, numerous alluvial and eluvial tin deposits are known and have been worked extensively. Many of these sites revealed greisenized lodes on sluicing, which indicated an extensive area of primary tin mineralization over a large part of the massif. In addition to the Cascade and Wyniford Leads, other economically important leads included the Endurance, Echo and Arba. North of Mount Cameron, leads located at the break in stream gradient also occur. Best known are the Monarch, Scotia and Lochaber Leads. To the east of Gladstone, a main lead is the Mussel Roe.

The placer tin deposits in Ringarooma Bay probably represented an extension of the onshore leads and were formed when sea level was lower than in the present day. These offshore deposits were explored by drilling in the 1960s by Ocean Mining AG (Lampietti et al. 1968;

Wellington 1982). Based on core assays and marine geophysical surveys, northwesterly trending lead features similar to those onshore were identified by Hellyer Mining & Exploration Proprietary Limited (1983). The deposits are estimated to contain 15 000 tonnes of metallic tin, but very little is known about the stratigraphy of the placers. In these deposits, the concentration of tin by marine processes may be ruled out because tin content is highest adjacent to bedrock, a feature which is in common with the onshore leads.

Along the present day course of the Ringarooma River near South Mount Cameron, terrace deposits have been worked for tin. These deposits appear to be related to the present floodplain of the river but their precise age is not known. It is likely that episodic reworking of the deposits has taken place until the present day. Downstream of Gladstone in the Great Northern and Boobyalla Plains, tin-bearing estuarine deposits were recognised by King (1963). However, the identification of an estuarine origin based on shingle is not conclusive. Even when sponge spicules are present (Bowden 1981), other explanations are possible (see Section 2.5.2).

2.7 Mining and contamination

Because of the large scale mining disturbance in northeastern Tasmania, it is necessary to consider past and present mining activity and contamination. A location map of placer tin mines including mines in operation during 1978 to 1980 and disused mines is shown in Fig. 2.10. This map is compiled from publications by the Tasmania Department of Mines and includes mines shown on the 1 : 50 000 Boobyalla and Ringarooma geological map sheets.

2.7.1 Past

According to Reid & Henderson (1928), the development of the Blue Tier tin field was in two stages; there was an early stage of placer mining followed by vein mining and rock excavation. For the latter

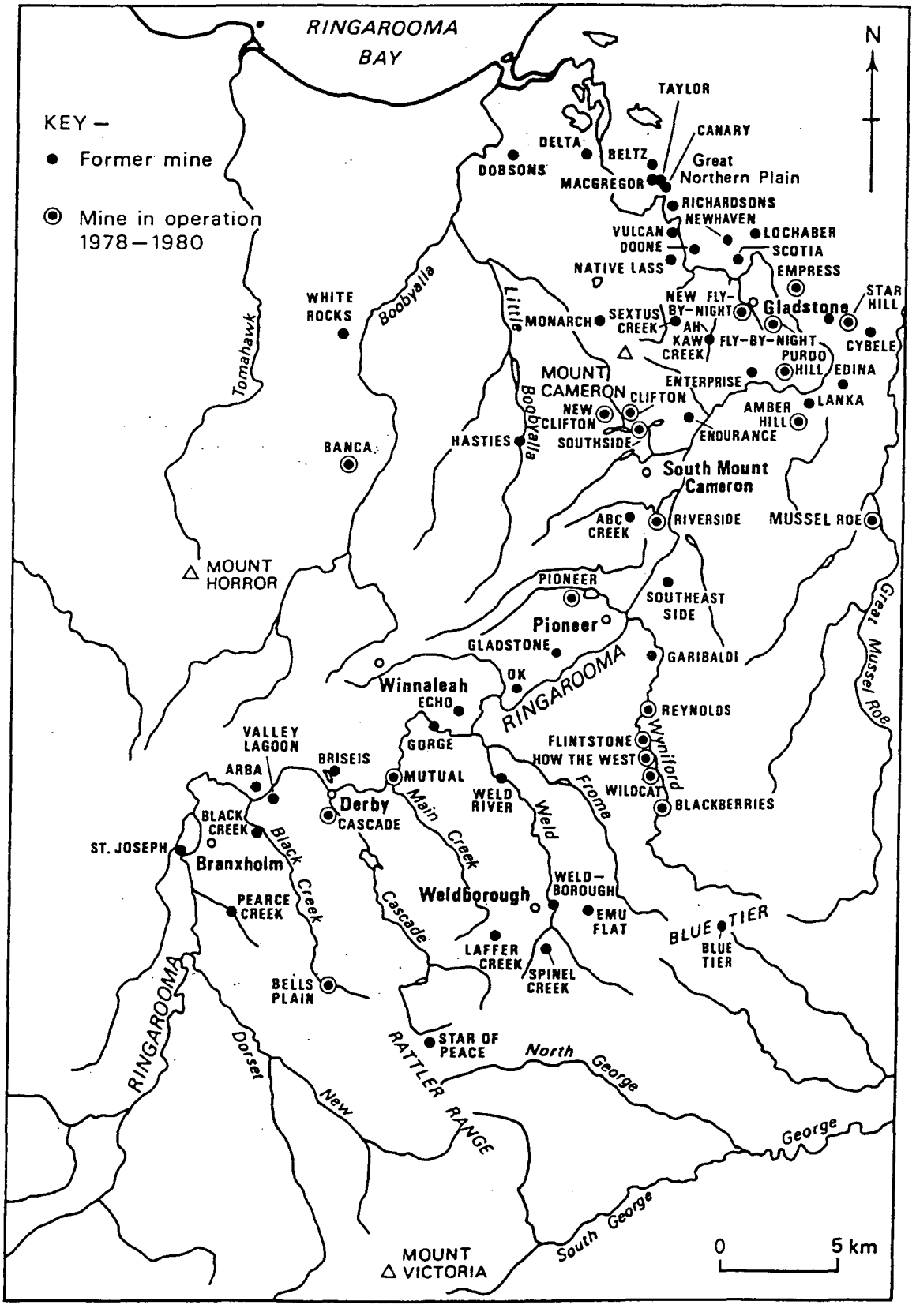

Fig. 2.10 Location map of disused and operating placer tin mines in the study area during 1978-1980.

stage, an estimated 2 000 000 tonnes of rock ore giving an average yield of 0.16 % metallic tin was mined, of which the output of the Anchor Mine amounted to 1 778 000 tonnes. Both forms of mining led to the release of considerable volumes of mining tailings, which travelled long distances downstream through the rivers and streams. Steane (1972) pointed out that the impact of mining was increasingly obvious below Branxholm and that the silt load of the river changed continuously with changes in mining activity. Both were confirmed by surveys of the river bed level along the Ringarooma River by Steane (1983). An estimate of the volume of silt discharged into the river by the Briseis Mine alone between 1876 and 1949 when the mine closed was about 13 400 000 cu. m as tailings. The probable annual maximum of 240 000 cu. m was reached in 1945. It is therefore important in the present study to avoid sampling contaminated sites.

Table 2.5 provides placer tin production figures for some of the tin mines in the study area. In order to facilitate comparison, the total production is given in tonnes of metallic tin. For the conversion of long tons to tonnes, a factor of 1.016 was used while cassiterite ore concentrate was taken as 70 % cassiterite. Although the tonnages shown are not up to date and only limited number of mines have been included, the large contribution to production by deep lead mines is evident.

2.7.2 Present

The introduction of a tin production quota in Australia and the collapse of international tin metal prices in 1984 led to the closure of all placer mines in northeastern Tasmania by 1985. However, during the period when fieldwork was carried out for the present study in 1978 to 1980, tin metal prices were high and many mines were operating (see Fig. 2.10). The largest producing mines at this time were Pioneer and Endurance, both owned by Amdex Mining Limited. Production reported for the year ended December 1978 for the two mines were 35 and 38 tonnes

Mine	Source	Period	Metallic tin production tonnes[1]
Briseis	Ingram (1977)	1876 - 1960	21 120
Pioneer	King (1963)	To 1963	9 327
Endurance	King (1963)	To 1963	2 672
Arba	King (1963)	To 1963	2 215
Clifton	Ingram (1977)	To 1970	2 135
Dorset Flat[2]	King (1963)	1906-1962	1 827
Valley Lagoon	King (1963)	To 1962	369
Echo & Weld	Nye (1925)	1902 - 1922	206
Mussel Roe	King (1963)	1960 - 1963	55
Monarch	Ingram (1977)	1970 - 1972	52
Mutual	Nye (1925)	1912 - 1918	45

1 - see text; 2 - including the Dorset Dredge.

Table 2.5 Record of tin production in selected placer tin mines of the study area.

cassiterite (27.5 and 30 tonnes metallic tin) respectively (Anon. 1979). The figures given for the Endurance Mine was a combined total for the Clifton, Southside and Riverside workings (see Fig. 2.10).

PART 2 HEAVY MINERAL PROVENANCE AND DISTRIBUTION

CHAPTER 3 FIELD AND LABORATORY PROCEDURES

3.1 Introduction

Because heavy minerals may be of economic value and are sensitive indicators of provenance (Morton 1985), it is important to obtain understanding of their distribution in placer deposits. Since very little information is available on the distribution of heavy minerals in northeastern Tasmania, studies were carried out to identify the mineral species present and their provenance. This chapter presents the methods used in the field and the laboratory.

3.2 Field procedure

All field samples were collected in 1978 and 1980 during a tin mining boom period when many mines in northeastern Tasmania were in operation. Fig. 3.1 shows a location map of the sampling sites excluding sediments in active streams.

A variety of sample types were collected in the field including in situ samples from natural and mine exposures, sluiced heavy mineral concentrates and tailings from tin mines, sediment in active streams and borehole samples. Because it is important to identify the main heavy mineral species occurring at each locality, where possible more than one sample type was obtained from most localities in order to reduce sampling errors. At localities where only one sample type was collected, heavy mineral concentrates from sluicing were preferred because they represent the range better. In a few selected localities, large volume bulk samples were also collected to check sampling accuracy.

Heavy mineral concentrates preconcentrated by panning using a 5.5 litre gold pan were collected. For each sample, the gold pan was filled with dirt to the level of the rim to provide a rough estimation of the volume of material panned. In the case of samples low in heavy mineral content, up to three pans of material were used to minimise sampling errors. Panning was carried out carefully to avoid the loss of heavy

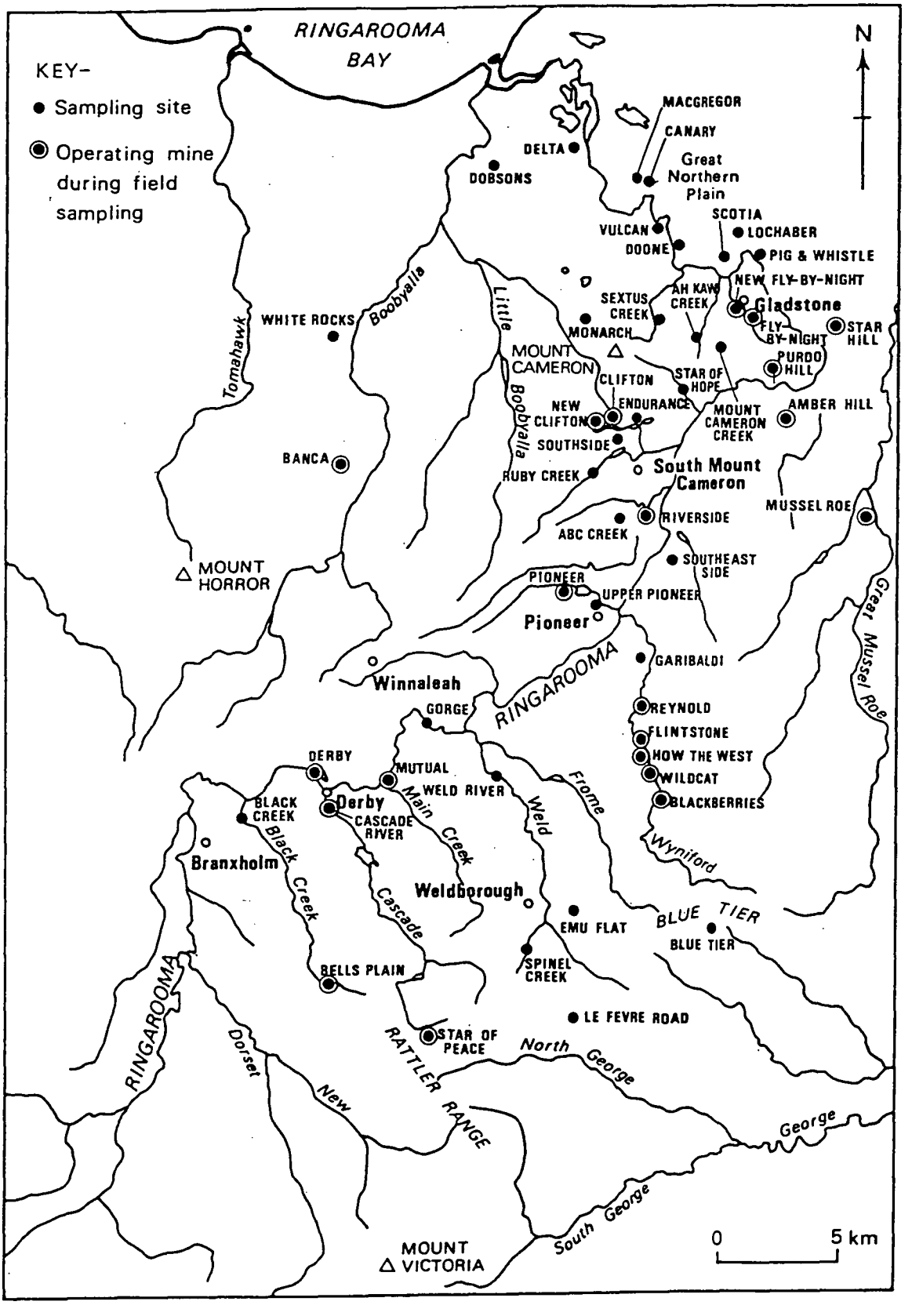

Fig. 3.1 Location map of sampling sites excluding sediments in active streams.

minerals exceeding the specific gravity of tourmaline (SG 3.1-3.3).Because tourmaline is a common light heavy mineral recognisable by its distinctive colour and shape, it was used as an indicator during panning. As soon as loss of the mineral was detected visually, panning was terminated.

Borehole and bulk samples were pre-concentrated using a short sluice box (Plate 3.1) prior to panning. Tailings passing through the cradle were collected and passed through the cradle again three times to minimise the loss of heavy minerals.

3.2.1 In situ samples from natural and mine exposures

In situ samples were collected from natural exposures and excavations in both operating and disused tin mines. In selected mine workings where the interface between bedrock and sediment was well exposed, basement sampling traverses were carried out in order to determine the control of bedrock topography on heavy mineral distribution. Where possible, the palaeocurrent direction was determined from cross-bedding using a dip direction indicator (Pryor 1958). Such basement traverses were carried out at the Pioneer, New Clifton and Sextus Creek Tin Mines (Fig. 3.1).

3.2.2 Heavy mineral concentrates from sluicing

Heavy mineral concentrates produced by sluicing were collected from most of the operating tin mines. Since these concentrates were derived from large volumes of in situ material, they are likely to be more representative of the heavy minerals present than the small in situ samples. In some of the abandoned tin mines, heavy mineral concentrates left behind in sluice boxes were also collected.

Mine tailings discarded during tin ore dressing through sluicing also contain important information on the distribution of heavy minerals. Such mine tailings may, for example, include monomineralic and composite cassiterite grains exceeding 2 mm in diameter which are lost

Plate 3.1 A short sluice box used for the concentration of heavy minerals.

during sluicing but are important in providing information on the maximum size availablility and liberation characteristics of mineral grains. They were collected in some tin mines in the vicinity of sluice boxes because they could not be washed away easily.

3.2.3 Sediments in active streams

Present day stream sediments were collected to assist the identification of heavy mineral provenance. Because past and present mine tailings discharged into streams are a major source of contamination downstream, the sampling of sediments in active streams was carried out mainly in the upper course of the Ringarooma River where mining activity is absent. In other areas, this type of sampling was used when other sample types cannot be collected. Fig. 3.2 shows a location map of stream sediment sampling sites.

3.2.4 Borings

A number of onshore and offshore borehole samples were supplied by Amdex Mining Limited and the Tasmania Department of Mines for this study. The onshore borings were obtained using either a percussion drill which is a mechanical adaptation of the Banka type hand drill or a Wallis reverse circulation drill. The offshore borings from Ringarooma Bay were collected using a Horton sampler (see Lampietti et al. 1968).

3.3 Laboratory procedure

In the laboratory, the heavy mineral concentrates were separated using physical techniques to assist mineral identification. The scheme adopted is based on heavy liquid and magnetic separations (Fig. 3.3) and the follow up methods used in mineral identification are summarised in Fig. 3.4. Particle size measurements were also made to determine the size availability of selected heavy mineral species to facilitate provenance identification. For all sample splitting steps, a Jones riffle was used to minimise sampling error caused by heavy mineral segregation.

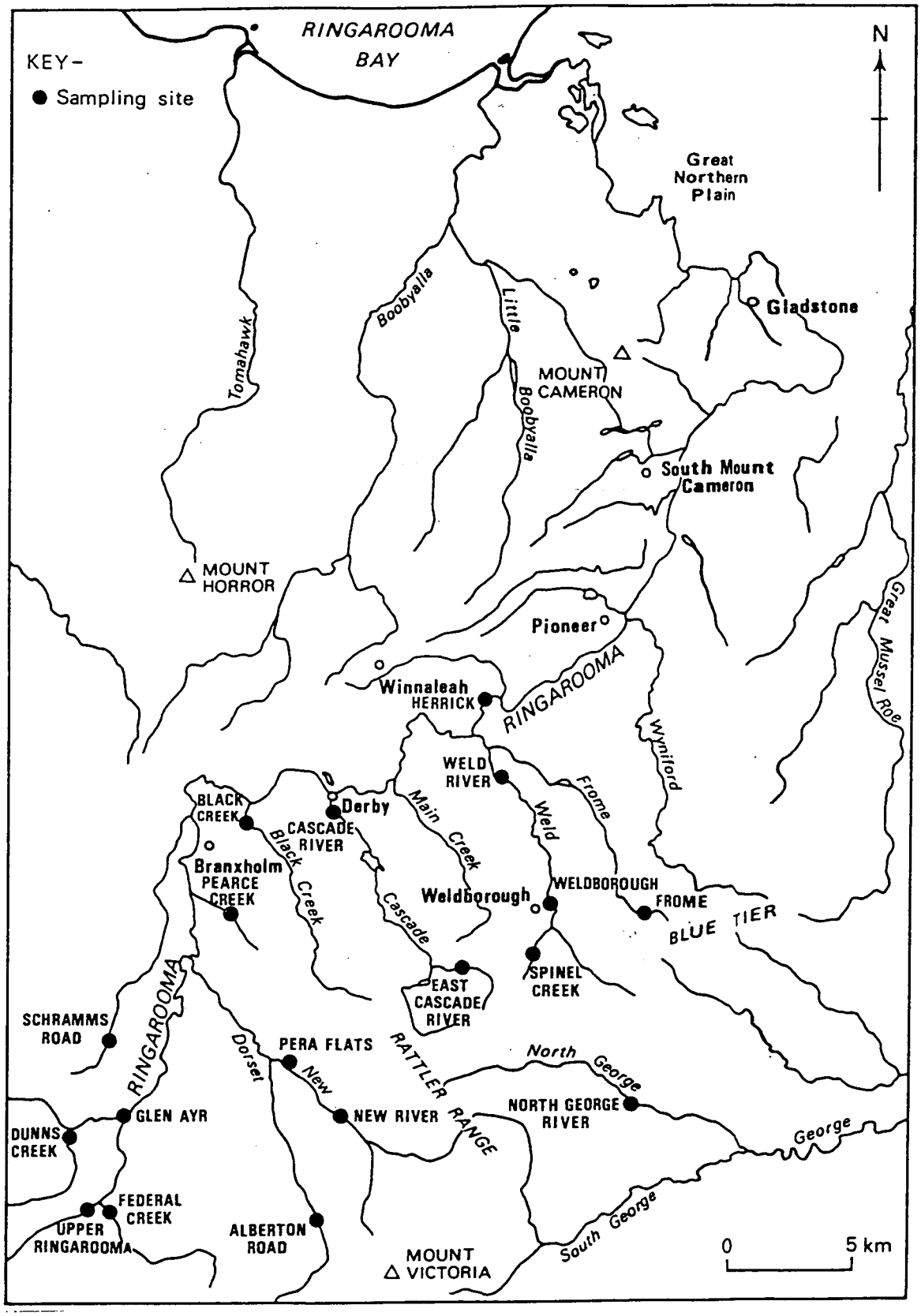

Fig. 3.2 Location map of sampling sites of sediments in active streams.

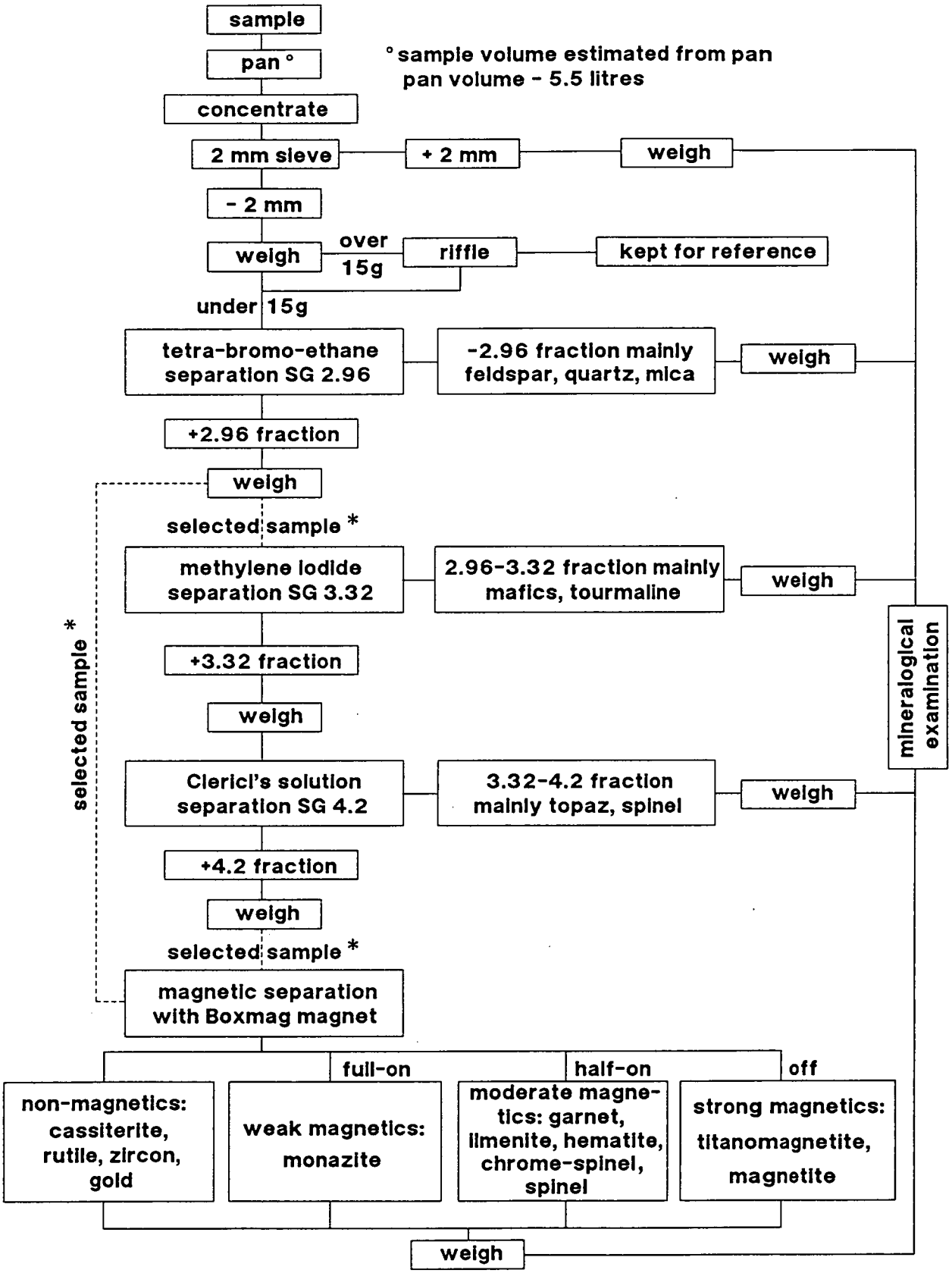

Fig. 3.3 Flow chart of sample treatment procedures involving heavy liquid and magnetic separations. * - Only a limited number of samples was processed because of the time-consuming nature of the work.

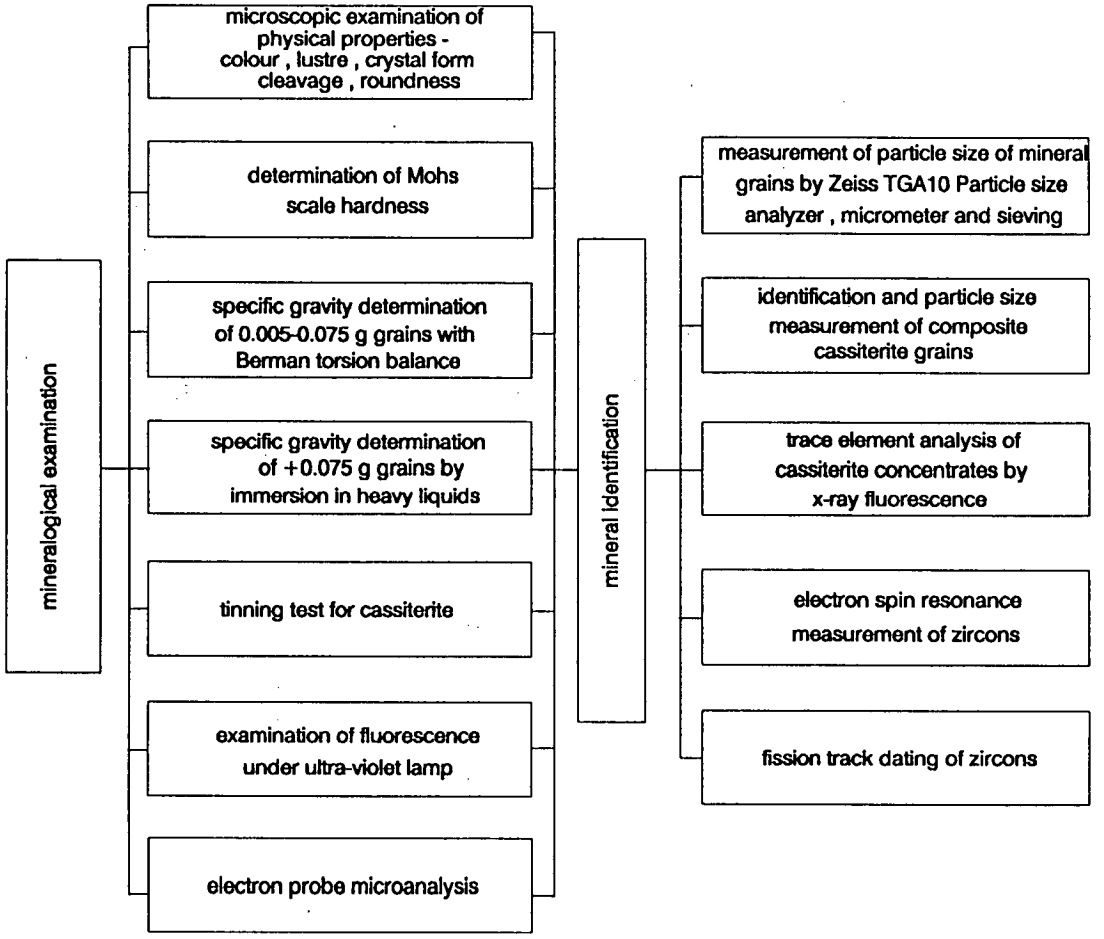

Fig. 3.4 Flow chart of follow-up mineralogical examination procedures.

3.3.1 Heavy liquid separations

Heavy liquids are widely used as a rapid means of separating heavy minerals. For example, Yim (1984) used tetra-bromo-ethane (SG 2.96), methylene iodide (SG 3.32) and Clerici's solution (SG 4.2 at room temperature) for the separation of tin-bearing sands from Cornwall for the estimation of tin liberation characteristics. In the present study, the same heavy liquids were used.

Tetra-bromo-ethane was preferred to bromoform (SG 2.89) for the following reasons:

(1) The higher specific gravity of the former. Light heavy minerals such as micas which are of little interest in the present study are more likely to be removed.

(2) The better wetting qualities of the former (M. P. Jones, pers. comm.).

(3) The lower cost of the former.

(4) The paler colour of the former. Bromoform often turns deep red on exposure to light making it difficult to recognise immersed minerals during the separation.

(5) The higher vapour density of the former makes it less volatile and dangerous, especially when a downward suction fume cupboard is used. Both tetra-bromo-ethane and bromoform emit carcinogenic fumes which are known to cause liver damage on inhalation.

A flow chart of the sample treatment procedure is shown in Fig. 3.3. Methylene iodide and Clerici's solution were used for the separation of some samples to obtain three heavy mineral fractions. These include the light heavy minerals (SG 2.96-3.32), the medium heavy minerals (SG 3.32-4.2) and the heavy heavy minerals (SG >4.2) (Fig. 3.3). The apparatus used in all three types of heavy liquid separation is shown in Plate 3.2. A sample weight not exceeding 15 g was separated in open conical filter funnels fitted with silicone rubber tubing and

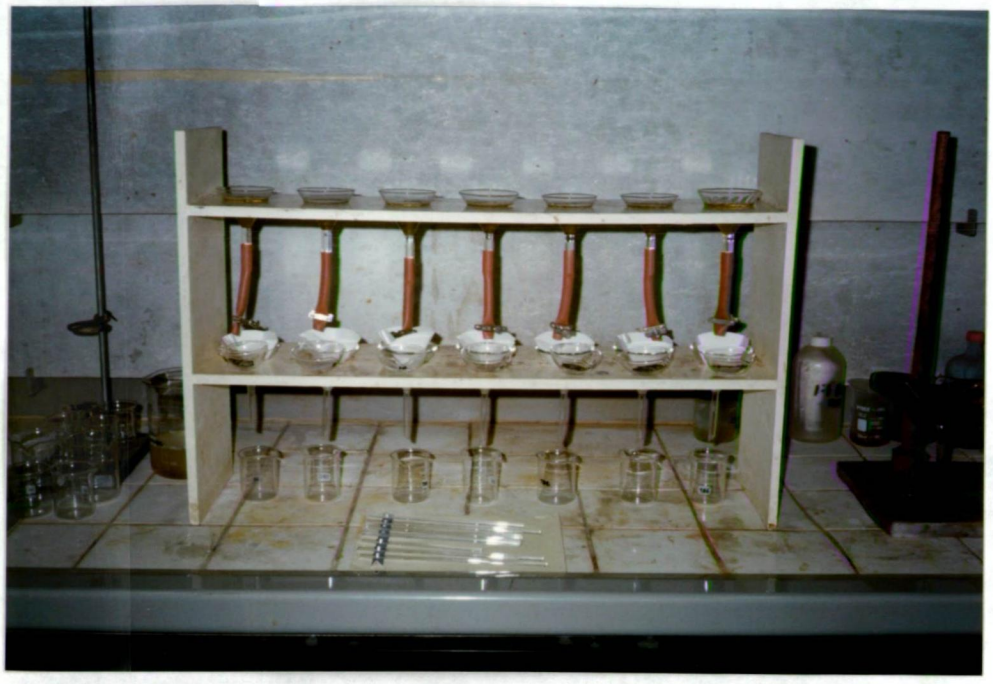

Plate 3.2 Apparatus used in the heavy liquid separations. Note that it is essential to carry out the separations in a well-ventilated fume cupboard to minimise the inhalation of toxic fumes.

Plate 3.3 Berman torsion balance used for specific gravity determination of heavy mineral grains.

screw clips. Glass rods were used for stirring to improve the efficiency of the separation. As a precaution against toxic fumes during the tetra-bromo-ethane separation, the apparatus was placed inside a fume cupboard. Gloves were worn when handling Clerici's solution and extra care was taken to avoid spillage. Further information on the handling of the heavy liquids may be found in Hauff & Airey (1980).

3.3.2 Magnetic separations

Magnetic separations were carried out to facilitate the identification of opaque heavy minerals. Although the Frantz electromagnetic separator may be used for separating minerals, it is slow and necessitates preliminary sizing to produce good results. In the present study, a Boxmag adjustable polepiece hand magnet was used to achieve rapid separation without sizing. When this magnet is switched to a full on, half on and off positions, weakly magnetic, moderately magnetic and strongly magnetic mineral fractions respectively may be separated from the non-magnetic fraction (Jones 1987).

3.3.3 Hand sorting and microscopic examination

Heavy mineral particles exceeding 2 mm (British Standard Sieve 8-mesh) in diameter were identified and hand sorted using a pair of forceps. Physical properties including colour, lustre, transparency, hardness, crystal form and cleavage were used in their identification. Because of the large grain size of some mineral particles, hardness points were used to determine the Mohs' scale of hardness. A summary of the relative hardness of heavy minerals found in the present study is shown in Fig. 3.5. For cassiterite, visual description of roundness and occurrence of composite grains were recorded to provide clues on the distance of transport.

A stereomicroscope was used to assist the identification of mineral particles passing a 2 mm diameter sieve. Semi-permanent mounting of

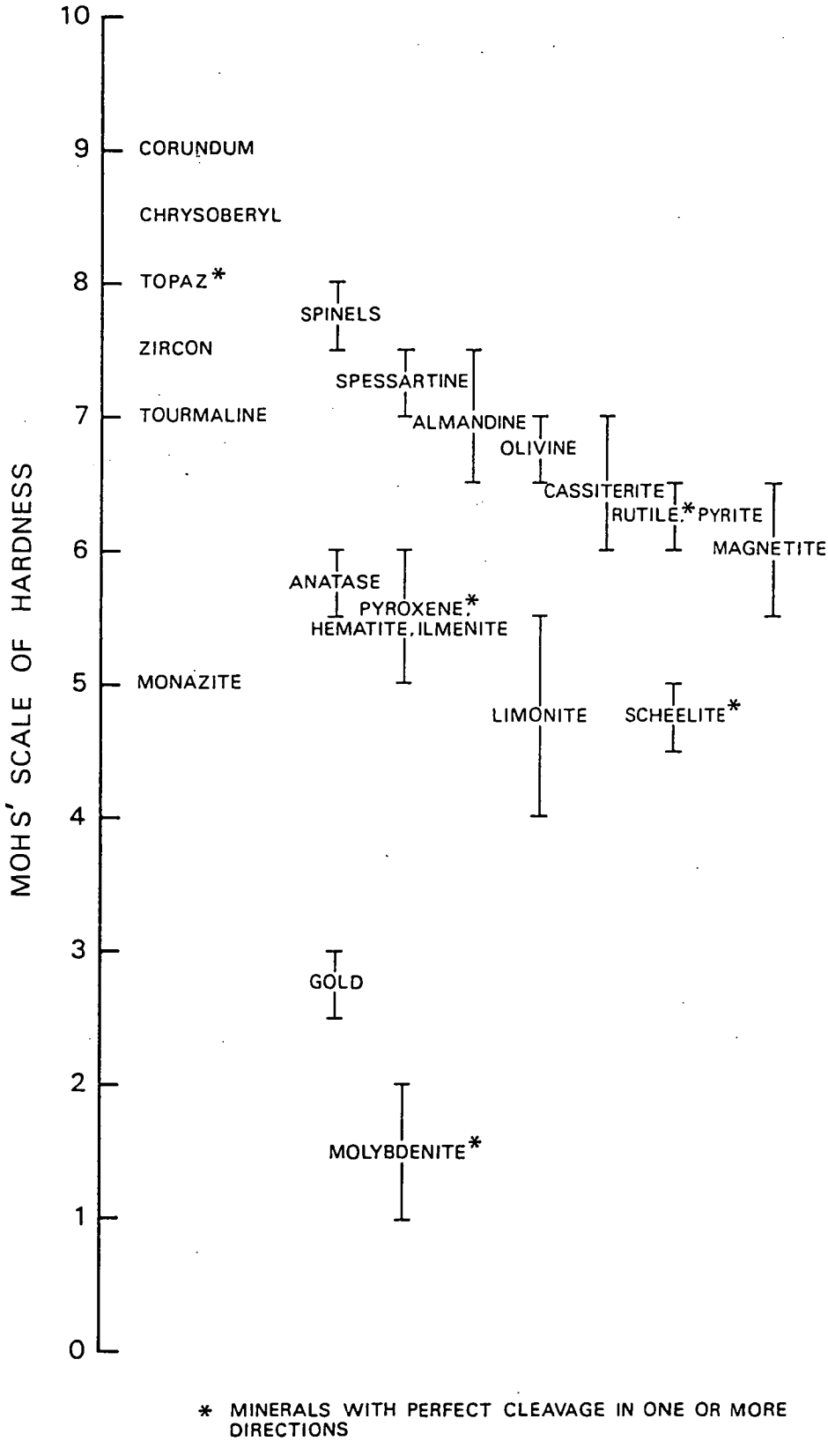

Fig. 3.5 Diagram showing the Mohs' scale of hardness of selected heavy minerals present in northeastern Tasmania.

mineral grains were made on glass slides by means of double-sided cellotape.

3.3.4 Specific gravity determination

A torsion type microbalance (Berman 1953) shown in Plate 3.3 was used for the specific gravity determination of heavy mineral grains. Because of the high sensitivity of this method, specific gravity values to three decimal places may be obtained. For heavy minerals with a narrow range of specific gravity, this is a particularly reliable confirmatory test for mineral identification by reference to Mursky & Thompson (1958) and Deer et al. (1966). However, the weight of the mineral grain required should be within the range of 5 to 75 mg but mineral particles exceeding 75 mg in weight may be broken down to size before measurement.

The specific gravity of valuable heavy mineral specimens with specific gravity <4.2 and exceeding 75 mg in weight which cannot be broken down were determined by the immersion method. The specimen was immersed in Clerici's solution at room temperature (SG 4.2) before drop by drop dilution with distilled water until the mineral began to float. The specific gravity of the diluted Clerici's solution being the same as that of the mineral was obtained by indexes.

3.3.5 Tinning test for cassiterite

Monomineralic and composite cassiterite grains were both confirmed by the 'tinning' test (Jones & Fleming 1965; Hosking 1974). The sample to be tested was placed on a zinc tray and then covered with 5 N hydrochloric acid. Any 'clean' cassiterite present is covered with a grey matt coating after a few minutes. If coatings of iron oxides and/or iron sulphides are present on cassiterite grains, they must be cleaned by boiling in concentrated nitric acid before carrying out this test.

3.3.6 Fluorescence

A Mineralight ultraviolet lamp model UVGL-25 was used to identify the strongly fluorescent minerals zircon and scheelite. This lamp has multibands and is switchable from short to long wave.

3.3.7 Electron microprobe analysis

The chemical composition of selected heavy minerals and their varietal types were determined by electron microprobe analysis to assist the interpretation of provenance. A Jeol model 50A electron microprobe equipped with an EDAX energy dispersive x-ray analysis system was used. The latter is computerised to carry out structural formula determination using oxygen number input (Griffin 1979).

Electron microprobe analysis is particularly valuable as a confirmatory test for opaque minerals of specific gravity >4.2. Without such chemical analysis it is for example extremely difficult to distinquish between chrome-spinel and ilmenite. Another important application in the present study is the identification of mineral varieties showing isomorphous substitution. This provided additional information on heavy minerals with multiple sources such as spinel, garnet and ilmenite.

3.3.8 Particle size measurements

Particle size measurements of selected heavy minerals was carried out mainly for two purposes - firstly, to determine their size of availability including the maximum length in millimetres, and secondly, to permit the determination of hydraulic equivalence (Rittenhouse 1943) between heavy minerals for the estimation of distance of transport from source rock. Note that the size of availability is used to refer to the grain size distribution of a mineral in a source rock.

The British Standard Code of Practice was used for all particle descriptions unless otherwise specified. Heavy mineral particles in excess of 1 mm in length were measured using a scale while smaller

grains were measured using a micrometer under a stereomicroscope. In order to speed up measurements, a Zeiss TGA10 semi-automatic particle size analyzer connected to a stereomicroscope via a drawing tube was set up. Details on this method is given in Yim (1986).

Twelve tin ore concentrates including two from the Pioneer Tin Mine (see Fig. 3.6) were dry sieved using Wentworth sediment scale sieves to provide information on the size of availability of cassiterite grains. Prior to this, mineral impurities were removed by magnetic separations, and, hand sorting under a stereomicroscope and an ultraviolet lamp. The sieves used were:

B.S.S. no.	Micrometer	Phi value	Sediment type (Wentworth scale)
8	2057	-1.041	Very coarse & coarse sand
30	500	1.000	
60	250	2.000	Medium sand
120	124	3.011	Fine sand
Pan	<124	<3.011	Very fine sand & silt

Graphic mean size and graphic sorting coefficent were determined from the particle size distribution curves obtained using the formulae of Folk (1968):

$$\text{Mean size} = \frac{\text{phi } 16 + \text{phi } 50 + \text{phi } 84}{3}$$

$$\text{Sorting coefficient} = \frac{\text{phi } 84 - \text{phi } 16}{4} + \frac{\text{phi } 95 - \text{phi } 5}{6.6}$$

The verbal scale of Folk & Ward (1957) used for describing sorting was:

Terminology	Sorting coefficient
Very well sorted	<0.35
Well sorted	0.35 - 0.5
Moderately sorted	0.5 - 1.0
Poorly sorted	1.0 - 2.0
Very poorly sorted	2.0 - 4.0

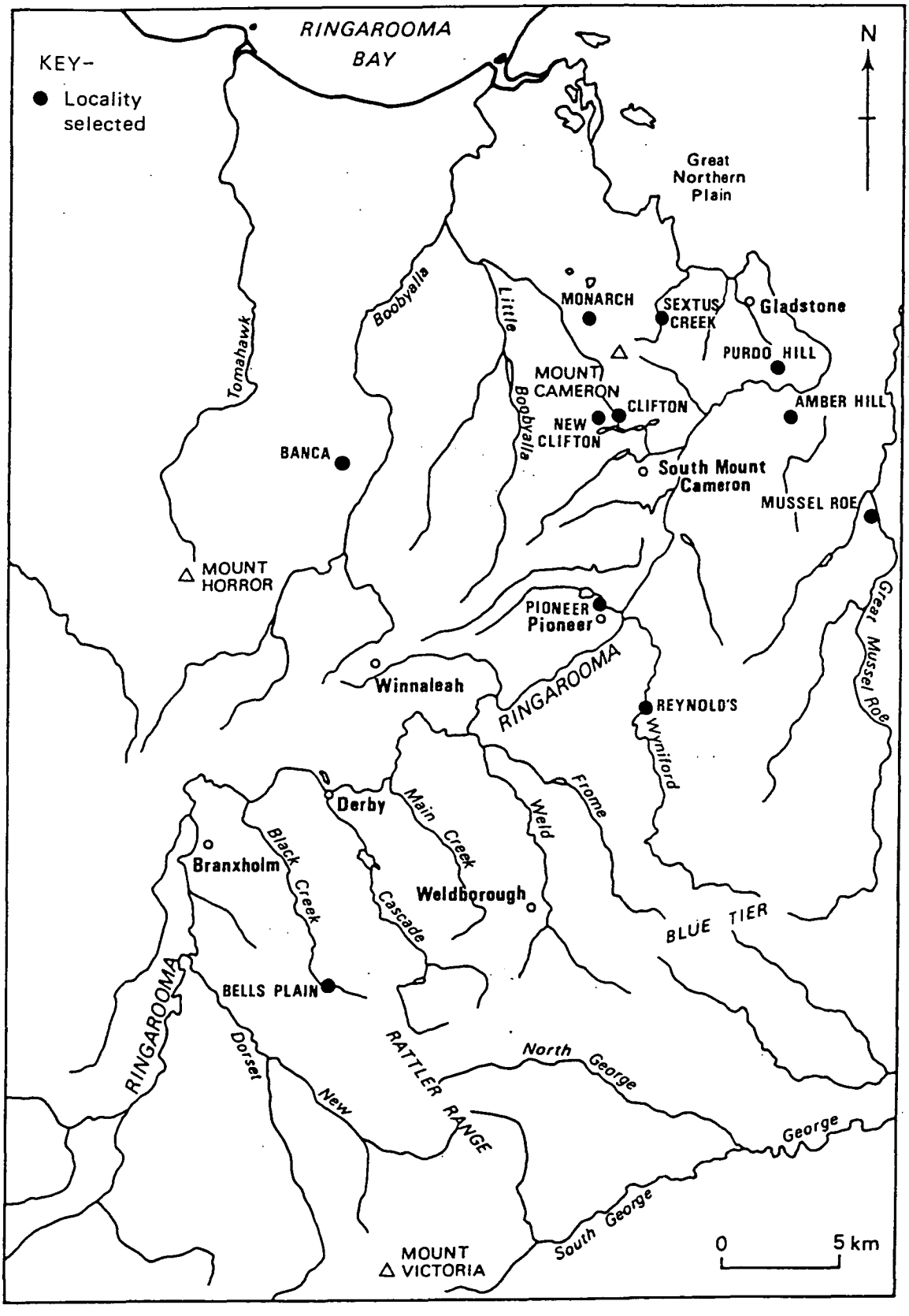

Fig. 3.6 Location map of tin mines where cassiterite concentrates were collected for particle size measurements and trace element analysis by x-ray fluorescence.

Extremely poorly sorted	>4.0

3.3.9 Trace element analysis of cassiterite

In order to identify whether multiple sources of cassiterite exist in northeastern Tasmania, x-ray fluorescence analysis of cassiterite concentrates from eleven localities shown in Fig. 3.6 was carried out. The content of four trace elements, niobium (Nb), tantalum (Ta), tungsten (W) and zirconium (Zr), which are known to be present in variable amounts in cassiterites derived from greisens and pegmatites (Taylor 1979) were determined. The twelve cassiterite concentrates subjected to particle size analysis in Section 3.3.8 were ground in a tungsten carbide Tema mill before preparation for x-ray fluorescence analysis using a method similar to that described by Hutchinson (1974). Table 3.1 provides a summary of the conditions used for each of the four trace elements. The precision obtained from replicate determinations for all elements is better than $\pm$ 5 % at the 95 % confidence level.

The relationship between pleochroism and Nb content in cassiterite from selected localities was investigated for fingerprinting pegmatitic sources of cassiterite in the follow-up studies. Polished cassiterite grains mounted on glass slides without a cover slip were examined under the petrological microscope using transmitted light to determine the degree of pleochroism. This was divided visually into three categories, strong, moderate and weak. The Nb content was estimated by wavelength x-ray analysis with a Jeol model 50A electron microscope using a natural columbite standard containing 36.07 % Nb.

3.3.10 Fission track dating of zircons

Fission tracks in zircons are extremely resistant to the effects of weathering so that results on alluvial zircons should represent the source rock ages (Gleadow & Lovering 1974). The provenance of two distinctive types of zircons found in the present study was subjected to fission track dating. Three zircon samples were submitted to Professor

Element	Tube	Line	Energy	Crystal	Background
Nb	Rhodium	L_1	60 KV 40 mA	LiF 220	$\pm$ 0.65°
Ta	Gold	L_1	60 KV 40 mA	LiF 200	-0.61°, +1.21°
W	Rhodium	L_1	50 KV 50 mA	LiF 200	$\pm$ 0.6°
Zr	Rhodium	K_{B1}*	60 KV 50 mA	LiF 200	+ 0.5° only

* - K_{B1} has strontium interference.

Table 3.1 Summary of conditions used for x-ray fluorescence analysis of cassiterite concentrates.

A. W. Gleadow formerly of the Department of Geology, University of Melbourne, who carried out the work. The laboratory details of this work was reported by Yim et al. (1985) (Appendix II). Further information on the principles and techniques of fission track dating may be found in Gleadow (1984).

3.3.11 ESR studies on zircon

Previous investigations by Zeller et al. (1967) and Zeller (1968) concluded that zircon was of little use for age determination by ESR. However, Taguchi et al. (1985) suggested that the age of pre-Pleistocene zircons may be determined.

In the present study, there are two important objectives in carrying out ESR measurements on zircon. Firstly, to obtain information on the provenance of zircons, and secondly, to use it as a semi-quantitative method of dating. The ESR signal measured from zircon is caused by the presence of unpaired electrons in the mineral, either related to trace elements in the lattice or through spin unpairing through radiation such as due to uranium and thorium. The amount of damage is roughly proportional to the age of the zircon in that older zircons show a stronger signal response than younger zircons. Therefore, electron spin resonance is a possible method for dating zircons as well as a method for assisting their provenance determination.

Pure zircon concentrates were used for this work. Zircon grains exceeding medium sand size were hand sorted under an ultraviolet lamp. Finer zircons below 1 mm were concentrated using a micropanner before magnetic separation and hand sorting under a stereomicroscope with the aid of a fine brush. About 0.3 g weight of each type of zircon determined on the basis of physical characteristics namely colour, crystal shape, particle size and degree of fluorescence, were ground into a powder using a percussion steel pestle and mortar (Hutton 1950) and an agate pestle and mortar. 0.09 g of the ground sample was placed

in an annealed silica tube for measurement using a Jeol model JES-FE3X ESR spectrometer in the 'x' band modulation. Geological ages are determined by using the absorption spectra of previously fission track dated zircons for calibration.

Several types of heavy minerals including cassiterite, corundum, topaz and spinel were also tested for ESR response. However, of these only topaz was found to show a weak response.

CHAPTER 4 PROVENANCE OF HEAVY MINERALS

4.1 Introduction

In a detrital heavy mineral provenance study of Dartmoor, southwestern England, Brammall (1928) stated that the varietal features of a mineral species in a heavy mineral assemblage may be of greater significance than the presence of that species. In the present study, both the heavy mineral assemblage and the varieties of each heavy mineral species are considered to be valuable as a source of information to assist provenance identification. Because of difficulties in identifying opaque heavy minerals and their varieties, electron microprobe analysis is used extensively as an aid to mineral identification and the determination of mineral composition. This chapter presents results on the provenance of heavy minerals in the study area including the main types of heavy mineral assemblage found, and, a comparison of the distribution pattern of the heavy minerals with the experimentally obtained transportation resistance of Freise (1931).

4.2 Provenance of heavy minerals

A summary of the specific gravity, frequency and probable provenance of the heavy minerals found in northeastern Tasmania is presented in Table 4.1. In this table, the stability and frequency of heavy mineral occurrence according to Milner (1962) is shown for comparison. Although four categories of heavy mineral frequencies were used by Milner (1962) and in the present study, a 'very common' category is preferred over the 'local' category because it is considered to be more appropriate in a regional study.

The heavy minerals present are attributed to four main types of source rocks including:

(1) Granite

(2) Mathinna Beds

(3) Older Tertiary basalts (Blue Tier)

		After Milner (1962)		Present study	
Mineral name	SG	Stability	Frequency	Frequency	Probable provenance
Gold	19.3	S	R	R	quartz veins in Mathinna Beds
Cassiterite	6.9-7.1	S	L	VC	greisens, pegmatites & veins
Scheelite	5.9-6.1	U	L	VR	pneumatolytic veins near granite/country rock contact
Magnetite	5.2	S	R	R	Tertiary basalts
Hematite	5.1	M	C	C	ferricretes
Monazite	5.0-5.3	S	R	C	accessory mineral in granites
Pyrite	5.0	M	C	VC	authigenic mineral; accessory mineral in granites
Marcasite	4.9	M	L	C	authigenic mineral
Ilmenite	4.7-4.8	M	C	VC	Mg-rich - megacrysts & accessory mineral in Tertiary basalts; Mg-poor - accessory mineral in granites
Molybdenite	4.7-4.8	M	L	VR	pegmatites
Ulvospinel/ Titanomagnetite	4.6-4.8	-	-	R	Tertiary basalts
Zircon	4.6-4.7	S	C	VC	fine euhedral - accessory mineral in granites; coarse anhedral - megacrysts in older Tertiary basalts
Xenotime	4.4-4.6	S	VR	R	accessory mineral in granites
Chromite	4.3-4.6	S	VR	VR	Juarassic dolerites
Rutile	4.2	S	C	R	Mathinna Beds; rutilated quartz in pegmatites
Garnet- Almandine	4.1-4.3	S	C	R	quartz-feldspar-porphyries; granites; aureoles of thermal metamorphism
Spessartine	4.1-4.3	S	VR	R	pegmatites
Goethite	4.0-4.4	M	L	VC	weathering product of iron-bearing minerals
Corundum	4.0	S	R	C	megacrysts & xenoliths in older Tertiary basalts
Cr-spinel	3.8-4.2	-	-	R	megacrysts & xenoliths in older Tertiary basalts
Anatase	3.8-4.0	S	C	VR	alteration product of sphene & ilmenite
Pleonaste/ Hercynite	3.7-3.9	M	R	C	megacrysts & xenoliths in older Tertiary basalts
Limonite	3.6-4.0	S	C	VC	ferricretes
Topaz	3.6	S	C	VC	greisens, pegmatites & aplites
Chrysoberyl	3.5-3.8	S	R	VR	pegmatites
Pyroxene	3.4-3.5	M	R	R	Tertiary basalts; Jurassic dolerites
Olivine	3.3-3.4	U	R	VR	Tertiary basalts
Tourmaline	3.1-3.3	S	C	VC	pneumatolytic veins & pegmatites

S - stable; M - moderately stable; U - unstable; VC - very common; C - common; L - local; R - rare; VR - very rare.

Table 4.1 Summary of specific gravity, stability, frequency and probable provenance of selected heavy minerals in northeastern Tasmania. Specific gravities are based on Mursky & Thompson (1958) and Deer et al. (1966).

(4) Younger Tertiary basalts (Winnaleah-Ringarooma).

The main attention of this work is on the stable heavy minerals with different provenance. Description of the occurrence and characteristics of heavy minerals in the probable source rock types is presented in Sections 4.2.1 to 4.2.5. A tabulation of electron microprobe results for various heavy minerals is presented in Appendix I.

4.2.1 Granite

In addition to cassiterite, very common and common heavy minerals found in granitic source rocks in northeastern Tasmania include monazite, ilmenite, fine euhedral zircons usually below 2 mm in length, topaz and tourmaline (Table 4.1). Very rare and rare heavy minerals include scheelite, molybdenite, xenotime, rutile, spessartine and chrysoberyl, most of which are usually found associated with pegmatites.

Cassiterite is present both in the form of monomineralic and composite grains with the latter occurring commonly in association with quartz. Because of the high specific gravity of cassiterite (6.9 - 7.1), it has low mobility; coarse particles exceeding about 40 mesh B.S.S. (ca. 380 μm) resist fluvial transport (Taylor 1986) and are always found within short distances of the source rock. In a comprehensive review on tin distribution patterns by Hosking (1979), both the grain size and shape of cassiterite were found to vary greatly with the type of mineralized bedrock. Pegmatites contain coarse, equant crystals whereas endogranitic stockworks, greisen bordered veins and vein deposits close to granite contacts contain both fine and coarse prismatic crystals. Exogranitic deposits on the other hand, contain fine granular to needle-like crystals. The distribution characteristics of cassiterite in an alluvial field would be expected to reflect the types of primary tin deposits present.

In the present study, unliberated cassiterite within the mineralized rock basement of alluvial tin mines have been observed only in a few localities during field sampling. They include Fly-by-night, Blackberries, Blue Tier, Star of Peace and Pearce Creek (Fig. 2.10). The local granitic provenance of cassiterite is therefore confirmed even though the representivity of these localities may be questioned.

The distribution of maximum diameter of monomineralic and composite cassiterite grains found in the present study is shown in Figs. 4.1 and 4.2 respectively. It can be seen that the biggest grains occur around both Mount Cameron and Blue Tier. A summary of the characteristics including colour, maximum grain size of monomineralic and composite cassiterite grains, visually estimated dominant grain size and grain shape is shown in Table 4.2. The maximum dimensions of both monomineralic and composite cassiterite grains are found to be mostly in excess of 2 mm. Since a decrease in particle size of cassiterite downstream of leads is not discernible in Figs. 4.1 and 4.2, local sources of input from an extensive area of bedrock tin mineralization in northeastern Tasmania is the most plausible explanation.

Of the heavy minerals found in association with cassiterite in granitic rocks, topaz is by far the coarsest. Because of the difficulty in sampling large topaz, a distribution map of the maximum diameter of topaz is likely to be misleading and has not been shown. A large crystal from Mount Cameron exceeding 0.2 m in length was reported in Twelvetrees (1916). However, while large crystals of such dimensions must have been derived from pegmatites, smaller crystals may have originated from aplites and greisens. In spite of a Mohs' scale hardness of 8, the naturally perfect basal cleavage of topaz causes it to break into small fragments relatively easily. Therefore, it is probable that the grain size of the mineral downstream of the source rock would decrease rapidly.

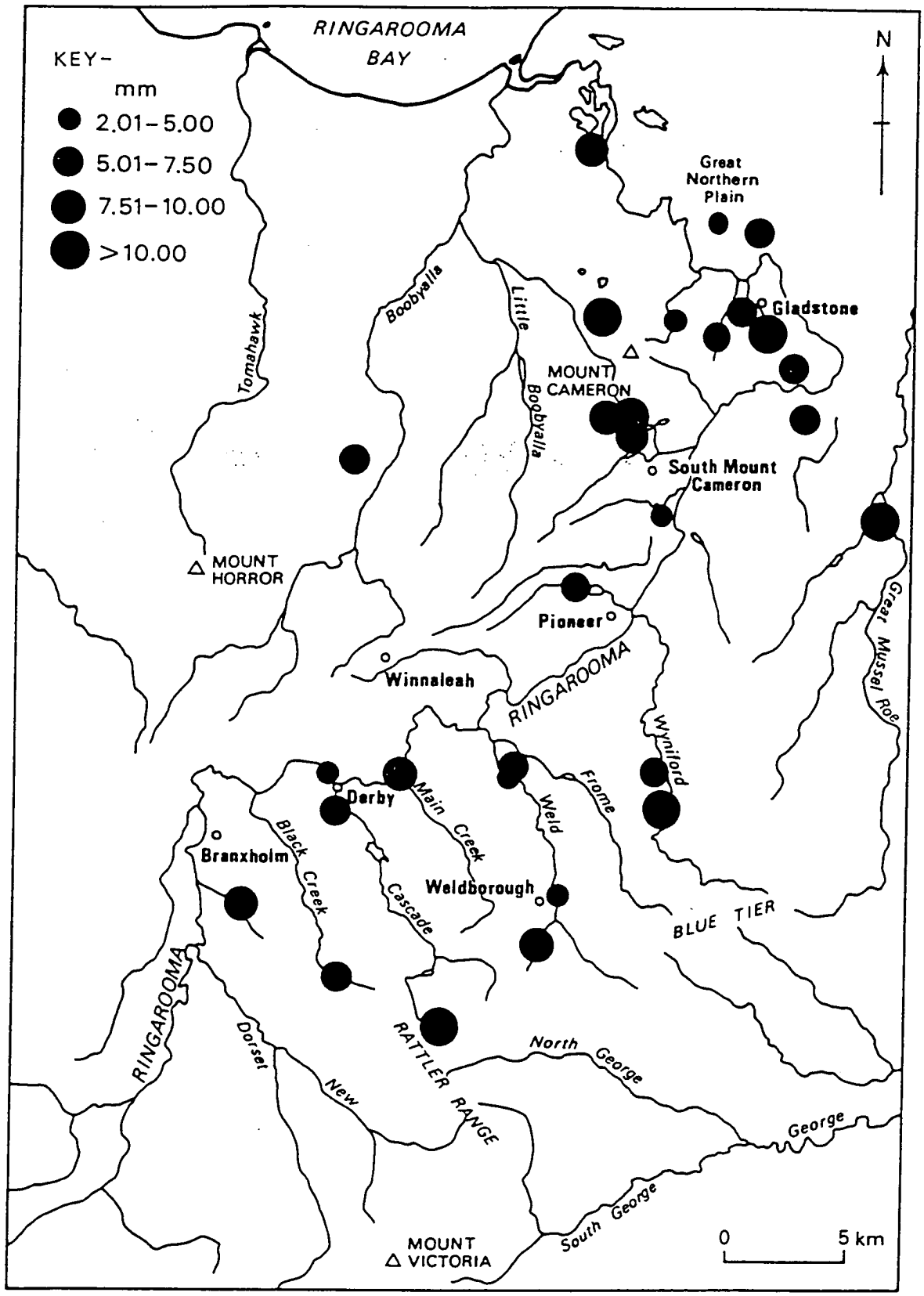

Fig. 4.1 Distribution of maximum diameter of monomineralic cassiterite grains found in the present study.

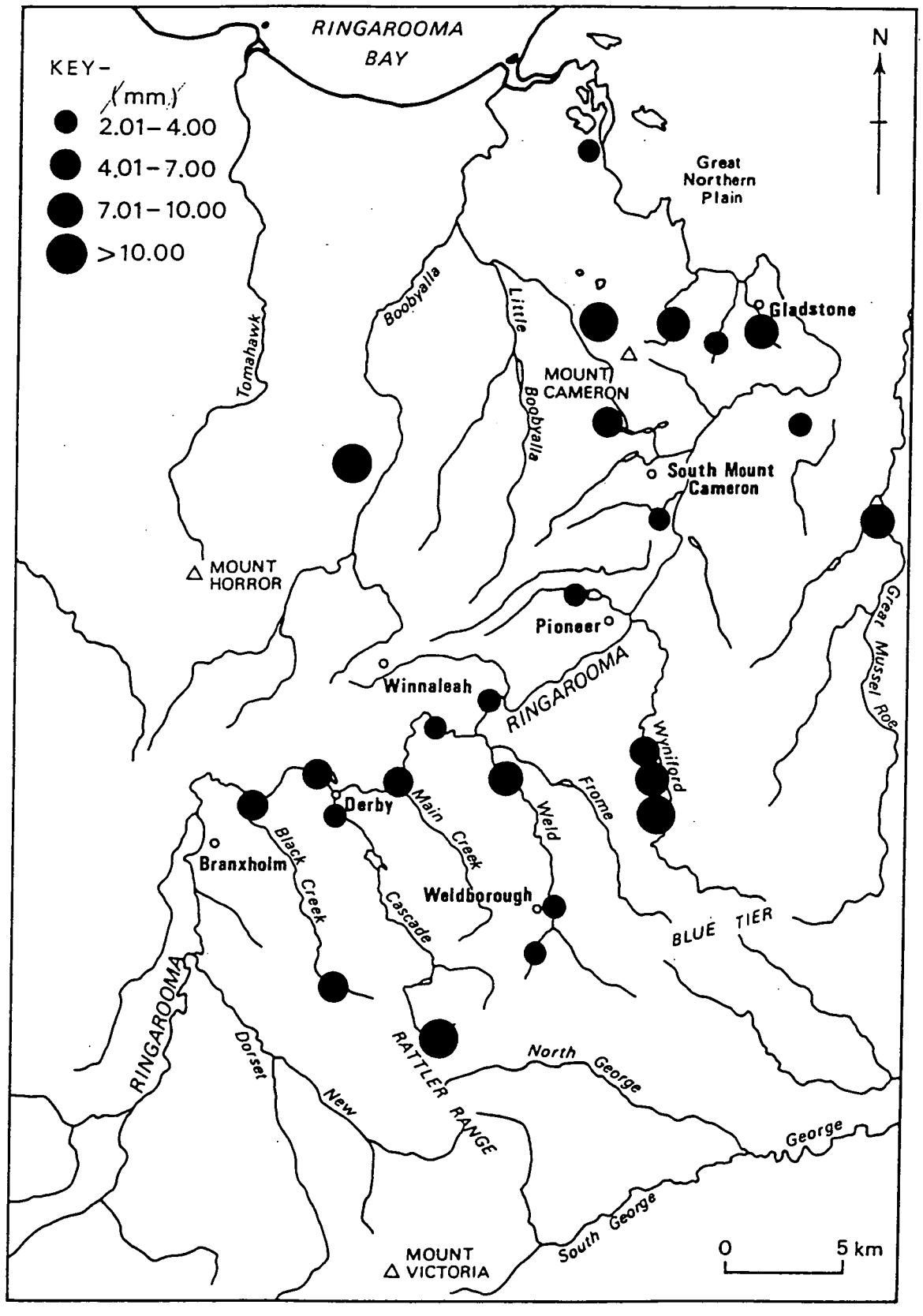

Fig. 4.2 Distribution of maximum diameter of composite cassiterite grains found in the present study.

Locality[1]	Sample type[2]	Colour	Maximum grain size (mm)		Dominant grain size[3]	Roundness[4]
			Monomineralic grains	Composite grains		
ABC Creek	b	dark to yellowish & reddish brown	<2	<2	fine sand	SA-SR
Ah Kaw Creek	b,c	dark to yellowish & reddish brown	5.8	3	coarse sand	SA-SR
Amber Hill	a,b	dark brown to yellow	6	3.8	medium sand	SA
Banca	a,b	mostly dark brown	6.5	18.5	gravel to coarse sand	SA
Bells Plain	a	dark to yellowish & orange brown	5.2	5.8	gravel to coarse sand	SR
Blackberries	a,b	dark to yellowish & reddish brown	12.5	38	gravel to coarse sand	SR
Blue Tier	a	black to black brown	>2	>2	coarse sand	SA-SR
Canary	b	dark to yellowish & reddish brown	<2	<2	fine sand	SA-SR
Cascade Creek	a,b,c	dark to reddish brown	7.5	4.2	coarse sand	SR
Clifton	a,b	dark to yellowish & reddish brown	13.2	>2	coarse sand	SA-SR
Corduroy Creek	a,b	dark to yellowish & reddish brown	<2	<2	medium sand	SA-SR
Dobson	a,b	dark to yellowish & reddish brown	<2	<2	fine sand	SA-SR
Delta	a,b	dark to yellowish & reddish brown	8.5	3.4	coarse to fine sand	SA-SR
Doone	b	dark to yellowish & reddish brown	<2	<2	medium sand	SA-SR
Emu Flat	b	dark to yellowish brown	>2	>2	coarse to medium sand	SA-SR
Endurance	a,b	dark to yellowish brown	9	>2	coarse to medium sand	SA-SR
Flintstone	a	dark to yellowish & reddish brown	>2	>2	coarse sand	SA-SR
Fly-by-night	a	dark to yellowish brown	12	14.5	gravel to coarse sand	SA-A
How the West	a	dark to yellowish & reddish brown	<2	4.2	coarse to medium sand	SA-SR
Lochaber	b	dark to yellowish brown	3	>2	coarse to medium sand	SA-SR
MacGregor	b	dark to yellowish & reddish brown	<2	<2	fine to medium sand	SA-SR
Monarch	a,b	black to dark brown	14	25	gravel to coarse sand	SA-SR
Mussel Roe	a,b	dark to orange brown	7	10	coarse sand	SA
Mutual	a	dark to yellowish & reddish brown	10	6.4	coarse sand	SR
New Clifton	b	black to dark reddish brown	9	5.8	coarse sand	SA-SR
New Fly-by-night	a	dark to reddish & orange brown	7	>2	coarse to medium sand	SA-SR
Pioneer	a,b	dark to yellowish brown	5.8	3.8	coarse to medium sand	SA-SR
Purdo Hill	a	dark yellowish brown	3.2	>2	coarse to medium sand	SA
Reynold	a	dark to yellowish & reddish brown	<2	<2	coarse sand	SA-SR
Ringarooma Bay	b	dark to yellowish brown	<2	<2	fine sand	SA-SR
Riverside	a,b	dark to yellowish & reddish brown	3.5	3.2	medium to fine sand	SA-SR
Ruby Creek	b	dark to yellowish brown	<2	<2	coarse to medium sand	SA-SR
Scotia	a,b	dark to yellowish brown	5	<2	coarse to medium sand	SA-SR
Sextus Creek	b	black to dark brown	4.2	7.2	coarse sand	SA-SR
Spinel Creek	b,c	dark to yellowish brown	9.5	4	coarse to medium sand	SA-SR
Star Hill	a,b	dark brown to yellow	<2	<2	coarse to medium sand	SA-SR
Star of Peace	a,c	dark to yellowish brown	15	18	gravel to coarse sand	SA-SR
Vulcan	a	dark to yellowish & reddish brown	<2	<2	fine sand	SA-SR
Weld River	b	dark to orange brown	6	6.2	coarse sand	SA-SR
Weldborough	c	dark to yellowish brown	3.8	<2	fine sand	SA-SR
White Rocks	a,b	dark to yellowish & reddish brown	>2	>2	coarse to medium sand	SA-SR
Wildcat	a	dark to yellowish & reddish brown	7	8	coarse sand	SA-SR

1 - For location see Fig. 3.1; 2 - (a) ore concentrate, (b) in situ sample, (c) active stream sediment;
3 - After British Standard Code of Practice; 4 - Three categories (A) angular, (SA) subangular, (SR) subrounded.

Table 4.2 Summary of cassiterite characteristics including colour, maximum grain size of monomineralic and composite grains, visually estimated dominant grain size and grain shape.

Euhedral prismatic crystals of zircon consisting of tetragonal bipyramids not exceeding 3 mm in grain size, averaging 0.5 mm and showing a high degree of fluorescence are found to be widespread in areas where source rocks other than granitoids may be safely ruled out. They are typically colourless to pale yellowish and are shown in Plate 4.1. The main source rock for this type of zircon in alluvial deposits is probably mineral inclusions liberated from the breakdown of micas in granitic rocks.

The presence of garnet in granitic rocks from northeastern Tasamania has been reported by Cocker (1977), Groves et al. (1977), McClenaghan et al. (1982) and McClenaghan & Williams (1982). A large source area is possible including the Boobyalla and Poimena plutons which are characterised by almandine (Groves et al. 1977) and spessartine (McClenaghan & Williams 1982) respectively (Fig. 4.3). Furthermore, the source rock may include quartz-feldspar-porphyry dykes (McClenaghan et al. 1982). In the present study, spessartine-bearing pegmatites were discovered in a road cut exposure of granite on the south side of the Gladstone Road (grid reference 790517) just outside Pioneer, suggesting that they could have been an important source of spessartine in alluvials. Therefore, the two types of garnets fall into a pegmatitic and a metamorphic field respectively as is suggested in Fig. 4.3.

The presence of the ilmenite-series granitoids was considered by Ishihara (1977) and Ishihara et al. (1979) to be a prerequisite to the formation of major tin fields. In northeastern Tasmania, a study of iron-titanium oxide minerals from the Poimena Pluton and the Scottsdale Batholith by Calcraft (1980) is consistent with this view. Abundant ilmenite with a magnesium oxide content of below 1 % was identified. Therefore the presence of ilmenite with similar composition in alluvials (Fig. 4.4) is in agreement with a derivation from granitic rocks.

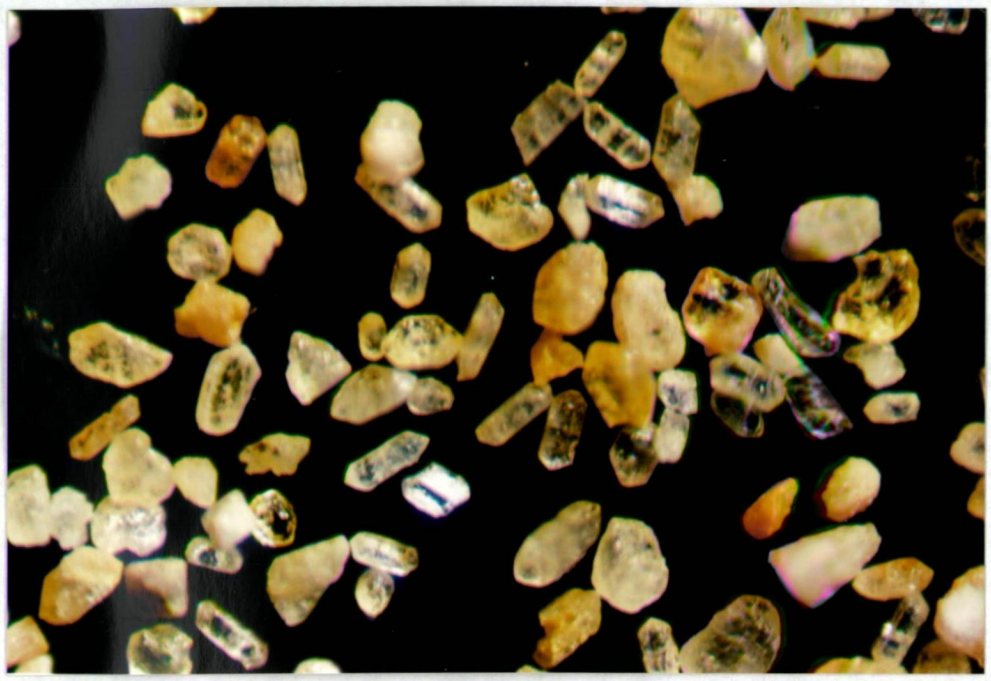

Plate 4.1 Fine euhedral zircons originating from Devonian granitic rocks. Weld River near Moorina. X 25.

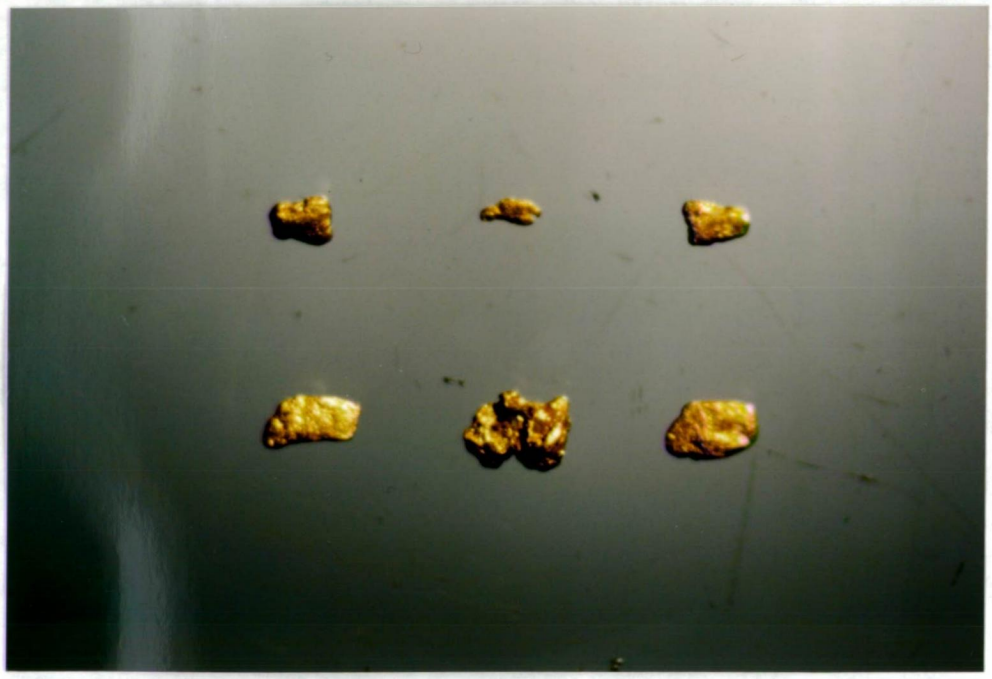

Plate 4.2 Small gold nuggets derived from quartz veins within Mathinna Beds. Ringarooma River near Derby. X 8.5.

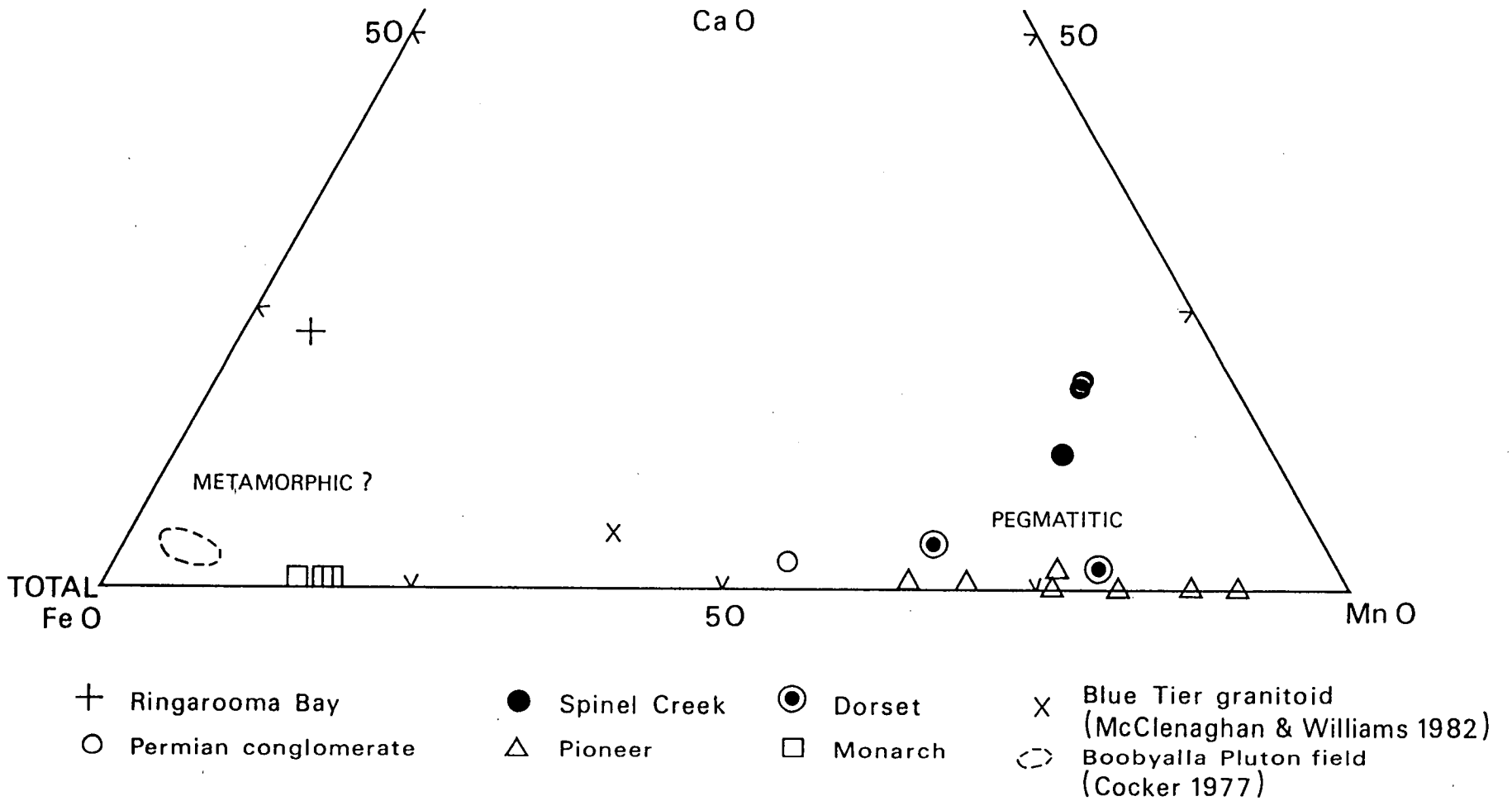

Fig. 4.3 CaO-total FeO-MnO diagram (mol %) for garnets in northeastern Tasmania.

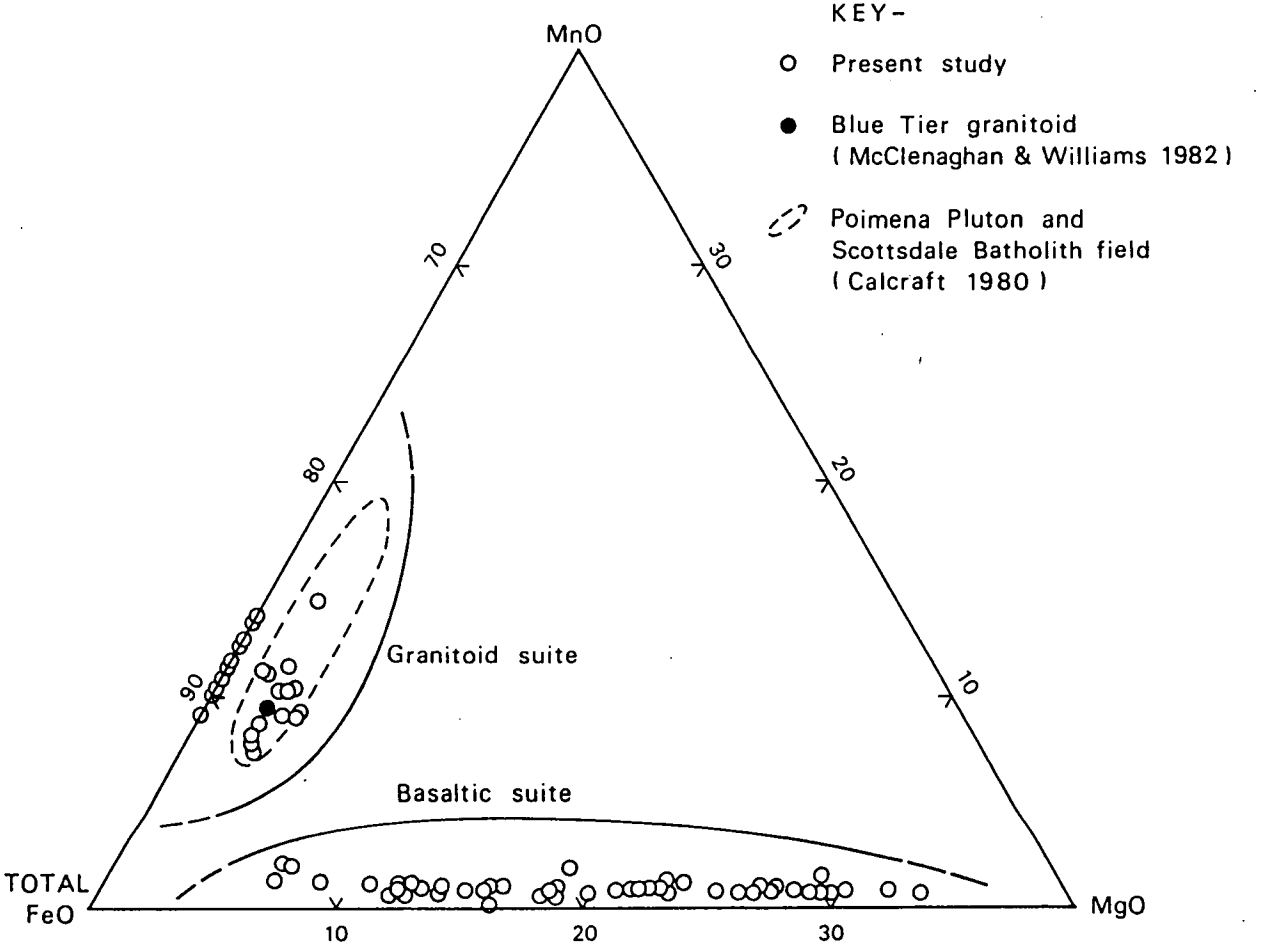

Fig. 4.4 MnO-total FeO-MgO diagram (mol %) for ilmenites in northeastern Tasmania.

Several specimens of chrysoberyl collected from the Weld River were obtained from the mineral collection of the Tasmanian Museum and Art Gallery in Hobart for confirmatory tests. These were carried out because chrysoberyl has not been found in the samples collected for the present study. All the grains exceeded 10 mm in grain size and were found to show the physical characteristics of chrysoberyl including hardness and specific gravity.

4.2.2 Mathinna Beds

In northeastern Tasmania, primary gold deposits occur almost exclusively in discordant quartz veins in the Mathinna Beds at considerable distances from exposed granitic rocks (Groves et al. 1977). Although the evidence is not conclusive, a genetic relationship between the gold deposits and the granodiorite plutons is suggested by the chemical similarity of these granitic rocks to that of other granitic rocks from other gold provinces of the world (Klominsky & Groves 1970). However, this idea as applied to northeastern Tasmania, would find little support at present as the gold is believed to be related to shear zones and deep metamoprphic origins (Gee & Legge 1979).

Figure 4.5 shows the distribution of known bedrock gold mineralization areas and alluvial gold localities confirmed in the present study. The centres of bedrock gold mineralization occurring within the study area include Alberton, Warrentinna, Gladstone and Portland, which are all associated with small quantities of alluvial gold. Gold nuggets up to a maximum grain size of 2 mm shown in Plate 4.2 were found in samples along the course of the Ringarooma River between Derby and Herrick. Although a possible source for these gold nuggets is the Warrentinna goldfield, it is more probable that they have been derived from the weathering and erosion of mineralized Mathinna Beds formerly existing in the vicinity with possible modifications by in situ growth. This is supported by remnants of Mathinna Beds at Main Creek

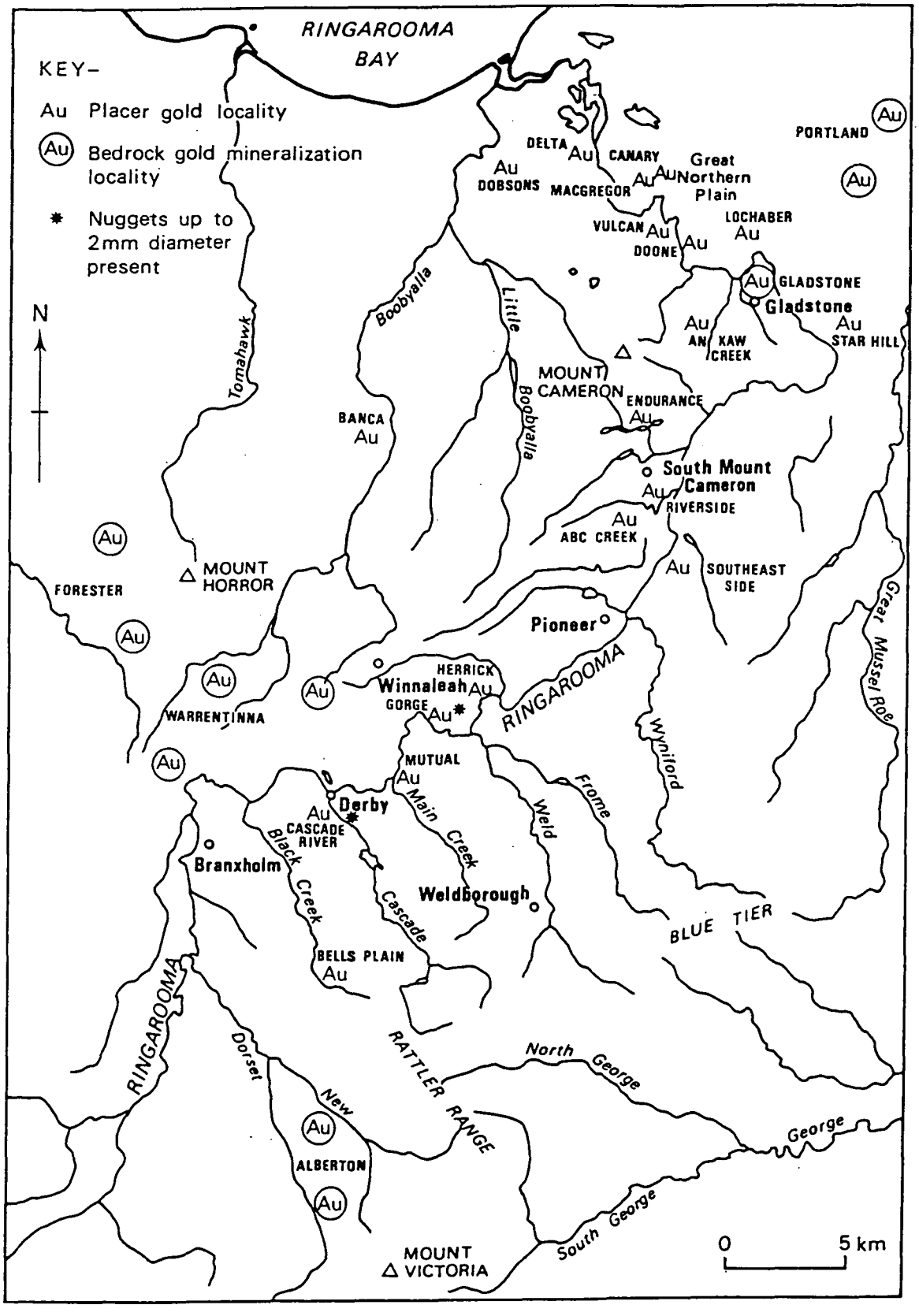

Fig. 4.5 Map showing area of known bedrock gold mineralization and and placer gold localities found in the present study. The former is based on the 1 : 50 000 geological map sheets of Tasmania Department of Mines.

which are partially concealed by the Winnaleah-Ringarooma basalts and the abundance of Mathinna clasts downstream.

Little is known about other heavy minerals occurring in the Mathinna Beds. With the exception of almandine which may occur in aureoles of metamorphism adjacent to granite (Fig. 4.3), other heavy minerals present in the predominantly arenaceous Mathinna Beds are likely to be too fine in particle size because of hydraulic equivalence to be of significance.

4.2.3 Older Tertiary basalts

The older Tertiary alkaline basaltic volcanics on top of the Blue Tier have yielded a distinctive stable heavy mineral assemblage identical to that of the gem fields of southeast Asia reported by Barr & MacDonald (1981). This assemblage comprises zircon (zir), corundum (co), spinel (sp) and ilmenite (il) (Plate 4.3). The occurrence of the same suite of minerals in southeastern Australia was given the name 'zircospilic' by Hollis (1984). In the zircospilic suite of minerals in northeastern Tasmania, the minerals in decreasing order of abundance are spinel, ilmenite, zircon and corundum. Although these heavy minerals occur mostly in or near granitic areas, an older Tertiary basalt derivation was recognised by Yim (1980). In eastern Australia, fieldwork and dating by Hollis & Sutherland (1985) confirmed alkali basalts and some trachytes as their hosts; the wide range of zircon crystal habits suggested diverse but, as yet, unknown parental sources. They were recognised by Wass & Irving (1976) and Sutherland & Hollis (1982) as megacrysts and xenocrysts of high pressure origin.

Unlike the fine and euhedral zircons occurring within the granitic rocks, zircons deriving from the older Tertiary basalt are typically coarse and anhedral (Plate 4.4). Large specimens may exceed 10 mm in grain size with an average of about 3 mm, and usually show some degree of rounding. The latter is explained by corrosion in the transporting

Plate 4.3 The zircospilic suite of heavy minerals. From left to right, the minerals are zircon, corundum, spinel and ilmenite. Mutual Mine. X 6.5.

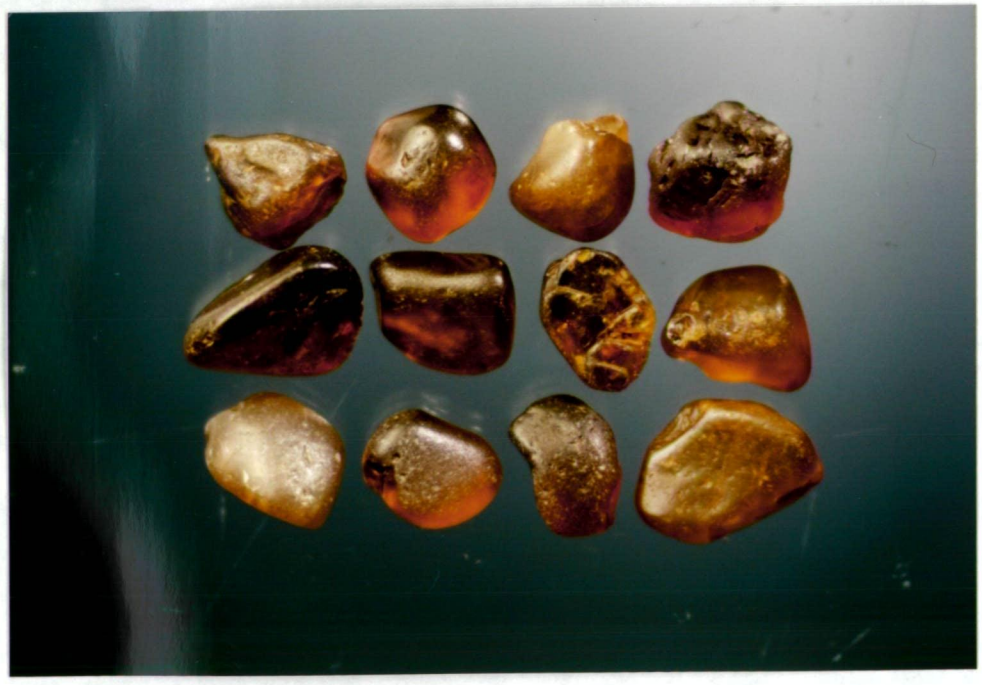

Plate 4.4 Coarse anhedral zircons from the older Tertiary basalts. Mutual Mine. X 6.5.

magmas (Hollis & Sutherland 1985) because subrounded zircons have been found short distances from the host rocks in the present study. The colour of the mineral varies from colourless to pale yellow to orange, pink and brown with the paler colour varieties showing the greatest degree of fluorescence. On the other hand, intermediate and deeply coloured types show moderate to weak fluorescence respectively. The derivation of coarse anhedral zircons from the Blue Tier basalts is confirmed by the identification of the mineral in active stream sediments along the Weld River and Spinel Creek, and in colluvial soil samples at Le Fevre Road (Fig. 3.1).

Corundum including the distinctive pale to deep blue gem variety, sapphire, was considered by Anon. (1970) to occur as an accessory mineral in igneous rocks and as a result of high grade metamorphism of aluminous rock types. The second origin is however not supported by the widespread distribution of corundum shown in Fig. 4.6. There are four main reasons to suggest an older Tertiary basalt source rock for corundum in northeastern Tasmania. Firstly, the largest recorded sapphire in Tasmania which presumably must occur fairly close to the source rock, is a 52.8 g stone found in the Weld River (Anon. 1981a). The site of occurrence is located within a short distance of the Blue Tier basalts. Secondly, sapphires have been found in basalt clasts in alluvium in eastern Australia near Inverell, New South Wales (MacNevin 1972). Thirdly, the widespread occurrence of corundum is indicative of the great transportation resistance of the mineral rather than a multiple source rock origin. Fourthly, sapphires were discovered near Inverell in Tertiary pyroclastics (Lishmund & Oakes 1983). The pyroclastic rocks containing the corundum are rarely exposed because of their concealment by corundum-barren basaltic flows making it difficult to find in situ corundum in the source rock. In the case of the Blue Tier basalts, pyroclastic rocks which are likely to be also

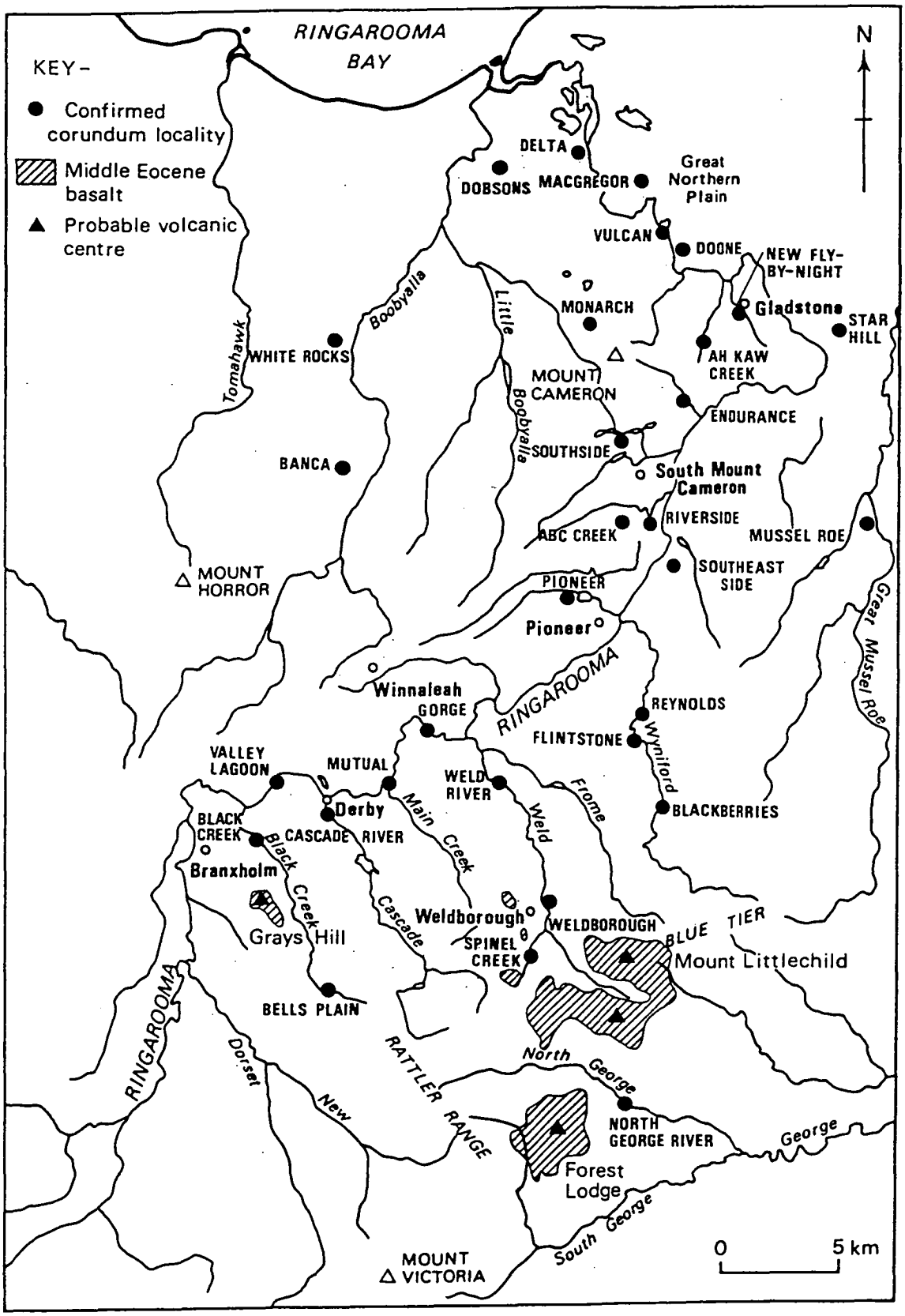

Fig. 4.6 Localities of corundum occurrences and the distribution of Middle Eocene basalts in northeastern Tasmania.

corundum-bearing are shown to outcrop extensively on the 1 : 50 000 Ringarooma geological map sheet probably as the result of the steeply sloping volcanic cone. They are therefore not concealed by corundum -barren basaltic flows.

The largest specimen of corundum found in the present study weighing over 5 g is from Black Creek. Because the catchment area of this locality is outside that of the Mount Littlechild and Forest Lodge volcanic centres, Grays Hill (Fig. 4.6) is likely to be the source.

A variety of spinel minerals have been found in the present study including pleonaste, hercynite, chrome-spinel and ulvospinel/titanomagnetite. Of these minerals, pleonaste (MgO-rich) and hercynite (FeO-rich) are by far the commonest and may exceed 10 mm in grain size. Based on the electron microprobe analysis of seventy-one mineral grains of these two types of spinel, hercynite is found to be just over twice as common as pleonaste. Both are jet black in colour and are well-rounded to subrounded. Fig. 4.7 shows a compositional plot of the chromian varieties. Spinels with high and low chromium content together with ulvospinel/titanomagnetite, pleonaste and hercynite, are found to be present in samples deriving from the Blue Tier basalts.

The ilmenite present in the zircospilic suite was found to differ in chemical composition from that originating in granitic rocks. It is distinctly lower in manganese oxide and higher in magnesium oxide content than that originating from granitoids (Fig. 4.4).

4.2.4 Younger Tertiary basalts

Younger Tertiary basalts differs from the older Tertiary basalts in that zircon, corundum, and the spinels, pleonaste, hercynite and ulvospinel/titanomagnetite have not been found. At Cascade Creek near Derby, where large lherzolite xenoliths are found to occur in the Winnaleah-Ringarooma basalts, peridot exceeding 10 mm in grain size has been found in alluvials. Chrome-spinels and magnesium-rich ilmenites

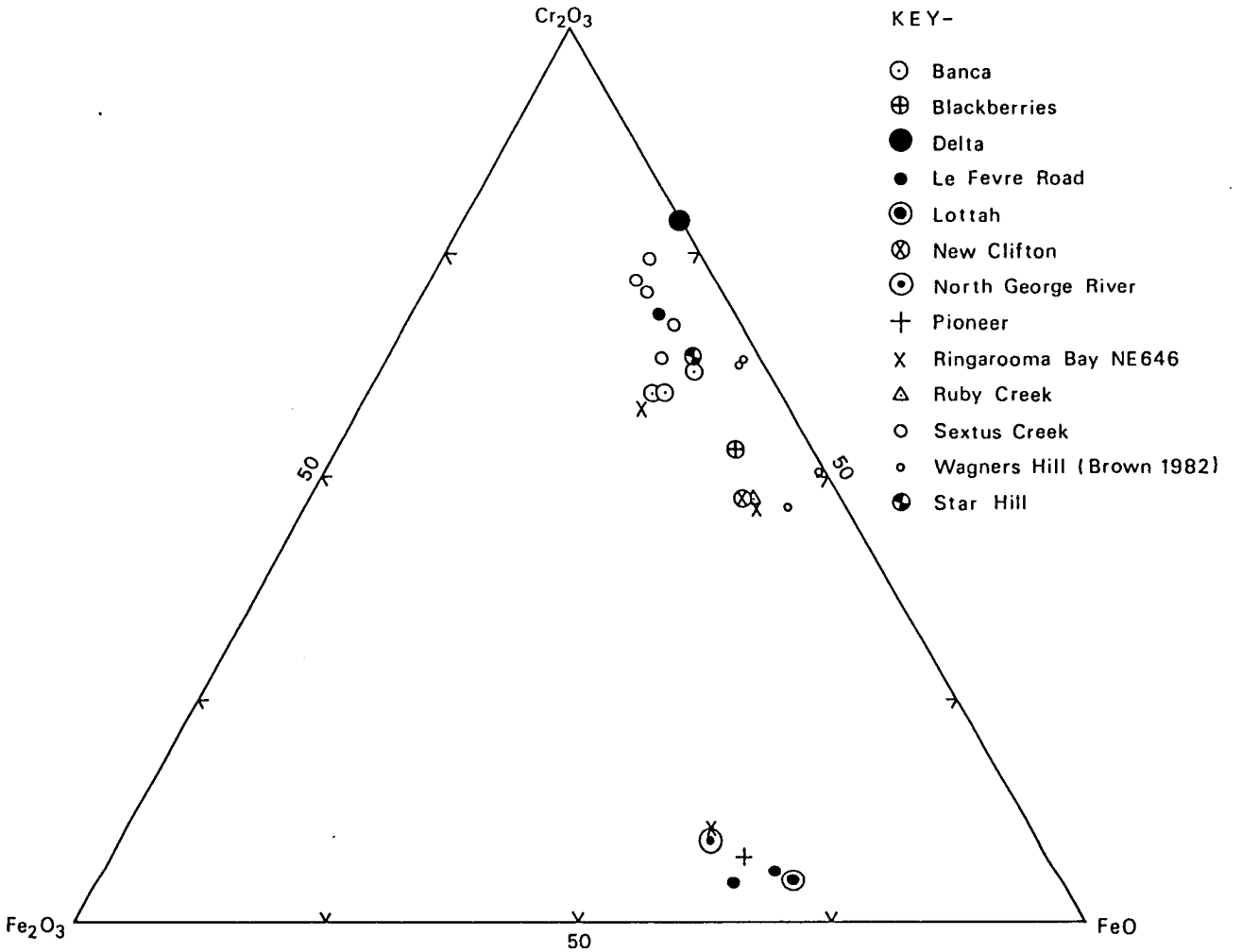

Fig. 4.7 Cr_2O_3-Fe_2O_3-FeO diagram (mol %) for chrome-spinels from northeastern Tasmania. Cr_2O_3 in all spinels shown exceed 1 % in weight.

which are present in the older Tertiary basalts also occurs. The composition of four chrome-spinels in spinel lherzolite from Wagners Hill near Herrick (Brown in McClenaghan et al. 1982) is similar to that of the mineral grain from Upper Le Fevre Road (Fig. 4.7).

4.2.5 Other source rocks

Two other source rocks for stable heavy minerals are possible. Firstly, Jurassic dolerite outcropping near Cape Portland and on the mountain tops of northeastern Tasmania such as Mount Maurice and Mount Victoria, and secondly, the Parmeener Supergroup. The former may account for a chromite grain found at the Delta Mine (Fig. 2.10) (N. Ortez via R.J. Ford, pers. comm.) while the latter would include stable heavy minerals such as fine euhedral zircons, manganese-rich ilmenites as well as cassiterite which had derived from the mineralized Devonian granite. However, to date no cassiterite has been identified in the conglomerates of the Parmeener Supergroup outcropping near the top of the Blue Tier.

4.3 Heavy mineral associations

Based on the heavy minerals present in northeastern Tasmania, three main types of heavy mineral association, all containing cassiterite and topaz are recognised. These associations are distinguished from each other using the two types of zircon and the occurrence of gold (Yim 1980). The three heavy mineral associations are:

(1) A garnet-spinel-corundum-zircon (both types) association (Plate 4.5) which may occur in deep leads below the Winnaleah-Ringarooma basalts. Localities include Briseis, Pioneer and Endurance (Fig. 2.10).

(2) A fine euhedral zircon association which may occur in creeks north and south of Mount Cameron including Clifton Creek and Sextus Creek (Fig. 2.10). No corundum and/or spinel, and Tertiary basalt are known at these localities.

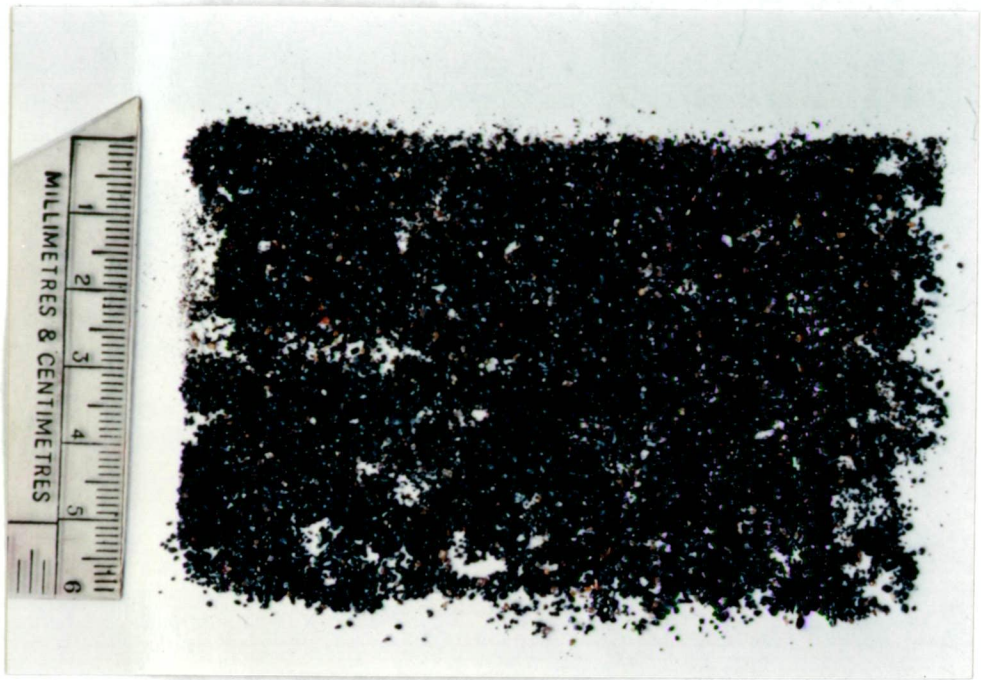

Plate 4.5 A typical heavy mineral concentrate exceeding SG 2.96 showing the cassiterite-garnet-spinel-corundum-topaz-zircon (both types) association. Pioneer Lead.

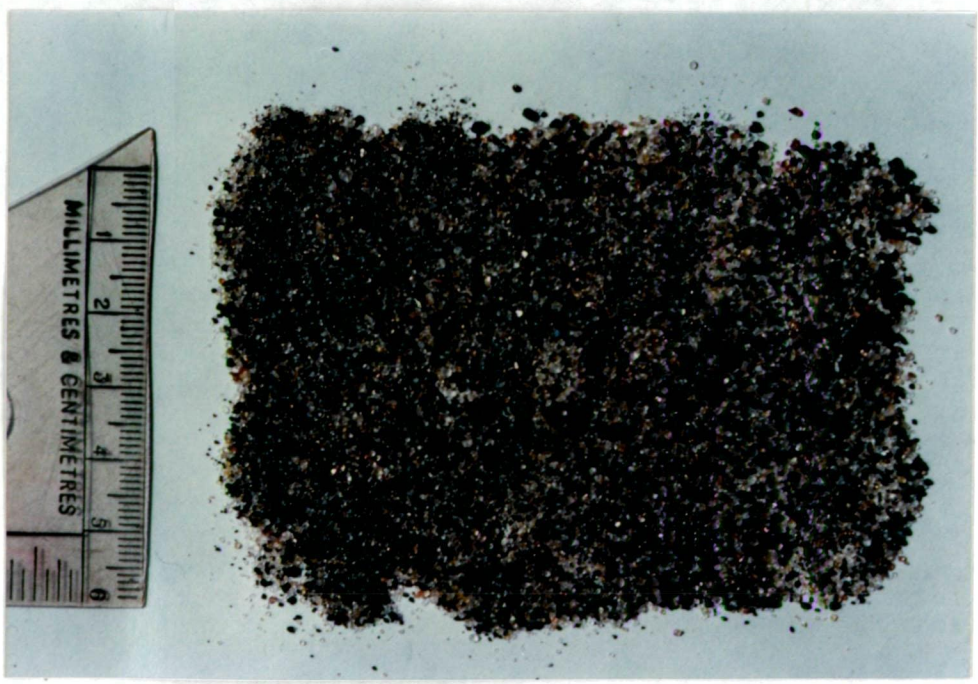

Plate 4.6 A typical heavy mineral concentrate exceeding SG 2.96 showing the cassiterite-gold-spinel-corundum-topaz-zircon (both types association). Riverside Tin Mine.

(3) A gold-spinel-corundum-zircon (both types) association (Plate 4.6) largely restricted to the present day floodplain of the Ringarooma River.

Based on the assumption that the fine euhedral zircons and coarse anhedral zircons were derived from Devonian granitic rocks and older Tertiary basalts respectively, the validity of the three heavy mineral associations was tested by fission track dating of the two types of zircon (Yim et al. 1985) (Appendix II). The postulated difference in age between the granitic zircons (ca. 367 Ma) and the basaltic zircons (ca. 47 Ma) is confirmed by the fission track ages obtained.

4.4 Transportation resistance and heavy mineral provenance

Raeburn & Milner (1927) stated 'As a general working rule, the greater the stability of the rock-forming minerals, the greater the distance they may be transported from parent-rocks without material change of state. The moderately stable and unstable species become progressively localised, their presence in any abundance in any alluvials is usually indicative of proximity to the source of supply'. From this, it can be seen that the distribution pattern of heavy minerals in northeastern Tasmania would reflect their transportation resistance.

Table 4.3 summarises the distribution characteristics, hardness, cleavage and transportation resistance of selected heavy minerals from northeastern Tasmania. Transportation resistance measures the resistance of a mineral to mechanical action during fluvial transport and was determined by experimental comparison under laboratory conditions with compact hematite arbitrarily taken as 100 (Friese 1931). It can be seen that cassiterite, a brittle but very dense mineral with poor cleavage and moderate hardness has a low transportation resistance of 360 in spite of its high chemical stability. Therefore it is expected to occur close to the source rock. In contrast to cassiterite, corundum, an

Mineral name	Hardness	Cleavage	Transportation resistance*	Distribution characteristics
Monazite	5	moderate	105-300	egg-shaped, fairly common
Olivine	6.5-7	none	250	usually well-rounded, restricted to near source rock
Zircon	7.5	imperfect	265	resistant to abrasion, basaltic zircons rounded by magmatic processes
Chrysoberyl	8.5	poor	300	found rounded in spite of hardness
Ilmenite	5-6	none	325	widespread moderately resistant mineral
Cassiterite	6-7	poor	360	brittle & very dense mineral, found close to source rock
Almandine	6.5-7.5	none	375	widespread resistant mineral
Magnetite	5.5-6.5	none	380	uncommon
Topaz	8	perfect	390	widespread mineral, decreases rapidly in grain size away from source rock
Rutile	6-6.5	perfect	455	common
Pleonaste/ Hercynite	7.5-8	none	550	widespread resistant mineral
Cr-spinel	7.5-8	none	680	widespread resistant mineral
Corundum	9	poor	750	widespread extremely resistant mineral
Tourmaline	7.5	poor	650-950	widespread extremely resistant mineral

* - Transportation resistance values are from Friese (1931).

Table 4.3 Summary of hardness, cleavage, transportation resistance and distribution characteristics of selected heavy minerals from northeastern Tasmania.

extremely hard, chemically resistant and moderately dense mineral has the highest transportation resistance of 750. Consequently, corundum can be found great distances from the source. Similarly the two spinels, pleonaste and chrome-spinel because of their great hardness, absence of cleavage, moderate density and high chemical stability may travel considerable distances from the source because of their moderately high transportation resistance. In the case of topaz, the presence of perfect cleavage in one direction causes the mineral to decrease rapidly in grain size away from the source rock in spite of its great hardness. Its transportation resistance of 390 is only marginally higher than cassiterite. On the other hand, zircon has a surprisingly low transportation resistance of 265. While the brittle nature of zircon can be demonstrated by the ease of grinding of the mineral into a powder with an agate pestle and mortar, it is one of the most common heavy minerals in polycyclic sediments. The abundance of fine euhedral zircons may be explained by trapping within the interstices of gravels due to its stability, shape and moderately high density.

It is significant that with the exception of tourmaline and zircon, the latter of the fine euhedral type, none of the heavy mineral species shown in Table 4.3 were found in a study of present day beach sands on the north coast of Tasmania by Davies & Hudson (1987). The absence of heavy minerals other than tourmaline and fine euhedral zircon is confirmative of the short distance of fluvial transportation for high density heavy minerals under and that the distribution of unstable heavy minerals in beaches reflected only local derivation.

CHAPTER 5 FOLLOW-UP STUDIES ON HEAVY MINERAL PROVENANCE

5.1 Introduction

To obtain further supporting evidence on the probable provenance of heavy minerals identified in the previous chapter, follow-up studies were carried out. The investigations reported in this chapter sought to accomplish three main objectives:

(1) To obtain evidence if any on the transport distance of cassiterite from the mineralized source rock - (a) Particle size distribution of cassiterite ore concentrates from selected localities were measured to provide information on their size distriution and distance of transportation. (b) The distribution within cassiterite of selected trace elements known to be diagnostic in recognising the type of primary tin mineralization was determined.

(2) Fission track dating and ESR studies were carried out to confirm the provenance of different types of zircon.

(3) To evaluate the application of hydraulic equivalence as a possible method for determining of the distance of transport of heavy minerals.

5.2 Transport distance of cassiterite

The transport distance of cassiterite is the maximum distance, measured from the primary occurrence, within which cassiterite concentrations can occur, in economic concentrations (currently over 0.1 kg metallic tin per square metre valley bottom surface).

5.2.1 Particle size distribution of cassiterite ores

Particle size analysis was carried out on twelve samples (Fig. 3.6). These samples included eight dressed ore concentrates, three in situ samples collected immediately above the bedrock basement, and one sluiced ore concentrate collected adjacent to the working face of a mine exposure. Although it is doubtful that the samples collected are sufficiently representative of individual mines, they are nevertheless

expected to provide some indication of the predominant grain size of cassiterite. With the exception of three samples, Pioneer, Purdo Hill and Mussel Roe, the majority of the samples satisfies the 50 g weight requirement specified for sand size sediment by Folk (1968). A summary of the particle size distribution is shown in Table 5.1.

The majority of the samples are dominated by cassiterite of very coarse sand (1 - 2 mm) to medium sand (0.25 - 0.5 mm) size with an overall graphic mean size of 1.39 mm. The coarsest mean size (3.84 mm) is from Bells Plain and the finest graphic mean size of 0.42 mm is from Pioneer. Significant quantities of coarse cassiterite exceeding 2 mm (8 mesh BSS) in size and 20 % by weight distribution are found in samples from Banca, Bells Plain, Monarch and Mussel Roe. Amber Hill, Pioneer and Purdo Hill are the only three samples with fine cassiterite below 0.25 mm (60 mesh BSS) exceeding 10 % by weight. There is great variation in graphic sorting coefficients ranging from very well sorted to poorly sorted. The general tendency is for well sorted samples in be finer in graphic mean size while poorly sorted samples are coarser in graphic mean size (Fig. 5.1). The three-fold classification of kulit, kaksa and mintjan deposits were applied to cassiterite placers by Krol (1960), van Overeem (1960), Taylor (1986) and others.

Three broad categories of economic cassiterite placers were recognised based on cassiterite grain size distribution characteristics in southeast Asia by Taylor (1986) including:

(1) Residual or 'kulit' deposits formed essentially in situ without major lateral transport or sorting of the minerals. Both coarse (exceeding 1.4 mm or 12 mesh BSS) and fine (below 0.075 mm or 200 mesh BSS) cassiterite are present but without any clear peak size.

(2) Washed out or elutriated 'kaksa' deposits where the coarser and heavier minerals remain close to the source while the finer and

Area	Locality (Fig. 3.6)	Sample type	Weight g	Size fractions % (Wentworth scale)						Graphic mean size		Graphic sorting coefficient	Sorting term*
				Gravel +2mm	Very coarse sand 1-2mm	Coarse sand 0.5-1mm	Medium sand 0.25-0.5mm	Fine sand 0.125-0.25mm	Very fine sand & silt -0.125mm	phi	mm		
Blue Tier Massif	Bells Plain	dressed ore	182.62	69.22	19.24	8.93	2.45	0.15	0.01	-1.940	3.84	1.54	P
	Pioneer	dressed ore	48.87	-	0.02	2.56	77.67	19.69	0.07	0.372	0.42	0.32	VW
	Pioneer T14	in situ sample	136.13	-	1.81	76.71	19.92	1.39	0.18	1.267	0.80	0.25	VW
	Reynolds	dressed ore	50.62	-	17.68	63.16	17.36	1.70	0.11	0.033	0.98	0.57	M
Mount Cameron Massif	Clifton	sluiced sample	56.12	-	1.57	68.19	28.77	1.21	0.26	0.393	0.76	0.29	VW
	Monarch	dressed ore	84.96	33.14	31.36	24.51	7.75	2.56	0.68	-0.917	1.89	1.07	P
	New Clifton 4	in situ sample	231.39	4.62	56.68	36.25	1.81	0.55	0.08	-0.547	1.46	0.62	M
	Purdo Hill	dressed ore	9.56	2.78	7.14	33.11	37.32	18.97	0.68	0.710	0.61	0.90	M
	Sextus Creek	in situ sample	241.56	0.62	49.34	45.63	3.48	0.79	0.14	-0.490	1.40	0.43	W
Others	Amber Hill	dressed ore	210.60	1.04	15.27	22.68	21.66	36.67	2.68	0.793	0.58	1.11	P
	Banca	dressed ore	161.40	45.62	47.21	6.46	0.25	0.19	0.29	-1.403	2.64	0.60	M
	Mussel Roe	dressed ore	17.66	23.73	8.13	24.15	37.38	6.11	0.50	-0.330	1.26	1.70	P

* VW - very well sorted; W - well sorted; M - moderately sorted; P - poorly sorted.

Table 5.1 Particle size distribution of tin concentrates from selected placer mines in northeastern Tasmania. Note that the sample representivity is increased by sample weight.

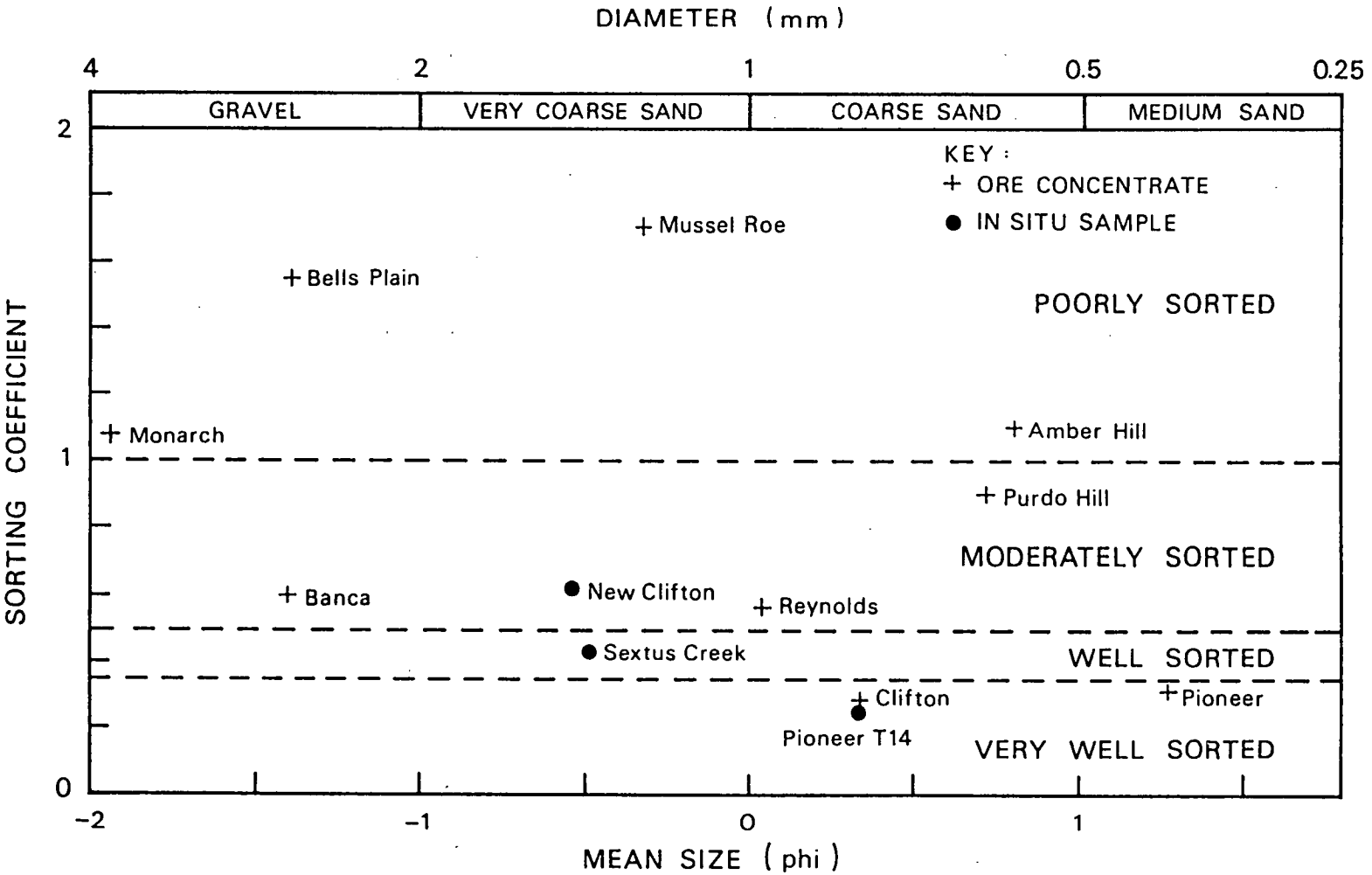

Fig. 5.1 Plot of mean size versus sorting coefficient for selected tin concentrates from northeastern Tasmania.

lighter minerals are removed. There is a marked depletion in the finer sizes and a sharply peaked size distribution.

(3) Transported or 'mintjan' deposits where the heavy minerals, after varying degrees of transport, have been trapped and retained in a suitable sedimentary environment. Cassiterite exceeding 0.425 mm (36 mesh BSS) and below 0.075 mm (200 mesh BSS) is lacking.

Based on the particle size distribution found, all three types of cassiterite placers have been recognised in this study.

Cumulative particle size distribution diagrams for the twelve samples from northeastern Tasmania and the three in situ samples are shown in Figs. 5.2 & 5.3 respectively. Both figures provide further insight into the nature of the cassiterite placers. Kulit deposits are represented by samples from Amber Hill, Monarch, Mussel Roe and Purdo Hill, while kaksa and mintjan deposits are represented by Banca, Bells Plain, Clifton, New Clifton 4, Sextus Creek and Pioneer T14, and Pioneer respectively. In the two samples from the Pioneer Tin Mine, it is important to note that one sample represented kaksa and the other a mintjan. Because the sample types are different, the dressed ore sample from Pioneer is probably more representative of the bulk of the tin ore at the mine which is dominated by mintjan deposits. On the other hand the in situ sample, Pioneer T14, shows that kaksa deposits immediately adjacent to the bedrock are present. The latter is supported by the identification of younger channel fill deposits cut into older channel fill deposits adjacent to the rock basement (Plate 5.1). Reworking is increasingly likely downstream from the source with kaksa replaced by mintjan.

All three in situ samples shown in Fig. 5.3 are identified as showing kaksa tendencies. They exhibit characteristically steep curves indicating their well sorted nature. However, Pioneer T14 which is the best sorted and the finest in mean size is considered to show

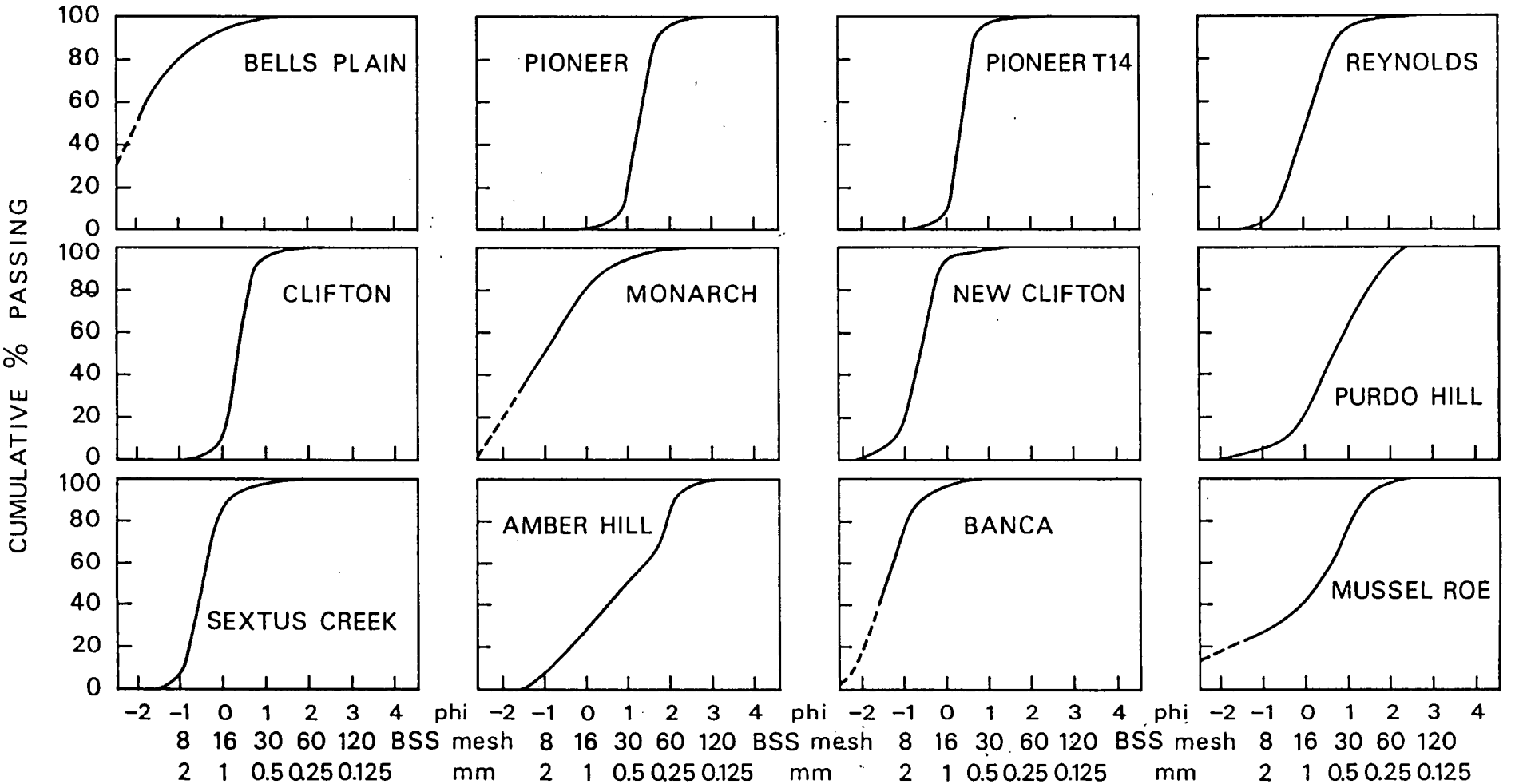

Fig. 5.2 Particle size distribution curves for twelve tin concentrates from northeastern Tasmania shown in Fig. 3.6.

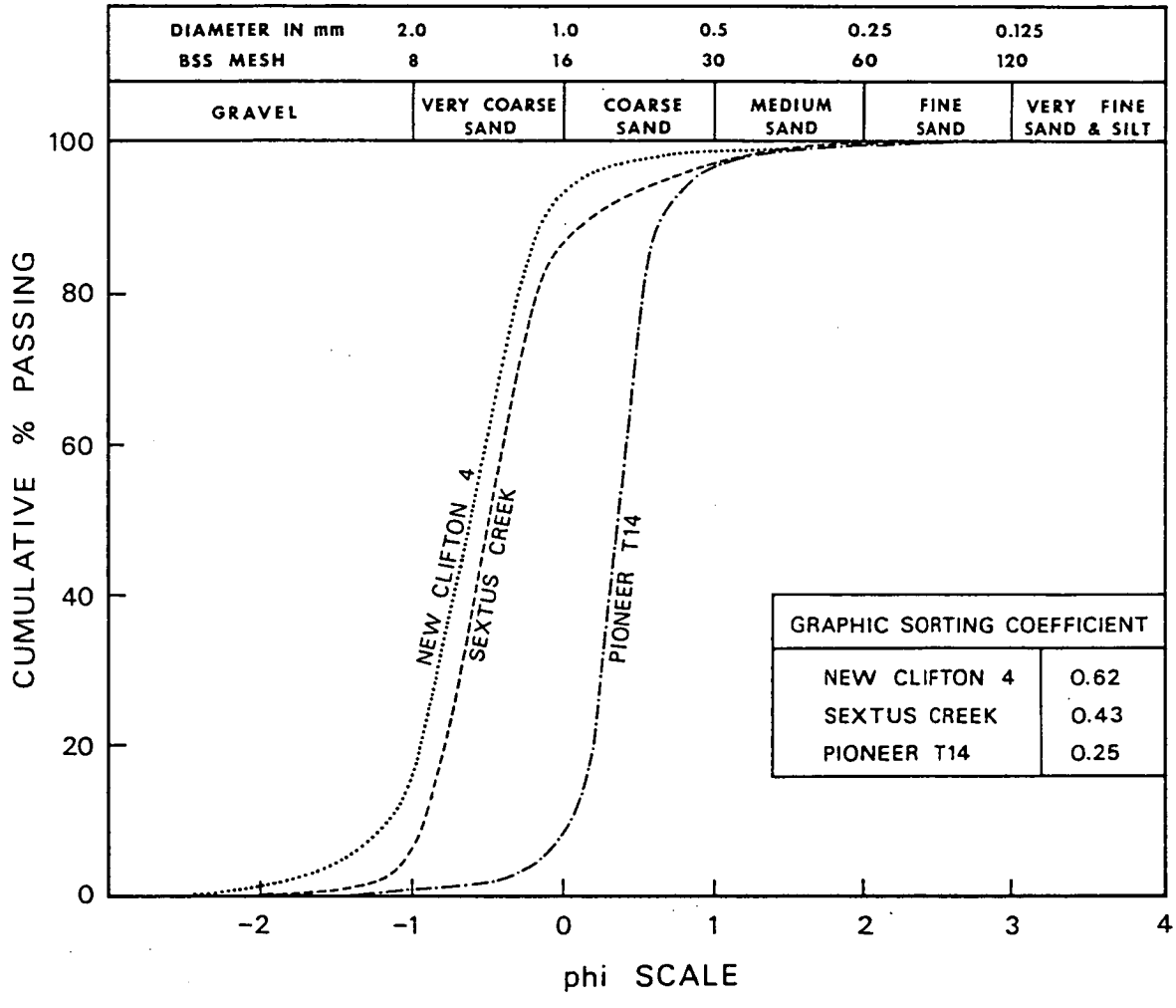

Fig. 5.3 Comparison of particle size distribution curves and sorting coefficients of three in situ samples.

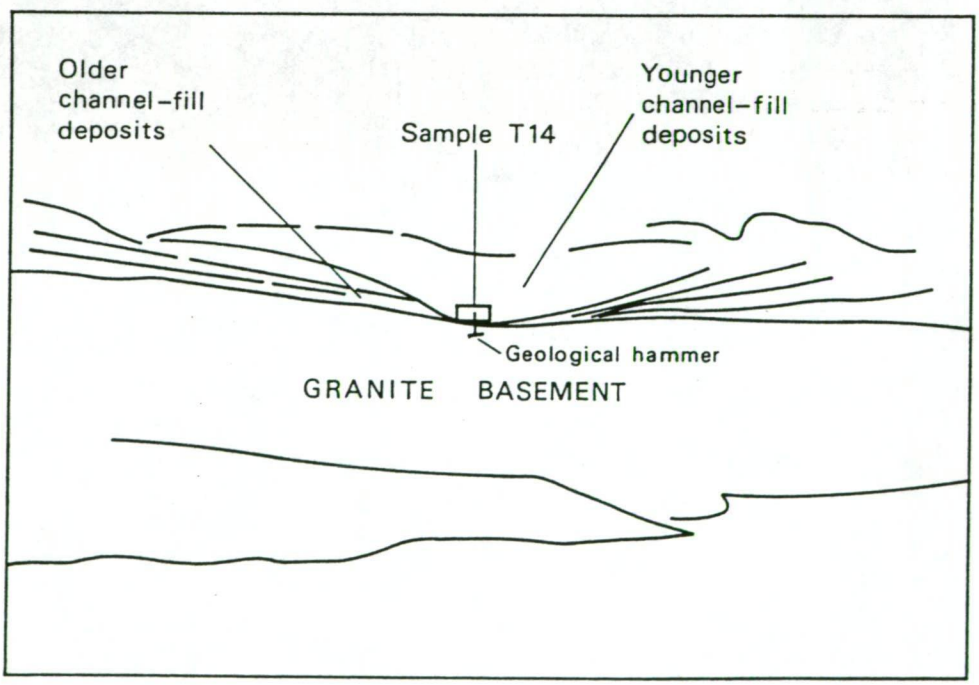

Plate 5.1 Rock basement view of the Pioneer Tin Mine showing the location of tin concentrate sample Pioneer T14. The sample formed by the reworking of lag deposits shows kaksa tendencies. Scale is shown by the geological hammer below sample T14.

intermediate tendencies towards mintjan. The steepness of the curve is best explained by selective sorting through elutriation during reworking as well as the increasing distance of transport from the source rock. A decrease in grain size and increase in sorting away from the source both laterally and vertically within placer deposits are to be expected. Kaksa and mintjan deposits, and, in some cases also kulit deposits, all coexisting at the same mine are probably more common than is suggested in the published literature. For example, all three types have been identified in Banca and Bells Plain where the dressed ore samples possess dominantly kulit and kaksa tendencies. Because of this, the distance of transport measured for different sites will vary depending on the stratigraphic and sedimentological details as well as the economic ore grade. In the absence of such details mainly due to the lack of continuous exposures for the collection of in situ samples, considerations of transport distances are probably meaningless. The distance of transport of cassiterite will be examined further in Section 9.3.

5.2.2 Trace elements in cassiterite

The mineralogy and aspects of crystal chemistry of tin including the occurrence of trace elements was reviewed in detail by Cuff & Taylor in Taylor (1979) and more recently by Barth (1986). Studies have been carried out on the trace element content of cassiterites from the U.S.S.R. (Dudykina 1959), eastern Australia (Steveson & Taylor 1973 and Barth 1986), Malaysia (Hassan 1982 and 1986) and many countries in Asia (Traub & Moh 1978). However, with the exception of Barth (1986), all these studies were carried out using semi-quantitative spectrochemical methods which are not noted for their precision and accurracy. Electron probe microanalysis was used by Barth (1986) to discriminate between lattice and non-lattice element contents.

Four trace elements found in cassiterite, Nb, Ta, W and Zr have been selected for the present study for three main reasons. Firstly, pegmatites and greisens are known to contain distinctive mean concentration of these elements (Table 5.2). Consequently, study on their distribution in cassiterites would be helpful to provide better understanding of the provenance and distance of transport from source rock. Secondly, all four elements may be determined by the x-ray fluorescence method which is superior in both precision and accuracy to spectrochemical methods, and, in that the method is less susceptible to interferences particularly when the sample matrix is uniform. Thirdly, all four elements may occur within the cassiterite crystal lattice, or in exsolved phases having valencies and ionic radii similar to those of tin (Steveson & Taylor 1973).

Table 5.2 shows that the mean Nb, Ta, W and Zr content of cassiterites from pegmatites, greisens and veins obtained by previous workers may be quite distinctive. Ta is always more enriched, while Nb and Zr are usually more enriched in pegmatites than in greisens and veins. On the other hand, W shows a tendency to be more enriched in greisens and veins than pegmatites.

The trace element content of cassiterites based on the analysis of bulk samples found in the present study is summarised in Table 5.3. For the comparison of regional geochemical characteristics of cassiterite, samples occurring within the Blue Tier and Mount Cameron Massifs are grouped for mean value determination. The results for each element and their interrelationship are presented in Sections 5.2.2A to 5.2.2E.

Because strongly pleochroic cassiterite rich in Nb is known to be associated with pegmatites,the Nb content and the degree of pleochroism of cassiterite were investigated. Thin sections of cassiterite were studied using two methods. Firstly, wavelength x-ray analysis of Nb content with a electron probe, and, secondly, estimation of the degree

Source	Type of deposit	No. of samples	PPM			
			Nb	Ta	W	Zr
Dudykina (1959)	pegmatites	37	6000	5300	730	2400
	greisens	38	5200	1570	4400	1020
	veins[1]	129	600	150	2140	750
Steveson & Taylor (1973)	pegmatites	6	10000	10000	283	458
	greisens	3	10000	600	200	200
	veins[2]	7	113	100	1000	161
Hassan (1986)	pegmatites[3]	19	6800	3900	180	1100
	greisens[3]	6	1125	625	500	188

1 - Including quartz veins with topaz, tourmaline and beryl; 2 - Quartz tourmaline; 3 - Values shown are based on a recalulation of data provided in Hassan (1986).

Table 5.2 Comparison of mean Nb, Ta, W and Zr content of cassiterites deriving from pegmatites, greisens and veins.

Area	Ref. no.	Locality name (see Fig. 3.1)	PPM Nb	Ta	W	Zr
Blue Tier Massif	1	Bells Plain	946	88	867	241
	2	Blackberries	532	44	796	236
	3	Blackberries 4	547	85	715	232
	4	Cascade Creek	1017	109	964	251
	5	Mutual	573	5	1071	236
	6	Pioneer	1502	566	1194	1425
	7	Reynolds	781	320	1027	234
	8	Star of Peace	1429	234	1570	85
	9	Wildcat	665	78	871	236
		Mean	888	170	1008	353
Mount Cameron Massif	10	Clifton	1744	435	912	350
	11	Fly-by-night	1513	356	604	225
	12	Monarch	1350	365	663	345
	13	New Clifton	1880	455	609	279
	14	Purdo Hill	3343	2488	699	1498
	15	Sextus Creek	4263	2922	637	651
		Mean	2349	1170	687	558
Others	16	Amber Hill	763	173	750	749
	17	Banca	895	30	1184	100
	18	Delta	767	400	644	341
	19	Mussel Roe	594	178	824	191
Detection limit at 3 standard deviation			10	9	20	24
Overall mean			1321	491	824	416
Overall range			532-4263	5-2922	604-1570	85-1498
Overall 1 standard deviation			983	801	251	402
Coefficient of variation (%)*			74.4	163.1	30.5	96.6

* - C = 100 S.D. / Mean.

Table 5.3 Nb, Ta, W and Zr content of cassiterites from northeastern Tasmania. Analytical details are presented in Section 3.3.9.

of pleochroism under a petrological microscope. A summary of the results based on measurement of different parts of cassiterite grains is presented in Table 5.4.

5.2.2A Nb

The overall mean found is 1321 ppm. This value is considerably lower than the mean content of pegmatites found by previous authors (Table 5.2), implying that the deposits studied may have been different. The standard deviation value of 983 ppm is the highest of all four trace elements. Mount Cameron Massif shows a mean concentration of 2349 ppm which is twice the mean for the Blue Tier Massif indicating the presence of two separate igneous intrusions. The range of Nb content found is confirmative of a wide range of geological environments for tin mineralization in northeastern Tasmania including pegmatites, greisens and veins.

5.2.2B Ta

Ta shows, as is usually the case, a pattern of distribution closely resembling Nb and is present at lower concentations than Nb. The latter is in agreement with Dudykina (1959) who considered that Nb was more widely distributed than Ta. As with Nb, the overall mean of 491 ppm for Ta is appreciably lower than the mean content found by previous authors (Table 5.2). The coefficient of variation of 163.1 % is by far the highest of the four elements studied. Again two populations are suggested, with Mount Cameron Massif distinctly higher in mean Ta content than to the Blue Tier Massif. The two samples with the highest Ta content, Purdo Hill (2488 ppm) and Sextus Creek (2922 ppm), are explained by a pegmatite origin.

5.2.2C W

For W, the overall mean of 824 ppm is near the middle of the concentration range found by previous workers (Table 5.2). Both the coefficient of variation of 28.7 % and the standard deviation value of

Area	Locality name (see Fig. 3.1)	Grain no.	Degree of pleochroism*	No. of analysis	Nb content PPM**
Blue Tier Massif	Briseis	1	W	1	ND
		2	M	1	2480
		3	W	3	ND - 1389
		4	M	2	ND
		5	W	2	ND
		6	M	3	5061 - 8336
		7	W	1	ND
		8	M	1	298
		9	W	1	571
		10	W	1	397
	Pioneer	1	W	1	ND
		2	W	1	1098
		3	W	1	ND
		4	W	1	ND
	Star of Peace	1	W	2	ND - 1195
		2	S	3	262 - 4595
		3	S	4	ND - 2105
		4	W	2	ND - 560
Mount Cameron Massif	Clifton	1	M	7	ND - 229
	Monarch	1	M	2	ND - 560
		2	W	1	ND
	Sextus Creek	1	S	2	1270 - 7509
		2	S	4	728 - 11058
		3	S	2	1382 - 6911
		4	S	5	784 - 5654

* W - weakly pleochroic, M - moderately pleochroic, S - strongly pleochroic;
** ND - not detectable.

Table 5.4 Pleochroism and Nb content of cassiterite grains from northeastern Tasmania. The latter was determined by x-ray wavelength spot mode analysis using an electron probe microanalyzer.

251 ppm are the lowest of all four elements. Unlike Nb and Ta, W is present in higher concentrations in samples from the Blue Tier Massif than in the Mount Cameron Massif. Although cassiterite from eastern Australia analysed by Steveson & Taylor (1973) failed to define any clear-cut relationship between W content and deposit type, this may be explained by the inhomogenous distribution of W in cassiterites (Barth 1986). The distriution of W found in the present study confirms the existence of regional differences between cassiterites from the Blue Tier and the Mount Cameron Massifs.

5.2.2D Zr

The overall mean and overall range found is 416 ppm and 85-1498 ppm respectively. Three samples with the highest Zr concentration, Amber Hill, Pioneer and Purdo Hill, are mainly responsible for the high coefficient of variation of 97.6 %. However, because all these samples contain substantial fine sand size cassiterite, contamination by incompletely separated zircon grains is likely. If these three samples are omitted from the determination of mean values, the Mount Cameron cassiterite with a mean concentration of 370 ppm is in excess of that from the Blue Tier Massif (218 ppm). The maximum value of 651 ppm is from a well-established pegmatite site at Sextus Creek (Twelvetrees 1916). This value is however appreciably lower than the maximum level of Zr (2400 ppm) found in cassiterites from pegmatitic veins by Dudykina (1959). The lower Zr content found in the present study again throws doubt on the previous data which were not determined by the x-ray fluorescence method.

5.2.2E Relationship between trace elements

Plots of the relationship between each pair of trace elements studied are shown in Fig. 5.4. The majority of the plots can be seen to fall clearly into two main fields one containing cassiterite originating from greisen, the other cassiterite from pegmatite sources. Both the

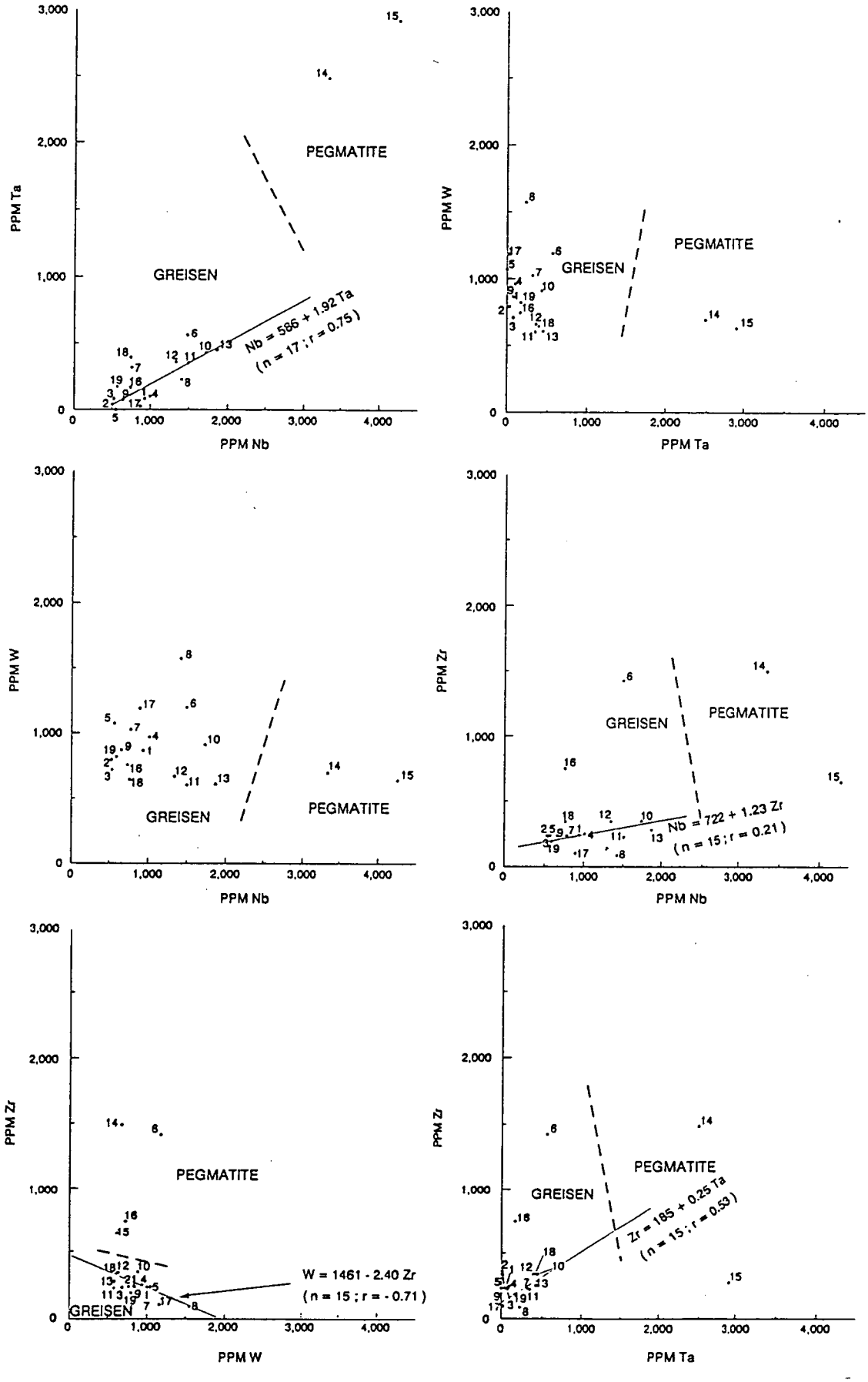

Fig. 5.4 Plots of Ta/Nb, W/Ta, W/Nb, Zr/Nb, Zr/W and Zr/Ta in cassiterites from northeastern Tasmania. Sample numbers are explained in Table 5.3. The probable hypothetical boundary between the greisen/pegmatite fields is indicated by dashed lines.

Sextus Creek and Purdo Hill samples plotted in the pegmatite field which is distinctly enriched in Nb and Ta, Nb over W and Ta over W. Ta/Nb, W/Nb, Zr/Nb and Zr/Ta were found to show a positively correlated linear trend while Zr/W and W/Ta show a negative trend.

The significance of the correlation coefficient depends on the number of samples involved. Although the number of samples used in the present study is small, Nb is found to show the strongest positive correlation with Ta ($r = 0.95$) followed by Ta with Zr ($r = 0.61$) and Nb with Zr ($r = 0.53$). The remaining pairs of elements all show weak negative correlation ranging from -0.11 to 0.31. However, if the Amber Hill, Pioneer and Purdo Hill samples are omitted from the determination of correlation coefficients, the positive correlation between Ta and Zr, and Nb with Zr is stronger at 0.86 and 0.77 respectively while the negative correlation between W and Zr increases from -0.11 to 0.60.

A comparison between the trace element content of two cassiterite samples from the Blue Tier Massif studied by Steveson & Taylor (1973) and that of another sample studied in the present study is shown in Table 5.5. With the exception of W content, Nb, Ta and Zr were all found to be significantly lower in the Star of Peace sample. The W content exceeds the concentration of the two localities studied by Steveson & Taylor (1973) by over seven times. This difference in results is best explained by the superior precision and accuracy of the x-ray fluorescence method over spectrochemical methods in the determination of all four trace elements.

The trace element contents of cassiterites in the Mount Cameron and Blue Tier Massifs are found to differ (Table 5.3). The former is relatively enriched in Nb, Ta and Zr but is depleted in W in comparison to the latter. This difference in trace element composition is thought to reflect the geochemical differences between the two mineralization centres, the widespread bedrock tin mineralization in northeastern

Locality	Source	PPM			
		Nb	Ta	W	Zr
Don	Steveson & Taylor (1973)*	10000	800	200	250
Summit	Steveson & Taylor (1973)*	10000	1000	200	250
Star of Peace	Present study	1429	234	1570	85

* - Determined by emission spectrographic method.

Table 5.5 Comparison of Nb, Ta, W and Zr content in cassiterites from the vicinity of Mount Paris on the Blue Tier Massif.

Tasmania, and the predominance of pegmatite and greisen source rocks on Mount Cameron and Blue Tier respectively. Because of these differences, the transportation of cassiterite from the Blue Tier to Mount Cameron (a minimum distance of 8 km) may be ruled out. Consequently, it is not necessary to use the 'Ringarooma Lead' of Nye (1925) to account for placer occurrences far away from the Blue Tier Massif.

5.2.2F Nb content and pleochroism of cassiterite

The pleochroic character of cassiterites from the tin belts of southeast Asia was noted by Hosking (1977). Four types of cassiterites displaying different degrees of pleochroism were recognised by him including:

(1) Intensely pleochroic - Much or all of the crystal displays intense red to pale (pale brown, colourless, etc.) pleochroism.

(2) Strongly pleochroic - The crystal contains zones that displays red to pale pleochroism.

(3) Moderately pleochroic - The crystal possesses zones or patches that display pink to other pale colour pleochroism.

(4) Non-red and non-pleochroic - Either the crystal displays pleochroism involving colours other than red or pink (such as dark brown to pale brown, yellow to light yellow) or exhibits no obvious pleochroism.

Furthermore, pegmatitic cassiterites were noted by Taylor (1979) to be intensely pleochroic while those from other types of environments show varying degrees of less intense pleochroism. Therefore the degree of pleochroism in cassiterite from northeastern Tasmania may be a possible means of distinquishing between pegmatitic and other types of mineralization. In the present study, Nb is selected for investigation because it is known to be enriched in pegmatitic cassiterite and is present in greater abundance than Ta in cassiterites. The abundance makes it easier to determine accurately.

The four degrees of pleochroism of Hosking (1977) is reduced to three in the present study. The intensely and strongly pleochroic types are combined into a strongly pleochroic category while the moderately pleochroic type remains unchanged and the non-pleochroic type becomes weakly pleochroic.

A summary of the degree of pleochroism and the Nb content in selected cassiterite grains from northeastern Tasmania is shown in Table 5.4. At Sextus Creek where a pegmatitic source for the cassiterite is supported by the presence of topaz exceeding 0.2 m in length (Twelvetrees 1916) and banded smoky quartz crystals up to 0.3 m long (J. C. van Moort, pers. comm.), all four grains studied are strongly pleochroic and a maximum Nb content of 11 058 ppm is found. However, within the Mount Cameron Massif, weak to moderately pleochroic cassiterite with low Nb content below the detection limit of about 100 ppm as in the case of grain no. 2 Monarch (Table 5.4) also exists. Similarly at Star of Peace in the Blue Tier Massif, strongly to weakly pleochroic grains coexists. Therefore both the Mount Cameron and Blue Tier Massifs are likely to contain other sources of cassiterite in addition to pegmatites.

In the strongly pleochroic cassiterite grains from Sextus Creek, the most deeply coloured part of cassiterite grains seen under a petrological microscope in transmitted light was found to show the highest Nb content. Since pentavalent Nb and Ta (both ionic radius 0.72 Å) may replace Sn (0.77 Å), a disturbance in the valency balance and crystal lattice of the cassiterite is possible. However, trace element mapping of Malaysian cassiterites with a scanning electron microscope by Santokh Singh & Bean (1968) revealed no evidence for lattice distortion and inclusions essentially of Nb, Ta, Fe and Mn were identified. Therefore it is probable that both Nb and Ta are present in the form of exsolved phases.

Pleochroism alone is concluded to be insufficient as a criterion for provenance identification in northeastern Tasmania because in both the Mount Cameron and Blue Tier Massifs cassiterites are not restricted to pegmatitic sources only. Nevertheless, this property is confirmed as valuable in identifying cassiterites from pegmatitic sources.

5.3 Dating of zircons

5.3.1 Fission track dating of zircons

The results and discussion of this study are reported in Yim et al. (1985) (Appendix II). The main conclusion is that the fine euhedral and coarse anhedral zircons shown in Table 4.1 differ in their provenance. The former with a combined age of 367 $\pm$ 15 Ma were derived from Upper Devonian granites while the latter with a combined age of 46.7 $\pm$ 0.6 Ma were derived from the older Tertiary basalts. The age of the latter is in good agreement with K-Ar radiometric ages (ca. 47 Ma) obtained from three Blue Tier basalts by Sutherland & Wellman (1986).

5.3.2 ESR dating of zircons

The zircon concentrates fission-track-dated by Yim et al. (1985) together with a number of coarse anhedral zircons from other localities were chosen for ESR study. Fig. 5.5 shows the ESR signals for the three previously dated samples. It can be seen that the fine euhedral zircons from the Weld River show appreciably stronger signals than the two samples of coarse anhedral zircons. This is in spite of a scale difference of less than a third that used for the fine euhedral zircons. It is not possible to show all the fine euhedral zircon sample on the same scale because of the strong signal found. Furthermore, the coarse anhedral zircons from the Weld River has a marginally weaker ESR signal in comparison to the coarse anhedral zircons from the Mutual Mine. This is in agreement with the combined fission track ages obtained of 46.3 $\pm$ 1.8 and 47.1 $\pm$ 1.4 Ma respectively, suggesting that the sensitivity of the ESR method is better than $\pm$ 2 % for zircons of Eocene age. Therefore

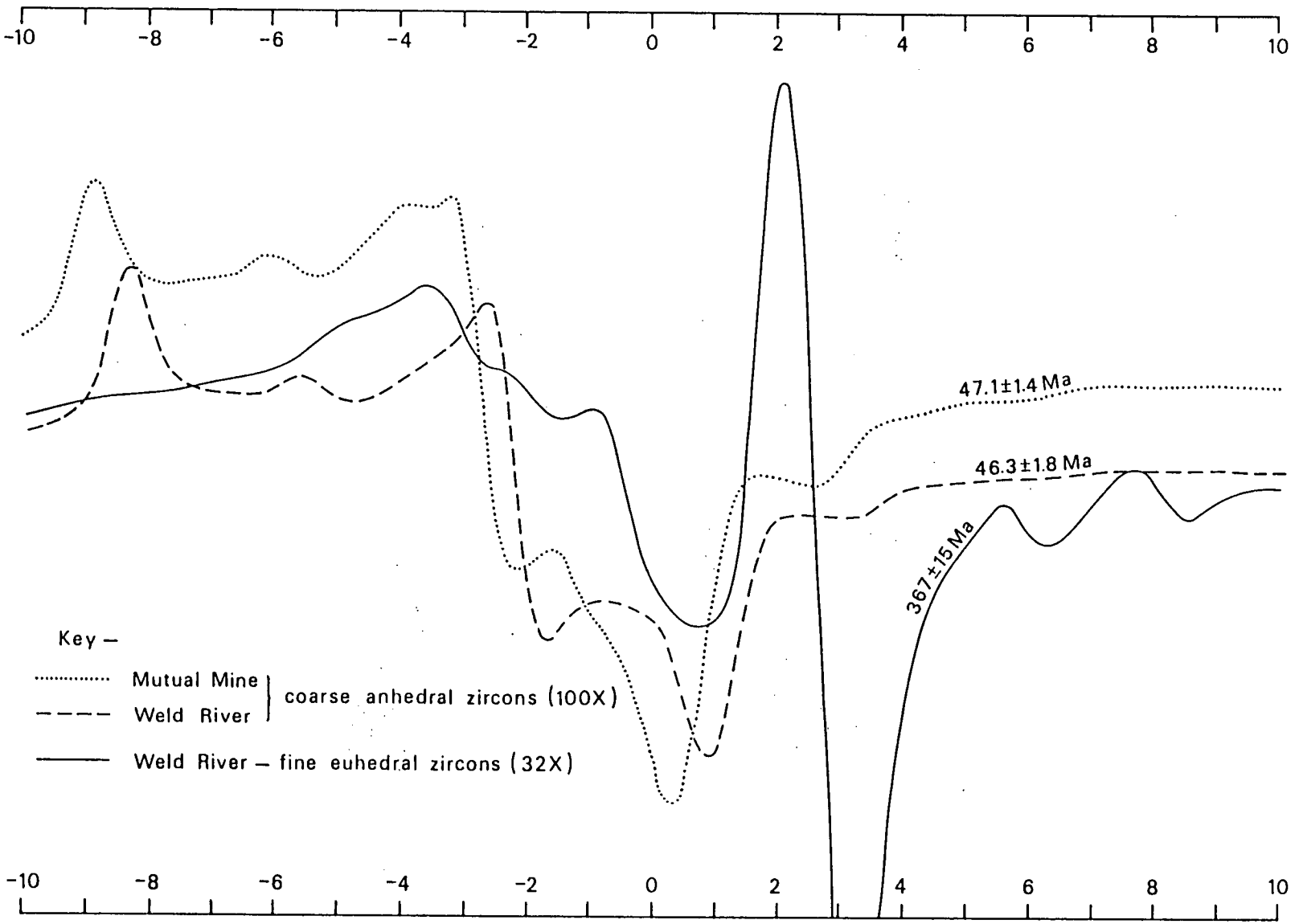

Fig. 5.5 ESR signals for three alluvial zircons previously fission track dated by Yim et al. (1985). Instrumental conditions used include radio frequency 9.26, magnetic field intensity 3305.5 ± 25G, sweep time 4 minutes, modulation 100K Hz 2 X 1G, and response 0.3. The difference in scale used for the fine euhedral and coarse anhedral zircons are as indicated.

the ESR results confirmed the granitic and basaltic derivation for the two types of zircon and the fission track ages of ca. 367 and 47 Ma respectively (Yim et al. 1985).

ESR signals obtained for coarse anhedral zircons from five other localities within the study area are shown in Fig. 5.6. With the possible exception of the Bells Plain sample which shows a slightly weaker signal, all the signals found are closely similar to each other and to the fission track dated coarse anhedral zircons from Mutual Mine and Weld River (Fig. 5.5). Therefore it is concluded that these zircons are all ca. 47 Ma in age and have been derived from the older Tertiary basalts. The weaker ESR signal shown by the Bells Plain sample may be explained by zircons with a derivation from Grays Hill (Fig. 2.6) which may be younger in age than the Blue Tier basalt or by variation in radioactive element content within the zircons. Furthermore, it is possible that zircons deriving from basalts intermediate in age between the younger and older Tertiary basalts have been missed because of the small number of zircon grains measured. It should be noted that minor variations shown by individual samples thought to be of the same age are not well understood at present and requires follow-up investigation which is outside the scope of the present study. Nevertheless by using zircon samples dated previously by the fission track method, it is possible to calibrate the ESR signals and correlate them with other measurements on alluvial zircons. ESR measurements are therefore a powerful tool for determining the provenance of zircons as well as an indirect method of dating. Major advantages of the ESR method over the fission track method is that the former is fast and non-destructive. One disadvantage is the relatively large sample weight required.

5.4 Hydraulic equivalence of heavy minerals

Hydraulic equivalence was originally introduced by Rubey (1933) in a theoretical study to explain the size distribution of heavy minerals

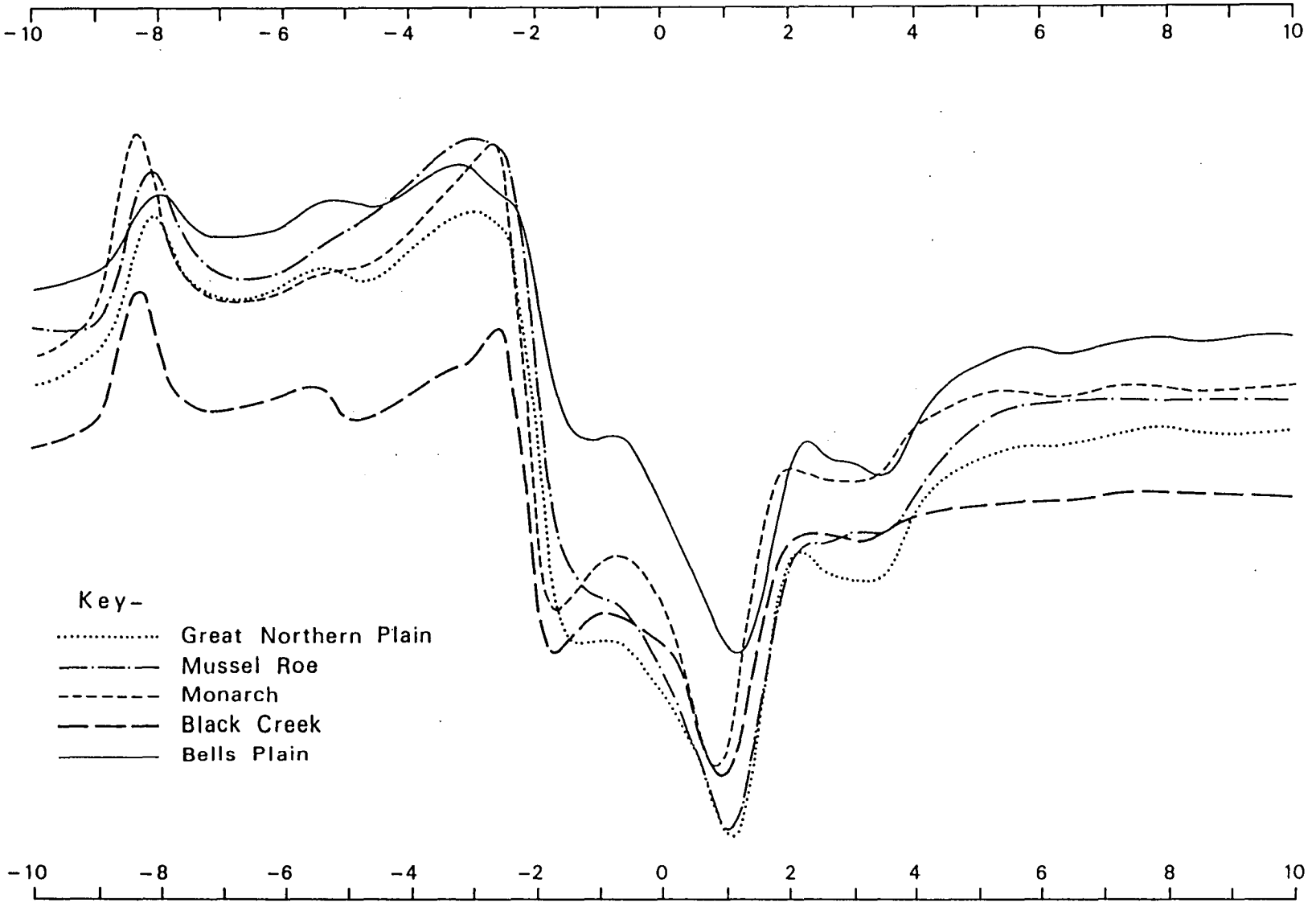

Fig. 5.6 ESR signals for coarse anhedral zircons from miscellaneous localities in northeastern Tasmania. Instrumental conditions used are the same as in Fig. 5.5. All signals are shown on the same scale.

within a water-laid sandstone. The concept was stated by Rittenhouse (1943) as 'under given hydraulic conditions grains of heavy minerals would, because of their greater specific gravity, tend to be deposited with quartz and other light minerals of somewhat larger size'. In an attempt to use heavy minerals to evaluate the sediment sources in the Rio Grande valley of New Mexico, Rittenhouse (1943) found that the size distribution of a heavy mineral in a fluvial deposit depended upon:

(1) its relative availability in each size grade in the stream load,

(2) its equivalent hydraulic sizes,

(3) the hydraulic conditions at the time and place of deposition, and

(4) some factors or factors now unknown.

The term 'hydraulic ratio' was introduced as a method of representing the heavy mineral composition of sediments. It measures directly the relative availability of heavy and light minerals of equivalent hydraulic value.

The main interest of hydraulic equivalence in the present study is the possibility in using it to assist identification of the distance of transport of heavy minerals deriving from different source rocks within the same drainage catchment. Previous studies, such as by Tourtelot (1968) and Hazelhoff Roelfzema & Tooms (1969) made use of the hydraulic equivalent grain size of quartz to the heavy minerals of interest. Since Stokes Law states that the settling velocity of a spherical particle vary as the square of the particle diameter, as the effective density of the particle in the fluid, and inversely to the viscosity of the fluid, it is controlled by the following relationship:

$$V = \frac{g}{18} \cdot \frac{Pq - Pw}{n} dq^2 = \frac{g}{18} \cdot \frac{Pm - Pw}{n} dm^2$$

(where V - settling velocity of both grains in cm/sec

Pq - specific gravity of quartz

Pw - specific gravity of water = 1.00

Pm - specific gravity of heavy mineral

dq - diameter of quartz in mm

dm - diameter of heavy mineral in mm

n - coefficient of viscosity of water

g - acceleration due to gravity)

For example, in the case of cassiterite (S.G. = 7.00)

$$(2.66 - 1.00)\, dq^2 = (7.00 - 1.00)\, dm^2$$

$$dq^2 = \frac{6.00}{1.66} \cdot dm^2$$

and $$dq = 1.901\ dm$$

However, Stokes law is adhered to only under certain conditions including:

(1) Particles are spherical.

(2) Mineral grains are monomineralic. It is not practical to use composite mineral grains because of their variable specific gravities.

(3) Particles are below 0.2 mm in diameter. For grains exceeding 0.2 mm in diameter, the settling velocity is proportional to the square root of the diameter rather than the square (Rubey 1933).

(4) The particles should be settling through an infinitely large quiescent volume of water under free settling conditions.

(5) The proportion of solids does not exceed 0.5 % by volume.

Because of the coarse particle size of heavy minerals (Table 5.6), the subangular to subrounded nature of cassiterite in northeastern Tasmania (Table 4.2) and the problem of sampling heavy minerals, the hydraulic equivalence concept may not be applicable. Furthermore, other types of heavy mineral concentrating processes including entrainment and dispersive equivalence, and interstitial entrapment are possible. The

Particle size (mm)						
Source rock	Granite			Basalt		
Locality name (see Fig. 3.1)	Monomineralic cassiterite	Composite cassiterite	Topaz	Zircon	Corundum	Spinel
SG	6.9 - 7.1	-	3.6	4.6 - 4.7	4.0	3.7 - 4.2
Banca	6.5	18.5	-	13.2	7.8	4.3
Bells Plain	5.2	5.8	10	6	13	9.8
Blackberries	12.5	38	11.8	4.5	9.5	2.5
Cascade Creek	7.5	4.2	15.8	7	16	11.2
Monarch	14	25	7	4.8	7	6.8
Mussel Roe	7	10	5.2	8	7	8.1
Mutual	10	6.4	4	6	7.6	7
Pioneer	5.8	3.8	5	5.8	4.1	4
Spinel Creek	9.5	4	-	5.8	11.5	4.8
Weld River	6	6.2	-	6	11.8	6

Table 5.6 Maximum particle size of selected granitic and basaltic heavy minerals from northeastern Tasmania.

latter is favoured by Reid & Frostick (1985) in accounting for the frequent association of placers with coarse-grained sediments.

By far the most serious problem in applying hydraulic equivalence for the determination of the distance of transport of heavy minerals found in the present study is the difficulty in collecting representative samples across the same time plane. Both vertical and lateral variability in sediments, and the lack of continuous exposures make this impossible. The only means of putting hydraulic equivalence into practice is restricted to the study of sediments in active streams. This is ruled out in northeastern Tasmania for two reasons. Firstly, most streams are contaminated by mine tailings, and secondly, active stream sediments may not be relevant in the study of palaeo-placers because the present environment may be very different from the past.

In order to take into account hydraulic equivalence as well as interstitial entrapment, the maximum particle size of selected granitic and basaltic heavy minerals was measured and used to provide some indication of the distance of transport (Table 5.6). The following observations may be drawn from the results:

(1) The coarsest particle size heavy minerals consist usually of monomineralic and composite cassiterite grains, and spinel. Because of the density difference between cassiterite and spinel, the former is likely to be autochthonous or locally derived while the latter is allochthonous or foreign in origin.

(2) The maximum size of a heavy mineral is dependant on the size of the mineral within the source rock. This is expected to be variable from place to place if multiple sources are present.

(3) The lower density heavy minerals are not in hydraulic equivalence with the monomineralic cassiterite grains. This is shown by their smaller particle size.

(4) The smaller particle size of corundum and zircon than cassiterite in many localities is indicative of their transported origin in contrast to the locally derived cassiterite monomineralic and composite grains.

In addition to the above observations, the transportation resistance of the heavy minerals including their resistance to abrasion and impact, solubility and reactivity are also likely to affect particle size distribution. Although hydraulic equivalence may exist locally on a restricted scale, in a regional study of involving coarse-grained sediments, the difficulties in sampling and the time consuming nature of particle size measurements does not permit its use. Consequently, the determination of the mean size of individual heavy minerals from in situ samples was not carried out.

5.5 Conclusions

The main conclusions drawn are:

(1) Particle size analysis of tin concentrates have revealed significant amounts of cassiterite exceeding 2 mm. Based on the particle size distribution, kulit, kaksa and mintjan types of economic cassiterite placers have been identified in northeastern Tasmania. However, at least in some of the tin mines, all three types of placers may occur in close association with each other.

(2) Cassiterites from the Blue Tier and Mount Cameron Massifs have been found to show differences in Nb, Ta, W and Zr content. In the former and latter localities, the cassiterites are relatively enriched in W, and, Nb, Ta and Zr respectively. Because of the geochemical differences found in trace element distribution within cassiterites from the Mount Cameron and Blue Tier Massifs, long distance of transport of cassiterite exceeding the 10 km distance between the two massifs is ruled out.

(3) Based on the particle size distribution of monomineralic and composite cassiterite grains, it is concluded that bedrock tin mineralization in the study area is widespread and the distance of transport does not exceed 1 km.

(4) Both fission track dating and ESR study of zircons have confirmed the granitic and basaltic provenances of the fine euhedral and coarse anhedral zircons respectively. There is evidence from ESR measurements for a younger age group of coarse anhedral zircons probably deriving from Grays Hill.

(5) Difficulties in the application of hydraulic equivalence to placer studies in coarse-grained sediments exist. In the present study, sampling difficulties and the time consuming nature of particle size measurements of individual heavy mineral species are considered to be the main obstacles.

(6) Based on the maximum particle size of granitic and basaltic heavy minerals found in northeastern Tasmania, it is suggested that the lighter heavy minerals including topaz, zircon, corundum and spinels are appreciably more mobile than monomineralic and composite cassiterite grains.

PART 3 STRATIGRAPHIC CONTROL, CLASSIFICATION AND GENESIS OF STANNIFEROUS PLACERS

CHAPTER 6 STRATIGRAPHIC CONTROL OF STANNIFEROUS PLACERS

6.1 Introduction

In this chapter, stratigraphic control of the placer deposits in northeastern Tasmania is determined using lines of evidence other than heavy mineral provenance and distribution. The main objective is to identify the age or ages of placer formation so that a better understanding may be obtained on the processes and palaeoenvironmental events involved in concentration of heavy minerals. In order to date such events, plant remains, palaeosols, palaeo-oceanography, K-Ar dating of basalts, and fission track dating of zircons are examined. The fit between different lines of evidence is considered to be important in indicating the stratigraphic control of placer deposits, and consequently promote understanding of their genesis.

6.2 Evidence from plant remains

Plant remains occurring within a placer sequence may provide information on age as well as on the palaeoenvironment. Although palaeo-botanical studies of such materials is outside the scope of the present investigation, based on studies carried out by previous workers, it is possible to draw useful conclusions.

A summary of the stratigraphic information on placer deposits in northeastern Tasmania based on the study of plant remains is summarised in Table 6.1. It is of interest to note that in spite of the geographic distribution of localities investigated, the inferred ages are all greater than the Middle Miocene age of the Winnaleah-Ringarooma basalts (Brown 1977) occurring to the west of the Pioneer Tin Mine. In the deep lead sequence occurring in the mine, the plant fossil-bearing layers in the upper part were thought to represent areas cut off from the main flow resulting in bodies of still water from which fine sediments and plant debris settled (Morrison in Hill & Macphail 1983). Because the sediments were deposited in a braided fluvial fan under a high energy

Source	Locality	Stratigraphic information	
		Age	Palaeoenvironment
Harris (1965)	various leads (Endurance, Mussel Roe, Star Hill)	Early Miocene	cooler than the time of marine sediment deposition during the Late Oligocene & Early Miocene
Harris (1965a)	Arba, Star Hill	Late Oligocene to Early Miocene	not specified
Morrison (1980)	Pioneer	Late Oligocene to Early Miocene	temperate rainforest
Hill (1983); Hill & Macphail (1983)	Pioneer	Oligocene	closed temperate rainfore-st
Bigwood & Hill (1985)	Hasties	Middle to Late Late Eocene	subtropical to tropical

Table 6.1 Summary of stratigraphic information on Tertiary sediments in northeastern Tasmania based on the study of plant remains by previous workers.

environment (Morrison 1980), it is likely that each layer represents a short-term event. An example of one such layer is shown in Plate 6.1. Since the main placer-bearing sequence in the deep lead lies immediately above the granitic rock basement beneath the fossil-bearing layers studied by Macphail in Morrison (1980), Hill (1983) and Hill & Macphail (1983), the sequence is stratigraphically confined by the age of the plant remains studied. The Early Miocene ages indicated in Table 6.1 provide a minimum age of placer burial. Consequently, the age of the deep leads is Early Miocene or older. At the Hasties Tin Mine, the age determined from Araucarian macrofossils by Bigwood & Hill (1985) is likely to be as old as the Middle to Late Eocene even though the stratigraphic relationship to the tin deposits is uncertain. Note that the cassiterite present may have been recycled previously prior to deposition with the zircospilic suite of heavy minerals.

In the present study, organic lag deposits containing abundant plant remains have been found immediately above the granitic rock basement (Plate 6.2). Since age information obtained from this deposit is likely to provide a more accurate maximum age for the placer sequence, one sample collected from this horizon was submitted to the Bureau of Mineral Resources, Geology and Geophysics for palynological studies. However, the results are not yet available for inclusion.

6.3 Evidence from palaeosols

A palaeosol is defined as a buried soil or a soil of the past (Bates & Jackson 1984). A hard layer in the upper horizons of a soil representing remnants of palaeosols is referred to as a duricrust (Woolnough 1927). In northeastern Tasmania, duricrusts occur in the form of ferricretes and silcretes. They represent remnants of Tertiary soil development events which may be useful as stratigraphic markers when they occur either within or overlying deep lead sequences. However, the origin of ferricretes and silcretes are both not well understood.

Plate 6.1 A plant fossil-bearing layer sandwiched by kaolinitic clays within the upper part of the deep lead sequence at the Pioneer Tin Mine.

Plate 6.2 An organic lag layer occurring above the granitic basement at the base of the deep lead sequence at the Pioneer Tin Mine.

Nevertheless, favourable local factors including the existence of Middle Miocene basaltic lava flows, suitable climatic and groundwater conditions are likely to have played a part in northeastern Tasmania. In this section, the value of ferricretes and silcretes as a stratigraphic marker for placer deposits is examined. Fig. 6.1 shows a distribution map of ferricretes and silcretes in the South Mount Cameron Basin based on the 1 : 50 000 Ringarooma geological map sheet.

6.3.1 Ferricretes

Ferricrete is defined as a conglomerate consisting of surficial sand and gravel cemented into a hard mass by iron oxide or a ferruginous duricrust (Bates & Jackson 1984). In the field, laterites and bauxites may occur in close association with ferricretes. These are defined by the same authors as a highly weathered red subsoil or material rich in secondary oxides of iron, aluminium or both, nearly devoid of bases and primary silicates, and commonly with quartz and kaolinite, and, a highly aluminous laterite respectively.

Palaeosols of lateritic and bauxitic nature are common in parts of Tasmania. They are best developed on dolerites and basalts (Owens 1954; Edwards 1955) and many were formed prior to the Early or Middle Miocene (Carey 1947). In northeastern Tasmania, the formation of ferricrete was considered by Brown & Moore in McClenaghan et al. (1982) to be due to iron enrichment and cementation of Tertiary sediments during weathering and erosion of the Winnaleah-Ringarooma basalts which covered a large part of the Scottsdale and South Mount Cameron Basins. The main supporting evidence used is the occurrence of ferricrete horizons at the Tertiary sediment-basalt interface (Plate 2.1). In the present study, further supporting evidence is found at two sites. Firstly, at the Pioneer Tin Mine, irregular nodules (Plate 6.3) have been identified in situ in the top soil approximately one metre below the ground surface. Thin sections of selected fragments of nodules show a basaltic texture

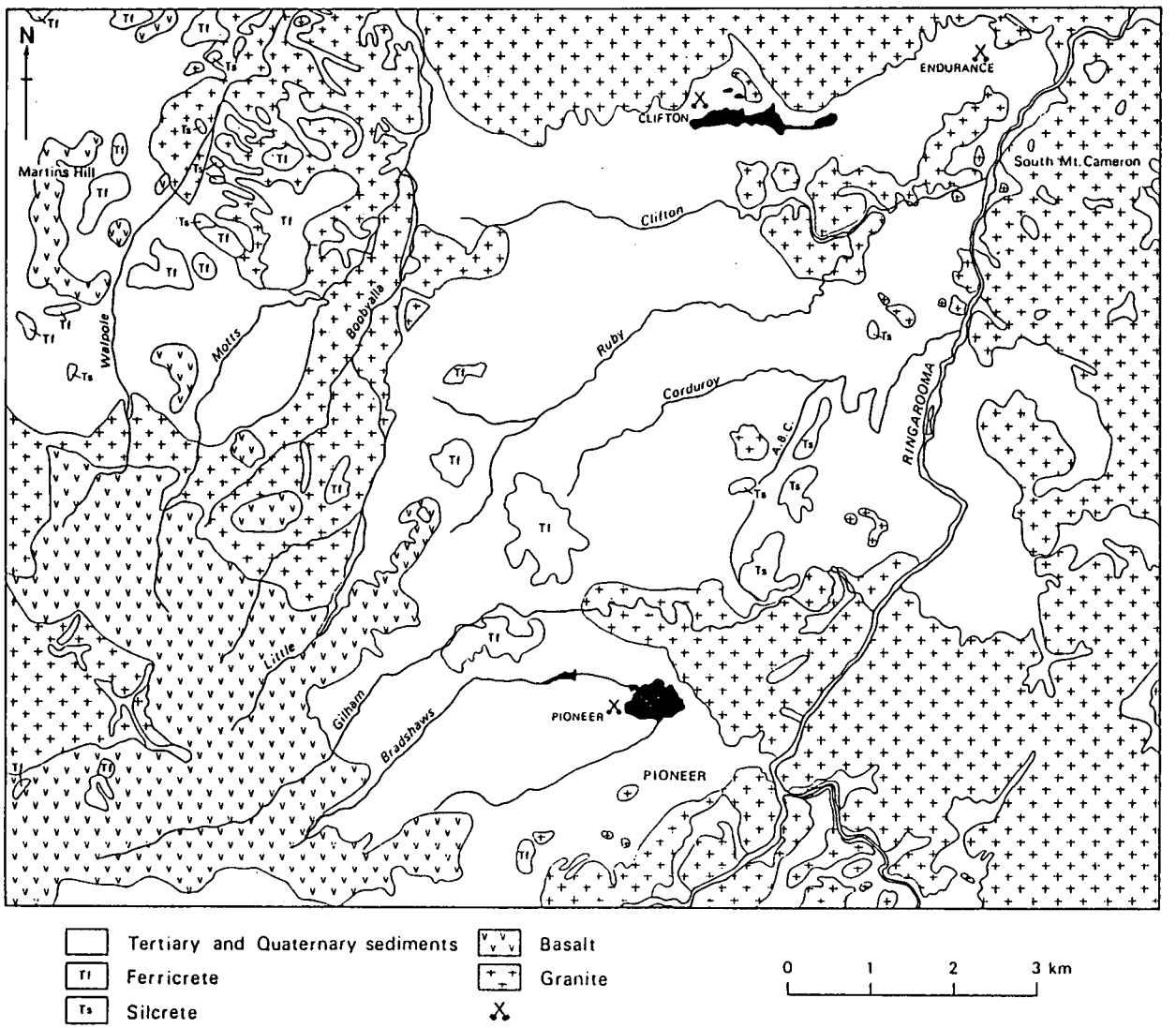

Fig. 6.1 Distrubution map of ferricretes and silcretes in South Mount Cameron Basin. Based on 1 : 50 000 Ringarooma geological map sheet.

Plate 6.3 Selected bauxitic nodules from the overburden of the Pioneer Tin Mine.

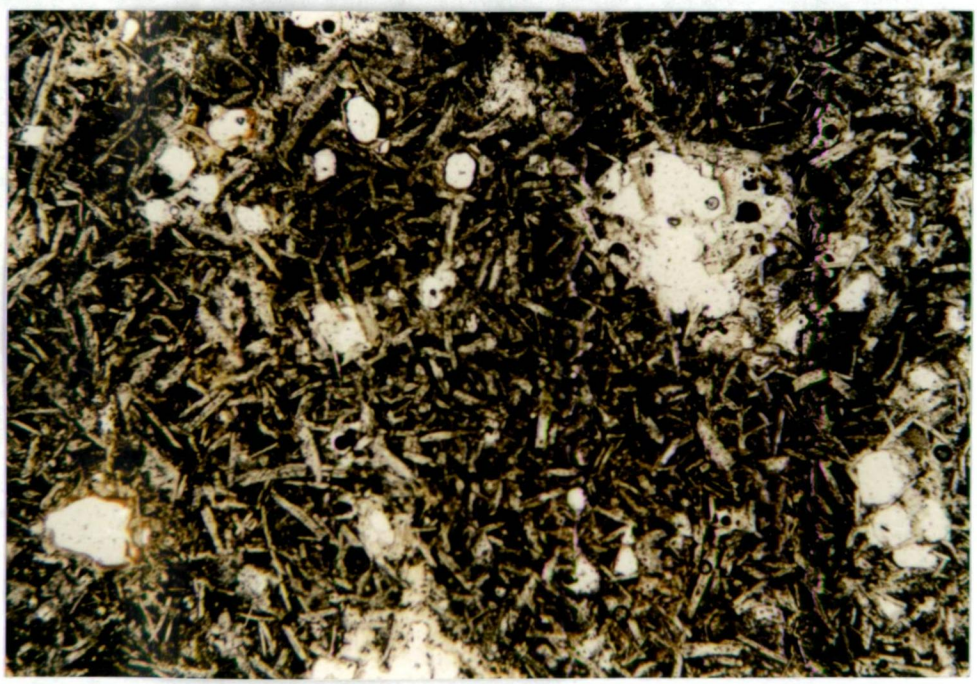

Plate 6.4 Photomicrograph of a bauxitic nodule showing basaltic texture from the overburden of the Pioneer Tin Mine. Plane polarized light. X25.

(Plate 6.4) preserved in different degrees while trace element distribution mapping by means of a scanning electron microscope confirmed their alteration to bauxite (Plate 6.5). They are confirmed to be enriched in aluminium while platy structures present are found to be depleted in aluminium and enriched in iron and titanium. Secondly, at ABC Creek where shallow alluvial mining for tin had taken place in the past, nodules similar in appearance to those of the Pioneer Tin Mine have been identified. Because the nodules at the two localities were likely to represent former extension of the Winnaleah-Ringarooma basalts dated at ca. 16 Ma (Brown 1977), an extensive former cover of basalts in the South Mount Cameron Basin is probable. Consequently, the horizons of nodules are useful as stratigraphic markers for both pre- and post-Middle Miocene placer deposits. The Pioneer deep lead belongs to the former type while deep leads including Briseis and Endurance are likely to be the same because of their similar topographic position and heavy mineral assemblage.

The presence of lateritic ferricretes in the South Mount Cameron Basin and the Scottsdale area which are both areas of low relief meets the relief requirements for the formation of bauxite (McFarlane 1983). Because of the close association between ferricretes and bauxites, their occurrence within Tertiary alluvial basins which are relatively depleted in iron and aluminium is best explained by the presence of a formerly more extensive cover of Middle Miocene basaltic lava flows. Without subaerially exposed basalts, relative and absolute accumulation, upward enrichment and residual accumulation would not be able to account satisfactorily for the distribution of ferricretes found. Since ferricretes occur in close proximity to bauxite nodules showing remnant basaltic texture, they are valuable as stratigraphic markers for stanniferous placer deposits underlain by them.

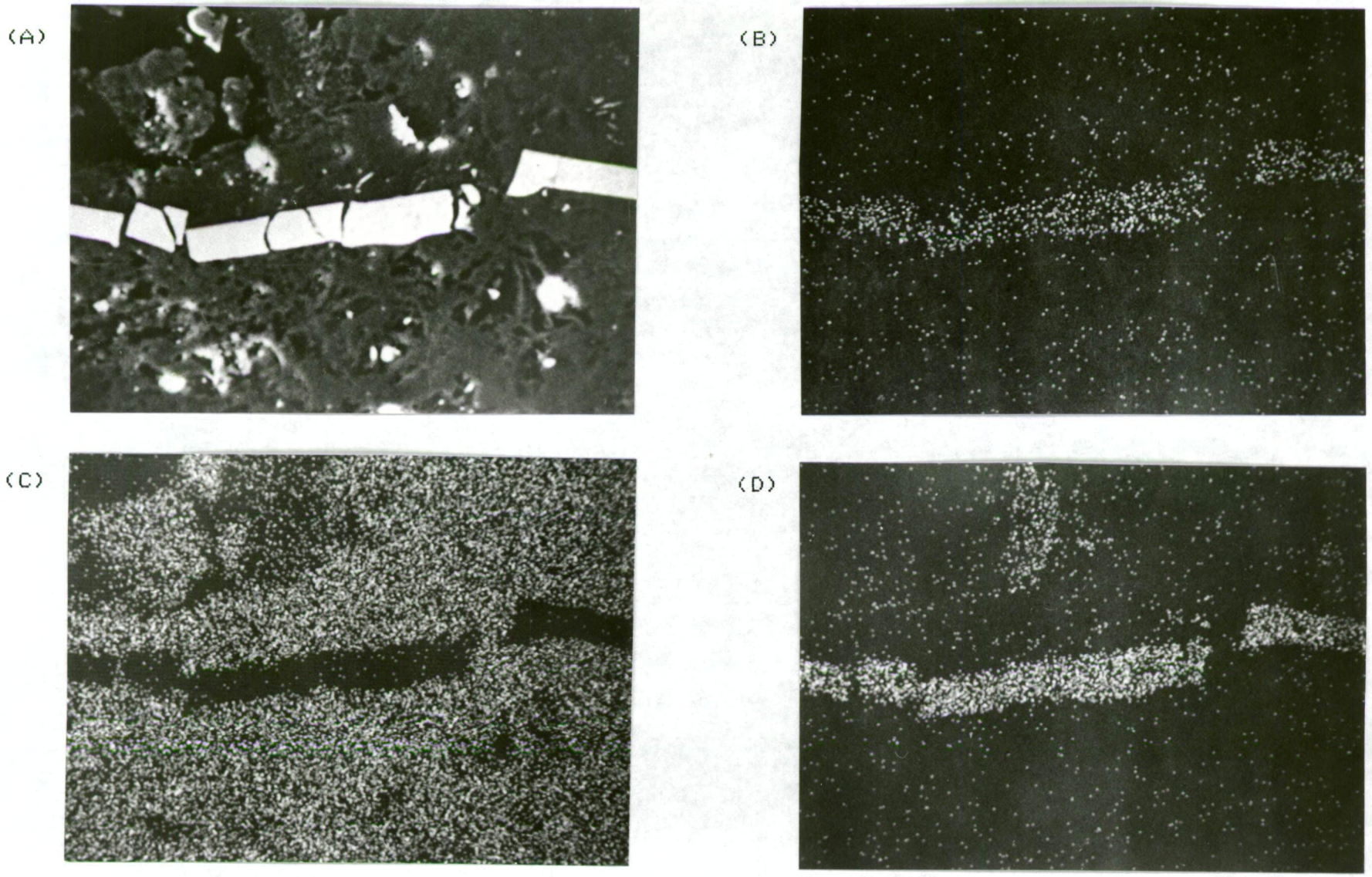

Plate 6.5 Scanning electron image (A) and distribution maps of Fe (B), Al (C) and Ti (D) in a bauxite nodule from the Pioneer Tin Mine. X800.

6.3.2 Silcretes

Silcretes are defined as siliceous duricrusts of conglomerates consisting of surficial sand and gravel cemented into a hard mass by silica (Bates & Jackson 1984). Two salient points were emphasized by Ollier (1978) in a review of silcrete and weathering. Firstly, weathering generally leads to loss of silica, and secondly, silcrete is formed only by absolute accumulation of silica. The term 'grey-billy' was used by Browne (1972) to distinquish silcretes originating from basaltic weathering from other silcretes. In the present study, silcrete of the grey-billy type is of special interest because of the close field association between basalt and silcrete in the South Mount Cameron Basin (Fig. 6.1). However, no agreement on the role played by basalt in silcrete formation was found in an Australian review by Langford-Smith (1978).

As in the Middle Shoalhaven Plain in New South Wales which was studied by Taylor & Ruxton (1987), duricrusts of iron, aluminium and silca occur in close proximity to one another in northeastern Tasmania. Because of alluvial tin mining in the present study area, excellent exposures of the duricrusts are present. In the South Mount Cameron Basin, large in situ silcrete blocks up to about 5 m in length and just below 1 m in thickness (Plate 2.2) are found. Occasionally isolated silcrete blocks referred to by tin miners as 'floaters' are encountered during alluvial tin mining (Plate 6.6). At ABC Creek (Fig. 6.1), large in situ silcrete blocks which impeded alluvial tin mining have been abandoned over parts of the site. Based largely on field and laboratory studies, the following lines of evidence are found to be in support of a basalt-silcrete association:

(1) The discovery of nodular fragments of bauxite similar in appearance to those found in the overburden of the Pioneer Tin Mine on the surface of silcrete blocks at ABC Creek. Although none of these

Plate 6.6 A silcrete 'floater' exhumed as the result of alluvial tin mining at the New Clifton Tin Mine, South Mount Cameron Basin.

fragments have so far been found in situ at ABC Creek, their size and abundance suggests that they have been derived locally and were exhumed by tin mining operations. Therefore the Winnaleah-Ringarooma basalts were likely to have extended into this area and must have been far more extensive than at present. Furthermore, it is likely that the silcrete at ABC Creek was sub-basaltic in the past.

(2) A more extensive cover of Winnaleah-Ringarooma basalts in the South Mount Cameron Basin as indicated by (1) implies that much weathering and erosion of basalts had taken place since the Middle Miocene. The release of silica during the weathering of basalts is a possible cause for silicification as was suggested by Stephens (1971), Browne (1972), Gunn & Galloway (1978) and Ollier (1978).

(3) Out of the possible source rocks present in the South Mount Cameron Basin, silica produced by the deep weathering of basalt is more likely than from the weathering of granite and alluvial sediments. Since the basalts were extrusive, their subaerial exposure and mineralogical composition would make them particularly susceptible to chemical breakdown. Furthermore, the granitic rocks within and surrounding the basin because of their much longer subaerial exposure had already been subjected to chemical weathering prior to the extrusion of the Winnaleah-Ringarooma basalts, and, consequently are less likely to yield the silica required for silcrete formation.

Based on the identification of bauxitized basalt nodules in the overburden of the Pioneer Tin Mine and ABC Creek, and the presence of silcrete only in the latter locality, favourable geomorphological and groundwater conditions in addition to a suitable palaeoclimate are likely to be required for silcrete formation. Since silcrete is chemically and mechanically resistant, isolated ellipsoidal hills or low ridges are formed (Brown et al. in McClenaghan et al. 1982). The lower topographic elevation of the silcretes in comparison to the ferricretes

is consistent with them being stratigraphically overlain by the Winnaleah-Ringarooma basalts. Both types of duricrusts would therefore serve as markers when they overlie Tertiary sediments.

Silcrete in Australia is a prominent element of the landscape, particularly when it is in the form of a duricrust and constitutes the capping to plateaux and mesas, thereby preserving remnants of a plateau surface. Numerous authors, e.g. Taylor & Smith (1975) and Young (1978) noted that many of the silcrete occurrences have no relation to basalt occurrences. Consequently a main objection exists against a basaltic origin for all silcretes, particularly for the many areas in the arid interior of Australia where basalts are unknown. However, in eastern Australia, there is far more silcrete in the supposed laterite zone than was previously realised (Young 1985). In the Monaro silcretes studied by Taylor & Smith (1975), with one possible exception, are all spatially related to basalts showing that basalt is in some way related to their formation (Taylor & Smith 1976). The theories put forward to explain such occurrences were reviewed by Taylor & Smith (1975) and include:

(1) Silica came directly from the basalt.

(2) The basalt heated interstitial water in the underlying sediments resulting in solution and, later, precipitation of silica.

(3) Silica was released during weathering of the basalts.

(4) Silica was leached from the basalt by late stage deuteric activity.

There is evidence that during lateritic weathering aluminium is immobile compared to silica. It is consequently concentrated in the weathering profile. Experimental evidence indicates that under all but very acid conditions, pseudo-boehemite and gibbsite are far more immobile than silica (Krauskopf 1956; Wey & Siffert 1962). Consequently silcretes in weathering profiles should be seen as precipitates out of descending water carrying silicic acid liberated in the hydrolysis of silicates.

In a study of silcretes of south-central Queensland, Gunn & Galloway (1978) have drawn attention to the close association between many silcretes and the original extent of basalt flows. They concluded that weathering of the basalt released silica which was deposited under the basalt or in deep weathering profiles. Because of this, the age of silcrete formation must be younger than the basaltic rocks from which the silica was derived. Therefore silcretes may be valuable as a stratigraphic marker when they are associated with deep lead sequences.

The post-Middle Miocene age of silcrete formation for northeastern Tasmania falls within the Oligocene to Pleistocene age range for silcretes in eastern Australia postulated by Young (1985). The age in the area of study is of necessity controlled by the ca. 16 Ma age of the Tertiary basalt. Although conditions favourable for silcrete formation may have occurred since the Oligocene, suitable source rocks for the release of silica were not available until after the Middle Miocene. This principle would help to resolve the difference in ages of silcrete formation in many parts of eastern Australia where silcretes are suspected to be genetically related to Cainozoic basalts. However, where multiple eruptions of basalt had taken place, silcretes formed by earlier and later episodes of basalt weathering are possible. It is therefore essential to study the field evidence with great care particularly to identify disconformities present such as was found in southern New South Wales by Young & McDougall (1982).

6.4 Correlation with palaeo-oceanographic evidence

The placer sequences in northeastern Tasmania may be correlated with palaeoclimatic and sea-level change evidence deduced from palaeo-oceanography. Three main types of evidence are available:

(1) The palaeotemperature record obtained from stable oxygen isotope studies of planktonic foraminifera base on DSSP sites off the coast

of Tasmania (Shackleton & Kennett 1975). Sea-surface temperatures obtained may be compared to the present day mean of about 11°C.

(2) The geological history of the Bass Basin and its onshore extension to the north of the study area available through oil and gas exploration. A recent review of such information was given by Williamson et al. (1987).

(3) The global cycles of relative sea-level change identified by seismic stratigraphy (Vail et al. 1977).

The purpose of Shackleton & Kennett (1975) in studying DSDP sites 277, 279 and 281 located in Fig. 8.4 was to establish the development of the Antarctic ice sheet and the related deep temperature structure of the oceans. However, the close spacing of the samples analyzed was found to provide a highly detailed palaeoclimatic sequence. Based on oxygen isotope data for planktonic foraminifera, sea-surface temperatures were estimated (Fig. 6.2). During the Early Eocene the temperature was about 20°C, falling to about 13°C in the Middle Eocene and about 11°C in the Late Eocene. There was a further drop to about 7°C in the Early Oligocene followed by a rise and fall of about 3°C during the Early Miocene. In the beginning of the Middle Miocene, there was a rise after which there was a general decline into the Pleistocene. The duration of time for which sea-surface temperature record is available when used together with radiometric dating information provides a means of correlating between events important in the formation of terrestrial placer sequences. For example, periods of relative climatic stability and instability may be identified and related to changes in the rates of weathering and erosion. The relatively high palaeotemperatures during the Late Palaeocene to Early Eocene is probably favourable for deep weathering while the lower palaeotemperatures during the 15 Ma period between the Oligocene and Early Miocene is associated with rapid sedimentation in deep leads.

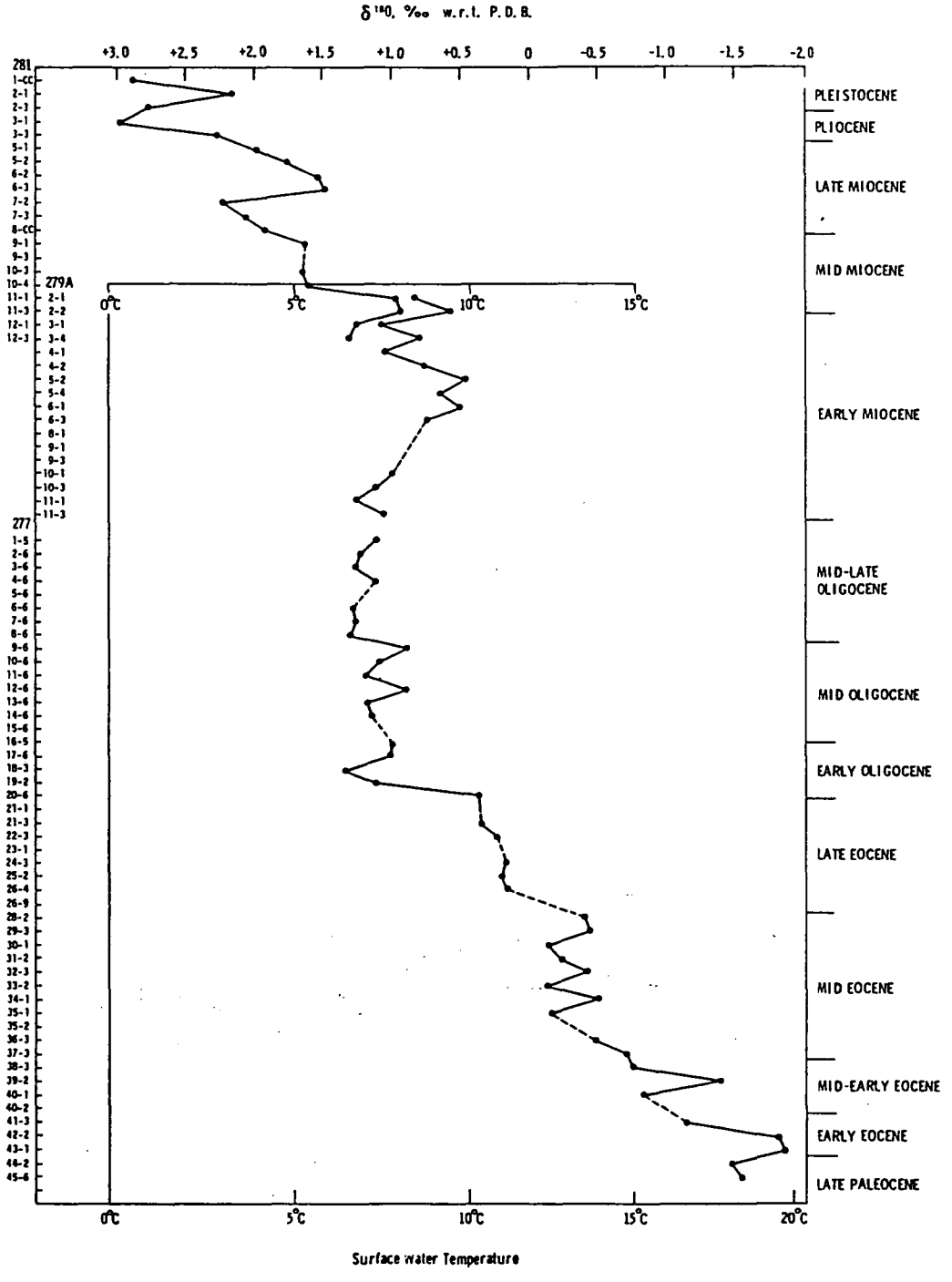

Fig. 6.2 Sea-surface temperatures estimated from oxygen isotope data of planktonic foraminifera at sites 277, 279 and 281 in the Tasman Sea. From Shackleton & Kennett (1975).

By using stratigraphic information obtained by seismic profiling, well data, and analogues with sedimentation models in modern rift valleys, the geological history of the Bass Basin was reviewed and summarised by Williamson et al. (1987) (Fig. 6.3). In Lower Cretaceous early rift-fill sedimentation caused by alluvial fan and braided river systems feeding into local, structurally controlled depocentres was the main process. Uplift during the rift phase was probably accompanied by substantial erosion of high areas. The development of alluvial fan and associated sediments was the most important event in the Late Cretaceous with the rift valleys filled to form a largely interconnected drainage system on an extensive alluvial floodplain by Late Palaeocene. Floodplain sediments continued to build up during the Eocene but by the Middle Eocene, fluvial activity had increased owing either to climatic change, tectonism, lowering of sea level, or a combination of these factors. The first major marine event in the basin began in the northwest during the Late Eocene. Between the Oligocene and Middle Miocene, sand was deposited along the northern and southeastern parts of the basin whereas carbonate sedimentation predominates elsewhere. The Upper Miocene to Holocene sediments consist predominantly of open-shelf calcarenite.

The Boobyalla Sub-basin (Moore et al. 1984), located in the southeastern sector of the Bass Basin constitutes the main depocentre for the highland area of northeastern Tasmania covered in the present study (Fig. 6.4). By correlating geological events between these two areas, a means of dating episodes important in placer formation have been obtained. The major rift episode of the basin occurred in the Late Cretaceous (Luskin et al. 1989) and the sediments consisting of poorly sorted boulder conglomerate, pebble conglomerate and ferruginous sandstone were recognised alluvial fan deposits (Moore et al. 1984).

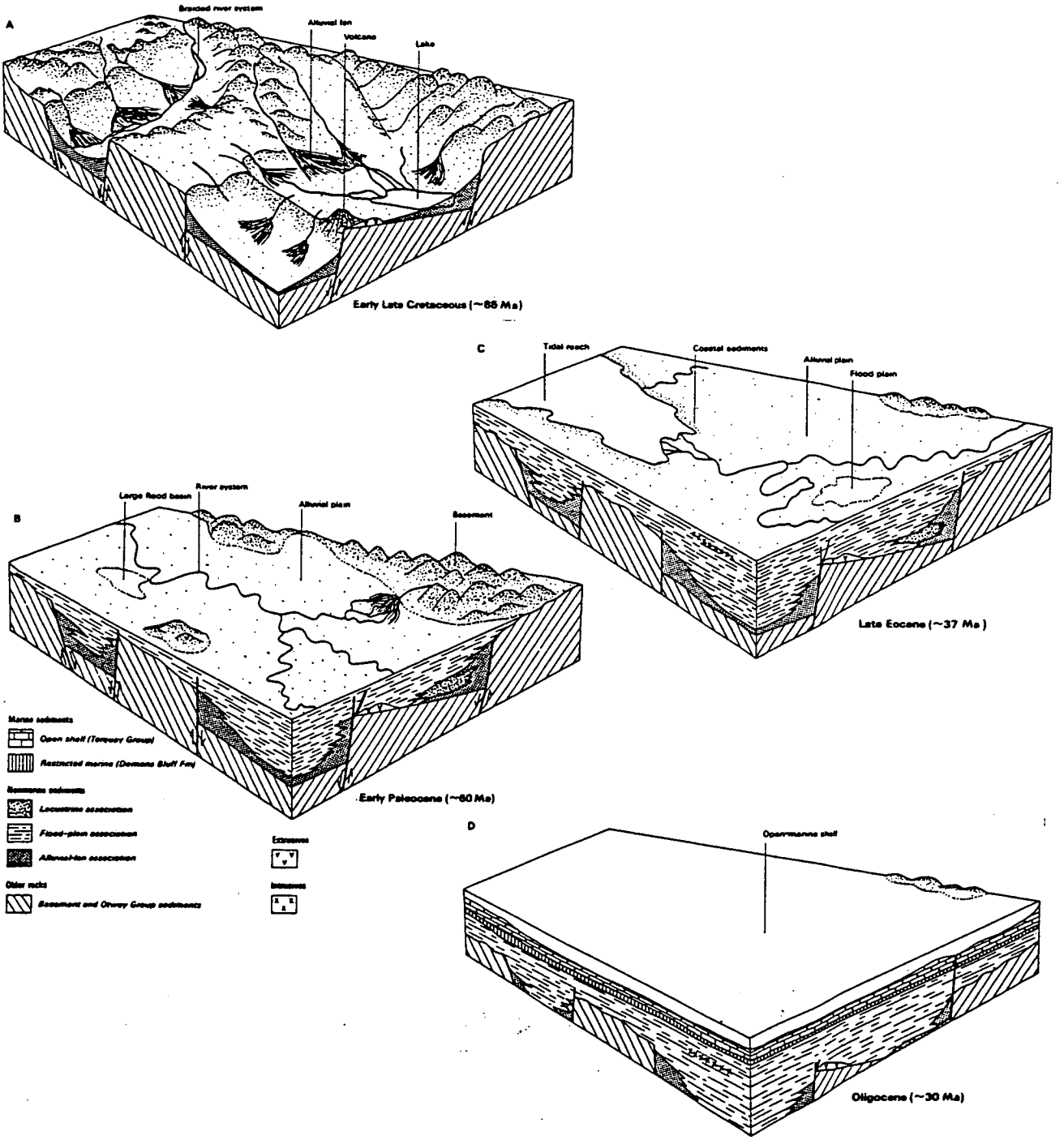

Fig. 6.3 Schematic evolution of sedimentary environments of Bass Basin from Williamson et al. (1987). (A) Middle Cretaceous base Eastern View Coal Measures (EVCM). Immediately postdates formation of basin by extensional tectonics. Alluvial-fan and braided-stream sedimentation is dominant; part of graben probably drained internally and formed lakes. Sedimentation rates were high, more than 50 m/Ma. (B) Palaeocene Lygistepollenites balmei horizon of EVCM. Most basement highs drowned, and extensive flood plain with marginal alluvial fans developed. (C) Late Eocene (Demons Bluff Formation). An extensive low-gradient flood plain passed westward into tidal-reach environment during rapid marine transgression. (D) Oligocene (Torquay Group). Establishment of shallow marine conditions led to carbonate shelf deposition, which persists to present day.

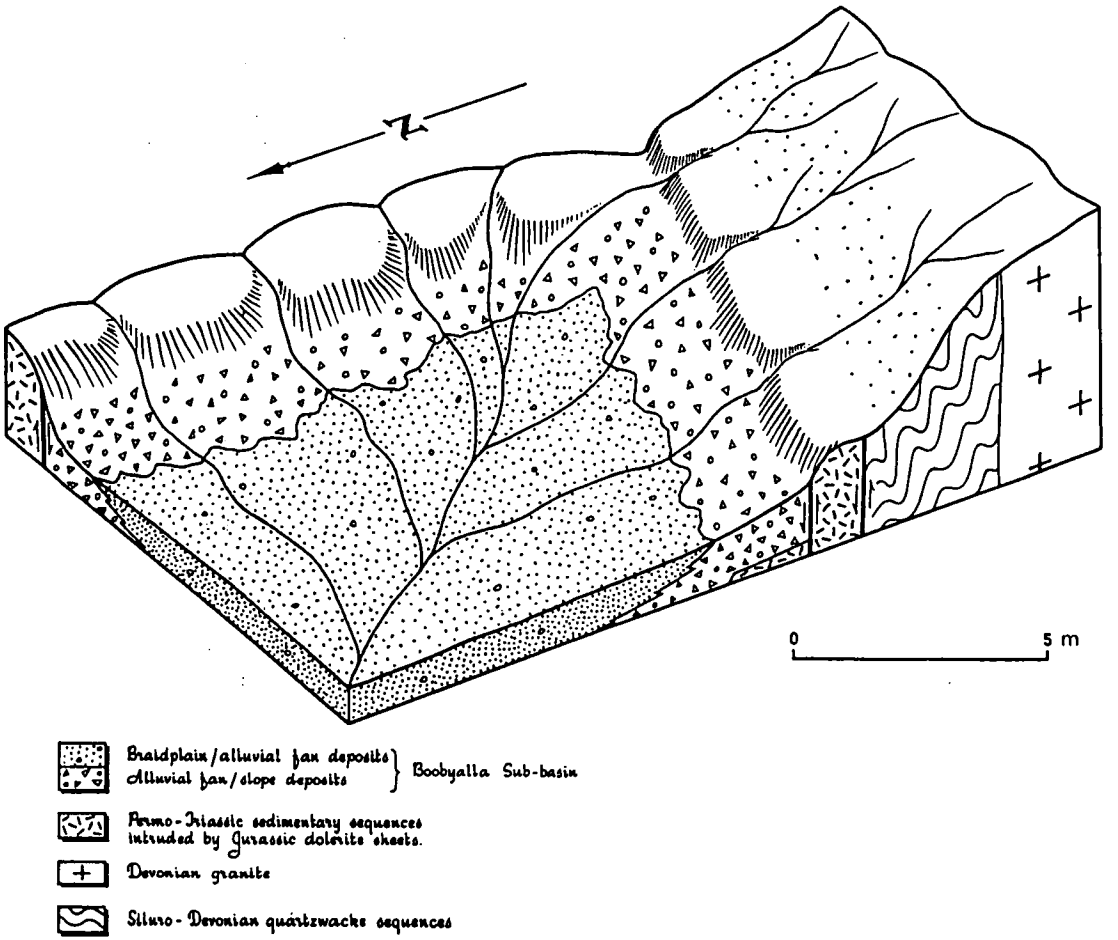

Fig. 6.4 Block diagram of the early Late Cretaceous palaeogeography of the Boobyalla Sub-basin. From Moore et al. (1984).

Based on this, erosional events in the highlands of northeastern Tasmania are likely to have prevailed from the Late Cretaceous onwards.

The global cycles of relative changes of sea level recognised by Vail et al. (1977) and recently updated by Haq et al. (1987) are likely to exert control over erosion and sedimentation rates. Fig. 6.5 shows a major regression in the Chattian resulting from the formation of the Antarctic ice sheet. The fall in sea level probably resulted in an increase in erosion rate over the highlands of northeastern Tasmania as well as an increase in sedimentation rate in the piedmont zone including the South Mount Cameron Basin and the Boobyalla Sub-basin. The cover of tin-barren Late Oligocene to Early Miocene sediments over the deep leads is in support of this.

6.5 K-Ar dating of basalts

K-Ar dating of basalts from northeastern Tasmania were undertaken by Brown (1977) and Sutherland & Wellman (1986). The samples dated include both the Winnaleah-Ringarooma and Blue Tier basaltic flows and the ages are summarized in Table 6.2. Brown (1977) obtained five dates on samples from the former, two of which including a pyroxene concentrate dated at 11 $\pm$ 1 Ma and a pyroxene glomeroporphyritic alkaline olivine basalt dated at 159 $\pm$ 6 Ma were considered anomalous. The dates of the other three samples ranging from 15.6 $\pm$ 0.3 to 16 $\pm$ 0.3 Ma were thought to be in good agreement with each other suggesting a Middle Miocene age. All three samples dated by Sutherland & Wellman (1986) were from the Blue Tier. The dates obtained are all Middle Eocene ranging from 46.2 $\pm$ 0.6 to 47.4 $\pm$ 0.5 Ma.

Because of the difference in age between the Winnaleah-Ringarooma and Blue Tier basalts, deep lead sites such as the Briseis Mine which is overlain by the former are stratigraphically confined by them and must pre-date the Middle Miocene. On the other hand, placer deposits occurring on the Blue Tier Massif may either be younger or older than

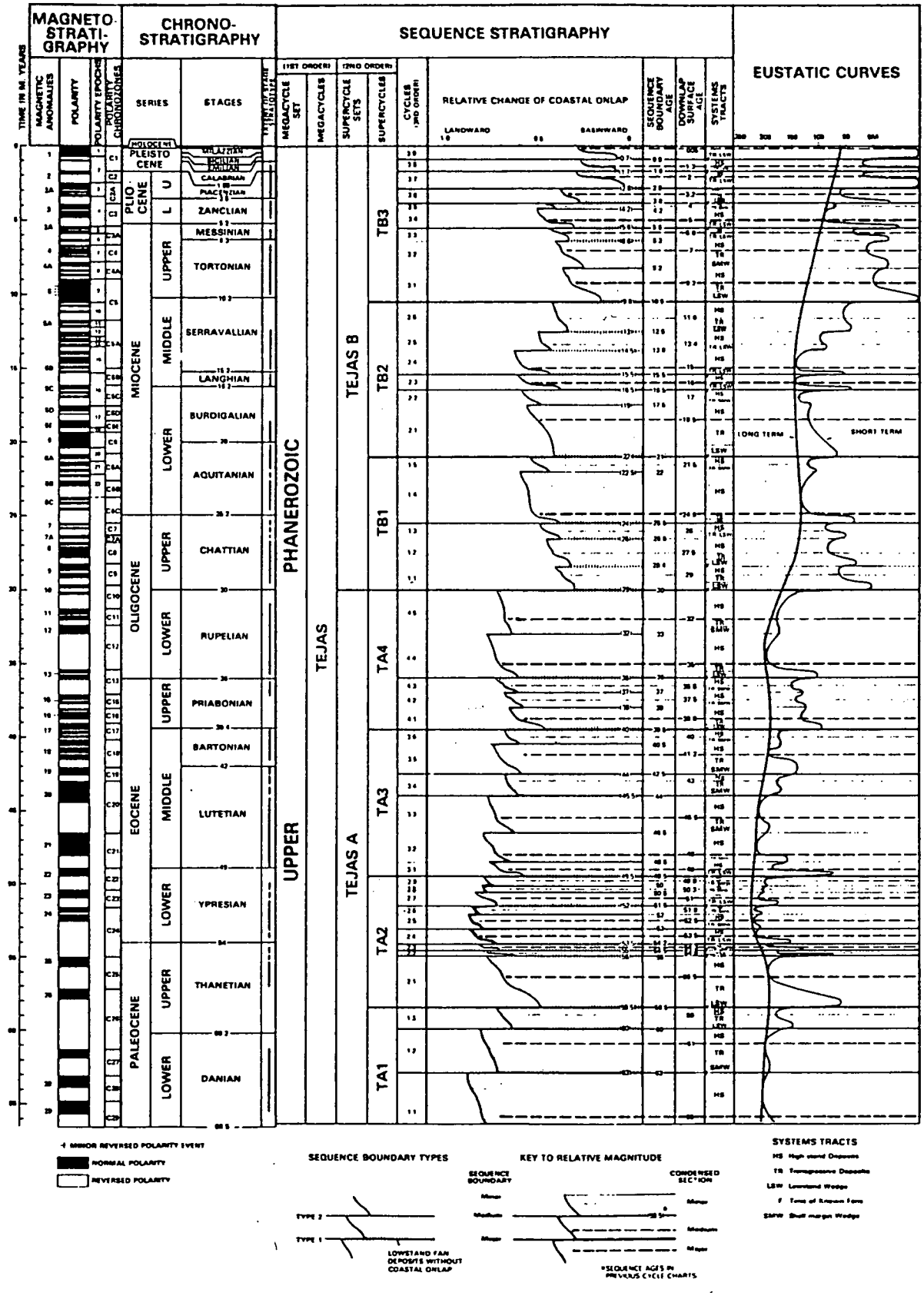

Fig. 6.5 Cainozoic chronostratigraphy and global cycles of sea-level changes. From Haq et al. (1987).

Locality	Basalts	Source	Age ± 1 SD (Ma)
David's Creek	Winnaleah-Ringarooma	Brown (1977)	15.9 ± 0.6
Swanee Creek	Winnaleah-Ringarooma	Brown (1977)	16.0 ± 0.3
Wagner's Hill	Winnaleah-Ringarooma	Brown (1977)	15.6 ± 0.3
Le Fevre Road	Blue Tier	Sutherland & Wellman (1986)	46.2 ± 0.6
Forest Lodge	Blue Tier	Sutherland & Wellman (1986)	47.3 ± 0.5
South of Weldborough Pass	Blue Tier	Sutherland & Wellman (1986)	47.4 ± 0.6

Table 6.2 Whole rock K-Ar ages of basalts in northeastern Tasmania.

the Middle Miocene when they occur at topographic elevations above the Winnaleah-Ringarooma basalts.

6.6 Fission track dating of zircons

Fission track dating was carried out to confirm the basaltic origin of the coarse, rounded zircons as compared to the fine, euhedral zircons which were thought to have been derived from the Devonian granites (Yim et al. 1985, see Appendix II). The results for single-grain fission track ages and combined fission track ages are summarised in Tables 6.3 and 6.4 respectively. The late Devonian age of the fine, euhedral zircons (sample 8022-113) is in agreement with a late Devonian age of the Blue Tier Batholith suggested by Groves et al. (1977). On the other hand, when the ages of the two coarse, rounded zircon concentrates (8022-114 and 8022-115) are averaged, an age of 46.7 $\pm$ 0.6 Ma in the Middle Eocene is obtained. This is in agreement to within experimental error with the K-Ar age of the Blue Tier basalts obtained by Sutherland & Wellman (1986). However, since the spread of results for individual grains is from 42 $\pm$ 3 to 50 $\pm$ 5 Ma (Table 6.3), multiple extrusion of zircon-bearing basalts is possible.

Based on the provenance of the coarse, rounded zircons, the fission track ages provide a means of dating placer deposits within alluvial sequences. Placers containing such zircons in northeastern Tasmania are reworked probably after the Middle Eocene and mixed with old and newly liberated cassiterite. In deep leads such as the Pioneer Tin Mine, the heavy mineral-enriched lower part were buried during the Late Oligocene to Early Miocene by tin depleted sediments. However, at elevations exceeding that of the Winnaleah-Ringarooma basalts, continuous recycling of heavy minerals in streams to the present day is possible.

6.7 Summary of conclusions

Based on the distribution of heavy minerals and the results of the different methods of age estimation presented in Sections 6.2 to 6.6,

Sample	Grain number	Spontaneous/induced track counts	Age ($Ma \pm 1\sigma$)
8022-113	1	426/235	405±33
	2	297/177	375±36
	3	186/128	326±37
	4	430/261	369±29
	5	221/158	314±33
	6	290/170	381±37
8022-114	1	281/341	48±4
	2	158/213	43±5
	3a	128/173	43±5
	3b	187/235	46±5
	4	344/422	48±3
	5	166/206	47±5
	6	154/194	46±5
8022-115	1	599/774	46±2
	2	525/622	50±3
	3	577/693	49±3
	4	472/610	46±3
	5	262/369	42±3
	6	154/184	50±5

Table 6.3 Single-grain fission track ages of alluvial zircons from northeastern Tasmania. From Yim et al. (1985).

Sample number	Grain-size (mm)	Number of grains	Neutron dose ($\times 10^{15}$ n/cm^2)	Fossil track density ($\times 10^6$ cm^{-2})	Induced track density ($\times 10^6$ cm^{-2})	Correlation coefficient	Age* (Ma)	Uranium (ppm)
8022-113	0.1–0.2	6	1.889 (5161)	31.88 (1850)	9.728 (1129)	0.977	367±15	188
8022-114	2–5	6	1.919 (5161)	2.367 (1413)	5.957 (1784)	0.998	46.3±1.8	113
8022-115	2–5	6	1.948 (5161)	5.403 (2589)	13.57 (3252)	0.991	47.1±1.4	254

Parentheses show number of tracks counted. All track densities as for internal surfaces ($g = 0.5$).
* $\lambda_f = 6.9 \times 10^{-17}$/yr, $\lambda_d = 1.551 \times 10^{-10}$/yr, $^{235}\sigma = 5.802 \times 10^{-22}$ cm^2, $I = 7.253 \times 10^{-3}$.
Neutron dosimetry for reference glass SRM612: $B = 6.005 \times 10^9$ neutrons per track, Zeta = 360±10.
Equivalent to NBS Cu dosimetry via reference glass SRM962.

Table 6.4 Combined fission track ages of alluvial zircons from northeastern Tasmania. From Yim et al. (1985).

valuable information on the stratigraphic control of placer deposits in northeastern Tasmania has been obtained. This is considered to be important in the understanding of placer genesis particularly in terms of the time scale required for their formation. The agreement in results shown by the different lines of evidence gives confidence to the conclusions drawn. The main conclusions reached in this chapter are:

(1) Previous work on plant remains occurring in sub-basaltic deep lead sediments at the Pioneer Tin Mine have revealed that the heavy mineral-enriched basal part of the deep lead sequence is overlain largely by Late Oligocene to Early Miocene sediments.

(2) Deep leads are stratigraphically confined by ferricretes which are found to have been derived from the weathering of the Middle Miocene Winnaleah-Ringarooma basalts. There is therefore support for the postulation of a lateritization event at least from the Middle Miocene.

(3) The Pioneer, Briseis and Endurance deep leads are stratigraphically lower than the silcretes. Silcrete formation in the area of study is a post-Middle Miocene event in which pre-existing alluvial sediments have been silicified through silica mobilization from the deep weathering of basalt outcrops.

(4) Reconstruction of sea-surface temperatures by oxygen isotopic analyses of planktonic formainifera in DSDP cores have provided valuable information on the palaeoclimatic history of the study area from the Late Palaeocene to the Pleistocene. This has permitted the recognition of periods of climatic stability and instability which are linked to changes in the rates of weathering, erosion and sedimentation. The early Tertiary remained warm and was probably still conducive to deep weathering. This was followed by a sharp decline in palaeotemperature during the Eocene prior to a period of relative climatic stability from the Oligocene to the Early Miocene.

(5) K-Ar dating of basalts by previous workers have revealed two episodes of volcanic activity in northeastern Tasmania. The Blue Tier basalts of Middle Eocene age (ca. 47 Ma) and the Winnaleah-Ringarooma basalts of Middle Miocene age (ca. 16 Ma). Because of the existence of deep leads beneath the latter, the two basalts provide stratigraphic control on the placer sequences.

(6) Fission track dating of alluvial zircons have proved to be a valuable adjunct to heavy mineral provenance studies. It allows at least one component mineral within the heavy mineral assemblage to be directly dated for the first time. Deep leads containing coarse, anhedral zircons must post-date the Middle Eocene.

(7) There is general agreement between the the different lines of evidence that deep leads are stratigraphically confined by a pre-Middle Miocene land surface. Although the lower heavy mineral enriched part of the sequence was reworked and mixed with zircospilic minerals from the older basalts, at least part of the cassiterite present must have been deposited prior to this event.

A summary diagram showing the possible relationship between Cainozoic sea-surface temperatures constructed from oxygen-isotope data, Cainozoic global changes in sea level and terrestrial events in northeastern Tasmania is presented in Fig. 6.6.

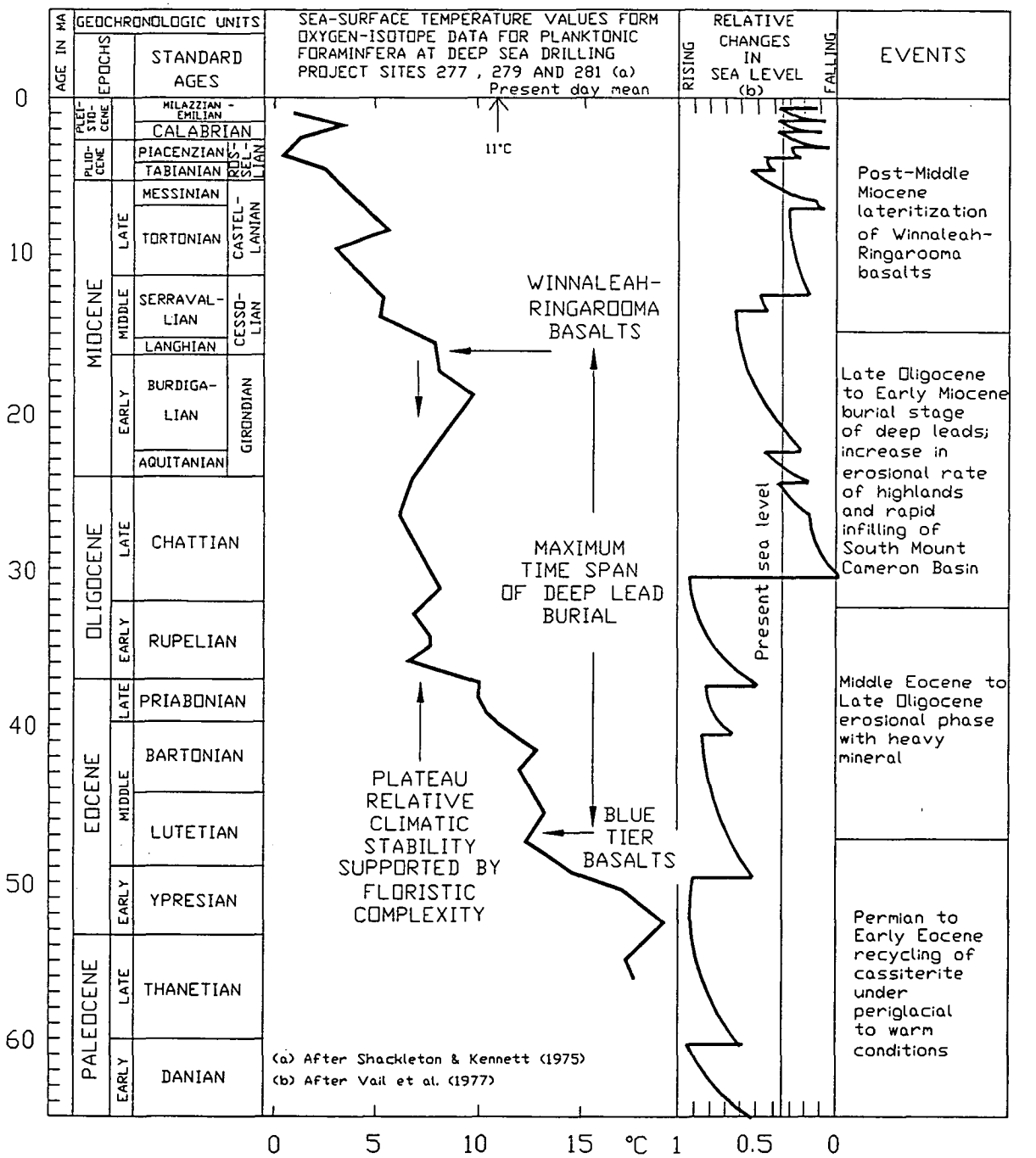

Fig. 6.6 Summary diagram showing the possible relationship between Cainozoic sea-surface temperatures reconstructed from oxygen-isotope data for planktonic foraminifera at DSDP sites 277, 279 and 281 (see Fig. 8.4), Cainozoic global changes in sea level and terrestrial events in northeastern Tasmania.

CHAPTER 7 DESCRIPTION AND CLASSIFICATION OF STANNIFEROUS PLACERS

7.1 Introduction

In this chapter, the stanniferous placer deposits in northeastern Tasmania are described and classified genetically into three main types. Information used in the classification included published work, unpublished reports, field and borehole data. The three types of placers identified are deep leads, eluvial and colluvial placers, and terrace deposits. All three types are described in the following sections with the aid of examples from the study area.

7.2 Deep leads

Deep leads are estimated to contain approximately 90 % of the total tin production in northeastern Tasmania. The four largest tin mines in terms of metallic tin production, Briseis, Pioneer, Endurance and Arba (Table 2.5) are all in this category.

The main characteristics of deep leads in northeastern Tasmania are:

(1) A relatively great depth below ground surface. Although the separation depth between deep leads and shallow leads is not of any geological significance, in the present study the former often exceeds 20 m below ground level and may in cases exceed 120 m.

(2) In many cases, deep leads are shown by field evidence to be sub-basaltic - beneath the Winnaleah-Ringarooma basalts.

(3) The zircospilic suite of heavy minerals (see Section 4.2.3) is sometimes found to occur in parts of the deep lead sequence.

(4) They contained the bulk of the past tin production as well as containing the largest untapped reserves.

(5) They also occur offshore under Ringarooma Bay.

(6) They are commonly found on the piedmont zone of massifs where there is a sharp flattening of palaeo-gradient. For example, Briseis and

Pioneer off the Blue Tier Massif, and Endurance off the Mount Cameron Massif.

Many deep leads were the site of formerly operational mines. Because of this, exposures of sedimentary sequences may not be available for field examination due to mining, drowning and/or the collapse of excavations. The only source of information available on some of the deep leads is as reports, published or unpublished. Further, some deep leads identified by exploratory boreholes were never mined and are not exposed. In such cases, exploration reports including borehole logsheets supplemented in some instances by borehole samples and geophysics provide the only source of information. During the period of field study, only one deep lead mine, the Pioneer Mine, was operational. Therefore, field study of the heavy-mineral-enriched basal part of a deep lead sequence was restricted to this site.

7.2.1 Briseis

The stanniferous drifts at the Briseis Tin Mine (Fig. 3.1) form the Cascade lead following the name of the Cascade River. This lead is located at the confluence point betwen the Cascade and the Ringarooma Rivers in the piedmont zone of the Blue Tier Massif. Although tin was discovered at the site in 1876, it was not until after 1890 that the deposit was recognised as a sub-basaltic deep lead (King 1963). The Briseis Mine was by far the richest in northeastern Tasmania if not in the southern hemisphere. It accounted for more than 50 % of the placer tin production within the region.

A summary of the stratigraphic sequence at the Briseis Mine is provided in Fig. 2.9. The main sedimentary sequence is overlain by three basaltic flows with the upper and middle flows separated by a thin horizon of quartz grits and sands. Based on the K-Ar age of the Winnaleah-Ringarooma basalts determined by Brown (1977), the sedimentary sequence beneath the lowest basalt layer is likely to be pre-Middle

Miocene in age. The 95 m sedimentary sequence (Fig. 2.9) is a fining-upward alluvial sequence considered by Jennings (1975) as one segment of a shallow alluvial cone formed at the break of stream gradient with its geometry disturbed by reworking.

Tin distribution within the Cascade lead was described by several authors. In an account of the tin deposits of Tasmania, Fawns (1905) provided vivid description on the occurrence of tin within the drift. The tin ore was reported to occur in irregular layers of varying thickness but the richness increased with depth until in the actual gutter of the lead a very high percentage of black tin was found. In places, the deposits had been cemented by iron oxides which might be tin-bearing but the pug was tin-barren. In a report on the sub-basaltic tin deposits of the Ringarooma valley, Nye (1925) gave details on the heavy minerals associated with cassiterite. Although no specific reference was made to the Cascade lead, it is evident from his descriptions that the heavy minerals included the zircospilic suite. This was confirmed subsequently by a visit made by the writer to the Queen Victoria Museum in Launceston to examine the mineral collections from the mine.

Details on the ore grade and the three-dimensional shape of the Cascade lead was given in an ore reserve assessment by Braithwaite (1964). Information on the lead was obtained by six borehole traverses about 100 m apart with a borehole spacing of about 30 m (Fig. 7.1). The ore grade found in the boreholes of the traverses are summarised in Fig. 7.2. The main characteristics shown by the tin distribution are:

(1) The basal 20 m of the deep lead shows the greatest tin concentration. A maximum ore grade of 38.3 kg/m^3 is found in one 1.5 m borehole section.

(2) Traverses 1 to 3 show a bedrock channel between 120 and 180 m wide which is markedly enriched in tin.

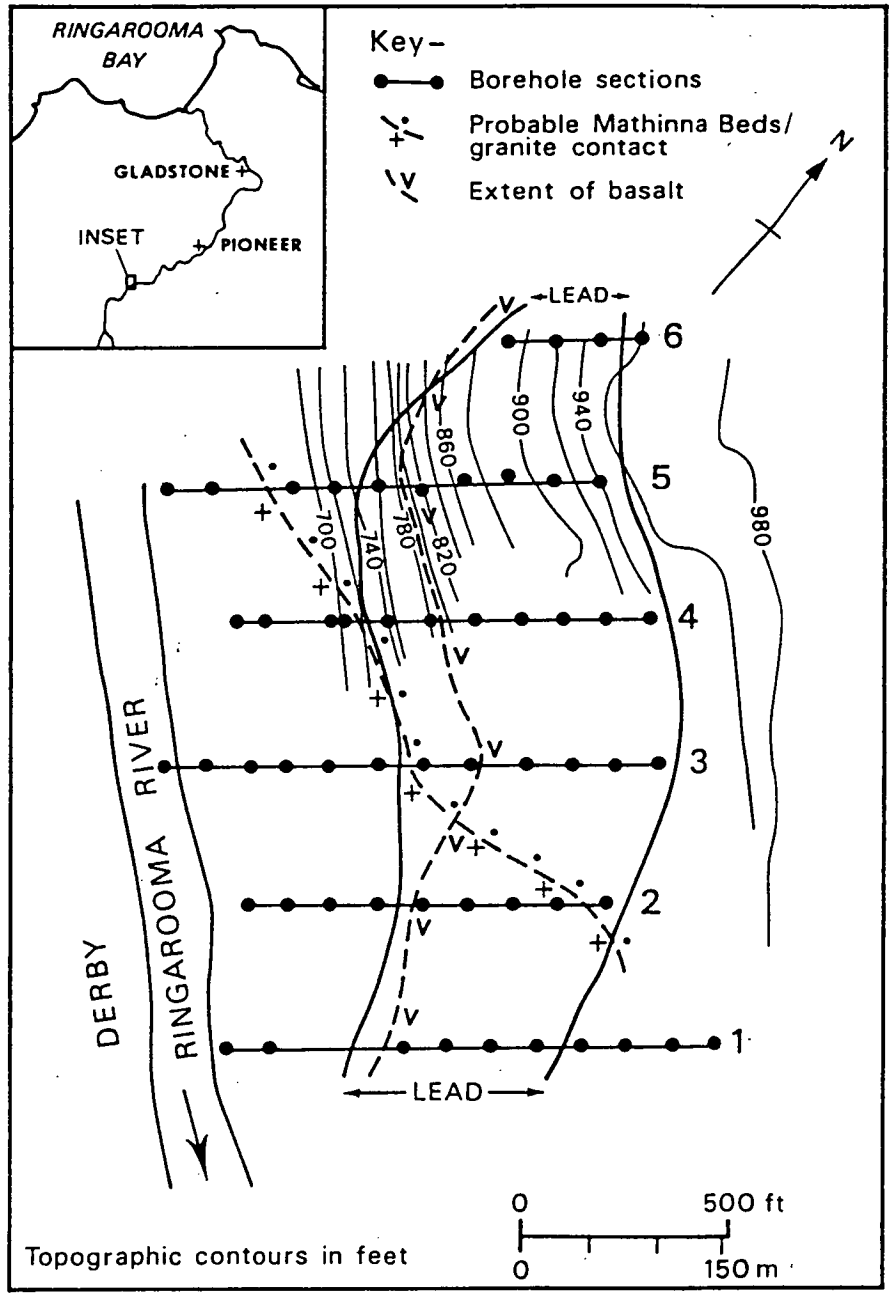

Fig. 7.1 Location map of borehole sections across the Cascade Lead. Redrawn from Braithwaite (1964). Metric equivalents of the contour heights above sea level are 700ft = 213.4m; 740ft = 225.6m; 780ft = 237.7m; 820ft = 249.9m; 860ft = 262.1m; 900ft = 274.3m; 940ft = 286.5m; 980ft = 298.7m.

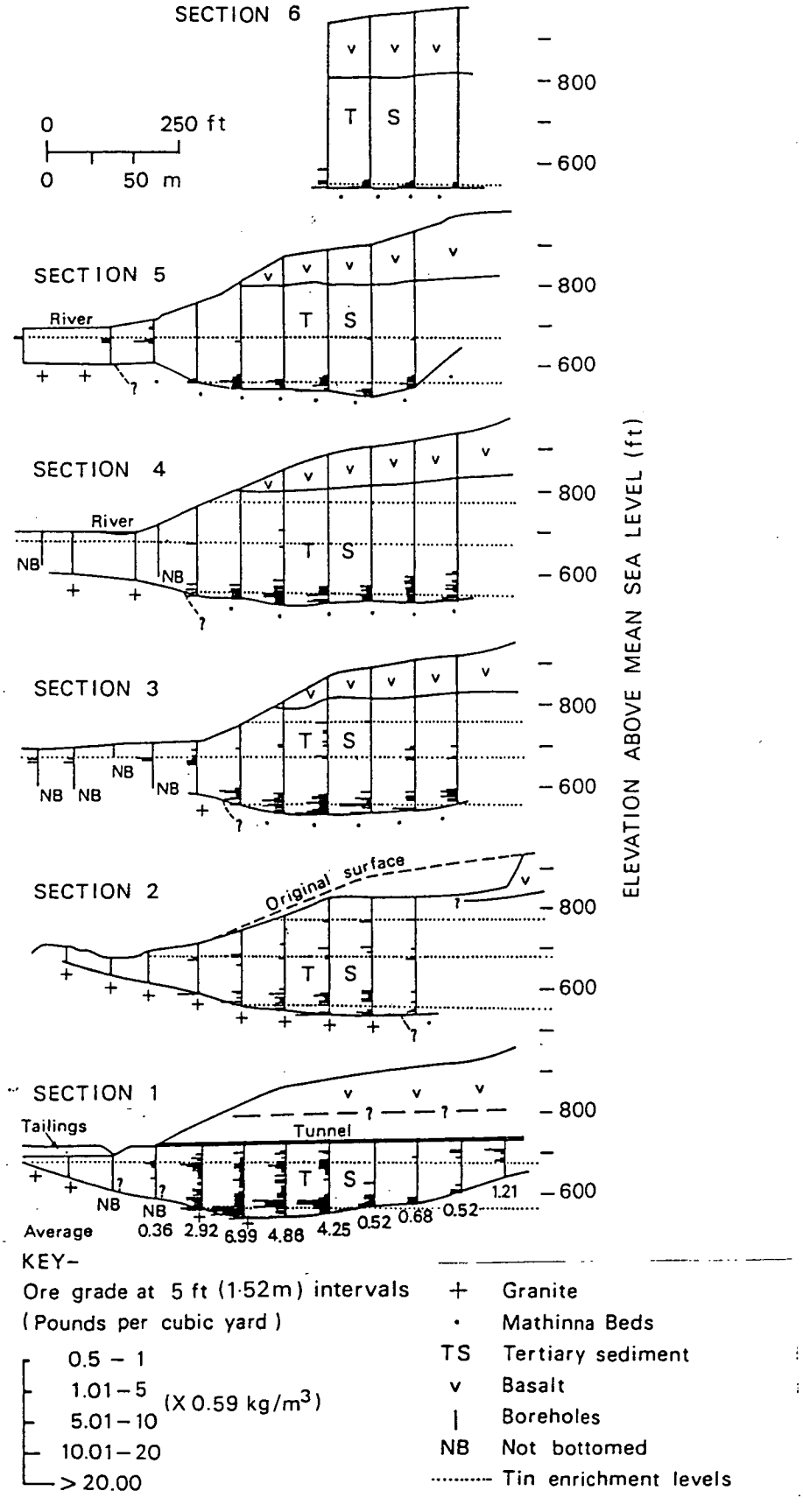

Fig. 7.2 Distribution of tin ore grade in borehole sections shown in Fig. 7.1. Redrawn from Braithwaite (1964). Three tin enrichment levels representing erosional surfaces are also shown.

(3) There is a sharp decrease in tin concentration in a northwesterly direction downstream of the deep lead. Within a distance of 510 m between traverse 1 and 6, there is a consistent declining trend.

(4) Boreholes along the centre of the bedrock channel in traverse 1 which is closest to the upstream end of the Cascade lead contains not only the highest tin concentration but also high levels of tin throughout the length of the borehole. This is in agreement with an upstream source of tin via the Cascade River.

(5) Three tin enrichment levels at about 168, 204 and 232 m above mean sea level are present. Tin concentration is at a maximum in the bottom level decreasing to the top level.

Based on the above characteristics, it is evident from the tin enrichment in the basal part of the lead, that at least part of the cassiterite existed as a lag deposit prior to burial. The sharp decrease in ore grade in sediments further above the rock basement and downstream of the deep lead is in support of the low mobility of the cassiterite. The three enrichment levels found are therefore likely to be caused by the existence of erosional surfaces or hiatuses within the sequence.

7.2.2 Pioneer

Since the Pioneer Mine was the only operating deep lead mine at the time of field study, it provides the only direct source of field information. Because the sedimentology of the deep lead was previously investigated in detail by Morrison (1980), only features considered to be relevant are included in this section. Fig. 7.3 shows the basement topography and the ore grade determined from boreholes based on data available at the end of 1980. The main lead which is known as the Wyniford Lead flows in a northwesterly direction from the Blue Tier Massif. The mine site is a confluence point between the South Pioneer Lead (Nye 1925) and the Wyniford Lead. Upstream and downstream direction of the lead are confirmed by increases and decreases in ore grade. The

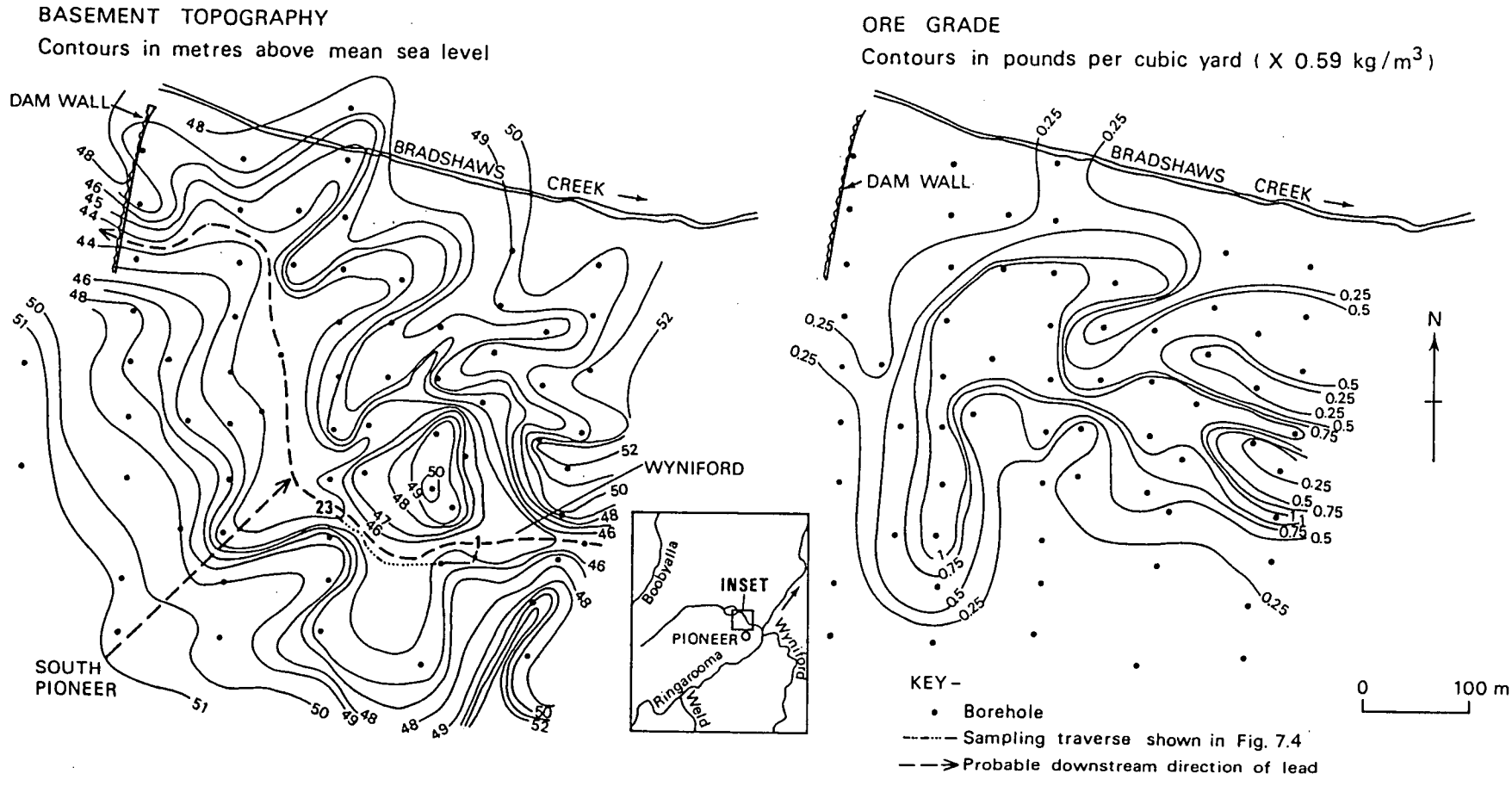

Fig. 7.3 Reconstructed basement topography and cassiterite ore grade for the bottom 15-m interval of the Pioneer Tin Mine. Based on unpublished data of Amdex Mining Limited.

basal sediments which are on average between 5 to 10 m in thickness contain the highest ore grade. The zircospilic suite of heavy minerals is present.

A sampling traverse of the basal sediments was carried out on the pit exposure of the Pioneer Tin Mine in order to study the relationship between bedrock topography and heavy mineral distribution (Fig. 7.4). One pan of sediment was collected from the basal wash immediately above bedrock at an average spacing of about 3 m. The heavy minerals in each sample was concentrated by panning before heavy liquid separation at SG 2.96 and heavy mineral analysis. Based on the distribution of heavy minerals found, the conclusions drawn are:

(1) Heavy mineral concentrations show a general tendency to increase in the centre of gutters.

(2) Besides the control exerted by bedrock topography, the reworking of basal sediment such as by cut and fill structures (Plate 5.1) also caused heavy mineral enrichment through selective sorting processes.

(3) Representative sampling of deep lead is difficult even with a borehole spacing of 10 m. Narrow gutters with high tin grade may be missed.

(4) The transportation distance of tin to form economic placers is about 1 km. This is indicated by the distance between the worked upstream and downstream point of the Pioneer Mine.

(5) The zircospilic suite of heavy minerals is present in some but not all of the samples. Alluvial channels infilled with sediments containing zircospilic minerals cut into older non-zircospilic mineral bearing sediments are identifiable.

(6) The absence of gold within the deposits is in support of source areas from the South Pioneer and Wyniford Leads, neither of which are known to be gold bearing.

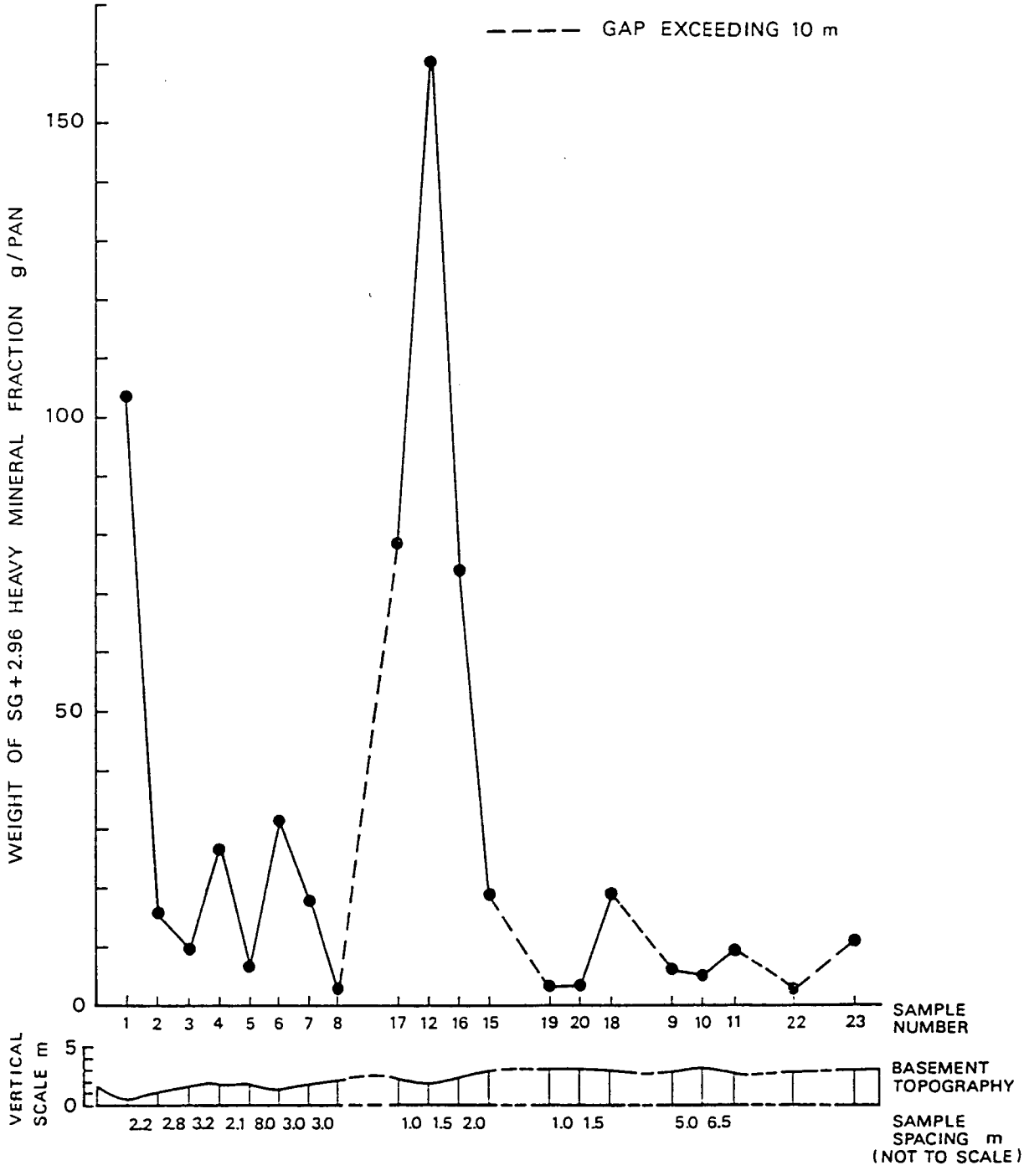

Fig. 7.4 Section showing the weight distribution of (SG +2.96) heavy minerals immediately above the rock basement of the Pioneer Tin Mine.

The Pioneer Lead is best explained by a mixed eluvial and alluvial origin. Eluvial tin concentrations which do not necessarily contain zircospilic minerals are enriched adjacent to the bedrock while alluvial tin typified by the presence of zircospilic minerals is dominant higher up in the sequence. However, the uppermost sequence is tin barren and consists of low energy deposits lacking significant amounts of coarse gravels.

7.2.3 Endurance

The Endurance Lead located on the piedmont zone south of Mount Cameron was studied by Blue Metals Industry Proprietary Limited during the early 1970s (Standard 1973). Detailed analysis was carried out on seventeen traverses of auger and percussion boreholes taken at the spacing of about 15 m. This led to the recognition of a east-north-east trending bedrock channel which is cut by a north-north-west trending fault (Fig. 7.5). Cross-sections of the bedrock channel are shown in Fig. 7.6. On the western side of the fault, the channel is more steep-sided, narrower and richer in tin grade than on the eastern side of the fault. The explanations given by Standard (1973) were:

(1) The downthrow side of the fault was to the west and the faulting was older than the deposits infilling the channel.

(2) The lead was flowing to the west.

(3) The fault plane created a waterfall about 15 m in height.

(4) Alluvial tin nearby was transported westward by the lead and was trapped in the plunge pool.

However, in regard to (1), displacement of bedrock contours show that the fault is younger than the channel.

Boreholes further to the west of the fault have shown that there is another lead flowing eastwards joining up at the sinuous elongated channel to the west of the fault (Fig. 7.5) (Standard 1973). The total thickness of sediment is variable from about 24 to 53 m but the upper 18

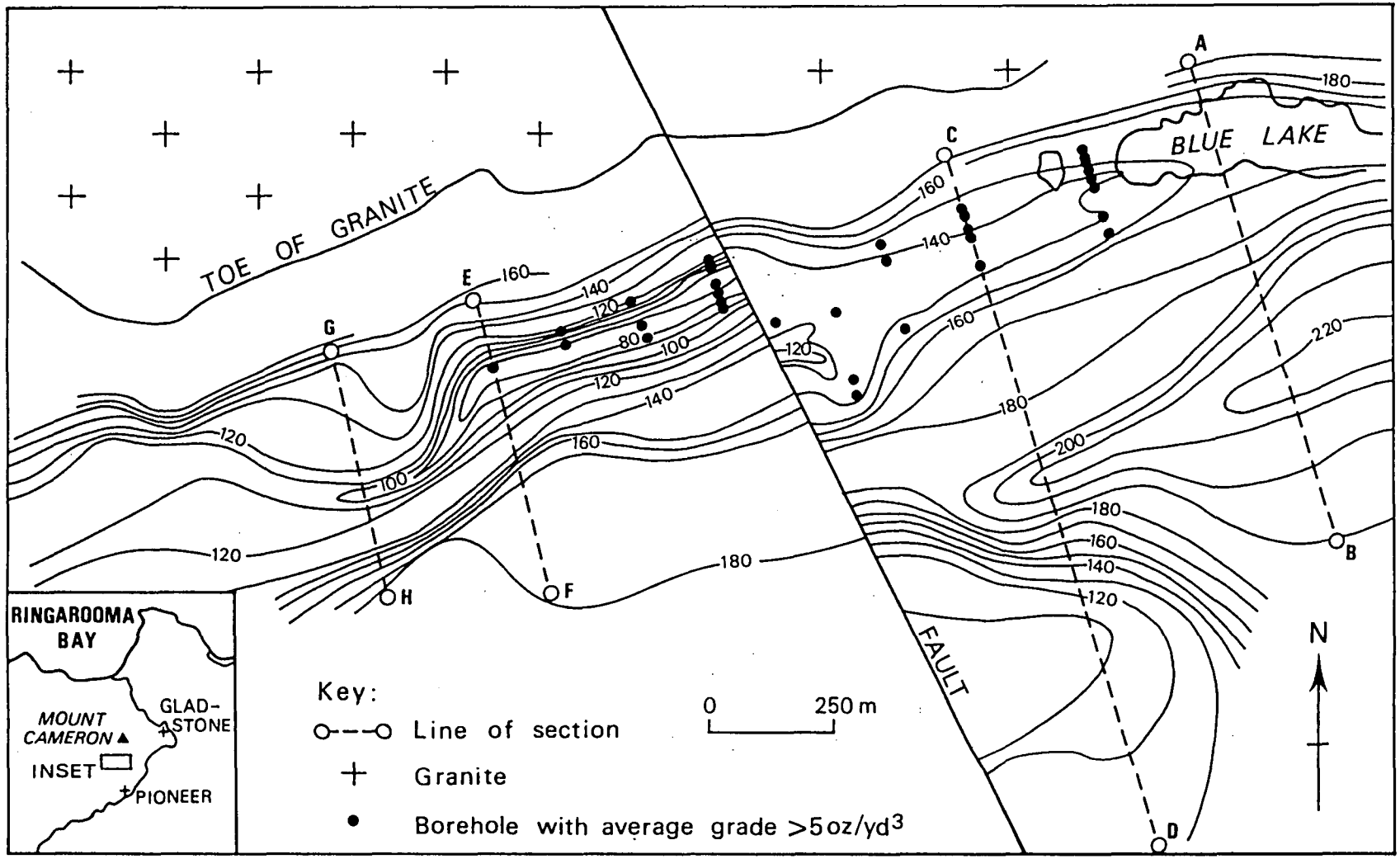

Fig. 7.5 Location map of borehole sections shown in Fig. 7.4 and reconstructed basement topography of the western portion of the Endurance Tin Mine. Contours shown are at 10-ft intervals above mean sea level. Redrawn from Standard (1973). Metric equivalents of the contour heights above sea level are 80ft = 24.4m; 100ft = 30.5m; 120ft = 36.6m; 140ft = 42.7m; 160ft = 48.8m; 180ft = 54.9m.

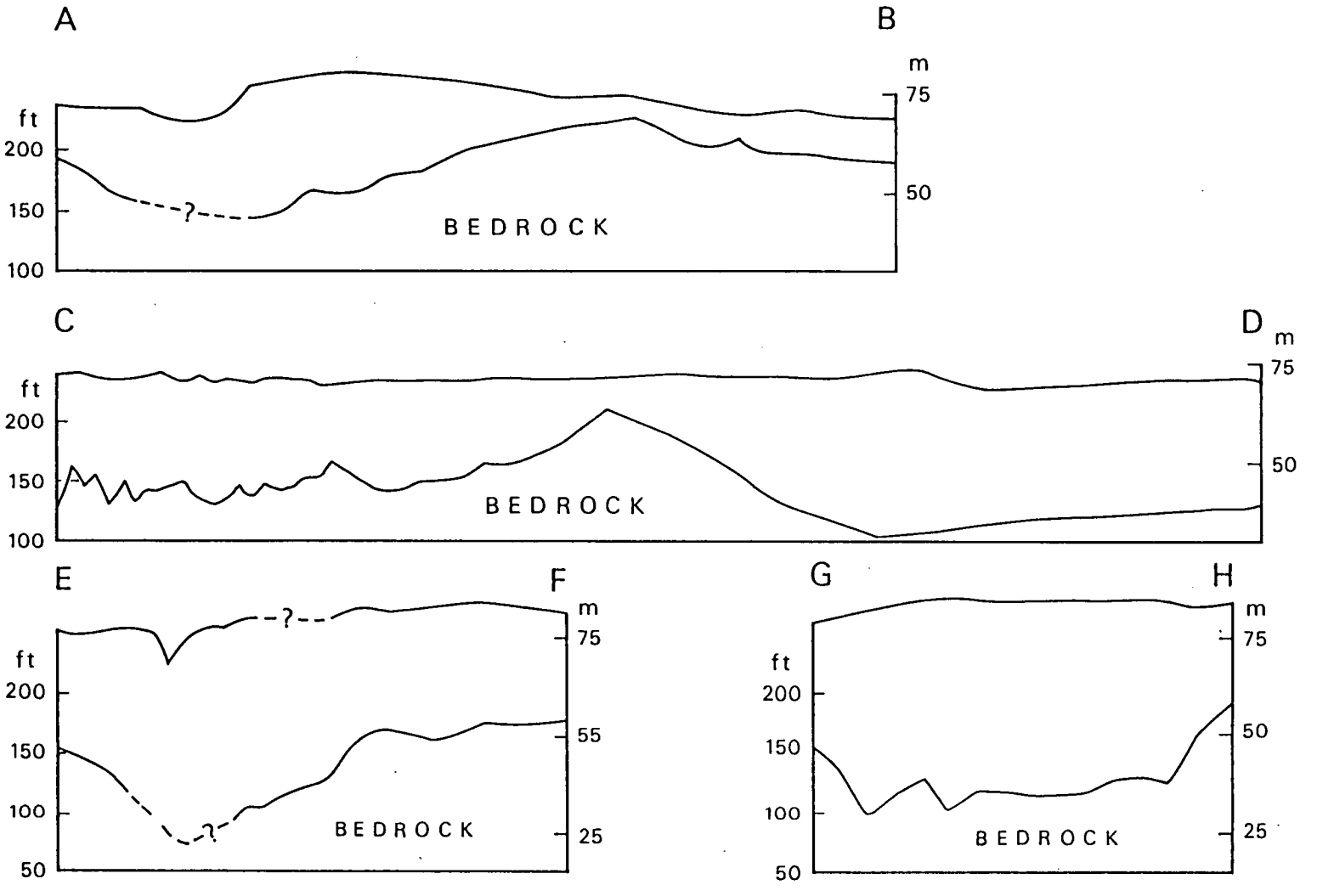

Fig. 7.6 Sections A-B, C-D, E-F and G-H across the Endurance Lead. Vertical exaggeration 4.6X and horizontal scale 1 : 7000. Redrawn from Standard (1973).

m carries only minor amounts of tin. The tin-bearing wash which occurs in the basal sediments is up to 18 m in thickness and is traceable for a distance of about 765 and 495 m to the east and west of the fault respectively.

A east to west cross section of the deep lead at the old Endurance Mine from unpublished records of the Blue Metals Mining Industries Proprietary Limited is shown in Fig. 7.7. Tin is seen to be enriched in two horizons approximately between 9 and 12 m below ground level (68 to 71 m above mean sea level) and in the basal sediments at a depth of about 25 m below ground level (55 m above mean sea level). A simplified version of Fig. 7.7 was shown in Jack (1965) who stated that there was no evidence for the existence of a basaltic cap above the deposits. There is also no information available to confirm the presence of the zircospilic suite of heavy minerals in the basal sequence of the lead. In the upper part of the sequence, the tin enrichments found are, as in the Cascade Lead, likely to be related to the presence of former erosional surfaces.

7.2.4 Scotia

From 1935 to 1944, an extensive drilling campaign in the Great Northern Plains was carried out by the Tasmania Department of Mines (Owers 1970). A total of 855 boreholes were sunk to an average depth of about 27 m. This led to the identification of a north-north-west trending deep lead with an average width of 45 m which was inferred to be an extension of the Scotia Lead (Fig. 7.8).

Summaries of the characteristic features of the Scotia Lead were provided by Blake (1955) and Standard (1973a). The total length of the lead exceeds 6 km and the rock basement elevation varies from a maximum and minimum of 48 and 6 m above mean sea level in the southern and northwestern part respectively. From the above, the average gradient of the lead is only 1 in 143. The lead also shows a sinuous course which is

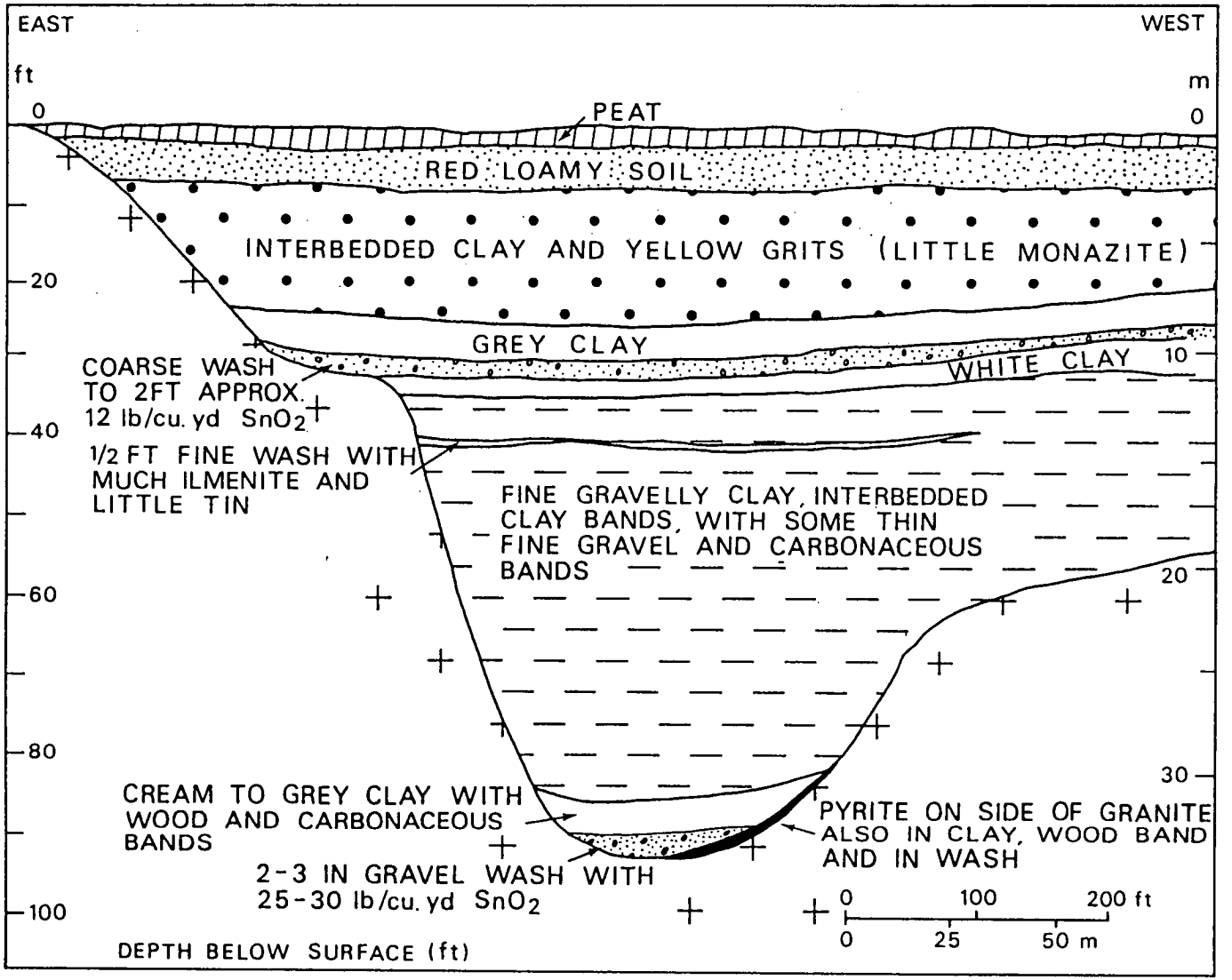

Fig. 7.7 East to west cross-section of the old Endurance Tin Mine. Redrawn from Blue Metals Industries Mining Proprietary Limited unpublished map.

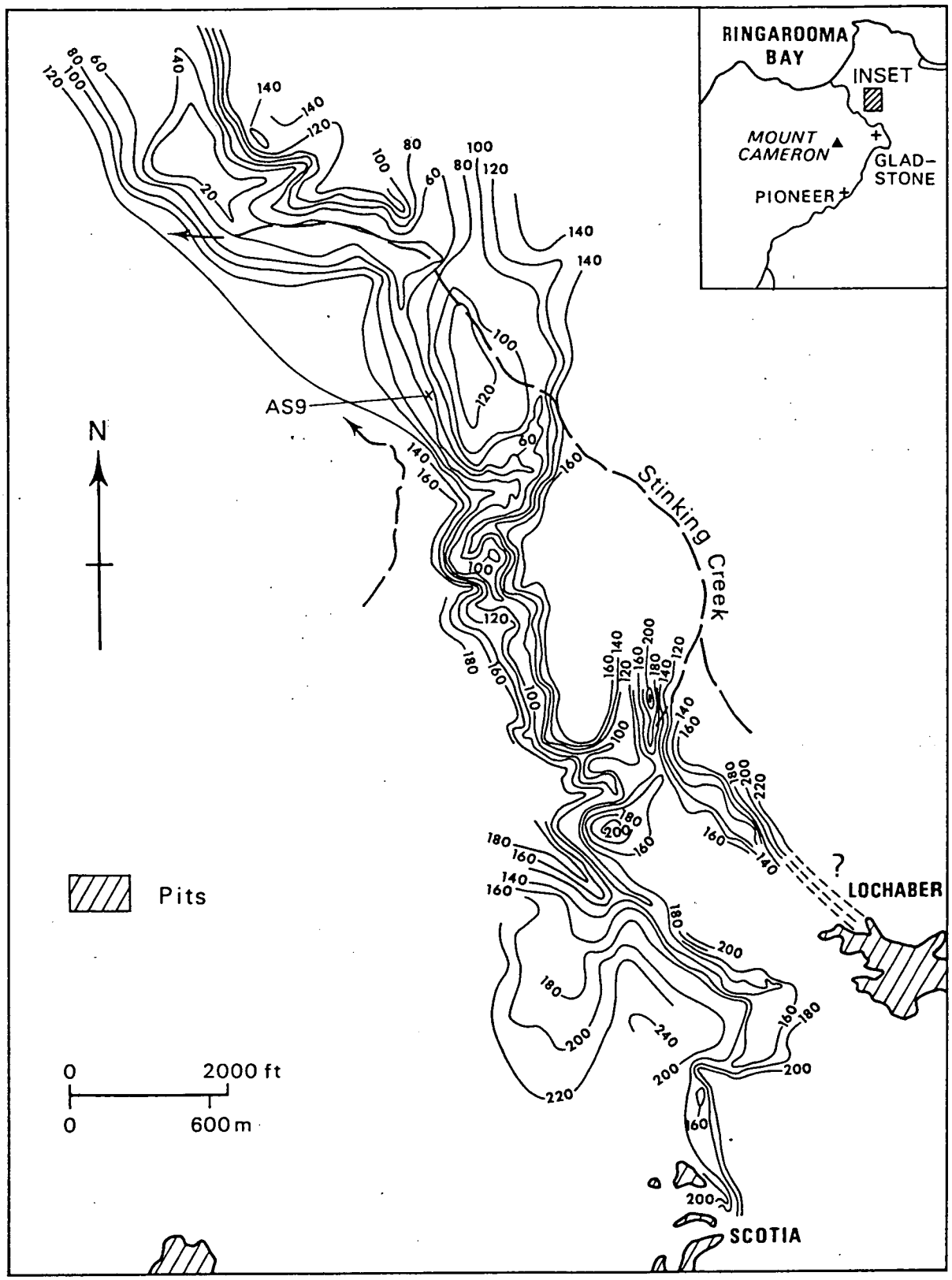

Fig. 7.8 Bedrock contour map of the Scotia Lead. Contours shown are at 20-ft intervals above mean sea level. Redrawn from Standard (1973a). Metric equivalents of the contour heights above sea level are 20ft = 6.1m; 40ft = 12.2m; 60ft = 18.3m; 80ft = 24.4m; 100ft =30.5m; 120ft = 36.6m; 140ft = 42.7m; 160ft = 48.8m; 180ft = 54.9m; 200ft = 61.0m; 220ft = 61.0m; 220ft = 67.1m; 240ft = 73.2m.

occasionally branched and the tin content is confined to basal sediments in gutters 3 to 9 m in thickness. About one-third of the total length of the lead was estimated by Blake (1955) to contain 937 tons of 70 % cassiterite concentrate. More recently, seismic and borehole investigations by the Tasmania Department of Mines (Braithwaite 1977) revealed the existence of a possible Tertiary basin northwest of the Scotia Lead.

In 1979, samples of heavy mineral concentrates from one percussion borehole (AS 9) located in the main gutter of the deep lead (Fig. 7.8) was obtained by Amdex Mining Limited for heavy mineral analysis. The stratigraphy of this borehole is shown in Fig. 7.9. A summary of the weight distribution of the three heavy mineral fractions obtained is shown in Table 7.1, and, a diagrammatic presentation of the correlation between the proportion of each heavy mineral fraction and the ore grade is shown in Fig. 7.10. As in the Cascade and Endurance Leads, tin enrichment levels also attributed to the presence of erosional surfaces are present. The three peaks in tin enrichment levels are identified at a depth of 10-12, 28-30 and 36-38 m below ground level or approximately 53 m, 25 m and 17 m above mean sea level respectively. The confirmation of the identification of one spinel mineral grain in the basal sediments is thought to indicate the presence of the zircospilic suite of heavy minerals.

7.2.5 Other onshore deep leads

Numerous boreholes undertaken by the Tasmania Department of Mines and various mining companies have provided much information to indicate the possible extension of deep leads beneath and beyond the Winnaleah-Ringarooma basalts. However, even though these studies have confirmed the extension of some deep leads, they have failed to reveal economically viable tin or gold placers.

BORE HOLE AS9

Surface elevation 54 m above mean sea level

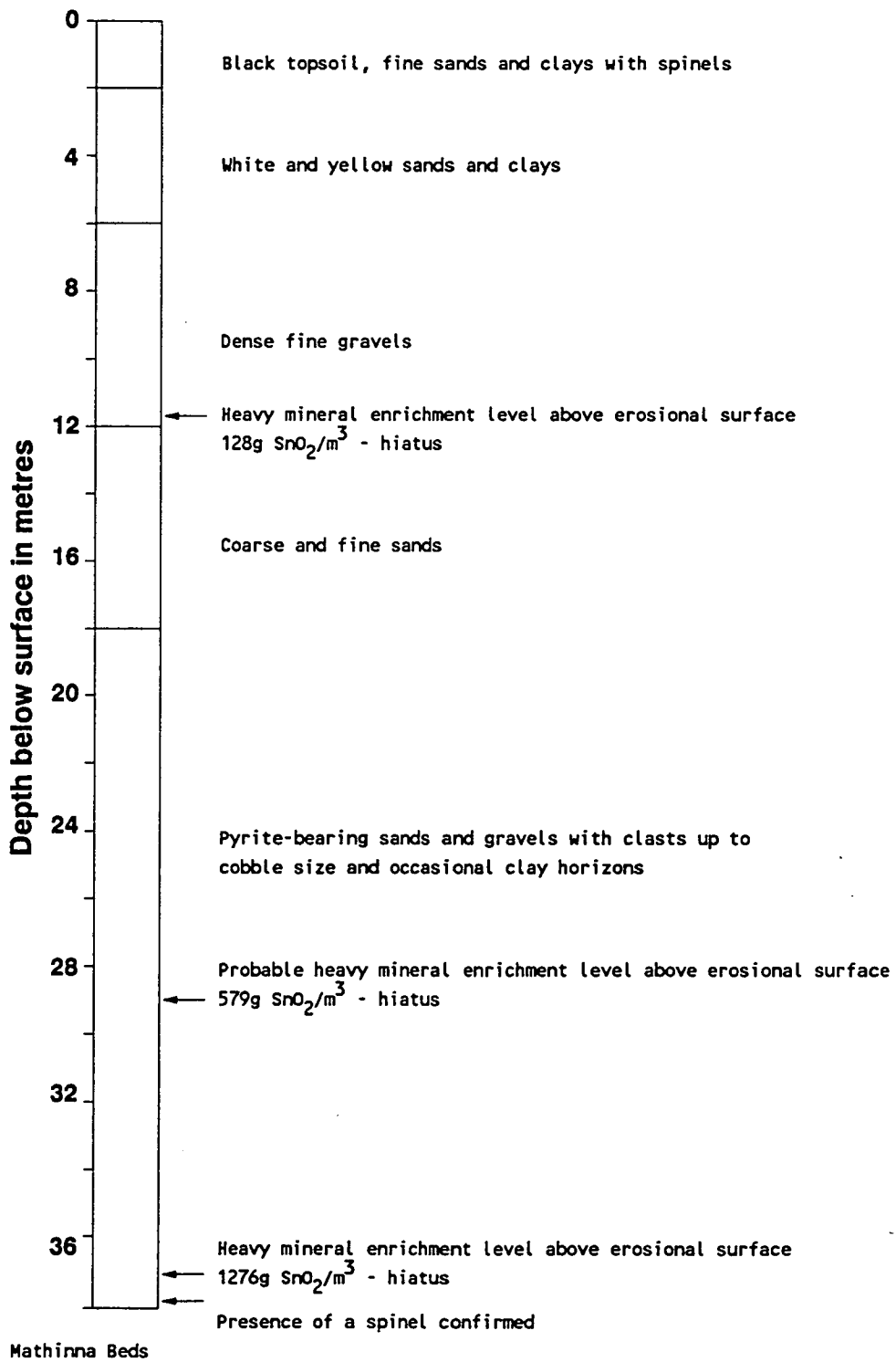

Fig. 7.9 Simplified logsheet for borehole AS9, Scotia Lead. Based on unpublished data of Amdex Mining Limited.

Sample no.	Borehole section M below ground level	Weight of concentrate (g)	Heavy mineral fraction					
			Weight (g)			Weight (%)		
			2.96-3.32	3.32-4.2	+4.2	2.96-3.32	3.32-4.2	+4.2
9264	2- 4	17.25	0.16	0.79	0.22	13.68	67.52	18.80
9266	6- 8	15.12	0.15	0.41	0.12	22.06	60.29	17.65
9268	10-12	30.02	0.48	1.61	4.54	7.24	24.28	68.48
9270	14-16	39.39	0.31	0.52	0.04	35.63	59.77	4.60
9272	18-20	24.61	0.28	2.27	0.71	8.59	69.63	21.78
9274	22-24	21.34	0.26	1.93	0.83	8.61	63.91	27.48
9276	26-28	52.39	0.38	3.28	11.92	2.44	21.05	76.51
9278	30-32	41.45	0.29	2.09	6.77	3.17	22.84	73.99
9280	34-36	45.70	0.55	3.26	34.33	1.44	8.55	90.01
9282	38-40	24.04	0.35	3.13	7.97	3.06	27.33	69.61

Table 7.1 Weight distribution of heavy mineral fractions in borehole AS9, Scotia Lead.

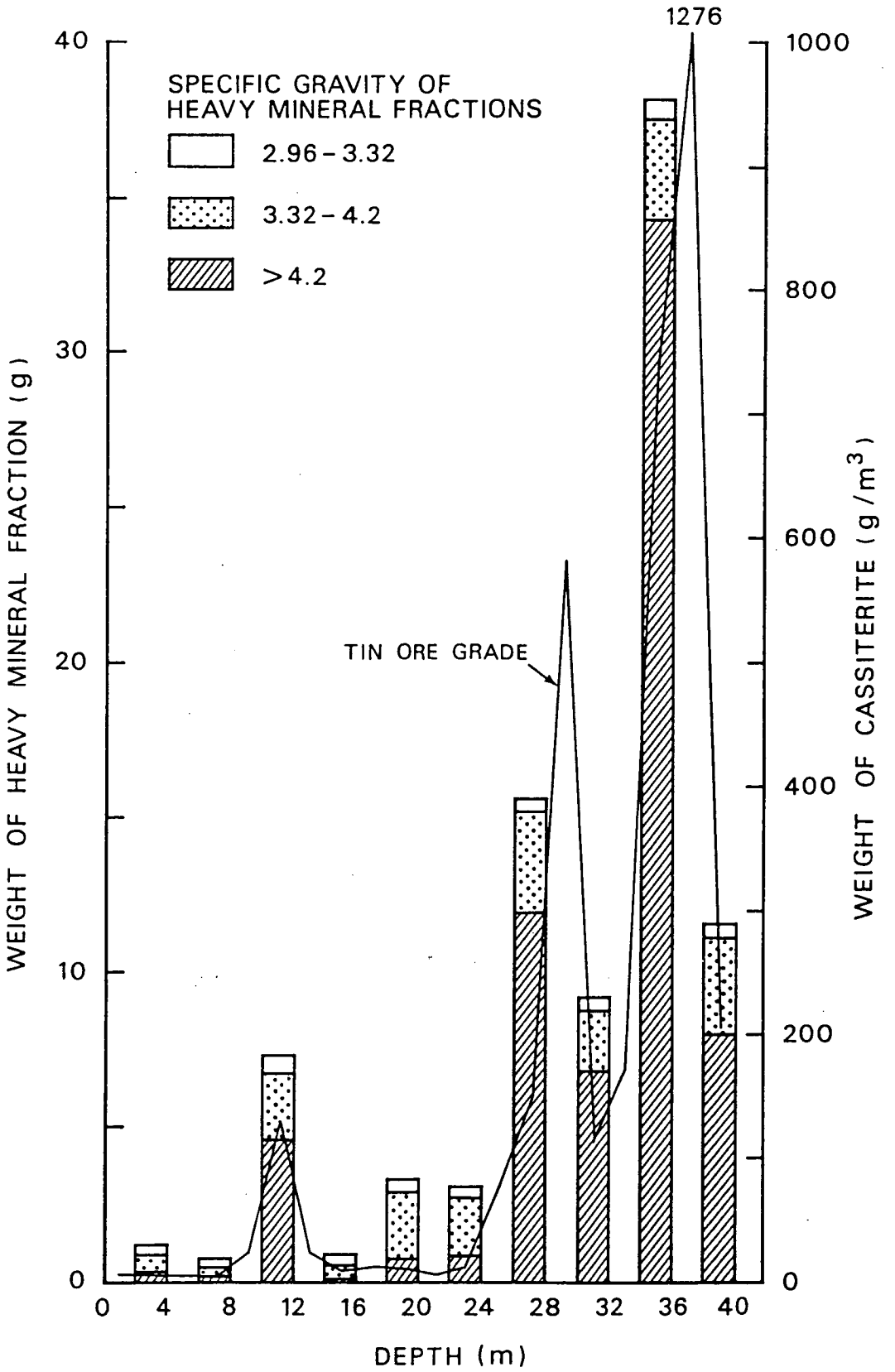

Fig. 7.10 Tin ore grade and weight distribution of heavy mineral fractions in borehole AS9, Scotia Lead. See Table 7.1 for weight distribution of the fractions.

Eight boreholes were made by the Tasmania Department of Mines (Brown in McClenaghan et al. 1982) along a line north of the present course of the Ringarooma River (Fig. 7.11). These boreholes were aimed at obtaining maximum data on the topography of the old Tertiary river valley and the underground water potential of the area. A summary of the lithological variation within the boreholes is shown in Fig. 7.12. The maximum thickness of drift found in borehole 7 exceeded 130 m while four layers of basalts separated by sediment have been encountered in borehole 4. Boreholes 1 and 4 with a Mathinna Beds rock basement show a fining-upward sequence typical of alluvial infilling. On the other hand, boreholes 5 to 9 which were all located in granitic rock basement do not show any clear-cut trend and were generally coarser in particle size. However, because of the wide borehole spacing used, it is not possible to delineate the deep lead channels precisely.

Two traverses of jetstream boreholes were made by Australian Anglo-American Prospecting Proprietary Limited at Trout Creek (Fig. 7.13) and Gellibrand Plains (Fig. 7.14) for placer tin and gold exploration respectively. Although the borehole samples were too disturbed to permit accurate determination of the sedimentary stratigraphy, valuable information on the bedrock topography and the distribution of heavy minerals has been obtained. This is summarised by the cross-sections in Figs. 7.15 and 7.16. Both traverses are located to the north of the main Winnaleah-Ringarooma basalts along possible former extension of leads originating from the Blue Tier Massif. Trout Creek and Gellibrand Plains may represent former extension of the Weld Lead, and the Main Creek and/or Cascade Leads respectively. In the Trout Creek boreholes, only small quantities of tin were found while spinels are present in basement samples as well as within the sequence (Fig. 7.15). The spinel is indicative of the presence of the zircospilic suite of heavy minerals within the sub-basaltic Tertiary sediments pre-dating the

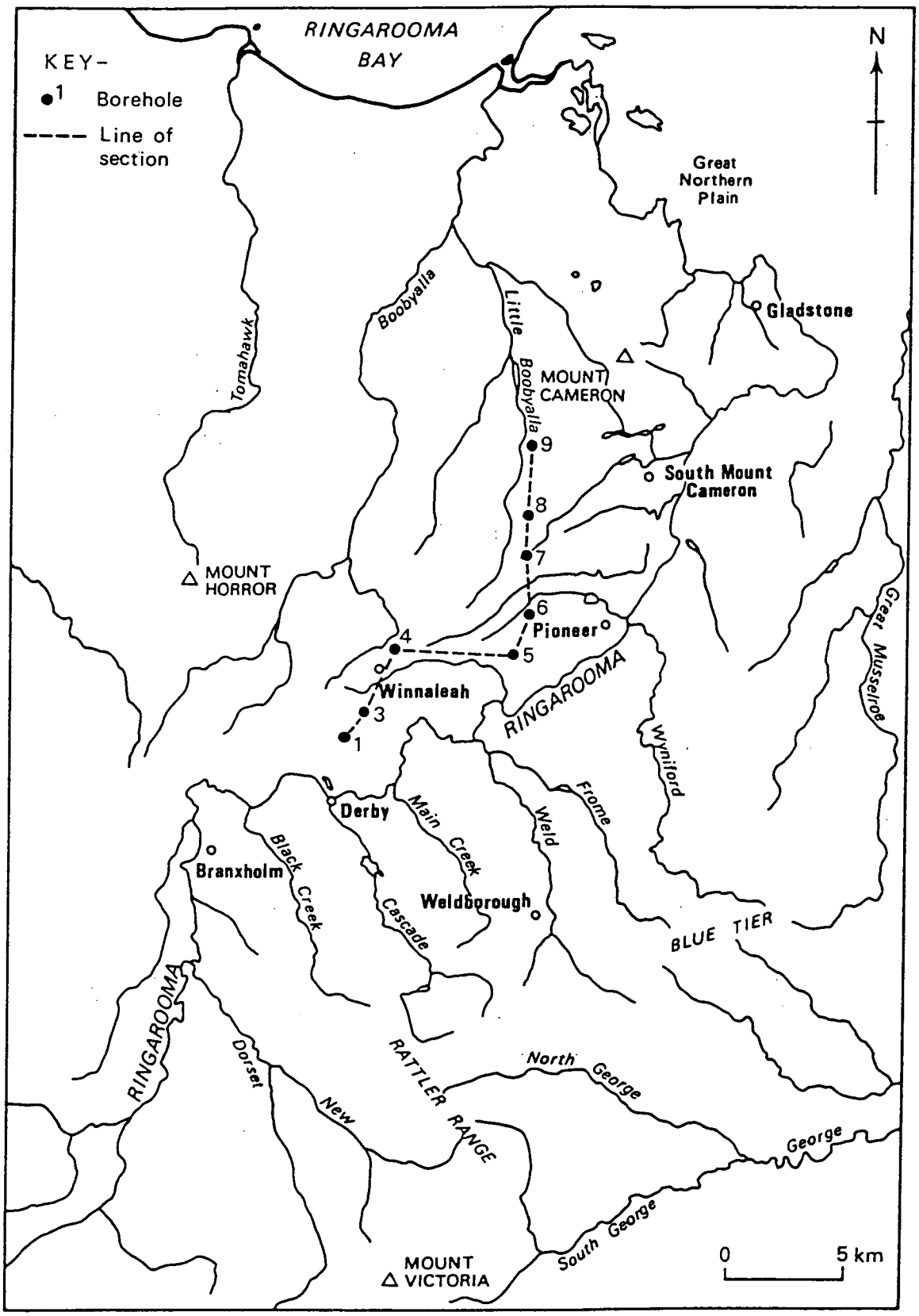

Fig. 7.11 Location map of boreholes in the South Mount Cameron Basin bored by the Tasmania Department of Mines (see Brown 1982).

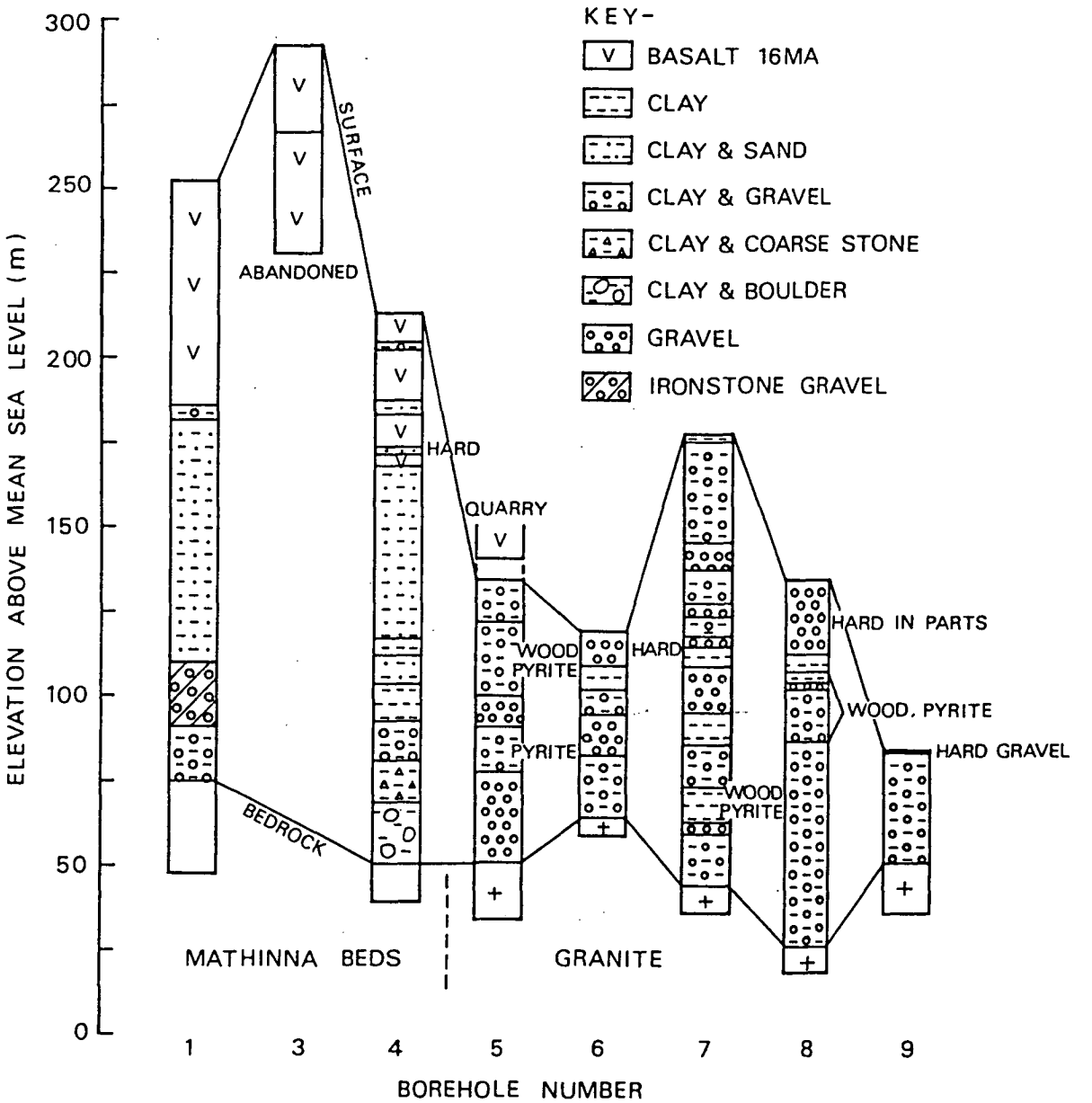

Fig. 7.12 Possible correlation between the stratigraphic sequence of boreholes shown in Fig. 7.11. Stratigraphic sequence of boreholes are based on borehole logs in Brown (1982).

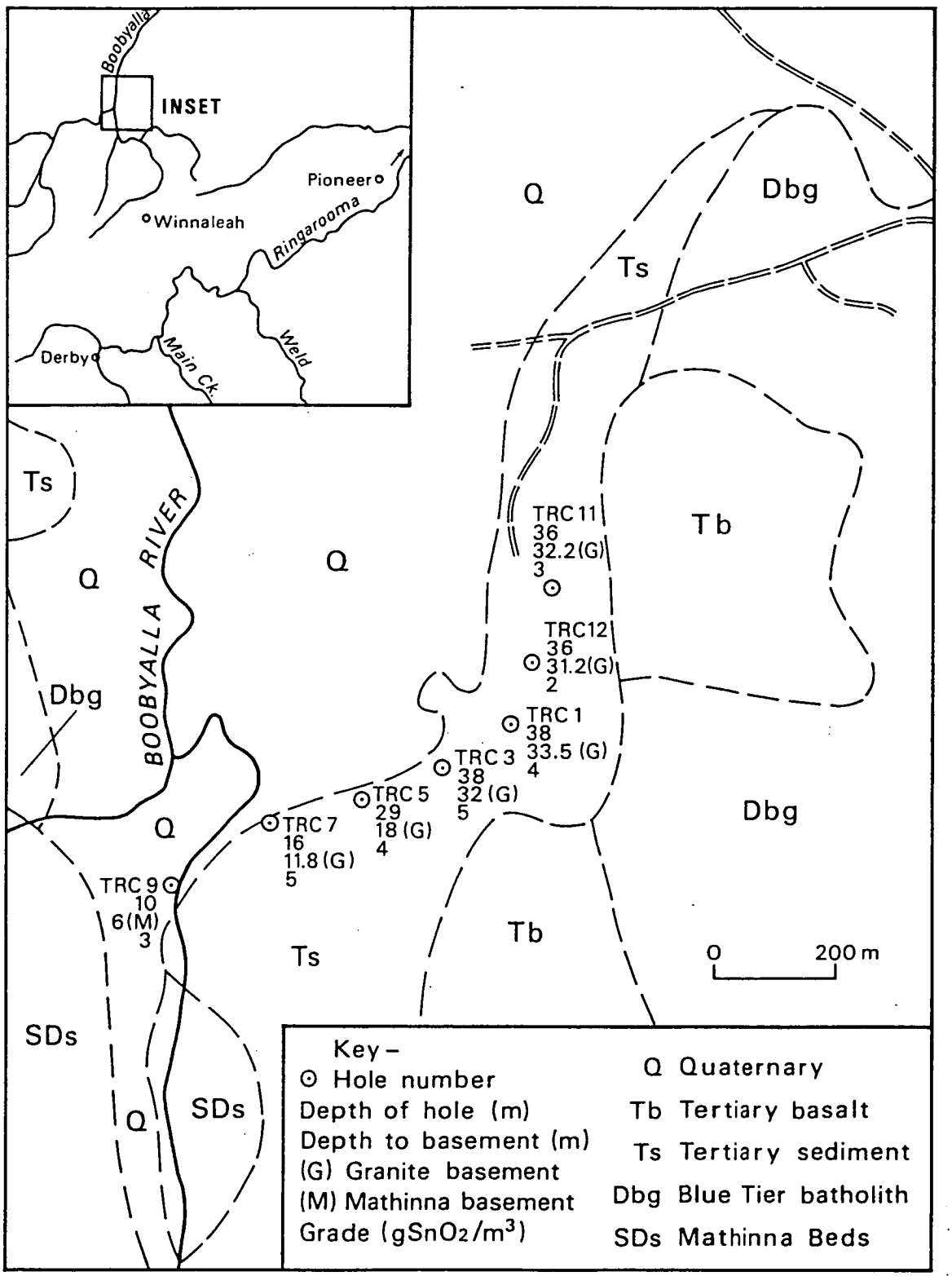

Fig. 7.13 Location map of borehole section across Trout Creek. Based on data supplied by Australian Anglo-American Prospecting Proprietary Limited.

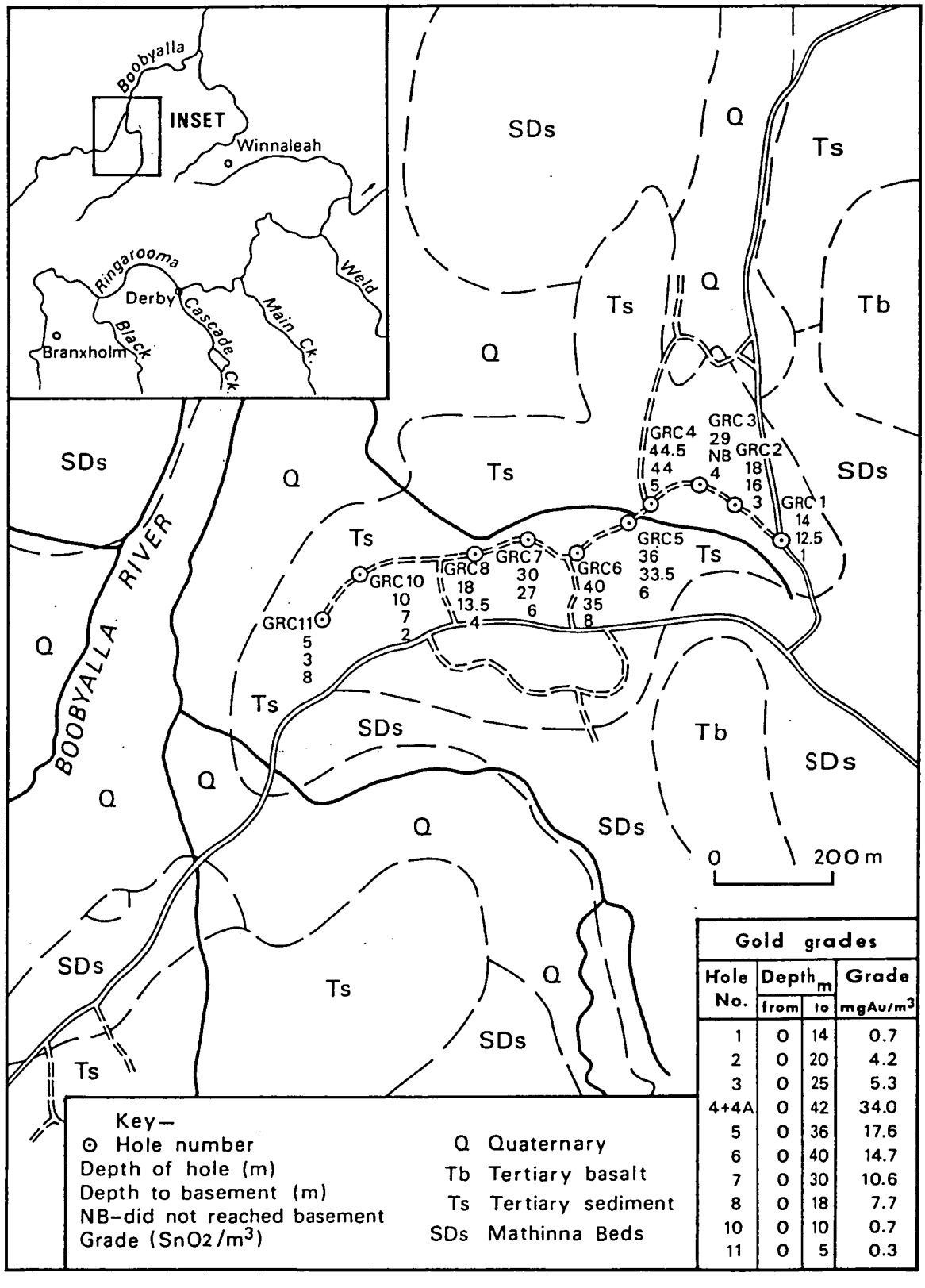

Gold grades			
Hole No.	Depth m		Grade
	from	to	mgAu/m³
1	0	14	0.7
2	0	20	4.2
3	0	25	5.3
4+4A	0	42	34.0
5	0	36	17.6
6	0	40	14.7
7	0	30	10.6
8	0	18	7.7
10	0	10	0.7
11	0	5	0.3

Fig. 7.14 Location map of borehole section across the Gellibrand Plains. Based on data supplied by Australian Anglo-American Prospecting Proprietary Limited.

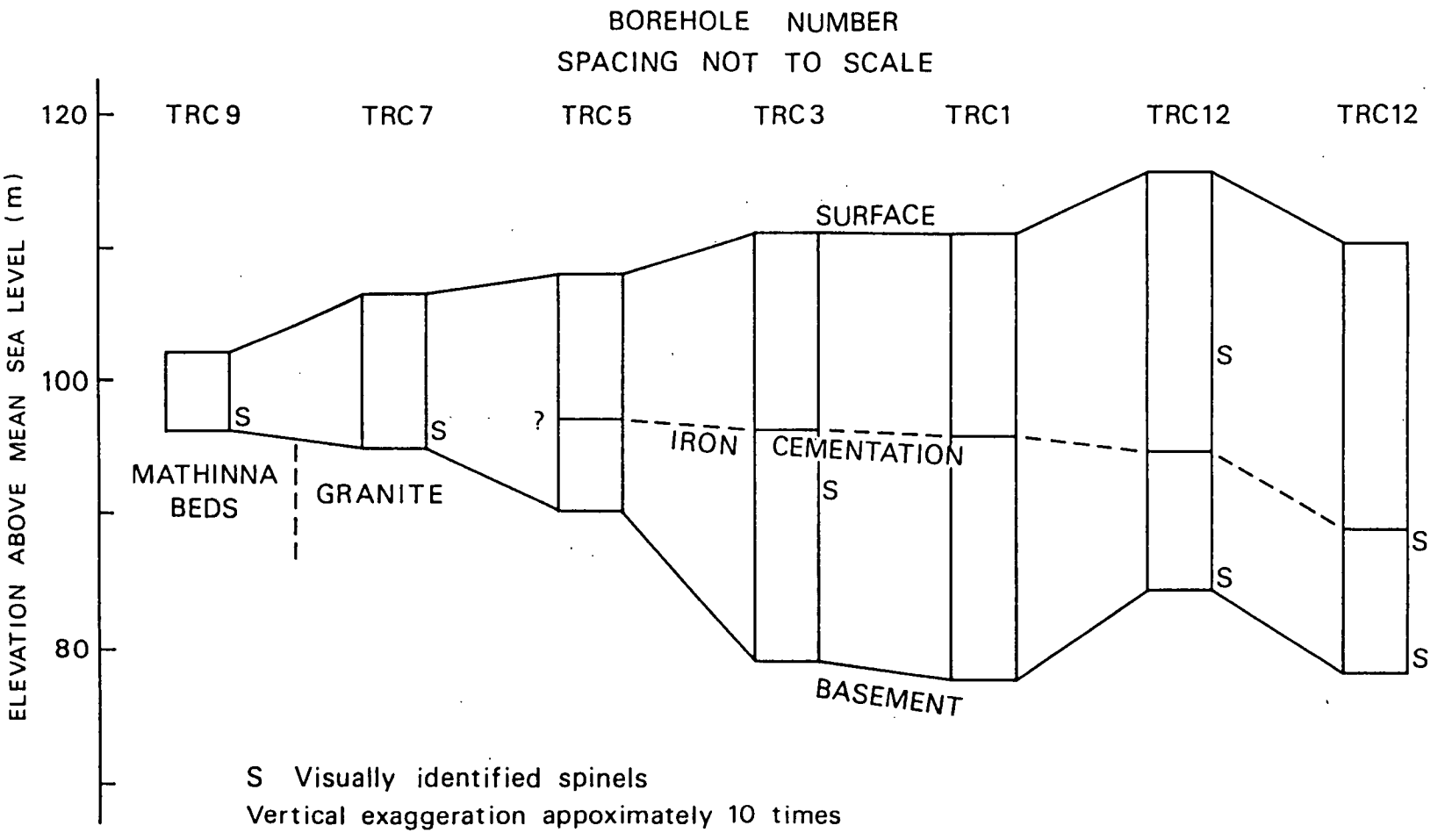

Fig. 7.15 Borehole section across Trout Creek showing the main stratigraphic features. Based on unpublished borehole data supplied by Australian Anglo-American Prospecting Proprietary Limited.

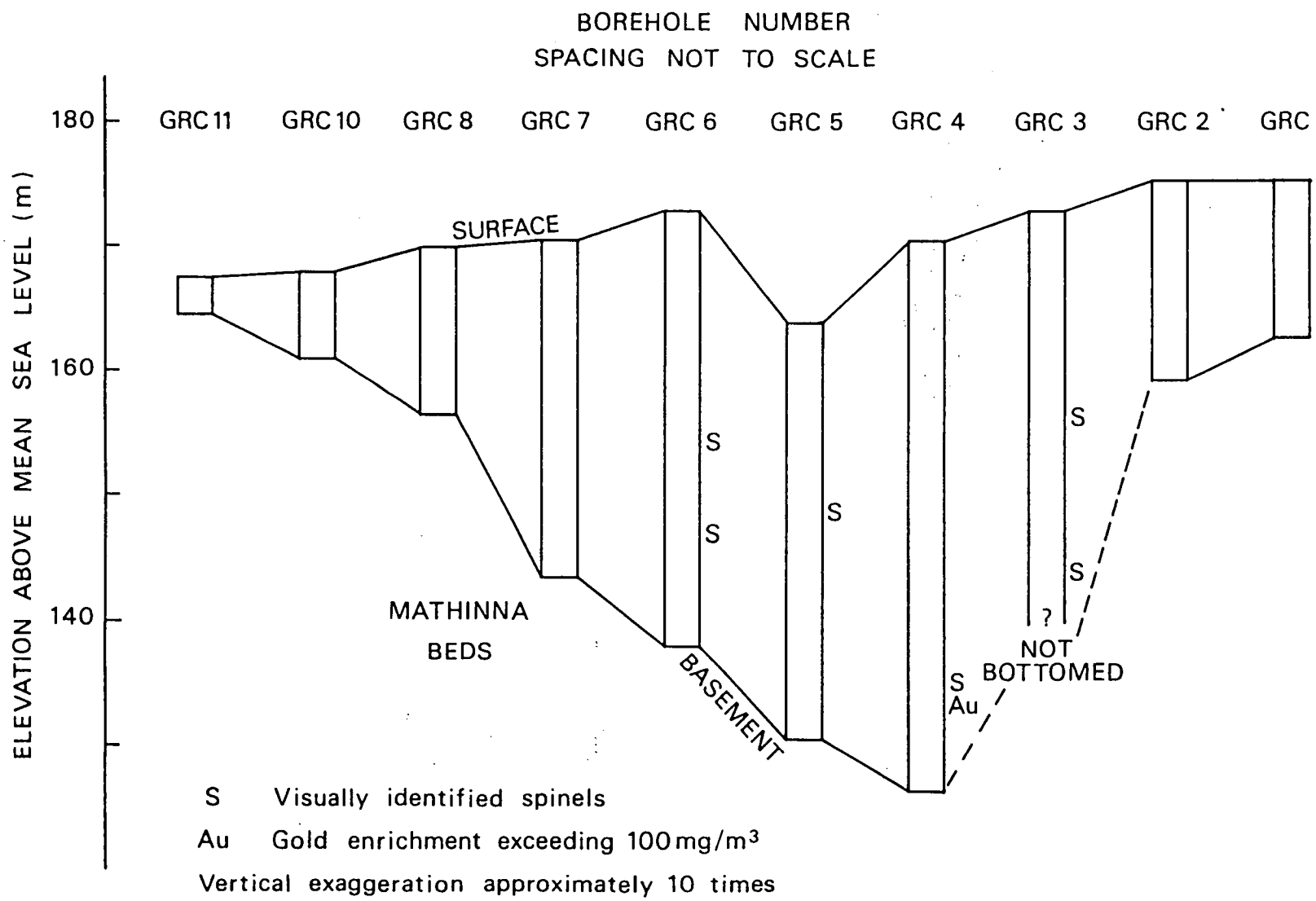

Fig. 7.16 Borehole section across the Gellibrand Plains showing the main stratigraphic features. Based on unpublished borehole data supplied by Australian Anglo-American Prospecting Proprietary Limited.

Middle Miocene. The iron cementation surface found in five of the boreholes is likely to be a relic feature formed by a Lower Tertiary pedogenic event. At least two bedrock channels are present between boreholes TRC 5 and 12, and, TRC 11 with the former reaching a maximum depth of 33 m. At the Gellibrand Plains, a single channel with sediment reaching 44 m in depth containing spinels and gold sporadically is present. The main difference between the two traverses is in the type of bedrock basement. Trout Creek with granitic rock basement is comparatively smooth in profile while the Gellibrand Plains with Mathinna Beds is comparatively steep. The gold present in the Gellibrand Plains is probably locally derived from auriferous quartz veins within the Mathinna Beds. Both channels are deep lead extensions even though their tin concentrations are low. For example, Trout Creek is a probable former extension of the Weld Lead. This conclusion is supported by the discovery of large sapphire specimens in creek sediments by the Tasmania Lapidary Club (S.H. Stevens, pers. comm.).

A number of boreholes were made by Australian Anglo-American Prospecting Proprietary Limited in the South Mount Cameron Basin during 1982. These boreholes (Fig. 7.17) revealed a maximum thickness of almost 100 m of pre-Middle Miocene Tertiary sediments even though the borehole spacing used is too wide to permit the identification of bedrock channels. Since borehole 9 lies only a short distance to the north of Tasmania Department of Mines borehole 7 (Fig. 7.12), the greatest thickness of Tertiary sediment may underly the tongue of Winnaleah-Ringarooma basalts near the upstream end of Ruby Creek (Fig. 7.17). An important discovery in these boreholes is the occurrence of basaltic rock fragments probably representing in situ lavas in the lower part of the sequence in four boreholes (2, 3, 5 and 16) (Fig. 7.18). Simplified logsheets of these boreholes are shown in Appendix III. The rock fragments from two of the boreholes (3 and 5) were confirmed by the

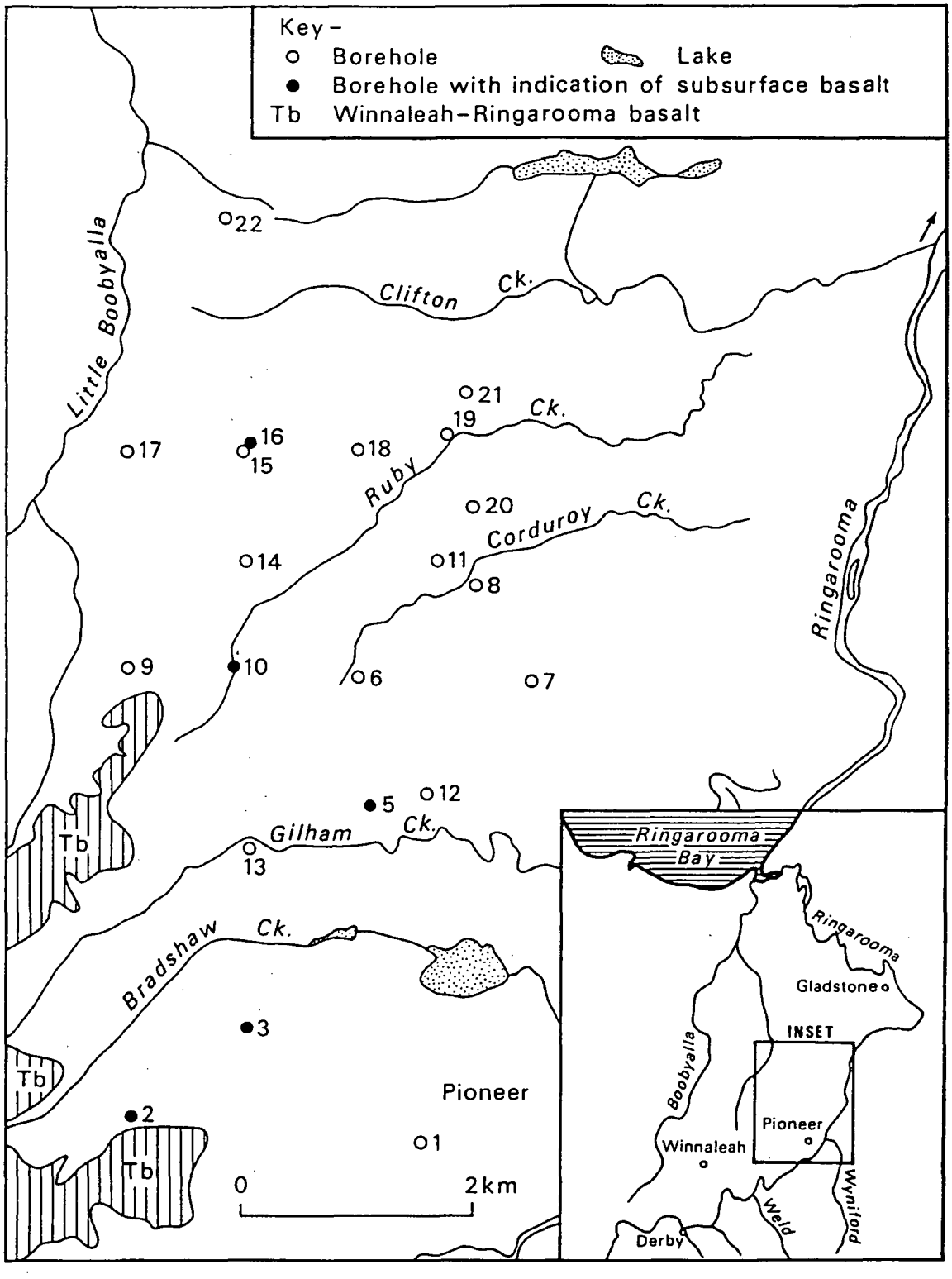

Fig. 7.17 Location map of jetstream boreholes in the South Mount Cameron Basin by Australian Anglo-American Prospecting Proprietary Limited.

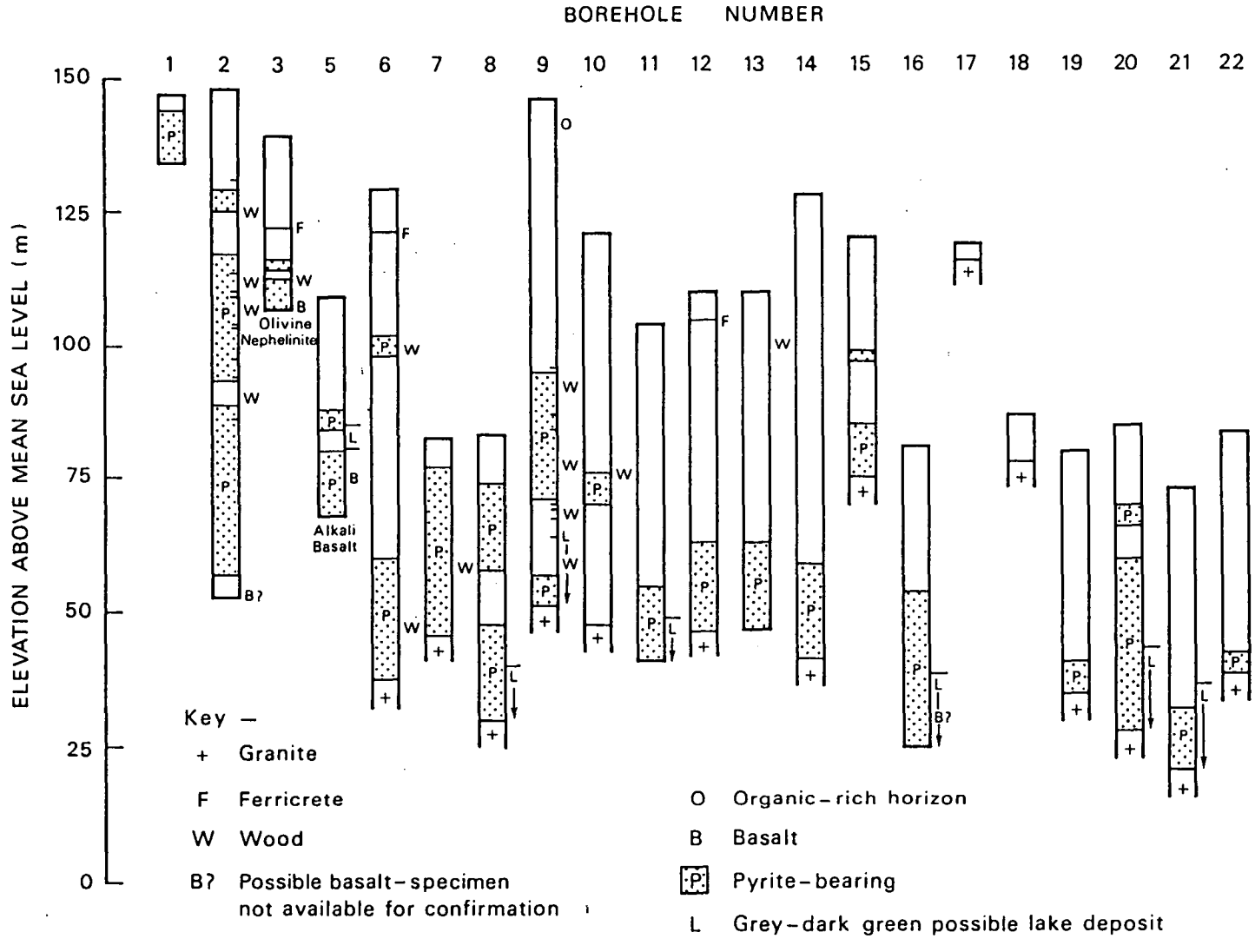

Fig. 7.18 Thickness and main characteristics of jetstream boreholes from the South Mount Cameron Basin. Based on unpublished borehole data supplied by Australian Anglo-American Prospecting Proprietary Limited.

petrographic identification of thin sections to be olivine nephelinite and alkali basalt respectively. Therefore, concealed basalts of pre-Middle Miocene age may exists at depth within the South Mount Cameron Basin. Both the abundance of pyrite in the basal sediments of all boreholes and the grey to dark green colouration near the base of many boreholes (5, 8, 9, 11, 16, 20 and 21) are indicative of anoxic deposits which may have formed in a lake prior to infilling and extrusion of the Winnaleah-Ringarooma basalts. The presence of ferricrete in the upper horizons of boreholes 3, 6 and 12 is explained by weathering of the Winnaleah-Ringarooma basalts caused by a post-Middle Miocene lateritization event.

7.2.6 Offshore deep leads

Offshore placer tin exploration by Ocean Mining A.G. in Ringarooma Bay involving seismic profiling and boreholes has resulted in the recognition of drowned offshore leads during the 1960s. The data available was reassessed by Hellyer Mining & Exploration Proprietary Limited (1982 and 1983). The main area of interest occurs at a water depth of less than 35 m below mean sea level (Fig. 7.19) and the maximum thickness of sediment is not more than about 20 m (Fig. 7.20). Although the depth below sea bed is less than those of deep leads occurring onshore, deep leads located in the Great Northern Plains were suggested by their bedrock depth to extend into Ringarooma Bay (Fig. 7.21). A frequency plot of metallic tin assay grades in borehole sections and the water depth below mean sea level is shown in Fig. 7.22. It can be seen that the bulk of the tin concentration occurs at a water depth of between 33 to 42 m below mean sea level. A number of northwesterly and northerly trending sediment filled channels were identified. Sediment samples obtained from three boreholes located on Fig. 7.19 for heavy mineral analysis have confirmed the presence of three zircospilic suite minerals, spinel, corundum and ilmenite. Based on this, the age of the

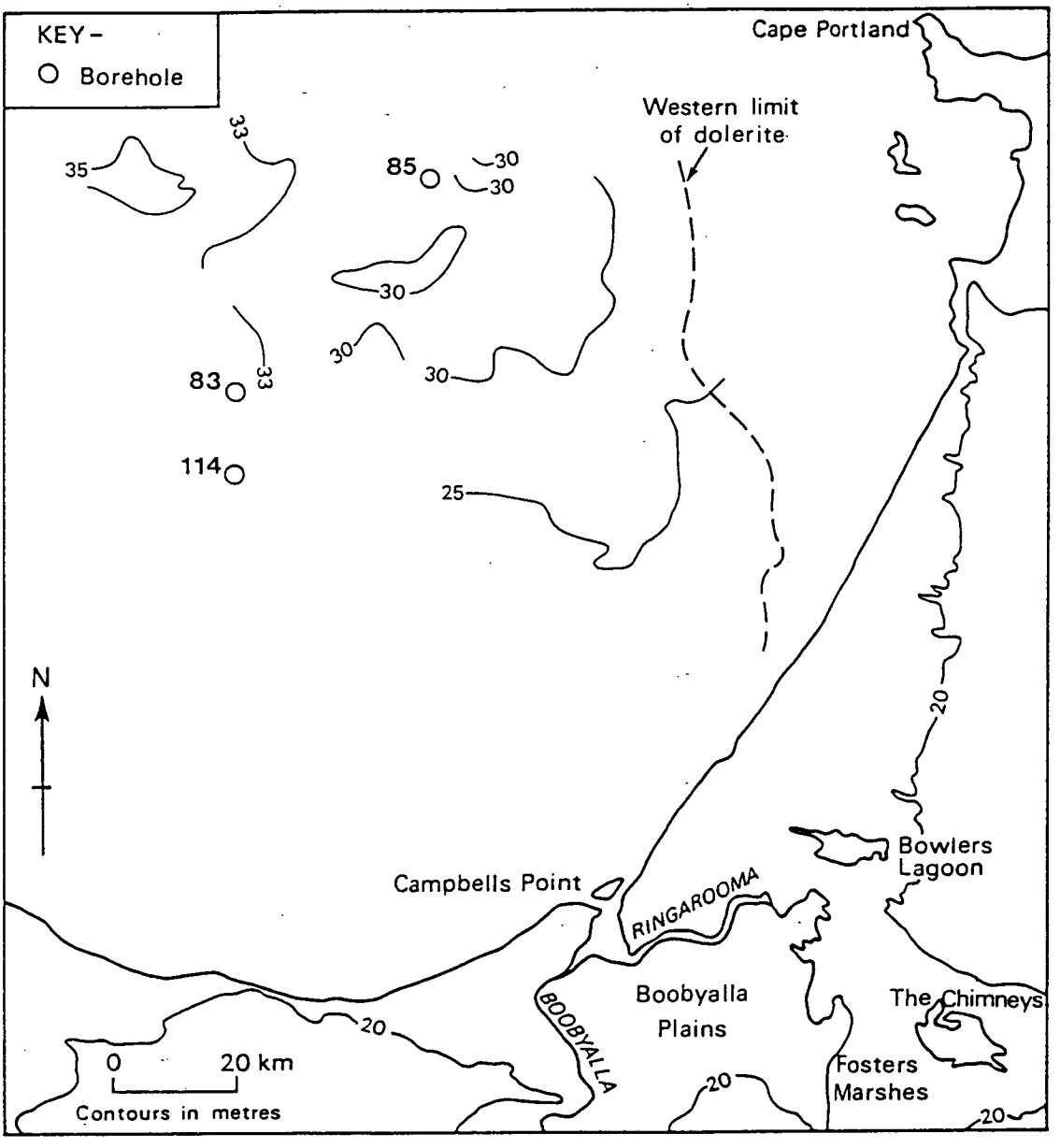

Fig. 7.19 Bathymetry and western limit of dolerite in the area of interest in Ringarooma Bay. Borehole locations referred to in the text are also shown. Redrawn from Hellyer Mining & Exploration Proprietary Limited (1983).

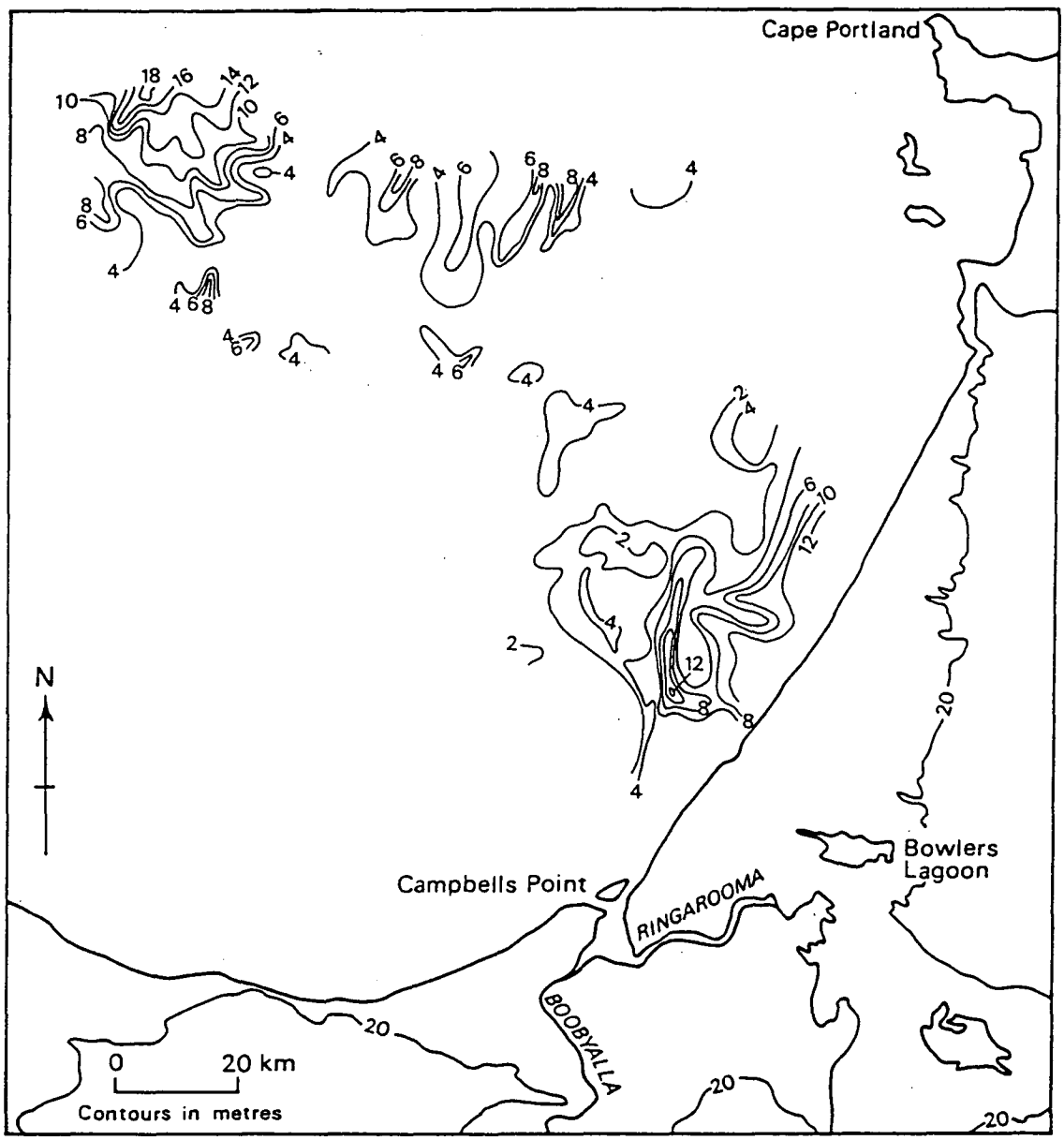

Fig. 7.20 Sediment thickness in the area of interest in Ringarooma Bay. Redrawn from Hellyer Mining & Exploration Proprietary Limited (1983).

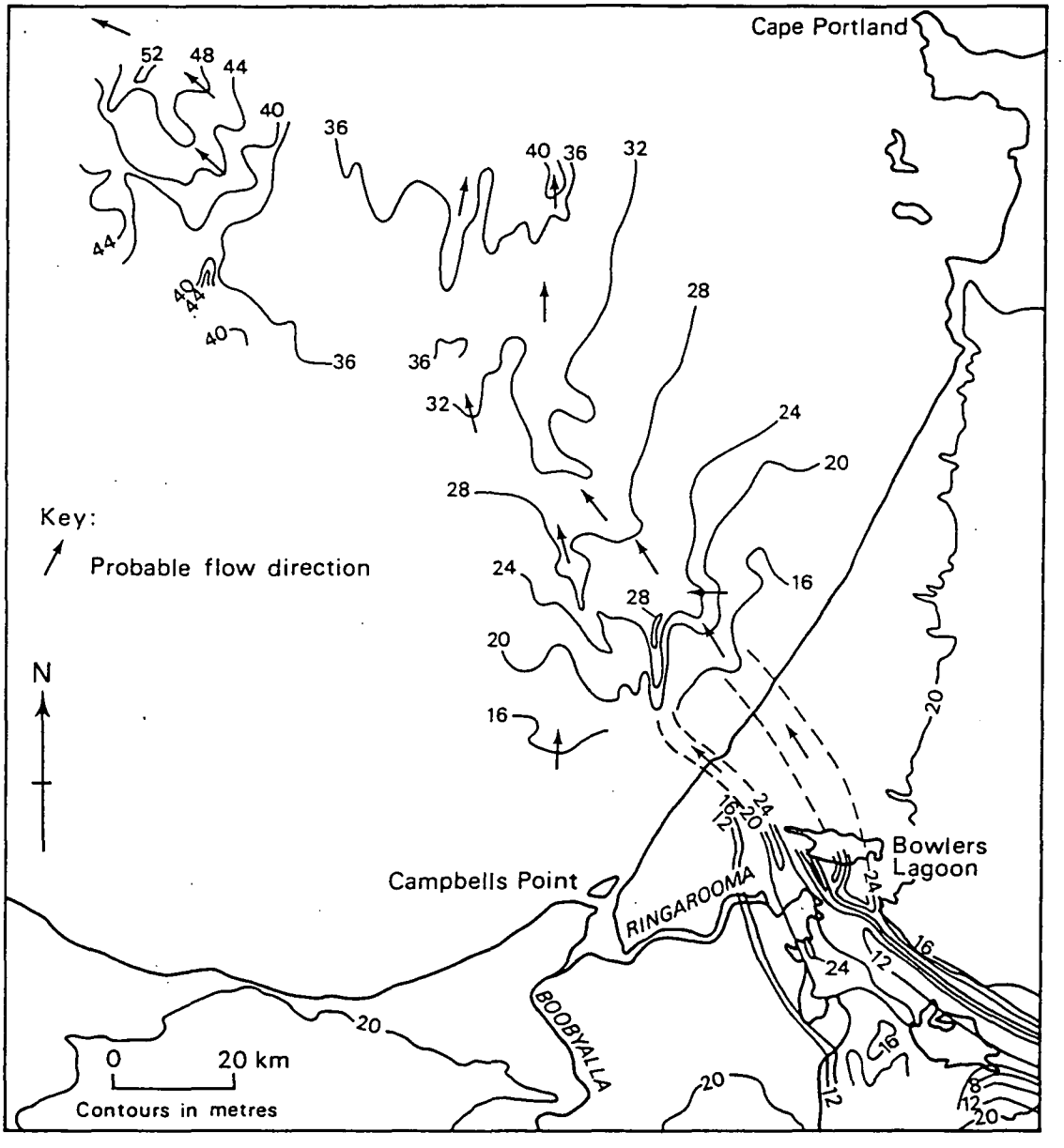

Fig. 7.21 Bedrock depth of Ringarooma Bay and part of the Great Northern Plains. Interpreted depths to bedrock in Ringarooma Bay are in metres below chart datum. Depths to bedrock on the Great Northern Plains are in metres below mean sea level. Redrawn from Hellyer Mining & Exploration Proprietary Limited (1983).

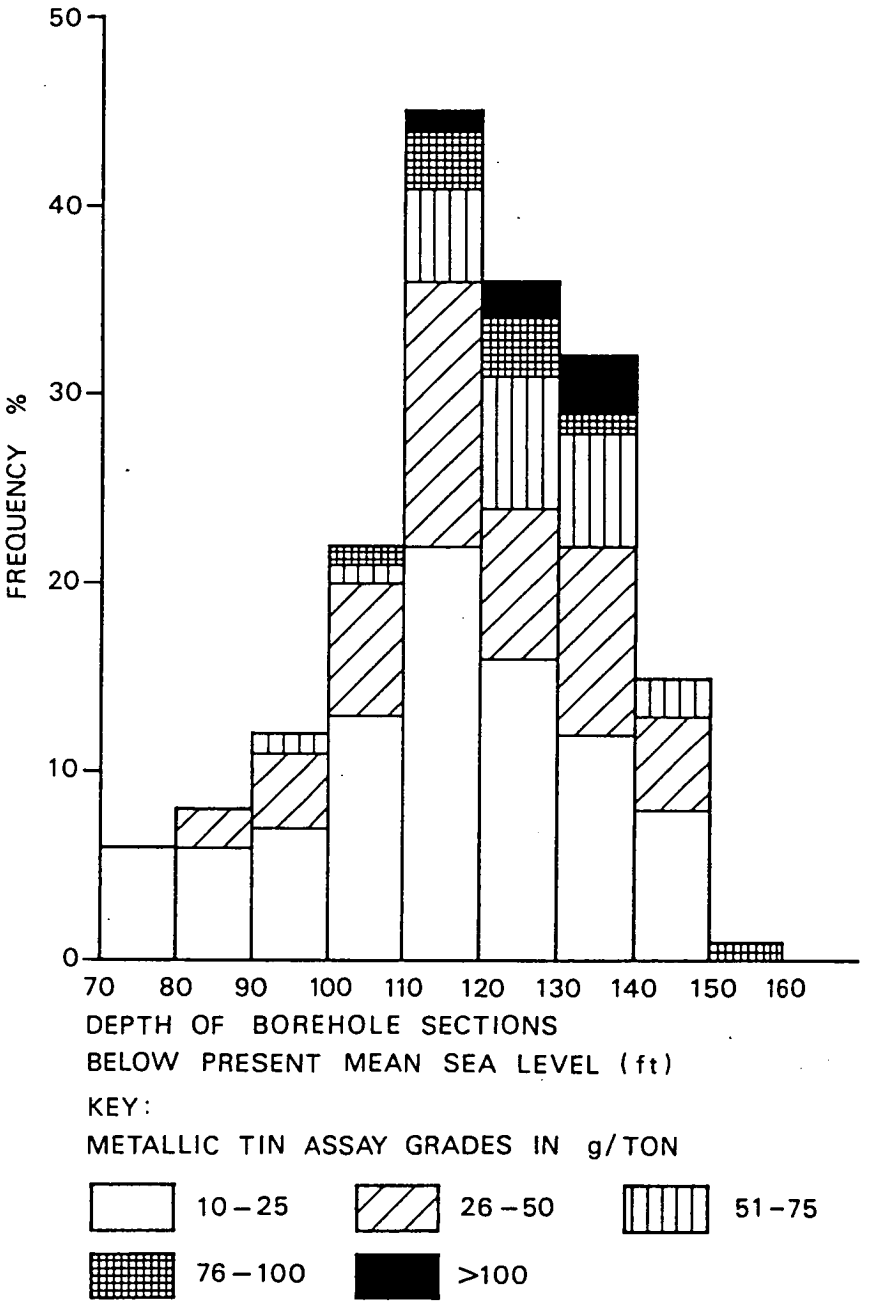

Fig. 7.22 Frequency distribution of tin assay grades in borehole sections of Ringarooma Bay plotted against depth below mean sea level. Based on unpublished data provided by the Tasmania Department of Mines. Metric equivalents of depths below sea level are 70ft = 21.3m; 80ft = 24.4m; 90ft = 27.4m; 100ft = 30.5m; 110ft = 33.5m; 120ft = 36.6m; 130ft = 39.6m; 140ft = 42.7m; 150ft = 45.7m; 160ft = 48.8m.

offshore deep leads are likely to be similar to those of the onshore counterparts.

7.3 Eluvial and colluvial placers

Eluvial placers were considered by Batchelor (1983) to be purely residual deposits which have undergone no horizontal transportation, while in colluvial placers cassiterite has been transported within the soil up to hundreds of metres. Since eluvial and colluvial placers grade into each other and into alluvial placers, they may occur in the field within short distances of each other. In the present study, eluvial and colluvial placers at shallow depth beneath ground surface are considered together because of their close genetic relationship. The main feature of this group of placers is characterized by the short transportation distance of cassiterite which may be shown by the presence of coarse and angular monomineralic and composite grains of a poorly sorted nature.

Four explanations to account for the comparatively rare occurrence of eluvial and colluvial placers are possible. Firstly, eluvial and colluvial placers may already have been exhausted through mining due to their accessible nature causing examples in the study area to be uncommon. Secondly, because of their marginal economic interest they are not exposed in mine excavations. Thirdly, it is likely that the deposits were formed at the same time as the deep leads when cassiterite was liberated from the bedrock after deep weathering. Fourthly, they are naturally rare in occurrence.

7.3.1 Monarch

The Monarch Tin Mine occurring to the northeast of Mount Cameron (Fig. 7.23) is an example of mixed eluvial and colluvial placer. Boreholes made by Blue Metals Mining Industries Proprietary Limited revealed a tongue-shaped ore body on a gentle northerly slope with a bedrock gradient of 1 in 26 (Fig. 7.24). The average thickness of the

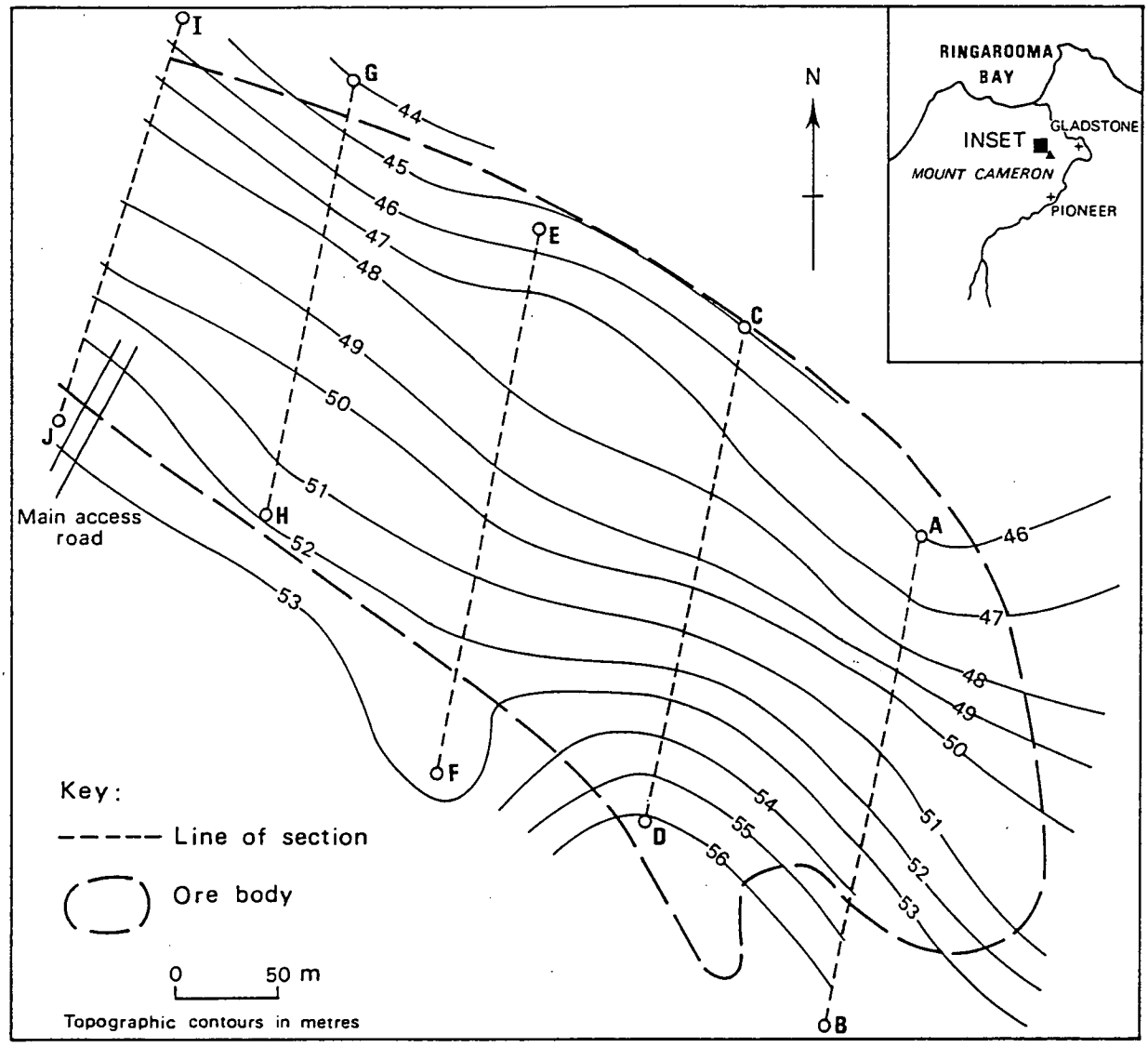

Fig. 7.23 Location map of the Monarch ore body showing the location of borehole sections. Based on unpublished data of Amdex Mining Limited.

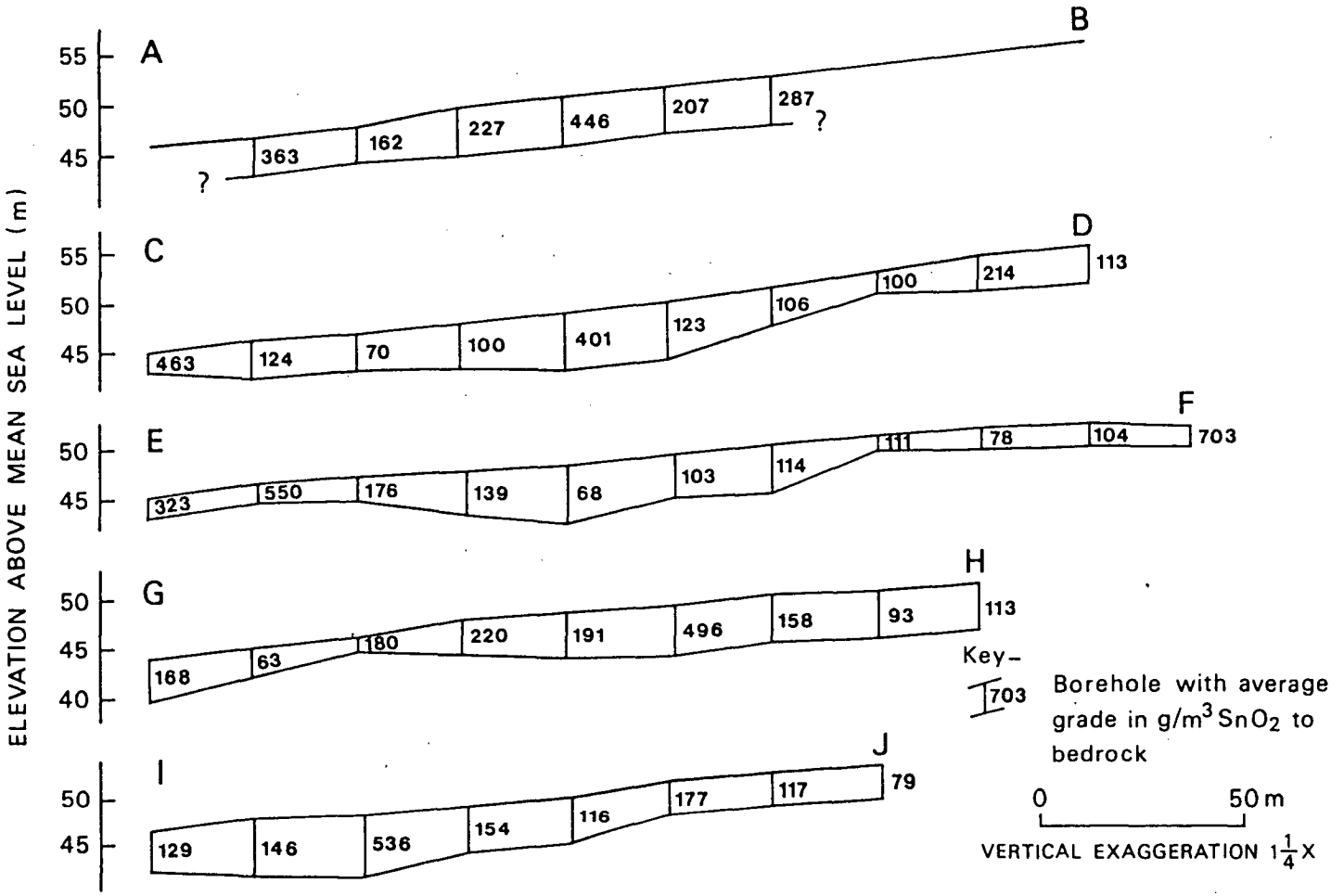

Fig. 7.24 Borehole sections across the Monarch ore body. Based on unpublished data of Blue Metals Mining Industries Proprietary Limited.

deposit is about 6 m with one borehole showing the maximum grade of 550 g/m^3 cassiterite.

Ore concentrates derived from the working of deposits adjacent to the tongue-shaped ore body have revealed the existence of abundant subangular to subrounded coarse cassiterite nuggets and composite grains of up to 14 and 25 mm grain size respectively. Based on their coarse nature, they are unlikely to have travelled far from the source rock. It is of interest to note that the zircospilic suite of heavy minerals has only been found rarely in the ore concentrates of the mine. Their restricted occurrence is explained by the presence of alluvial channels infilled by transported sediments including zircospilic minerals cut into the older eluvial and colluvial deposits.

7.3.2 Blackberries

One pit exposure of the Blackberries Tin Mine located along the Wyniford River (Fig. 3.1) provides a good example of a placer approaching a truly eluvial type. At this mine section (Plate 2.3), both mineralized and unmineralized quartz veins can be seen in the bedrock. On top of the granitic basement, subangular cobbles and boulders were embedded in a matrix of coarse-grained granitic fragments. Basement sampling of the matrix material has revealed low concentrations of cassiterite averaging between 5 and 20 g/pan which are present in the form of subangular to subrounded nuggets and composite grains up to 12.5 and 38 mm in grain size respectively. Because the cobbles and boulders are clast supported, they may have acted as a sieve deposits (Bull 1972) for trapping cassiterite. A mixed eluvial and colluvial origin is considered to be probable because of the uniformity of the size of cobbles. Elsewhere in the mine, the zircospilic suite of heavy minerals occur in alluvial deposits associated with the Wyniford Lead.

7.3.3 New Clifton and Sextus Creek

Two mines, New Clifton and Sextus Creek (Fig. 3.1), both located on the piedmont zone of the Mount Cameron Massif are thought to represent eluvial and colluvial placers in addition to alluvial placers. The former was operating at the time of field study while the latter was closed. However, both mines were sufficiently well exposed to permit basement sampling traverses to be carried out and the results are shown in Fig. 7.25.

At the New Clifton Mine (Plate 7.1), the sampling traverse made was at right angles to the downslope direction and the average sample spacing used was about 5.5 m. The heavy mineral content was found to vary between a maximum of 200 g/pan to below 5 g/pan. No correlation was found between heavy mineral concentration and the position of bedrock gullies. The presence of randomly oriented subangular to subrounded boulders which are clast supported beneath the present day piedmont zone of Mount Cameron is indicative of an eluvial-colluvial origin. However, further down, the deposits is found to grade into an alluvial deposit.

At the Sextus Creek Mine, the sampling traverse made was in the downslope direction of the lead and the sample spacing used was variable between 10 to 20 m. The heavy mineral concentration is found to decrease rapidly downstream suggesting that cassiterite concentrations falls rapidly away from downslope of Mount Cameron within a distance of 100 m. However, another interpretation is that the sampling procedure used was not representative.

Common features found at the New Clifton and Sextus Creek Mines include:

(1) Predominance of coarse sand and fine gravel size cassiterite grains.

(2) Presence of subangular to subrounded monomineralic cassiterite grains. The maximum grain sizes found are 9 and 4.2 mm respectively.

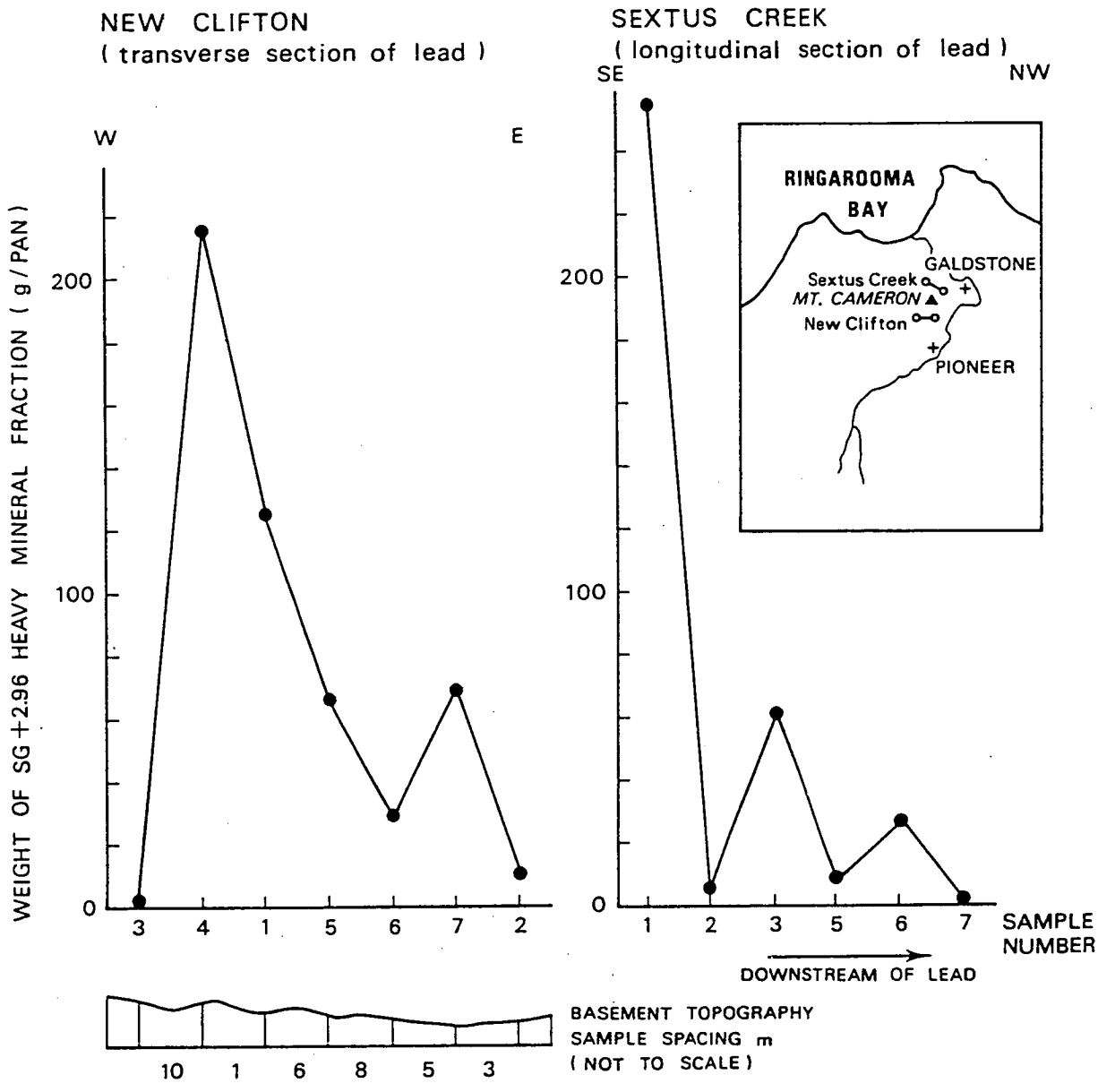

Fig. 7.25 Section showing the weight distribution of (SG +2.96) heavy minerals immediately above the rock basement of the New Clifton and Sextus Creek Tin Mines.

Plate 7.1 Pit exposure at the New Clifton Mine showing colluvial deposits with numerous randomly oriented sub-angular to sub-rounded cobbles and boulders resting on a granitic rock basement.

(3) Presence of subangular to subrounded composite cassiterite grains. The maximum grain sizes found are 5.8 and 7.2 mm respectively.

(4) Absence of the zircospilic suite of heavy minerals.

(5) Presence of topaz even though this mineral is less common at Clifton.

The common features listed above are in confirmation of the short transportation distance of cassiterite even on sloping ground. Downstream of the mineralized bedrock, a decrease in grain size and the abundance of composite cassiterite grains are to be expected. However, since mass movement downslope had taken place, both New Clifton and Sextus Creek are closer to colluvial than eluvial placers.

7.4 Terrace deposits

Unlike deep leads, eluvial and colluvial placers, terrace deposits are restricted in occurrence the Ringarooma River valley. They are typically fining-upward alluvial sequences up to about 10 m in thickness. Examples include Mutual, Riverside, Delta, Dobsons and several shallow workings on the Great Northern Plains including Macgregor, Canary, Vulcan and Doone (Fig. 3.1). The common feature shown by these mines is the presence of the zircospilic suite of heavy minerals as well as small quantities of alluvial gold. Based on their high stratigraphic position, they are younger than the other types of placer deposits. In the present study, the occurrence of alluvial gold has been traced upstream of the Ringarooma River to Derby where comparatively coarse gold has been found at the Cascade River Tin Mine (Fig. 3.1). Although the source rock for the gold may already have been eroded away, a probable location for the gold mineralization is within the Mathinna Beds which are known to contain small auriferous quartz reefs. These beds outcrop along the section of the Ringarooma River between the Cascade River and Main Creek. Through the provenance of gold, it appears that the terrace deposits are relatively young.

7.5 General discussion

Tin placers in southeast Asia were classified by Batchelor (1983) into seven types:

(1) Eluvial placers.

(2) Colluvial placers.

(3) Piedmont fan placers.

(4) 'Residual' and transported Kaksa placers.

(5) Transported fluviatile mintjan placers.

(6) Transported fluviatile cave placers.

(7) Marine placers.

Out of these, only types (3), (4) and (5) were considered by Batchelor (1983) to be of major economic significance. Furthermore, he noted that in many cases, the different types of placers were interrelated and intergradational, and, form an evolutionary series.

In the present study, the classification of placers into three main categories are considered to be more appropriate because of their age relationship. Deep leads which are buried by tin-barren sediments are relic and are of the greatest age because of their low stratigraphic position. Eluvial and colluvial placers close to the ground surface are liable to be episodically reworked and are likely to be younger than deep leads. On the other hand, terrace deposits are the youngest because they are found adjacent to present day river channels and floodplains, occupying the highest stratigraphic position as well as containing alluvial gold.

Although deep leads such as Briseis and Pioneer would fall into the piedmont fan type of placer of Batchelor (1983), the classification of a deposit into a single type is considered to be inappropriate because of complexities found within deep leads. For example, close examination of the Pioneer Lead has revealed the presence of 'residual' and transported Kaksa placers as well as transported mintjan placers in the upper part

of the basal sequence. Furthermore, the presence of the zircospilic suite of heavy minerals transported to the site by fluvial means indicated mixing with essentially locally derived cassiterite. Therefore a detailed classification of placers is not considered meaningful in the present study.

Placer deposits below the present sea level in Ringarooma Bay cannot be considered marine placers in a strict sense because they may have been formed subaerially. The absence of marine indicators such as the lack of surficial tin enrichment found on the present sea bed (Jones & Davies 1983) supports this view.

A summary of elevations of rock basement level of leads and heavy mineral enrichment levels is shown in Table 7.2. The rock basement elevation is seen to vary from a maximum elevation of 160 m in the Cascade Lead to a minimum of -45 m in the case of leads in Ringarooma Bay. Thus the total difference in elevation is in excess of 200 m. Because of the distance separating the localities, the cassiterite present within the basal sediments of leads is best explained by a local source of supply through bedrock mineralization. The presence of tin enrichment levels above the rock basement in the Cascade, Endurance and Scotia Leads is suggested to represent erosional surfaces associated with the reworking of lead sediments causing heavy mineral concentration by elutriation.

7.6 Summary of conclusions

Based on the types of placer deposit found in northeastern Tasmania and their characteristics, the following conclusions may be drawn:

(1) Deep leads are older than other types of placers and are of greater economic significance.

(2) Deep leads show a sharp decline in tin content downstream indicating that no 'new' cassiterite enters the river valley.

Locality /lead	Elevation above or below mean sea level (m)	
	Rock basement level*	Heavy mineral enrichment level(s)
Cascade	160	232, 204, 168
Pioneer	44 - 46	adjacent to rock basement
Endurance	24 - 48	70, 55
Scotia	6 - 48	43, 25, 17
Monarch	44 - 50	adjacent to rock basement
Gellibrand Plains	128	adjacent to rock basement
Trout Creek	78	adjacent to rock basement
Ringarooma Bay	-35 - -45	adjacent to rock basement

* - Rock basement may be deeply decomposed; where a range of elevation values is indicated, minimum downstream and upstream elevations are given.

Table 7.2 Summary of elevation of rock basement levels and heavy mineral enrichment levels in selected leads of northeastern Tasmania.

Furthermore, the low gradient of the rock basement is not conducive to long distance of transport.

(3) The occurrence of deep leads both onshore and offshore is indicative of their relic origin. It is possible that they have been formed by related events during periods of low sea-level stand.

(4) The bulk of the tin is found within the basal sequence of deep leads. Elutriation is likely to be important as an enrichment process.

(5) Erosional surfaces or hiatuses may be recognised by heavy mineral enriched layers within deep lead sequences.

(6) Tin distribution in basal sediment is dependent on selective concentration processes operating as well as the nature of bedrock mineralization. Cassiterite shows little of no mobility in contrast to the low density minerals and is therefore concentrated in the basal part of sedimentary sequences.

(7) Much relief in the former landscape was destroyed by alluvial infilling particularly during the period prior to the Middle Miocene.

(8) While some deep lead sites have remained buried to the present day, other leads are likely to be subjected to reworking by fluvial processes especially if they are shallow in depth.

(9) The zircospilic suite of heavy minerals and the occurrence of alluvial gold are useful age and provenance indicators of placer deposits. Because the provenance of these minerals is different from cassiterite, their presence together indicates the mixing and reworking of the deposits.

(10) Local sources of tin mineralization in the bedrock are indicated by the distribution of cassiterite grain size. Near to the source grain size increases to a maximum.

(11) All eluvial deposits are of residual origin. Such deposits are commonly of a mixed eluvial and colluvial origin.

(12) Eluvial and colluvial placers are characterised by subangular and subrounded cassiterite nuggets and composite grains present in the matrix of cobbles and boulders.

(13) The zircospilic suite of heavy minerals occurring in what appeared to be eluvial and colluvial deposits are introduced by alluvial channels cut into the older deposits. In other words, all three types of placers may occur in close association with each other.

(14) Terrace deposits containing the zircospilic suite of heavy minerals and gold are found to be restricted to the channels and floodplains of the present day Ringarooma River downstream of Derby.

(15) The sediment-filled bedrock channels at Trout Creek and Gellibrand Plains represent former extensions of the Weld Lead, and, the Main Creek and/or Cascade Lead respectively.

(16) Deep lead basins, such as the South Mount Cameron Basin, with no apparent outlet need to be explained.

CHAPTER 8 GENESIS OF STANNIFEROUS PLACERS

8.1 Introduction

In chapters 6 and 7, dating and classification permitted the identification of the time scale and the mode of formation of each type of placer to be determined. In the present chapter, the genesis of stanniferous placers is examined in the light of all available evidence.

Based on the stratigraphic control of deep leads and information obtained from heavy mineral provenance, it is possible to identify the geological events important in placer genesis in northeastern Tasmania. The sequence of events is grouped under five main time intervals:

(1) Pre-Triassic

(2) Triassic to Early Eocene

(3) Middle Eocene to Early Miocene

(4) Middle Miocene to Pliocene

(5) Quaternary.

The relationship between tin mine location, surficial geology and bedrock type along five lines of section located in Fig. 8.1 are illustrated in Figs. 8.2 and 8.3. These geological sections indicate the stratigraphic relationship between the mineralized granite, the younger and older basalts, and the placer deposits.

8.2 Pre-Triassic

The timing of unroofing of the mineralized Late Devonian to Early Carboniferous Blue Tier and Scottsdale Batholiths leading to the release of cassiterite is important in the formation of the placer deposits. Although unroofing occurred at different times in different places, the outcrop of lithified conglomerate of the Permo-Triassic Parmeener Supergroup resting unconformably on granitic rocks on the east side of Mount Littlechild at an elevation of ca. 780 m above present mean sea level (Fig. 2.6) must have taken place at least prior to the Middle Permian and possibly as early as the Late Carboniferous. Based on the

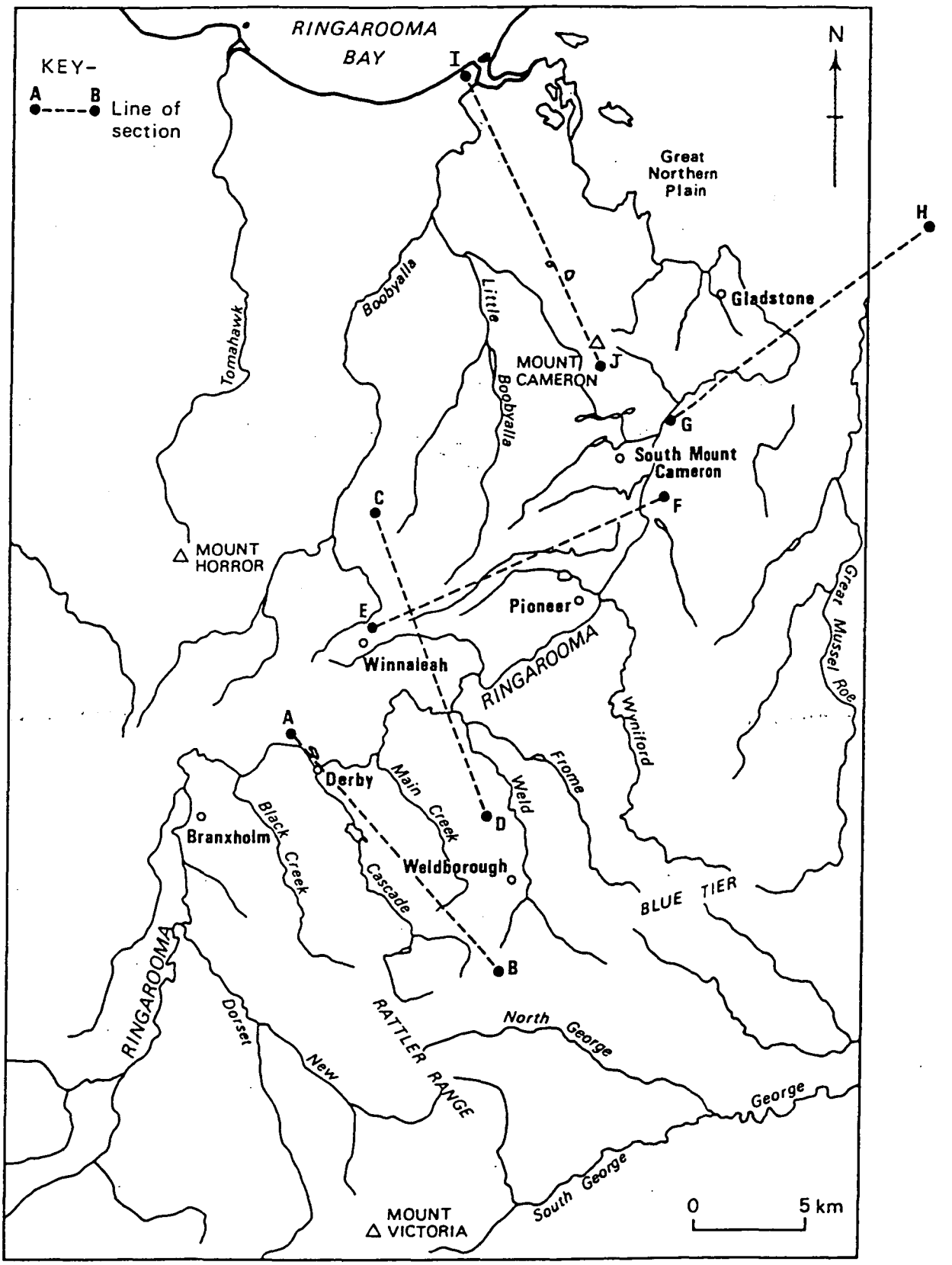

Fig. 8.1 Location map of five geological cross-sections in the study area shown in Figs. 8.2 and 8.3.

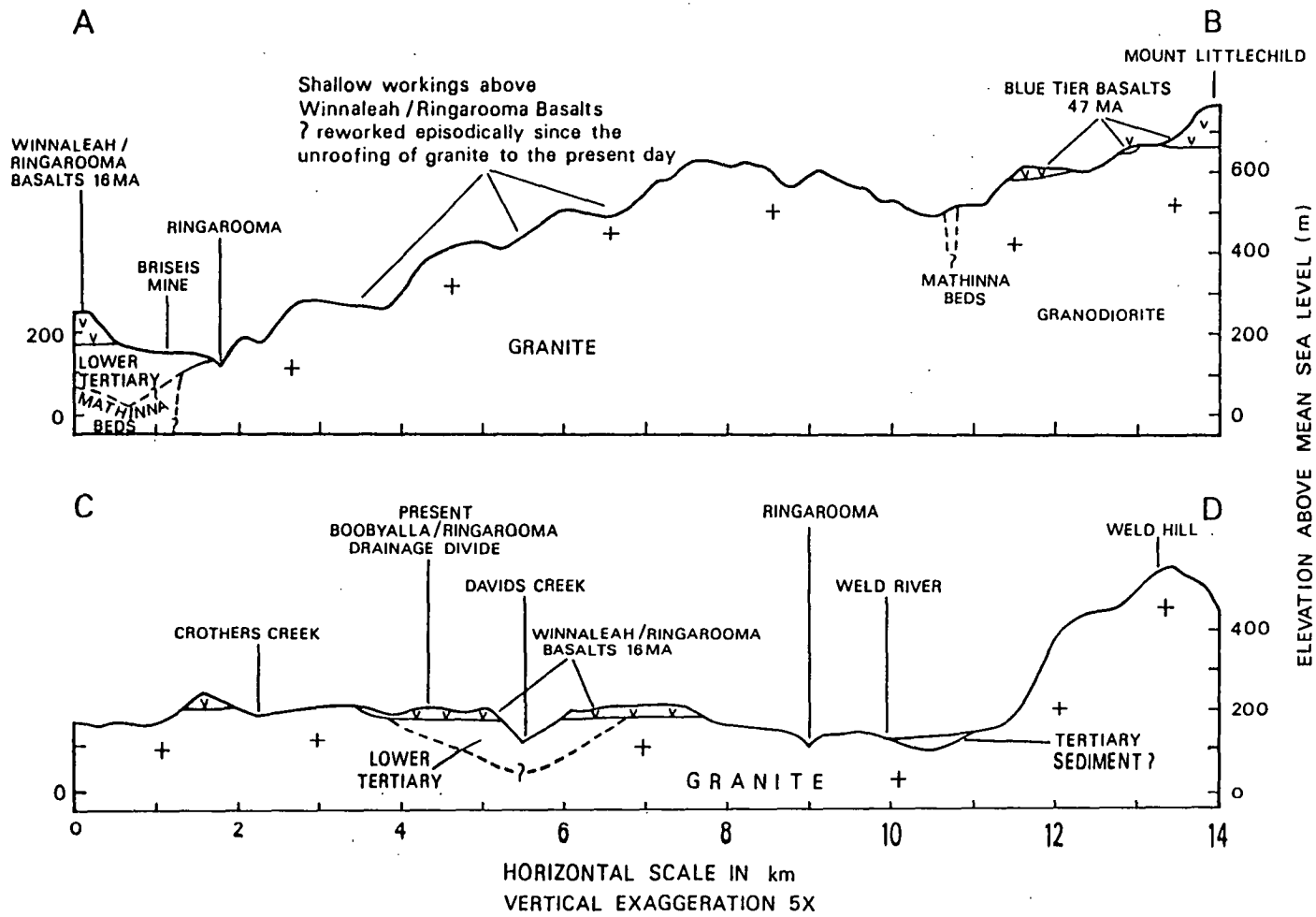

Fig. 8.2 Geological cross-sections along lines A-B and C-D shown in Fig. 8.1. Geological information shown inferred from 1 : 50 000 geological map sheets of the Tasmanian Department of Mines.

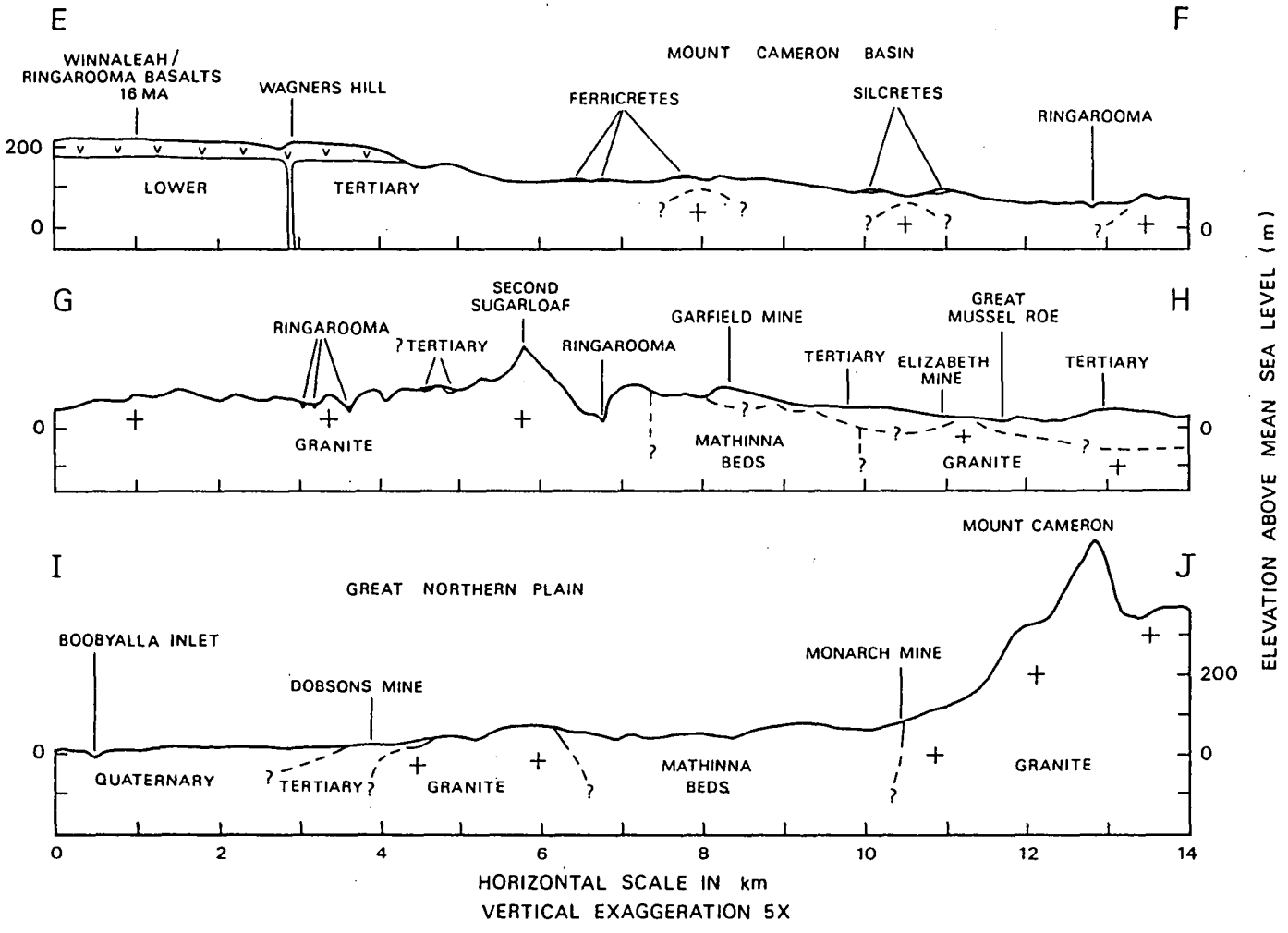

Fig. 8.3 Geological cross-sections along lines E-F, G-H and I-J shown in Fig. 8.1. Geological information shown inferred from 1 : 50 000 geological map sheets of the Tasmanian Department of Mines.

lithological characteristics described by McClenaghan et al. (1982), the sedimentary environment of the conglomerate was a channel of a high to moderate energy river. In the present study, attempts have been made to identify cassiterite within the conglomerate specimens. However, none was found probably due to the erratic distribution of cassiterite within sediments. Nevertheless, fluvial processes of erosion and deposition must have operated on the granite to create the erosional surface on which the conglomerate rests causing cassiterite liberation and concentration through recycling. At the same time, the absence of granite fragments within the conglomerate suggest that conditions favourable for chemical weathering may have been present in the Late Carboniferous or Early Permian.

Based on the occurrence of sparsely fossiliferous marine sandstone and siltstone with dropstones in the Permian rocks of the Great Northern Plain, glacial-marine conditions prevailed over parts of the study area during the Permian. Thus, glacial or periglacial erosion of the Blue Tier and Mount Cameron Massifs have occurred. Such conditions are likely to facilitate the release of cassiterite from the mineralized bedrock.

Although the stratigraphic relationship between the outcrops of Parmeener Supergroup on the Blue Tier and the Great Northern Plain is uncertain, the present difference in topographic elevation of 740 m was probably in existence during the Permian. A large difference in topographic elevation would have important implications on placer genesis. The presence of high relief is favourable to fluvial erosion. On the other hand, cold climatic conditions may result in glacial erosion and/or periglacial activity. The latter include frost shattering, solifluction and meltwater erosion caused by the seasonal thawing of snow fields. All these processes would not only contribute towards the release of cassiterite from the mineralized granite but also causing their selective sorting and concentration.

8.3 Triassic to Early Eocene

The intrusion of Jurassic dolerite sheets over Tasmania was probably accompanied by uplift followed by extensive erosion (F.L. Sutherland, pers. comm.). The sediment fill within the Boobyalla Sub-basin identified by Moore et al. (1984) which forms an onshore extension of the Bass Basin immediately north of the study area is in support of the continued uplift and erosion. These workers concluded that northeastern Tasmania was the major sediment source for the Cretaceous and later sediments in the southeastern sector of the Bass Basin. However, the cause of uplift is uncertain even though isostatic rebound, erosion and heating associated with dolerite intrusion may all have played a part. The Late Cretaceous palaeogeography of the Sub-basin was shown by matrix supported conglomerates with a great range of clast sizes to have been a fault scarp probably with adjacent debris flow and sheet flood deposits. Because of this, heavy minerals may be enriched in the piedmont zone of the granite massifs.

The climate during most of the Jurassic was less differentiated than now (Quilty in Veevers 1984). Townrow (1964) suggested a temperate climate for Tasmania in the Early Jurassic but later palaeontological evidence reveals a Late Triassic age for the beds used by Townrow as evidence. Based on evidence from palynological and foraminiferal analyses, Douglas & Ferguson (1976) suggested that southeastern Australia was cool until the Santonian, with rising temperature and humidity to the end of the Cretaceous. Consequently, favourable climatic conditions for deep weathering to prepare further the mineralized bedrock for cassiterite release may have existed from the Late Cretaceous onwards.

A reconstruction of the palaeogeography of Australia during the Middle Palaeocene after Kemp (1978) is shown in Fig. 8.4. Palynological evidence indicated that northeastern Tasmania was a region with

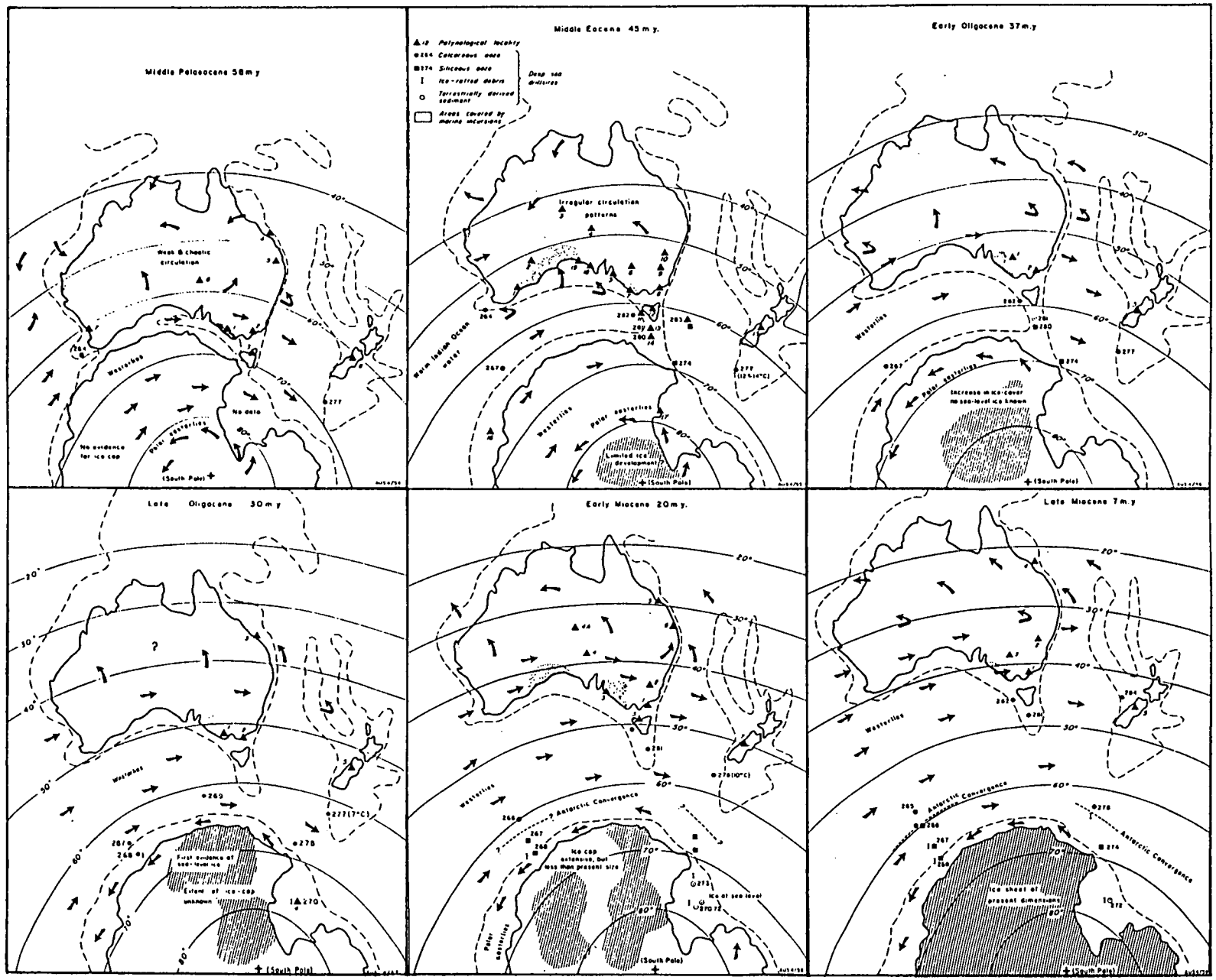

Fig. 8.4 Palaeogeographic reconstruction of the Australian region for the Middle Palaeocene, Middle Eocene, Early Oligocene, Late Oligocene, Early Miocene and Late Miocene after Kemp (1978). Locations of DSDP boreholes are also shown.

sufficient rainfall to support rainforest cover with warm temperatures. In addition to this, a sea-surface temperature of about 18°C was estimated for the Late Palaeocene by oxygen-isotope studies of planktonic foraminifera in DSDP cores around Tasmania (Shackleton & Kennett 1975) (Fig. 6.6). Therefore, warm climatic conditions conducive to deep weathering prevailed for up to 37 Ma from the Late Cretaceous into the Early Eocene.

Many of the major relief and drainage features in northeastern Tasmania still visible today appear to date back to the Triassic to Early Eocene time interval. Both the Blue Tier and Mount Cameron Massifs were already established highland areas with the former showing a dominance of north-north-west flowing streams well adjusted to the geological structure. The presence of highland areas from the Permo-Triassic is indicated by outcrops of Parmeener Supergroup to the east of Mount Littlechild (Figs. 2.2 and 2.6) and on Mount Victoria about 10 km south of the study area. Because radial drainage patterns are discernible from these outcrops in the present day, they appear to have remained high ground up to the present day. The north-north-west drainage trend found on the Blue Tier Massif was probably controlled by Devonian Tabberabberan structures (see Solomon 1962). Since much of the landscape features had already been established for a long time, the episodic recycling of heavy minerals probably led to cassiterite enrichment by elutriation.

8.4 Middle Eocene to Early Miocene

The extrusion of the Middle Eocene Blue Tier basalts dated at ca. 47 Ma (Sutherland & Wellman 1986) served as an important stratigraphic marker for the genesis of stanniferous placers because of the distinctive zircospilic suite of heavy minerals associated with these basalts. Since Mount Littlechild (Fig. 8.2) and the adjacent Forest Lodge acted as volcanic centres emitting the basaltic lavas (Sutherland

& Wellman (1986), they created new topographic high points on the plateau of the Blue Tier. The development of a radial drainage pattern around the volcanic cones caused the zircospilic suite of heavy minerals to be dispersed in all directions making them useful as indicators of post-Middle Eocene deposits. When present within deep leads, the deposits must have been reworked prior to their burial between the Middle Eocene and Early Miocene. On the other hand, deposits without these heavy minerals such as in part of the Blackberries Tin Mine are likely to be pre-Middle Eocene in age. Evidence for one or two reworking episodes above the basal sediments have been found in some of the deep lead sequences, e.g. Cascade, Endurance and Scotia. These episodes are recognised through the identification of erosional surfaces associated with heavy mineral enrichment.

Vegetation history (Kemp 1978) and oxygen-isotope data (Dorman 1966 and Shackleton & Kennett 1975) have provided indirect information on age as well as indications of the broad trends of climatic evolution from the Early Tertiary. Palaeogeographical maps of Australia during the Middle Eocene, Early Oligocene, Late Oligocene and Early Miocene compiled by Kemp (1978) are shown in Fig. 8.4. In southeastern Australia including Tasmania, sea-surface temperatures of around 20 °C in the Early Eocene fell to 12-14°C in the Middle Eocene, and to 10 °C by the Late Eocene (Shackleton & Kennett 1975) (Fig. 6.6). This is supported both by the absence of taxa indicative of tropical warmth beyond the Middle Eocene and the minimal zonation of vegetation found for this epoch (Kemp 1978). At the end of the Eocene, there was a major temperature decline and an associated decrease in floral diversity. From Oligocene to Early Miocene, the sea-surface temperature varied within a narrow range of between 6 and 10°C (Fig. 6.6) suggesting relative climatic stability. The persistence of rainforest is reflected in the vegetation data which showed evenly distributed rainfall (Kemp 1978). Some evidence was found

by Hill & Macphail (1983) for floristic complexity caused probably by evolutionary changes during the relatively long period of climatic stability.

The rapid decline in sea-surface temperature near the end of the Late Eocene (Fig. 6.6) which preceded the sharp fall in sea level at the beginning of the Late Oligocene probably marks the beginning of an erosional phase in the highlands associated with heavy mineral concentration. During this phase, pre-Middle Eocene placers with a granitic suite of heavy minerals were reworked and became mixed with the zircospilic suite of heavy minerals deriving from the older basalts. Episodic recycling of heavy minerals prior to the Middle Miocene is shown by the occurrence of erosional surfaces associated with placer mineral enrichment above the basal sediments within deep lead sequences. During the Late Oligocene to Early Miocene, when the global sea level fell dramatically as a consequence of the withdrawal of sea water caused by the formation of the Antarctica ice cap, the deep leads occurring in the piedmont zone where there is a sharp flattening of slope gradient were buried. This is explained by the increase in erosion rate over the highlands following a fall in base level. The infilling of the South Mount Cameron Basin is likely to have reached the level of the surface underlying the younger basalts.

8.5 Middle Miocene to Pliocene

Middle Miocene basaltic volcanic activity dated at ca. 16 Ma (Brown 1977) with extensive flows of the Winnaleah-Ringarooma basalts led to dramatic changes in the drainage pattern of the study area through drainage diversion and capture. The north-north-west flowing streams originating from the Blue Tier Massif were obstructed by the younger basalts along a line running from South Mount Cameron to Branxholm (Fig. 8.5) forming the Ringarooma River course which resembled that of the present day. A summary of the attributes of these diverted streams

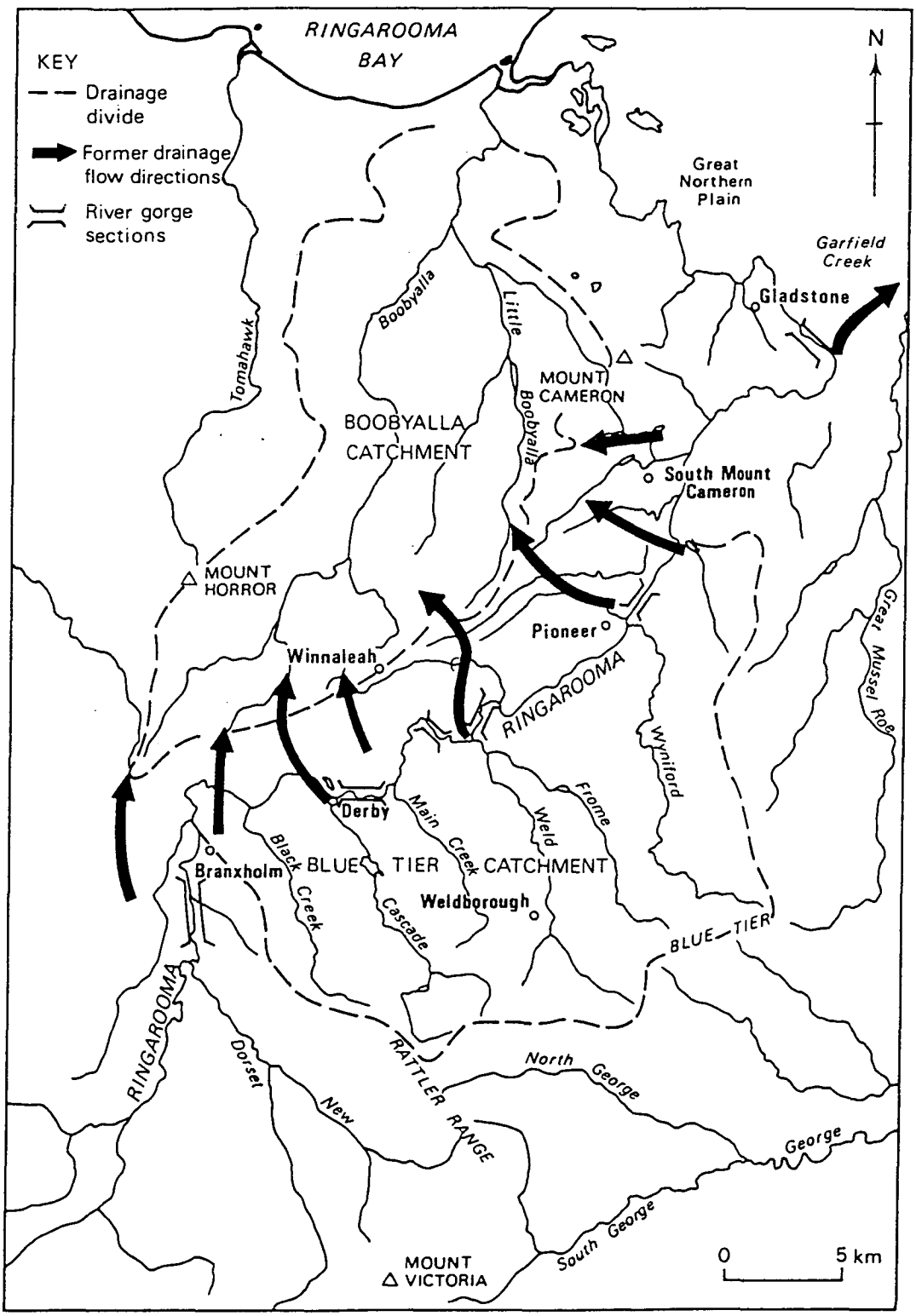

Fig. 8.5 Sketch map showing the probable former drainage extension of streams from the Blue Tier Massif into the Boobyalla catchment prior to diversion by the Winnaleah-Ringarooma basalts. Present river gorge sections along the Ringarooma River and former extension of the Great Mussel Roe catchment are also shown.

including Black Creek, Cascade River, Main Creek, Weld River and Wyniford River are summarised in Table 8.1. All these streams were connected formerly to the Boobyalla catchment and are evident today by their north-north-west sub-basaltic extensions found at e.g. Trout Creek and Gellibrand Plains. Other supporting evidence is:

(1) The heavy mineral provenance. The zircospilic minerals have been found in tin mines including Banca and White Rocks (Fig. 2.10) which occur north of the Winnaleah-Ringarooma basalts. These minerals were thought to have originated from the Blue Tier basalts and were transported to these sites by fluvial processes probably during the Middle Eocene to Early Miocene.

(2) The misfit nature of drainage within the present day Boobyalla River catchment (Fig. 8.5) in that the present day streams appear to be too small for their existing valley and channel. Prior to the drainage diversion event, these stream valleys were occupied by larger streams connected to the Blue Tier.

(3) The sources of most streams within the present day Boobyalla River catchment are located on the Winnaleah-Ringarooma basalts immediately to the north of the South Mount Cameron to Branxholm line. Because the age of the basalts is known, these streams must all post-date ca. 16 Ma.

(4) A number of river gorge sections along the present course of the Ringarooma River (Fig. 8.5) cannot be explained satisfactorily by downcutting since the Middle Miocene. If these gorges were cut since the Middle Miocene, the mean rate of downcutting may be estimated using the present day elevation of the Winnaleah-Ringarooma basalts adjacent to the gorges. However, the estimates made at four sites shown in Table 8.2 indicated a downcutting rate ranging from 4.5 to 7.2 m/Ma are low.

Tributary	Elevation above mean sea level (m)*		Length (km)	Average gradient	Catchment area (km^2)
	Headwater	Confluence point			
Guilding Star Creek	550	175	4.0	1:11	6.0
Black Creek	350	158	4.7	1:25	23.4
Black Creek (via Arba Creek)	800	158	13.2	1:21	-
Cascade River	870	150	16.2	1:23	39.1
Cascade River (via Tin Pot Creek)	610	150	9.3	1:20	-
Cascade River (via East Cascade River)	850	150	14.8	1:21	-
Main Creek	612	130	10.9	1:23	22.6
Weld River	594	109	17.6	1:37	69.8
Weld River (via Frome River)	850	109	15.3	1:21	-
Weld River (via Spinel Creek)	750	109	16.0	1:25	-
OK Creek	375	100	4.0	1:15	4.5
Gladstone Creek	400	78	4.2	1:13	4.6
Wyniford River	750	77	15.7	1:23	58.5
Chung Creek	290	65	6.2	1:28	14.4
Swain Creek	300	57	5.6	1:28	7.4

* - Estimated from Tasmania 1 : 25 000 topographic series map sheets.

Table 8.1 Comparison of present day attributes of north-north-west flowing streams originating from the Blue Tier Massif. These streams are thought to have been diverted by the Winnaleah-Ringarooma basalts. All major tributaries are located in Fig. 2.2.

Confluence Point	Elevation above mean sea level (m)*		Possible downcutting rate (m/Ma)
	Ringarooma River	Surface of adjacent basalt	
Weld River	109	210	6.3
Main Creek	130	245	7.2
Cascade River	150	250	6.2
Black Creek	158	230	4.5

* - Estimated from Tasmania 1 : 25 000 topographic series map sheet (Derby) and 1 : 50 000 Ringarooma geological map sheet.

Table 8.2 Estimates of mean downcutting rate at four confluence points along the present Ringarooma River. Based on the assumption that the Ringarooma River was entirely responsible for downcutting since the Middle Miocene (16 Ma).

(5) An examination of the present day attributes of the north-north-west flowing tributary streams of the Ringarooma River between South Mount Cameron and Branxholm (Table 8.1) shows that most major streams are similiar in length and gradient with a maximum of 17.6 km for the former and 1 in 11 for the latter. Since all these streams have originated from the Blue Tier Massif, their similarity in attributes is best explained by their diversion caused by the younger Tertiary basalts.

(6) The absence of major tributaries along the present day Ringarooma River downstream of Pioneer show the lack of adjustment, and, the relatively young age of this part of the river course.

Because of a combination of drainage obstruction and river capture, runoff from the Blue Tier Massif was diverted northeastwards into the South Mount Cameron Basin which became enclosed through blockage on its western side by the Winnaleah-Ringarooma basalts. A shallow lake may have been formed initially before an exit into the sea was found via Garfield Creek and the Great Mussel Roe River (Fig. 8.5). The lack of evidence for the existence of the lake may be explained by its short-term existence. This was followed by further river capture causing the proto-Ringarooma River to flow in a north-north-west direction from near Star Hill Mine (Fig. 2.10) along a course similar to the present one.

The weathering and erosion of the subaerially exposed Winnaleah-Ringarooma basalts have resulted in lateritization and silcrete formation. Based on the known distribution of ferricretes and silcretes, and lateritized nodules found in the present study, the former extension of these basalts is reconstructed in Fig. 8.6. It is argued that favourable environmental conditions for lateritization as well as silcrete formation may have existed from the Oligocene onwards, even though a favourable source rock in the form of the younger basalts was

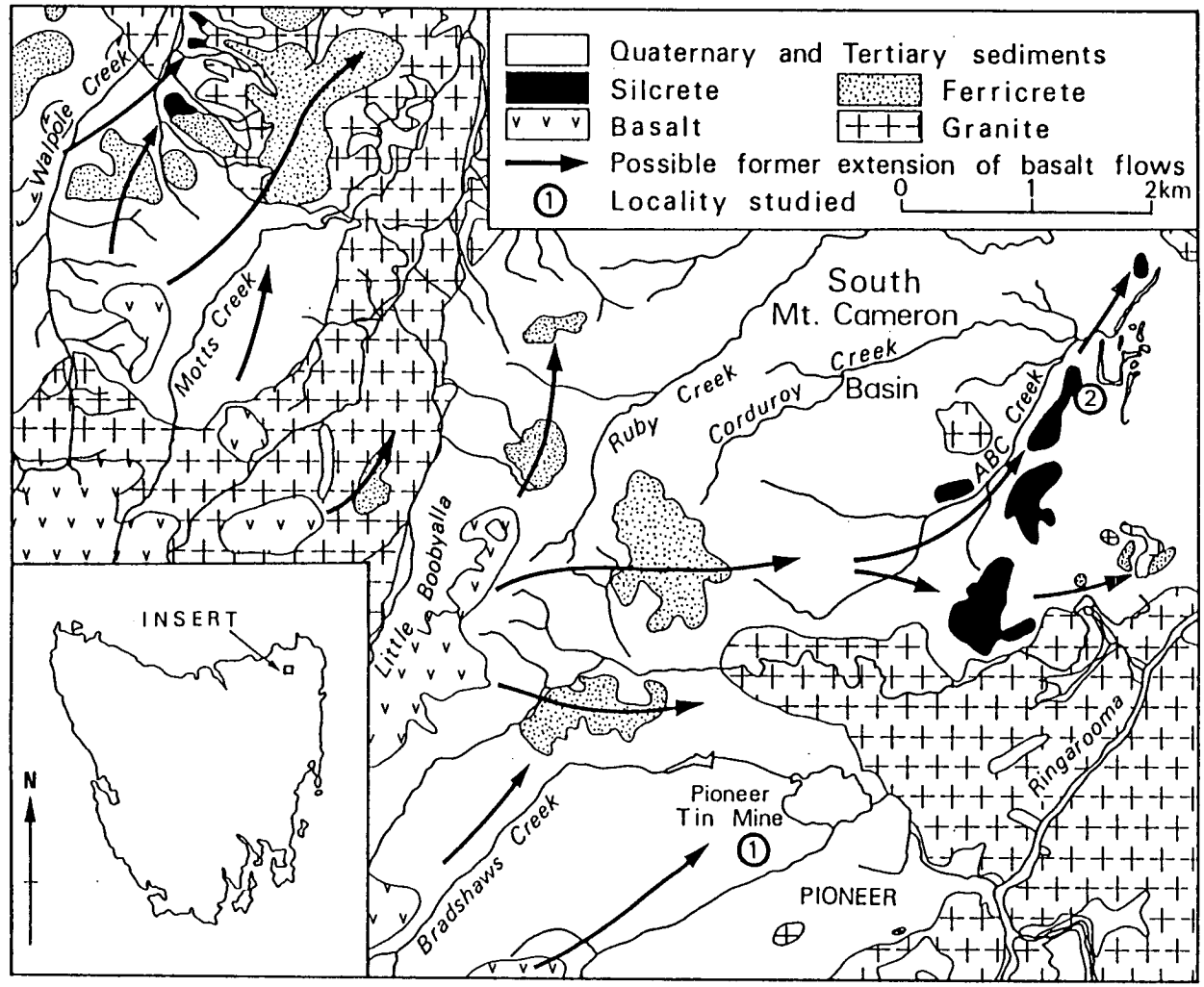

Fig. 8.6 Geological map of the South Mount Cameron Basin showing silcrete and ferricrete outcrops and possible former extension of the Winnaleah-Ringarooma basalts.

not available until the Middle Miocene. Their ca. 16 Ma age in comparison to the ca. 26 Ma age of the Moriarty Basalt (Baillie 1986) in the Devonport-Port Sorell area, northwestern Tasmania would help to explain why the latter is more deeply lateritized (Yim et al. 1985). The possible stratigraphic correlations between the Cainozoic successions established in the study area and the east of Devonport, northern Tasmania is shown in Table 8.3. Good agreement can be seen to exist between the two areas.

In the Middle Miocene, 'warmer' waters was indicated by the deposition of marine limestones with lepidocyclines at Marrawah and Cape Barren Island (Quilty 1972). From the Middle Miocene to the Pliocene, the South Tasman Rise showed marked decrease in sea-surface temperatures (Shackleton & Kennett 1975). This decrease reflected the increase in glacial activity in Antarctica with good correlation during the time interval between sea level and glacial activity. Furthermore, Kemp (1978) concluded that palynological data suggest a dominance of rainforest in southeastern Australia with little evidence of open vegetation for the Middle Miocene. From Late Miocene to Pliocene there was an increase in aridity during which there was probably an accompanying slow down in placer formation processes with the recycling of heavy minerals restricted mainly to the river courses.

8.6 Quaternary

In a review of Quaternary and geomorphological studies in Tasmania, Colhoun (1978) concluded that Tasmania did experience multiple glaciations. Frost and nivation processes operated on mountains above 1200 m. During the Last Glaciation, frost and solifluction processes operated above 450 m and occur occasionally down to 300 m (Davies 1967 and 1974; Derbyshire 1973). Based on sea-surface temperatures of approaching freezing found during the Pleistocene (Shackleton & Kennett 1975) in contrast to the present day sea-surface temperature of about

Age	Study area	Wesley Vale, East of Devonport Based on Cromer (1980; 1989) and F.L. Sutherland (pers. comm.)
Recent - Pliocene	Sediments of the Ringarooma-Boobyalla drainage system	Sediments of the Mersey-Rubicon drainage system
Late Miocene	Lateritization of the Winnaleah-Ringarooma basalts in the South Mount Cameron Basin	Pre-Early Pliocene lateritization of the Moriarty Basalt
Middle Miocene	Winnaleah-Ringarooma basalts (Brown 1977)	
Early Miocene	Alluvial floodplain sedimentation in the South Mount Cameron Basin	
Late Oligocene	Microflora in sub-basaltic tin-barren sediments studied by Harris (1965) and others	Moriarty Basalt; Wesley Vale Sand
Early Oligocene	Burial of stanniferous deep leads, probably Late Eocene to Middle Oligocene	Interbedded basalts and sediments at top of Thirlstane Basalt
Late Eocene		Thirlstane Basalt
Middle Eocene	Mount Littlechild and Forest Lodge basalts	
Early Eocene	Continuation of warm conditions for deep weathering since the Late Cretaceous	Harford Beds
Palaeocene		

Table 8.3 Possible stratigraphic correlations between the Cainozoic successions established in the study area and east of Devonport, northern Tasmania. Modified after Yim et al. (1985).

11 °C, the existence of seasonal snow fields over the highland areas of northeastern Tasmania was likely during glacial periods. Therefore, the reworking of alluvial deposits along the courses of the major rivers particularly in the case of the Ringarooma and its tributary streams on the Blue Tier Massif may have occurred through high discharge associated with seasonal thawing of snow fields. Although less emphasis was given to Quaternary placers in the present study, the terrace deposits along the floodplains of the Ringarooma River were probably formed during this time period. It is mainly because of their lower economic value in comparison to deep leads as well as severe mining disturbances in some cases that they have not been investigated in greater detail. An important characteristic shown by this type of placer is the presence of gold. This a reflection of drainage evolution causing the introduction of gold deriving from the Mathinna Beds.

8.7 General discussion

In studying the genesis of stanniferous placers in northeastern Tasmania, the importance of reliable stratigraphic information is stressed. Lines of evidence found to be particularly important in the present study include:

(1) The provenance of heavy minerals particularly those deriving from the mineralized granite and the older basalts.

(2) The presence of two dated episodes of Tertiary basaltic volcanic activity.

(3) The outcrop of Parmeener Supergroup resting unconformably on mineralized granite on the Blue Tier Massif.

(4) The occurrence and distribution of the Blue Tier basalts of Middle Eocene age on top of the Blue Tier Massif. Since the zircospilic suite of heavy minerals is exclusively associated with these basalts, this facilitated radial dispersion of zircospilic minerals and provided natural tracers as well as a means of dating deep lead

sequences. Stanniferous deep leads with or without such minerals are likely to either post-date or pre-date the Middle Eocene respectively.

(5) The sub-basaltic stratigraphic position of the deep lead sequence beneath the Winnaleah-Ringarooma basalts of Middle Miocene age.

(6) The distribution of monomineralic and composite cassiterite grains, and trace elements in cassiterite for indicating the distance of transport of cassiterite from mineralized rocks.

Based on the above, a 'long' geological history involving episodic recycling of heavy minerals must have occurred. The stanniferous placers in northeastern Tasmania are therefore polycyclic in their origin.

Deep weathering episodes preceeding erosional phases are considered to be important in the preparation of mineralized granite for the release of cassiterite into placers. Although hydrothermal alteration effects are difficult to distinquish from weathering (Ollier 1983), the Australian regolith was shown in reviews by Mabbut in Butt & Smith (1979), Ollier (1988) and others to date back to the Tertiary, Mesozoic or earlier. This relic weathering origin is confirmed by studies made by Bird & Chivas (1988) using the oxygen isotope composition of minerals developed by deep weathering/lateritization processes. Four ages of weathering were identified by these authors in eastern Australia including the Late Palaeozoic, Late Mesozoic to Early Tertiary, post-mid Tertiary and the present day. Out of these, the first three ages are in agreement with the weathering episodes in the Late Carboniferous, Late Cretaceous to Early Eocene and Middle Miocene to Pliocene found in the present study. In regard to the Middle Miocene to Pliocene episode, warm temperatures are however not supported by sea-surface temperatures determined by the oxygen isotope studies of Shackleton & Kennett (1975). Nevertheless, based on the two older episodes of weathering, a long

history of weathering is apparent in the genesis of tin placers in the study area.

Two dated episodes of basaltic volcanic activity have so far been identified in the study area. However, the discovery of basaltic rock fragments from boreholes within the South Mount Cameron Basin (see Section 7.2.5, Fig. 7.18 and Appendix III) may be indicative of a third episode of basaltic volcanic activity as well as an additional source of the zircospilic suite of heavy minerals. Because these rock fragments have been encountered in four separate boreholes at depths of up to 90 m below ground surface, they are widespread in extent and are unlikely to be feeders for the Winnaleah-Ringarooma basalts. Since they occur at or near the base of the deep lead sequence in the South Mount Cameron Basin, they may pre-date part of the deep lead sequence. On the other hand, no evidence has so far been found to show that these basalts contain zircospilic minerals. If they do, the distance of transport of zircospilic minerals indicated by the provenance of heavy minerals found would have to be reduced considerably.

The deep leads are found to show the following characteristics:

(1) They occur on the piedmont zone of granitic massifs. Because of their location adjacent to a relatively steep slope, a mixed colluvial-eluvial-alluvial origin is probable.

(2) Deep leads do not contain tin concentrations of economic importance unless they are located within short distances of the contact zone between the granite and the Mathinna Beds, e.g. the Briseis and Monarch Tin Mines.

(3) Although deep leads may contain the zircospilic suite of heavy minerals and cassiterite, the bulk of the latter is likely to have been recycled. The presence of cassiterite together with zircospilic minerals is confirmative of renewed recycling probably during the

Late Eocene and Middle Oligocene. However, the presence of most cassiterite is explained by pre-Middle Eocene deposition.

(4) Because of drainage diversion caused by the Winnaleah-Ringarooma basalts, new stream courses have been created. However, some stream courses such as the north-north-west flowing streams on the Blue Tier Massif have remained essentially unchanged at least since the Middle Eocene. In such stream courses especially when the deposits are shallow, the continuous recycling of heavy minerals is possible.

(5) The majority of deep leads show a north-north-west trend which coincides with the major structural trend of the region. Because of the adaptation to geological structure, sufficient geological time must have been available for their evolution. They are therefore features indicative of 'long' geological time scale.

(6) In deep leads, cassiterite shows low mobility in comparison with the zircospilic suite of heavy minerals. This is attributed to its greater density in addition to its residual origin and greater age.

Without the favourable conditions indicated above, deep leads are unlikely to have been formed.

8.8 Summary of conclusions

The genesis of stanniferous placers in northeastern Tasmania may be summarised as follow:

(1) Pre-Permian erosion and unroofing of the Late Devonian to Early Carboniferous Blue Tier and Scottsdale Batholiths were initially responsible for the release of cassiterite.

(2) Erosion and recycling of cassiterite by fluvial and glacial processes occurred during the Permo-Triassic.

(3) Jurassic uplift associated with the intrusion of dolerite followed by erosion and recycling of cassiterite.

(4) Deep weathering during the Late Carboniferous and Late Cretaceous to the Palaeocene under warm and humid conditions together with erosion and recycling by debris flow and sheet flood.

(5) Enrichment of cassiterite at the piedmont zone of massifs prior to the Middle Eocene.

(6) Extrusion of the Middle Eocene basalts followed by their erosion. Cassiterite recycling is confirmed by the occurrence of this mineral together with zircospilic minerals within deep leads.

(7) Burial of deep leads during the Late Oligocene to Early Miocene.

(8) Extrusion of Middle Miocene basalts accompanied by reworking in localities influenced by drainage diversion. The north-north-west flowing streams from the Blue Tier Massif were obstructed by these younger basalts causing a proto-Ringarroma River to form. This river initially flowed into the sea via the Great Mussel Roe River before diversion to the present day course via river capture.

(9) Post-Middle Miocene to Pliocene lateritization with recycling of heavy minerals restricted mainly to the course of the Ringarooma River.

(10) Erosion and recycling during glacial periods in the Quaternary restricted mainly to the floodplain of the Ringarooma River to form terrace deposits.

PART 4 FURTHER DISCUSSION, CONCLUSIONS AND RECOMMENDATIONS

CHAPTER 9 FURTHER DISCUSSION

9.1 Introduction

In this chapter, the implications of the major findings are discussed further under four headings. These include the causes of cassiterite concentration, the distance of cassiterite transport, the relative mobility of heavy minerals, and, implications of the stratigraphic control on stanniferous placers.

9.2 Causes of cassiterite concentration

The main causes of cassiterite concentration identified in northeastern Tasmania include:

(1) The presence of an extensive area of bedrock mineralization.

(2) The long geological history since the unroofing of the tin-bearing Devonian granites probably from the Carboniferous Period onwards.

(3) The existence of periglacial and warm climatic conditions to facilitate cassiterite liberation from the source rock. These conditions are favourable for the physical and chemical disintegration of granite respectively.

(4) The involvement of fluvial processes during the recycling of cassiterite.

(5) The existence of piedmont zones at the margin of the granite massifs to facilitate cassiterite deposition and concentration.

Bedrock tin mineralization is found to be widespread in northeastern Tasmania. Placers with locally derived cassiterite are indicated by the presence of large monomineralic (Fig. 4.1) and composite (Fig. 4.2) cassiterite grains in addition to the exposure of bedrock showing tin mineralization. Consequently, the position of leads inferred by previous workers and shown in Fig. 2.8 are either invalid or only partially valid. In the present study, deep leads are found to be highly complex in their origin. This is explained by their greater geological age than was formerly realised which may invlove dramatic

changes in drainage courses in addition to episodic recycling, e.g. the diversion of the north-north-west flowing streams on the Blue Tier Massif by the Winnaleah-Ringarooma basalts and recycling episodes during the Late Palaeozoic and post-Triassic.

The age of granite unroofing is considered to be important because a maximum time limit is set for the liberation of cassiterite to form placers. In northeastern Tasmania, the unroofing probably occurred in the Carboniferous Period since Carboniferous strata are missing from the region. Therefore cassiterite recycling from the Carboniferous onwards is possible. Deep leads underlying the Winnaleah-Ringarooma basalts are found to be subjected to recycling prior to their burial during the Late Oligocene to Early Miocene (Fig. 6.6). At sites not covered by these basalts, continuous recycling of cassiterite to the present day is possible.

The age of granite unroofing in northeastern Tasmania is considerably older than that of the Dartmoor Granite and the Southeast Asian tin field. In an examination of heavy mineral species derived from the former locality by Groves (1931), no clear-cut evidence for granite unroofing was found until the Cretaceous when topaz becomes noticeably more abundant in sediments. In the Southeast Asian tin field, Permo-Triassic episodes of granite magmatism at ca. 260, 240 and 210 Ma were found by Derbyshire (1987). While the age of granite unroofing has not been identified as far as the author is aware, it is likely to have taken place as early as the Jurassic and as late as the Cretaceous periods.

Periglacial and warm climatic conditions are both conducive to cassiterite release from tin-bearing granites. In northeastern Tasmania, the long duration of time since granite unroofing and the favourable climatic conditions acted together in assisting cassiterite recycling. While deep weathering under warm and humid conditions is suitable for

preparing cassiterite release from the bedrock, by itself weathering is insufficient to lead to cassiterite concentration. The weathered granite must be eroded before cassiterite can be selectively concentrated to form placers (Aleva et al. 1973; Aleva 1985). In the study area, this is likely to occur under periglacial conditions by glacial erosion in addition to fluvial erosion. Weathering episodes under warm climatic conditions during the Late Palaeozoic and the Late Mesozoic to Early Tertiary (Bird & Chivas 1988) are likely to be largely responsible for the cassiterite found within deep leads.

Because of the great chemical stability and high specific gravity of cassiterite, it is frequently concentrated selectively in alluvial sediments adjacent to bedrock. Sediment recycling would lead to further cassiterite enrichment through the elutriation of light minerals by winnowing. Since the bulk of the cassiterite in all placer localities in northeastern Tasmania occurs at or near the bedrock contact, the cause of enrichment is likely to be common to all. As noted by Gunn (1968), Tuck (1968) and Adams et al. (1978), the origin of bedrock values of placer deposits is found in the present study to be caused by recycling during erosive or downcutting phases of the valley rock basement. In other words, the bedrock values probably represented a lag deposit which has always remained close to the bedrock-sediment interface. Recycling is therefore the key to a good placer concentration as was noted by Henley & Adams (1979) and Clemmey (1985).

Large, fluvial placers occur at points of abrupt valley widening (Kuzvart & Bohmer 1978). These sites are also noted for their marked reduction in stream gradient leading to a decline in stream velocity and heavy mineral deposition. The existence of piedmont zones on the Blue Tier and Mount Cameron Massifs would provide favourable sites for alluvial fan deposition as was pointed out by Jennings (1975). Sieve

deposits (Bull 1972) within the alluvial fans would provide suitable traps for cassiterite transported by streams draining off the massifs.

9.3 Transport distance of cassiterite

In this section, the transport distance of cassiterite to form economic tin placers is further examined.

The distance of cassiterite transport may be determined if there is only one known source of supply of the mineral in an area and if the palaeoenvironmental conditions are known. However, under natural circumstances, not only is the area of bedrock mineralization extensive but multiple sources of cassiterite are probable. It is also possible for some of the sources to be missed because of inadequacies in the study methods used and/or poor exposures. Furthermore, cassiterite placers of alluvial, eluvial, colluvial or mixed origin are likely to show different distances of transport.

When determining the distance of transport, a map showing the distribution of past and present tin mines such as that shown in Fig. 2.10 is already indicative of the short distance involved. A major problem in recognising the distance of transport is caused by the complex geological settings possible in the formation of the placers. For example, drainage diversion as well as changes in stream gradient through tectonism may have taken place. The present study shows that deep leads were buried during the Late Oligocene and Early Miocene while the terrace deposits may have been recycled during the Pleistocene Period.

In an examination of the transportation of cassiterite in streams, Saks & Gavshina (1976) pointed out the difference in transportability between coarse and fine cassiterite. Although the grain diameter for these two types of cassiterite have not been specified, fine cassiterite was considered to be too easily moved to be found in alluvial placers while coarse cassiterite forms autochthonous placers because of low

transportability. Such pecularities of fine and coarse cassiterite transport may be used to explain the absence of alluvial placers that are distant from primary sources.

At two piedmont deep lead sites, based on ore grades found in borings of the Briseis Tin Mine (Braithwaite 1964, Fig. 7.2), and the mining record of the Pioneer Tin Mine, the distance of cassiterite transport may be estimated. In both cases, the total distance in which economic concentrations of cassiterite were present is approximately 1 km. Therefore it is likely that economic cassiterite placers are not normally transported distances greater than 1 km from the source rock. Possible exceptions are mass-flow deposits and where stream courses were able to maintain steep gradients for long distances. The 1 km distance is considerably less than the 7-10 km suggested by Toh (1978) for recoverable cassiterite (+200 um) on low gradient. It is also much less than the minimum distance of 10 km identified by Yim (1981) for tin-mine tailings transported by the Red River in Cornwall, England.

Since the distance of cassiterite transport is dependant on numerous variables, without specifying these variables, it is dangerous to give values. For example, the variables may include stream gradient, stream discharge, palaeoclimate and the geological time involved in recycling cassiterite will require careful consideration. Therefore the distance of cassiterite transport is considered to be a distraction in the study of stanniferous placers.

9.4 Relative mobility of heavy minerals

In the present study, cassiterite being the second heaviest mineral found after gold is only carried a short distance. This is in general agreement with the conclusions of Mackie (1923) that the heaviest mineral is carried the shortest distance. However, an exception to this rule is the greater mobility of flaky gold as compared to granular gold.

This is confirmed by the presence of the former in terrace deposits adjacent to the present day course of the Ringarooma River.

If the Blue Tier basalts are the only source rock for the zircospilic suite of heavy minerals in northeastern Tasmania, the distance of transport of each mineral can be estimated by measuring the distance between the basalts and the locality of mineral occurrence. From this, based on the occurrence of zircospilic minerals in boreholes from Ringarooma Bay (Section 7.2.6), the distance of transport is in excess of 50 km. However, the existence of other sources of zircospilic minerals would reduce the distance of transport considerably. The basalts at Grays Hill (Fig. 4.6) and the concealed basalts in the South Mount Cameron Basin (see Section 7.2.5) are also probable sources. They would reduce to distance of transport by more than 15 km.

The greater mobility of zircospilic minerals in comparison with cassiterite is explained by their greater mechanical resistance and their lower specific gravities. With the exception of ilmenite, cassiterite (H = 6-7) is lower in the Mohs' scale of hardness (Fig. 3.5). Furthermore, because cassiterite is brittle in nature, fine cassiterite produced by mechanical breakdown is lost too easily to be found in alluvial placers (Saks & Gavshina 1978). Based on the hardnesses and specific gravities of zircospilic minerals, the mobility in decreasing order is suggested to be corundum, spinel, ilmenite and zircon. The high mobility of corundum is attributed to its great hardness (H = 9) and relatively low specific gravity (SG = 4.0). However, in comparison to diamond (H = 10, SG = 3.42), the mobility of corundum is expected to be less because of its lower hardness and greater specific gravity. A minimum distance of transport of 42 km for diamonds along the Orange River cannot be disputed (Keyser 1974), and, diamonds originating in rather restricted source areas can be spread across many thousands of square kilometres by fluvial and marine

processes (Sutherland 1982). The order of mobility for zircospilic minerals found is in the same order as the transportation resistance of Friese (1931) (Table 4.3). Because of this, it is suggested that the mobility of heavy minerals is closely related to their transportation resistance.

Of the heavy minerals occurring in association with cassiterite within mineralized granite, tourmaline, fine euhedral zircon, monazite, Mg-poor ilmenite and topaz are the most common in alluvials. Less common minerals include garnets (almandine and spessartine), chrysoberyl and xenotime. Because of the widespread distribution of granite in northeastern Tasmania, it is difficult to determine the mobility of a heavy mineral with any degree of certainty unless the source of the mineral is known. Only three minerals, topaz, chrysoberyl and spessartine are found to be useful in the assessment of mobilities in this respect. Topaz is a common mineral found in greisens, pegmatites and aplites. Because of the presence of ultra-coarse-grained topaz in pegmatite localities such as Sextus Creek, the rapid decrease in particle size of topaz is found downstream of the source rock. This is attributed to the presence of a perfect basal cleavage causing the mineral to be broken up during transportation. In terms of mobility, topaz is moderate. Both chrysoberyl and spessartine are associated with pegmatites and are mechanically resistant. Their restricted distribution is explained by sampling error due to their low abundance and their low mobilities. The chrysoberyl specimens reported in the present study were from the Weld River locality near Moorina. All these specimens were on loan from the Tasmania Museum and Art Gallery because none were found in the samples collected in the field.

The distribution of granitic heavy minerals may be accounted for by their relative chemical stability. Hubert (1971) considered zircon and tourmaline to be ultrastable, garnet to be semistable, and ilmenite to

be unstable. The highly stable heavy minerals are likely to show the greatest persistence (Pettijohn 1941) which may not necessary be caused by their high mobilities.

Table 9.1 provides a summary of the relative mobility of selected heavy minerals during alluvial transportation in northeastern Tasmania. It should be noted that the three categories of mobility are not intended to reflect either the distance of transport or the transportation resistance, but more as an indication of the tendency for the heavy mineral to be transported. The reason for this is because very little purpose is served in classifying mobilities unless conditions such as palaeoenvironmental factors and the geological time scale are considered. It is also desirable to take into account grain shape in determining whether the source of the heavy mineral is likely to be local even though rounding is quite likely to be a product of recycling.

9.5 Implications of the stratigraphic control on stanniferous placers

In northeastern Tasmania, the long history of geological events involved in the genesis of tin placer deposits is identified through a wealth of information on stratigraphic control. In this section, the implications on other stanniferous placer deposits are discussed briefly.

Economic stanniferous placers present in consolidated sedimentary rocks are extremely rare in the geological record. Their scarcity may be explained by three reasons. Firstly, the importance of recycling in the concentration of cassiterite to form placers. Secondly, the long geological history involved in the formation of stanniferous placers, and thirdly, the unique circumstances required for the formation of the placers. South of the present area of study in northeastern Tasmania, cassiterite palaeo-placers in basal conglomerate of Late Carboniferous to Triassic age (Banks et al. 1989) are known near Rossarden (Connolly 1953), Roys Hill (Herman 1914) and Brookstead (Reid & Henderson 1929).

Mobility	Mineral name
Low	Granular gold Cassiterite
Medium	Topaz Garnet Ilmenite Monazite Coarse anhedral zircon Flaky gold Rutile
High	Tourmaline Fine euhedral zircon Spinel

Table 9.1 Summary of the relative mobility of selected heavy minerals during alluvial transportation in northeastern Tasmania.

However, the tin production in all three localities has been small. In the present study area, similar 'low grade' cassiterite palaeo-placers could be present in the basal conglomerate of the Parmeener Supergroup resting unconformably on the tin-bearing Devonian granites of the Blue Tier Massif. The small outcrop of conglomerate on Mount Littlechild probably represents a small remnant of a much more extensive former cover now stripped away. Therefore the recycling of cassiterite present within the Parmeener Supergroup has taken place and has been mixed with further cassiterite liberated from the Devonian granites to produce to the economic concentrations found in the deep lead-type placers.

In order to determine the stratigraphic control of a stanniferous placer, it is necessary to consider the fit in as many lines of evidence as possible. Agreement between the different lines of evidence is essential to give confidence that the conclusions drawn are valid. Due to the natural circumstances of the area of study chosen, particularly through the presence of younger and older Tertiary basalts which are directly datable by the K-Ar method and indirectly datable by the fission track and ESR measurements of alluvial zircons, it is possible to identify the timing of burial of deep leads because they are overlain by the younger basalts. Other important lines of evidence include the information provided by plant remains, the presence of palaeosols as stratigraphic markers, and, the sea-surface palaeotemperature and sea-level fluctuation record (Fig. 6.6).

It is clear from the present study that the cassiterite found in a placer deposit is often the product of a long history of recycling. Therefore cassiterite is usually present as a lag deposit. Consequently, sediments enclosing the cassiterite lag may be appreciably younger. Based on this, the conclusions drawn from the dating of tin placers in Southeast Asia are seen to be speculative. For example, radiocarbon dating have been used to indicate the age of placer deposits. Based

largely on infinite radiocarbon ages of wood in Kaksa, and, fossils and artifacts, Osberger (1967) concluded that the Indonesian placers including Bangka and Billiton were formed during the Pleistocene and Holocene. There are two main objections to this conclusion. Firstly, since the radiocarbon ages are all infinite, there are no good reasons why the actual age should not be pre-Pleistocene. The limitations of radiocarbon ages greater in age than the Holocene is well known, for example see Thom (1976) for a detailed review of the problems. Secondly, the radiocarbon ages obtained from the sediment enclosing the cassiterite if valid provides only the timing of burial. In a more recent study, Batchelor (1988) dated the fluvial tin placers of Malaysia using five lines of evidence. These included palaeomagnetism, radiocarbon dating, vertebrate palaeontology, palynology, and, other indirect age evidences. However, all these lines of evidence suffers from the same problem in that they do not necessarily provide the age of cassiterite deposition. The conclusion by Batchelor (1988) that the principal phase of economic tin placer formation to the Late Pliocene to Middle Pleistocene is therefore considered to be suspect, to be too young.

Table 9.2 provides a summary of geological ages attributed to the formation of stanniferous placers. Northeastern Tasmania shows an appreciably greater age of formation than the other localities. This gives rise to the question whether at least some of the other localities because of their inferior stratigraphic control are similar in age as those found in northeastern Tasmania. A short geological time scale is less favourable for the recycling and concentration of cassiterite. In addition to this, the rising eustatic sea-level trend from the Late Miocene to Pliocene (Vail et al. 1977) is probably not as conducive to high erosion rates in onshore areas as during a falling sea-level stand.

Source	Area of study	Age of formation
Camm & Hosking (1985)	Cornwall, UK	Late Miocene to Late Pleistocene
Batchelor (1988)	Malaysia	Latest Pliocene to Middle Pleistocene
Osberger (1967)	Indonesia	Pleistocene to Holocene
Present study	Northeastern Tasmania	Deep leads - buried within the Middle Eocene to Middle Miocene interval, the cassiterite present may have been deposited much earlier; terrace deposits with lower economic potential - reworked and buried during the Pleistocene

Table 9.2 Summary of the ages of formation of stanniferous placers according to various sources and the present study.

Placers are therefore concluded to be a product of the antiquity of the landscape.

CHAPTER 10 CONCLUSIONS AND RECOMMENDATIONS

10.1 Provenance of heavy minerals

Based on the distribution of heavy minerals found in northeastern Tasmania, the conclusions on the provenance of heavy minerals are:

(1) The heavy minerals found in the study area are derived from four main types of source rocks: granite, Mathinna Beds, and younger and older Tertiary basalts.

(2) The common heavy minerals derived from granitic source rocks include cassiterite, monazite, low-Mg ilmenite, fine euhedral zircons, topaz and tourmaline. Less common heavy minerals include xenotime, rutile, spessartine and chrysoberyl.

(3) Gold and almandine are related to the Mathinna Beds.

(4) Heavy minerals derived from the older Tertiary basalts near the top of the Blue Tier Massif include the zircospilic suite of coarse anhedral zircons, corundum, spinel and high-Mg ilmenite.

(5) Heavy minerals found in common between the older and younger Tertiary basalts include olivine, pyroxene, high-Mg ilmenite, chrome-spinel, ulvospinel and titanomagnetite.

(6) There are three main heavy mineral associations:

(a) Cassiterite-spinel-corundum-topaz-zircon (both fine euhedral and coarse anhedral types) association which may occur in deep leads below the younger Tertiary basalts.

(b) Cassiterite-topaz-fine euhedral zircon association which may occur in placer deposits either older and younger than the deep leads.

(c) Cassiterite-gold-spinel-corundum-topaz-zircon (both fine euhedral and coarse anhedral types) association largely restricted to terrace and floodplain deposits of the present day Ringarooma River.

(7) Because some of the heavy minerals are restricted to only one known source, their presence may be of value as a stratigraphic marker for the correlation of placer sequences.

(8) The trace element content of cassiterite is useful for distinquishing mineralization from different source areas. Cassiterite originating from the Mount Cameron and Blue Tier Massifs are found to differ in Nb, Ta, Zr and W content. The former locality is enriched in Nb, Ta and Zr, while the latter locality is enriched in W.

(9) The large particle size of both monomineralic and composite cassiterite grains indicates that the source is not far away.

(10) The fine euhedral zircons and coarse anhedral zircons are derived from granites and older basalts respectively.

(11) The input of gold along the Ringarooma River is indicated by the increase in grain size of gold particles near Derby.

(12) Fission track and ESR dating of alluvial zircons are helpful to define provenance. More specific conclusions are presented in section 10.2.

10.2 Dating of alluvial zircons

The conclusions on the dating of fine euhedral and coarse anhedral zircons are:

(1) Fission track dating is a valuable method for dating and provenance study of alluvial zircons.

(2) ESR measurement is a promising method for dating and provenance study of alluvial zircons.

(3) Both fission track dating and ESR measurements have shown that the ages of the fine euhedral and coarse anhedral zircons are distinctly different. The former with an average age of 367 $\pm$ 15 Ma is derived from Upper Devonian granites while the latter with an average age of 46.7 $\pm$ 0.6 Ma is derived from the Blue Tier basalts.

(4) The age of the coarse anhedral zircons is in agreement with the age of the Blue Tier basalts obtained by Sutherland & Wellman (1986).

(5) Based on the age of the coarse anhedral zircons, placer deposits containing both types of zircons must have been reworked since the Middle Eocene. On the other hand, placer deposits containing only fine euhedral zircons may either pre-date or post-date the Middle Eocene. Such deposits fall outside the catchment area of coarse anhedral zircons.

(6) Because of the difference in provenance between the two types of zircons, the presence or absence of coarse anhedral zircons may be of stratigraphical importance.

(7) Clues are provided by coarse anhedral zircons on the drainage diversion events which had taken place.

(8) The dating of alluvial zircons is likely to have widespread applications in eastern Australia, parts of Indo-China and China where alluvial zircons deriving from Cainozoic basalts are known.

(9) The ESR method has major advantages over fission track dating in that it is fast and non-destructive. A disadvantage is that it requires a relatively large sample weight of ca. 0.1 g. However, in the present study most coarse anhedral zircons are sufficiently large to permit measurements of single mineral grains.

10.3 Transportation of heavy minerals

The conclusions on the transportation of heavy minerals are:

(1) Economic cassiterite placers are not normally transported distances greater than 1 km from the source rock. Possible exceptions are mass-flow deposits and where the stream courses were able to maintain steep gradients for long distances.

(2) Gold shows greater mobility than cassiterite in spite of its higher specific gravity. This is explained by the finer particle size of

gold, their flaky particle shape, and their malleability, making them more susceptible to entrainment and long distance transport.

(3) Because of the lower specific gravity of the zircospilic heavy minerals in comparison with cassiterite, they all show greater mobility. The greater hardness of zircon, corundum and spinel also makes them more resistant to abrasion than cassiterite. These minerals are therefore more likely to be transported longer distances.

(4) The transportation resistance of heavy minerals is (in decreasing order) corundum, spinel, zircon, topaz, cassiterite and ilmenite. With the exception of zircon, this is in general agreement with the findings of Friese (1931). The discrepancy shown by zircon may be explained by multiple sources of the mineral.

(5) Fluvial processes appear to be dominant in the transportation of heavy minerals in deep leads and terrace deposits. All eluvial or colluvial placers found are small in size and are always closely associated with alluvial placers.

(6) The residual concentration of cassiterite at many localities is confirmed by the presence of significant quantities of monomineralic and composite cassiterite grains exceeding 2 mm in particle size.

(7) The maximum distance of transport of cassiterite depends on the gradient of palaeo-streams.

(8) A wider range of particle size of a heavy mineral is present near to the source rock because of lack of opportunity for sorting.

(9) Tin mineralization in the bedrock is present in many localities in northeastern Tasmania, and, it is unnecessary to account for tin placers by long distance transport.

(10) The particle size distribution of cassiterite at a given locality may be used to identify kulit, kaksa and mintjan types of economic placers in northeastern Tasmania.

(11) The maximum particle size is considered to be superior to hydraulic equivalence as a practical means of indicating the distance of transport of heavy minerals.

10.4 Deposition of heavy minerals

The conclusions on the deposition of heavy minerals are:

(1) Piedmont zones such as those off the Blue Tier and Mount Cameron Massifs are favourable sites for heavy mineral accumulation because of the fall in gradient which is accompanied by a decrease in stream flow velocity and energy.

(2) The confluence points of deep leads are favourable sites for heavy mineral accumulation.

(3) Cassiterite in deep leads was concentrated by selective sorting processes through the removal of light minerals by winnowing.

(4) The high specific gravity and the great chemical stability of cassiterite is mainly responsible for its low transportability.

(5) Recycling is an important process in the enrichment of heavy minerals to form placer deposits.

10.5 Genesis of stanniferous placers

Although alluvial, colluvial and eluvial placers may all be identified in northeastern Tasmania, alluvial placers predominate. This is explained by the importance of reworking of pre-existing alluvial, colluvial and eluvial deposits by fluvial processes prior to preservation. The widespread occurrence of deep leads both onshore and offshore confirms this.

Deep leads which are economically the most important type of placer deposit, reflect the antiquity of the landscape. The 'long' geological time scale dating back at least to pre-Permian with numerous recycling

episodes is considered to be of major importance in the genesis of stanniferous placers in the area studied. This permitted the reworking of heavy minerals and the selective concentration of cassiterite through the removal of light minerals by winnowing. From the unroofing of the Upper Devonian to Early Carboniferous Blue Tier and Scottsdale Batholiths, recycling episodes have taken place at least once during the pre-Permian, the Permo-Triassic, Jurassic to Middle Cretaceous, Late Cretaceous to Palaeocene, and Late Eocene to Middle Oligocene. However, in spite of the episodes of recycling, cassiterite shows low mobility and is found within short distances of the source rock. At some sites, the deep leads were buried by Late Oligocene to Early Miocene sediments which may in turn be overlain by the Winnaleah-Ringarooma basalts. Along the present day Ringarooma valley, the placer deposits were recycled from the Late Miocene, after the Ringarooma River was created by drainage diversion of streams draining from the Blue Tier Massif. The terrace deposits along the middle and lower part of the Ringarooma valley were probably formed during periods of high discharge during the Quaternary because of seasonal thawing of snowfields accumulating on high ground.

The importance of stratigraphic control in the understanding of the genesis of stanniferous placers is emphasised in the present study. In northeastern Tasmania, stratigraphic control is possible because of the special circumstances including:

(1) The availability of high quality geological maps on a scale of 1 : 50 000 published by the Tasmania Department of Mines.

(2) The availability of radiometric ages for the granitic plutons which are mineralized in tin.

(3) The availability of radiometric ages for a younger and an older episode of Tertiary basaltic volcanic activity.

(4) The presence of abundant data on the distribution of heavy minerals obtained by field and laboratory studies. These included distinctive heavy mineral assemblages derived from different bedrock types including granite, Mathinna Beds, the younger and older Tertiary basalts.

(5) The availability of two distinctive types of alluvial zircons, one deriving from granite and the other from the older basalts. In addition to differences in mineralogical characteristics, grain size and shape, the two types of zircons have been confirmed by fission track dating and ESR measurements to be of different ages.

(6) The availability of palynological evidence within the study area and on the Australian mainland to provide palaeoenvironmental information in addition to indirect evidence of age.

(7) The availability of geological knowledge on the Bass Strait basins during the Mesozoic and Cainozoic Eras obtained through oil, gas and groundwater exploration.

(8) The availability of sea-surface temperature data in the Tasman Sea throughout most of the Cainozoic Era via oxygen isotopic studies of planktonic foraminifera.

(9) The availability of a global sea-level curve determined by seismic stratigraphy to facilitate correlation between terrestrial and marine events.

(10) The presence of duricrusts including ferricrete, silcrete and bauxite to provide stratigraphic markers of the former landscape.

(11) The long history of weathering revealed through the oxygen isotope dating of the Australian regolith by Bird & Chivas (1988).

The agreement shown by a combination of the above methods gives confidence that the results obtained about the genesis of stanniferous placers determined in the present study are likely to be valid.

10.6 Relevance of conclusions

A major implication of the Tasmanian study is that tin placer deposits occurring elsewhere in southeast Asia are also likely to be a product of the antiquity of the landscape. Stratigraphic control involving numerical and indirect methods of dating including palynology, DSDP data, and geological information obtained from oil and gas exploration should be sought where possible. The absence of age information obtained using a combination of reliable methods is a good reason for suspecting that southeast Asian placers were also formed by 'long' time scale geological events. This conclusion is considered to be likely because global events dating back in time is found to be important in the genesis of deep leads in northeastern Tasmania. Broad agreement was found between sea-level change and the deep lead sequence both onshore and offshore.

10.7 Recommendations

The main recommendations are:

(1) Further work on pre-Eocene and post-Middle Miocene tin placers in northeastern Tasmania is desirable to improve stratigraphic control on them than is possible at present. The use of palynology and palaeomagnetic dating are likely to be particularly rewarding.

(2) Follow-up work on directional sedimentary structures would be useful to confirm the palaeocurrent directions indicated by the distribution of heavy minerals in the present study.

(3) The concealed basalts within the South Mount Cameron Basin should be investigated by K-Ar dating and heavy mineral studies. Results on the former would help to provide greater understanding on the early Cainozoic geological history. If the zircospilic suite of heavy minerals are present in these basalts, the additional source of these minerals may change some of the conclusions on the transportation of heavy minerals drawn here.

(4) Further dating on alluvial zircons from northeastern Tasmania using the fission track and ESR methods should be carried out to check the existence of other populations which may be present but missed in this study, and, possible resetting of zircon ages by episodes of volcanic activity.

(5) The stratigraphic control of tin placer deposits in southeast Asia should be investigated to permit intercontinental correlation of placers. This would assist greatly our understanding of the geology of tin placer deposits.

(6) Similar studies using fission track dating and ESR measurements of alluvial zircons should be carried out in eastern Australia, parts of Indo-China and China to provide a better understanding of Cainozoic geology in these regions.

(7) The ESR method for dating zircons shows promise and warrants further investigation. Follow-up work should be carried out on the zircons to determine the annual dose rate in order to permit the determination of independent ages.

(8) Follow-up trace element studies on cassiterite concentrates should be carried out to provide better fingerprinting of local sources of bedrock mineralization.

(9) Further studies should be carried out to investigate the relationship between stratigraphy of the placer sequences in northeastern Tasmania and local tectonic events.

(10) The nature of cassiterite in the source rocks of northeastern Tasmania should be investigated further to permit a better understanding of the controls on tin placer development.

(11) The grain size distribution of heavy minerals should be further investigated using closer spaced sieves and larger samples to provide a better understanding on transport distances.

(12) The pre-basaltic topography of the older and younger basalts as well as the concealed basalts in the South Mount Cameron Basin are critical to the understanding of deep lead evolution. Further boreholes and geophysical investigations are needed to provide better clues.

(13) Further studies should be carried out on the mechanics of heavy mineral accumulation.

(14) Oxygen-isotope dating of residual clays should be carried out to test the weathering events identified.

REFERENCES

Adams, J., Zimpfer, G.L. & McLane, C.F. (1978). Basin dynamics, channel processes, and placer formation: a model study. Econ. Geol., 73, 416-426.

Aleva, G.J.J. (1985). Indonesian fluvial cassiterite placers and their genetic environment. J. Geol. Soc. London, 142, 815-836.

Aleva, G.J.J., Fick, L.J. & Krol, G.L. (1973). Some remarks on the environmental influence on secondary tin deposits. Bull. Bur. Min. Res. Geol. & Geophys. Aus., 141, 163-172.

Anon. (1970). Catalogue of the Minerals of Tasmania. Rec. Geol. Surv., Tasmania Dept. Mines, 9.

Anon. (1979). Director of Mines report for the year ended 31 December 1978. Parliament of Tasmania no. 75, Government Printer, Hobart.

Anon. (1981). Atlas of Australia. George Philip & O'Neil Pty. Ltd., Melbourne.

Anon. (1981a). Occurrences of Gemstone Minerals in Tasmania. Tasmania Dept. Mines, 5th ed.

Baillie, P. (1986). A radiometric age for the Moriarty basalt, northwestern Tasmania. Unpub. Rep. Tasmania Dept. Mines, 1986/38.

Baillie, P., Turner, E. & Quilty, P.G. (1985). Late Pleistocene marine sediments and fossils from Mussel Roe Bay, northeastern Tasmania. Pap. Proc. Roy. Soc. Tasmania, 119, 83-87.

Banks, M.R. (1973). General geology. In Banks, M.R. ed. The Lake Country of Tasmania. Roy. Soc. Tasmania, Hobart, 25-34.

Banks, M.R., Bacon, C.A. & Clarke, M.J. (1989). Economic geology. In Burrett, C.F. & Martin, E.L. eds. Geology and Mineral Resources of Tasmania. Geol. Soc. Aus. Spec. Pub., 15, 335-338.

Banks, M.R. & Smith, E.A. (1968). A graptolite from the Mathinna Beds, northeastern Tasmania. Aus. J. Sci., 31, 118-119.

Barr, S.M. & MacDonald, A.S. (1981). Geochemistry and geochronology of late Cainozoic basalts of Southeast Asia. Geol. Soc. Amer. Bull., 92, 508-512 (Part I) & 1069-1142 (Part II).

Barth, W.H. (1986). Geology of the Cleveland Tin Mine, Tasmania, Australia with Special Reference to Mineral Chemistry and Rare Earth Distribution. Unpub. Ph.D. thesis, Ruprecht-Karls-Universitat Heidelberg.

Batchelor, B.C. (1973). Economic Geology and Exploration Potential of the Indonesian Tin Province. Unpub. M.Sc. thesis, University of London.

Batchelor, B.C. (1979). Discontinuously rising late Cainozoic eustatic sea-levels, with special reference to Sundaland, Southeast Asia. Geol. Mijn., 58, 1-20.

Batchelor, B.C. (1983). Sundaland Tin Placer Genesis and Late Cainozoic Coastal and Offshore Stratigraphy in Western Malaysia and Indonesia. Unpub. Ph.D. thesis, University of Malaya.

Batchelor, D.A.F. (1988). Dating of Malaysian fluvial tin placers. J. Southeast Asian Earth Sci., 2, 3-14.

Bates, R.L. & Jackson, J.A. eds. (1984). Dictionary of Geological Terms. Amer. Geol. Inst., Anchor Press, New York, 3rd ed.

Berman, H. (1953). A torsion microbalance for the determination of specific gravities of minerals. Amer. Miner., 24, 434-440.

Bigwood, A.J. & Hill, R.S. (1985). Tertiary Araucarian macrofossils from Tasmania. Aus. J. Bot., 33, 645-656.

Bird, M.I. & Chivas, A.R. (1988). Oxygen isotope dating of the Australian regolith. Nature, 331, 513-516.

Blake, F. (1955). Boring on Scotia-Lochaber tin leads, Great Northern Plain - Gladstone district. Unpub. Rep. Tasmania Dept. Mines.

Boswell, P.G.H. (1916). The application of petrological and quantitative methods to stratigraphy. Geol. Mag., 53, 105-111.

Bowden, A.R. (1978). Geomorphic perspective on shallow groundwater potential, coastal northeastern Tasmania. Aus. Water Res. Council Tech. Pap., 36.

Bowden, A.R. (1981). Coastal Sands of Northeastern Tasmania: Geomorphology and Groundwater Hydrology. Unpub. Ph.D. thesis, University of Tasmania.

Bowden, A.R. & Colhoun, E.A. (1984). Quaternary emergent shorelines of Tasmania. In Thom, B.G. ed. Coastal Geomorphology in Australia. Academic Press, Australia, 313-349.

Braithwaite, J.B. (1964). Ore reserves in the Cascade deep lead. Tech. Rep. Tasmania Dept. Mines, 9, 133-142.

Braithwaite, J.B. (1977). Great Northern Plain: a possible dredging area. Tech. Rep. Tasmania Dept. Mines, 20, 62-76.

Brammall, A. (1928). Dartmoor detritals - a study of provenance. Proc. Geol. Assoc., 39, 27-48.

Brown, A.V. (1977). Preliminary report on age determination of basalt samples from Ringarooma 1 : 50 000 sheet. Unpub. Rep. Tasmania Dept. Mines, 1977/25.

Brown, A.V. (1982). Tertiary leads and basin in the Winnleah-Mount Cameron area. Geol. Surv. Bull., Tasmania Dept. Mines, 61, 170-177.

Browne, W.R. (1972). Grey billy and its associates in eastern Australia. Proc. Linean Soc. New South Wales, 97, 98-129.

Bull, W.B. (1972). Recognition of alluvial-fan deposits in the stratigraphic record. In Rigby, J.K. & Hamblin, W.K. eds. Recognition of Ancient Sedimentary Environments. Soc. Econ. Paleon. & Miner. Spec. Pub., 16, 63-83.

Burrett, C.F. & Martin, E.L. eds. (1989). Geology and Mineral Resources of Tasmania. Geol. Soc. Aus. Spec. Pub., 15.

Butt, C.R.M. & Smith, R.E. eds. (1979). Conceptual models in exploration geochemistry, Australia. J. Geochem. Expl. Spec. Issue, 12, 89-365.

Caine, N. (1983). The Mountains of Northeastern Tasmania: A Study of Alpine Geomorphology. A.A. Balkema, Rotterdam.

Calcraft, H.J. (1980). Fe-Ti Oxide Minerals in Some Tasmania Granitoids. Unpub. B.Sc. Hons. thesis, University of Tasmania.

Camm, G.S. & Hosking, K.F.G. (1985). Stanniferous placer development on an evolving landsurface with special reference to placers near St. Austell, Cornwall. J. Geol. Soc. London, 142, 803-813.

Carey, S.W. (1947). Geology of the Launceston district, Tasmania. Rec. Queen Vict. Mus., 2, 31-46.

Clarke, M.J., Farmer, N. & Gulline, A.B. (1976). Tasmania Basin - Parmeener Supergroup. Mono. Ser. Australas. Inst. Min. Metall., 7, 438-443.

Clemmey, H. (1985). Sedimentary ore deposits. In Brenchley, P.J. & Williams, B.P.J. eds. Sedimentology - Recent Developments and Applied Aspects. Geol. Soc. London, Blackwell Scientific Pub., 229-247.

Cocker, J.D. (1977). Petrogenesis of the Tasmanian Granitoids. Unpub. Ph.D. thesis, University of Tasmania.

Cocker, J.D. (1982). Rb-Sr geochronology and Sr isotopic composition of Devonian granitoids, eastern Tasmania. J. Geol. Soc. Aus., 29, 139-158.

Colhoun, E.A. (1978). Recent Quaternary and geomorphological studies in Tasmania. Aus. Geog. Stud. Newsletter, 12, 2-15.

Colhoun, E.A. (1989). Quaternary. In Burrett, C.F. & Martin, E.L. eds. Geology and Mineral Resources of Tasmania. Geol. Soc. Aus. Spec. Pub., 15, 410-418.

Connolly, H.J.C. (1953). Aberfoyle tin-wolfram mine. 5th Empire Min. Metall. Cong., 1, 1200-1208.

Cromer, W.C. (1980). A Late Eocene basalt date from northern Tasmania. Search, 11, 294-295.

Cromer, W.C. (1989). Devonport-Port Sorell Sub-basin. In Burrett, C.F. & Martin, E.L. eds. Geology and Mineral Resources of Tasmania. Geol Soc. Aus. Spec. Pub., 15, 360-361.

Davies, J.L. (1959). High level erosion surfaces and landscape development in Tasmania. Aus. Geogr., 7, 193-203.

Davies, J.L. (1967). Tasmania landforms and Quaternary climates. In Jennings, J.N. & Mabbut, J.A. eds. Landform Studies from Australia and New Guinea. Australian National University Press, Canberra, 1-25.

Davies, J.L. (1974). Geomorphology and Quaternary environments. In Williams, W.D. ed. Biogeography and Ecology in Tasmania. Dr W. Junk Publications, Hague, 17-27.

Davies, J.L. & Hudson, J.P. (1987). Differential supply and longshore transport as determinants of sediment distribution on the north coast of Tasmania. Mar. Geol., 77, 233-245.

Deer, W.A., Howie, R.A. & Zussman, J. (1966). An Introduction to Rock-forming Minerals. Longman Group Ltd., London.

Denyer, J.E. (1972). The production of tin. Paper no. 2 presented at the Conference on Tin Consumption, London, Int. Tin Coun. & Tin Res. Inst.

Derbyshire, D.P.F. (1987). Rb/Sr and Sm/Nd isotope studies on granites of Southeast Asia. Warta Geologi, 13, 117-120.

Derbyshire, E. (1973). Periglacial phenomena in Tasmania. Buil. Periglac., 22, 131-148.

Dorman, F.H. (1966). Australian Tertiary paleotemperatures. J. Geol., 74, 49-61.

Douglas, J.G. & Ferguson, J.A. eds. (1976). Geology of Victoria. Geol. Soc. Aus. Spec. Pub., 5.

Dudykina, A.S. (1959). Paragenetic associations of element admixtures in cassiterite of different genetic types of tin ore deposits. Trudy Inst. Geol. Rudnykh Mestorozhdenii Pet. Miner. i Geok. Akad. Nauk SSSR, 28, 111-121.

Edwards, A.B. (1939). The age and physiographical relationships of some Cainozoic basalts in central and eastern Tasmania. Pap. Proc. Roy. Soc. Tasmania, 1938, 175-199.

Edwards, A.B. (1955). The Petrology of the Bauxites of Tasmania. Mineragraphic Invest. CSIRO, Geol. Dept., University of Melbourne.

Emery, K.O. & Noakes, L.C. (1968). Economic placer deposits of the continental shelf. C.C.O.P. Tech. Bull., United Nations, 1, 95-111.

Fawns, S. (1905). Tin Deposits of the World. Mining J., London.

Fleming, A.W. (1979). Exploration potential map of northeast Tasmania. Unpub. map, Amdex Mining Ltd., Sydney.

Folk, R.L. (1968). Petrology of Sedimentary Rocks. Hemphills, Austin.

Folk, R.L. & Ward, W.C. (1957). Brazos River bar: a study in the significance of grain size parameters. J. Sed. Pet., 27, 3-26.

Forsyth, S.M. (1982). Preliminary investigation of Boobyalla DDH1, 1977-1979, north-east groundwater investigation. Geol. Surv. Bull., Tasmania Dept. Mines, 61, 192-198.

Friese, F.W. (1931). Untersuchung von Mineralen auf Abnutzbarkeit bei Verfrachtung im Wasser. Miner. Petrog. Mitt., 41, 1-7.

Gee, R.D. & Groves, D.I. (1971). Structural features and mode of emplacement of part of the Blue Tier Batholith in northeast Tasmania. J. Geol. Soc. Aus., 18, 41-55.

Gee, R.D. & Legge, P.J. (1979). Beaconsfield, Tasmania. Geol. Surv. Tasmania Geol. Atlas 1 Mile Series Expl. Rep., Sh. 30, 2nd ed.

Gentilli, J. (1977). Climate. In Jean, D.N. ed. Australia: A Geography. St. Martins Press, New York, 7-37.

Gill, E.D. (1962). Cainozoic. J. Geol. Soc. Aus., 9, 233-253.

Gleadow, A.J.W. (1984). Fission track dating methods - a manual of principles and techniques. Workshop on Fission Track Analysis: Principles and Applications, James Cook University, Townsville.

Gleadow, A.J.W. & Lovering, J.F. (1974). The effect of weathering on fission track dating. Earth Planet. Sci. Lett., 22, 163-168.

Griffin, B.J. (1979). Energy Dispersive Analysis System Calibration and Operation with TAS-SUED, An Advanced Interactive Data-reduction Package. Geol. Dept. Pub., University of Tasmania.

Groves, A.W. (1931). The unroofing of the Dartmoor granite and the distribution of its detritus in the sediments of southern England. Geol. Soc. London Quat. J., 87, 62-94.

Groves, D.I., Cocker, J.D. & Jennings, D.J. (1977). The Blue Tier Batholith. Geol. Surv. Bull., Tasmania Dept. Mines, 55.

Groves, D.I. & Taylor, R.G. (1973). Greisenization and mineralization at Anchor tin mine, northeast Tasmania. Trans. Inst. Min. Metall. London, 82B, 135-146.

Gunn, C.B. (1968). Origin of the bedrock values of placer deposits. Econ. Geol., 63, 86.

Gunn, R.H. & Galloway, R.W. (1978). Silcretes in south-central Queensland. In Langford-Smith, T. ed. Silcrete in Australia. University of New England Press, Armidale, 51-71.

Hails, J.R. (1976). Placer deposits. Chap. 5 in Wolf, K.H. ed. Handbook of Strata-bound and Stratiform Ore Deposits Vol. 3 Supergene and Surfical Ore Deposits, Textures and Fabrics. Elsevier Sci. Pub. Co., Amsterdam, 213-244.

Hall, G. & Solomon, M. (1962). Metallic mineral deposits. J. Geol. Soc. Aus., 9, 284-309.

Haq, B.U., Hardenbol, J. & Vail, P.R. (1987). Chronology of fluctuating sea levels since the Triassic. Science, 235, 1156-1167.

Harris, W.K. (1965). Palynological examination of samples from the tin leads of north east Tasmania for Utah Development Company. Unpub. Rep. South Australia Dept. Mines, 60/15.

Harris, W.K. (1965a). Palynological examination of samples from north east Tasmania, Cape Barren and Flinders Islands. Unpub. Rep. South Australia Dept. Mines, 60/115.

Harris, W.K. (1968). Tasmania Tertiary and Quaternary microfloras summary report. Unpub. rep. South Australia Dept. Mines, 67/43.

Hassan, W.F. (1982). Aspects of Geochemistry and Mineralogy of Tin and Associated Minerals in the Malaysian Tinfields. Unpub. Ph.D. thesis, University of Leeds.

Hassan, W.F. (1986). Aspects of the geochemistry of Malaysian cassiterites. Bull. Geol. Soc. Malaysia, 19, 223-248.

Hauff, P.L. & Airey, J. (1980). The handling, hazards, and maintenance of heavy liquids in the geologic laboratory. Geol. Surv. Circ. 827, U.S. Dept. Interior, Reston.

Hazelhoff Roelfzema, B.H. & Tooms, J.S. (1969). Dispersion of cassiterite in the marine sediments of western Mounts Bay, Cornwall. Proc. 2nd Tech. Conf. on Tin, vol. 2, Int. Tin Coun., 491-516.

Hellyer Mining & Exploration Pty. Ltd. (1982). EL 42/80 Ringarooma Bay annual report 1981. Unpub. Rep. Tasmania Dept. Mines.

Hellyer Mining & Exploration Pty. Ltd. (1983). EL 42/80 Ringarooma Bay quaterly exploration progress report for period ending 20 March, 1983. Unpub. Rep. Tasmania Dept. Mines.

Henley, R.W. & Adams, J. (1979). On the evolution of giant gold placers. Trans. Inst. Min. Metall. London, 88B, 41-50.

Herman, H. (1914). Australian tin lodes and mills. Proc. Australas. Inst. Min. Eng., 14, 277-402.

Higgins, N.C., Solomon, M. & Varne, V. (1985). The genesis of the Blue Tier Batholith, northeastern Tasmania, Australia. Lithos, 18, 129-149.

Hill, R.S. (1983). Nothofagus macrofossils from the Tertiary of Tasmania. Alcheringa, 7, 169-183.

Hill, R.S. & Macphail, M.K. (1983). Reconstruction of the Oligocene vegetation at Pioneer, northeast Tasmania. Alcheringa, 7, 281-299.

Hollis, J.D. (1984). Volcanism and upper mantle - lower crust relationships: evidence from inclusions from alkali basaltic rocks. Pub. Geol. Soc. Aus., New South Wales Div., 1, 33-47.

Hollis, J.D. & Sutherland, F.L. (1985). Occurrences and origins of gem zircons in Eastern Australia. Rec. Aus. Mus., 36, 299-311.

Hosking, K.F.G. (1974). Practical aspects of the identification of cassiterite (SnO_2) by the 'tinning test.' Bull. Geol. Soc. Malaysia, 7, 17-26.

Hosking, K.F.G. (1977). Known relationships between the 'hard-rock' tin deposits and the granites of Southeast Asia. Bull. Geol. Soc. Malaysia, 9, 141-157.

Hosking, K.F.G. (1979). Tin distribution patterns. Bull. Geol. Soc. Malaysia, 11, 1-70.

Hubert, J.F. (1971). Analysis of heavy mineral assemblages. In Carver, R.E. ed. Procedures in Sedimentary Petrology. Wiley-Interscience, New York, 453-478.

Hutchinson, C.S. (1974). Laboratory Handbook of Petrographic Techniques. Wiley Interscience, New York.

Hutton, C.O. (1950). Studies of heavy detrital minerals. Geol. Soc. Amer. Bull., 61, 635-716.

Ingram, J.A. (1977). Australian tin deposits. Min. Res. Rep. no. 7, Bur. Min. Res. Geol. & Geophys. Aus.

Ishihara, S. (1977). The magnetite-series and ilmenite-series granitic rocks. Min. Geol., 27, 293-305.

Ishihara, S., Sawata, H., Arpornsuwan, Busaracome, P. & Bungbrakearti, S. (1979). The magnetite-series and ilmenite-series granitoids and their bearing on tin mineralization, particularly of the Malay Peninsula region. Bull. Geol. Soc. Malaysia, 11, 103-110.

Jack, R. (1965). Mount Cameron region - Endurance Tin Mine. In Geological Excursions for the Australian & New Zealand Assoc. for the Advancement of Science, 38th Conq., Tasmania Dept. Mines, 48-49.

Jennings, D.J. (1975). Alluvial tin deposits of Tasmania. In Knight, C.L. ed. Economic Geology of Australia and Papua New Guinea 1. Metals. Mono. Ser. no. 5, Australas. Inst. Min. Metall., 1053-1054.

Jennings, D.J. (1980). Tin in northeast Tasmania. In Abstracts, Coal, Tin, Surficial Deposits and Geology of North East Tasmania. Geol. Soc. Aus. 1, 18-19.

Jennings, D.J. & Sutherland, F.L. (1969). Geology of the Cape Portland area with special reference to the Mesozoic (?) appinitic rocks. Tech. Rep. Tasmania Dept. Mines, 13, 45-82.

Jones, H.A. & Davies, P.J. (1983). Superficial sediments of the Tasmanian continental shelf and part of Bass Strait. Bull. Bur. Min. Res. Geol. & Geophys. Aus., 218.

Jones, M.P. (1987). Applied Mineralogy. Graham & Trotman, London.

Jones, M.P. & Fleming, M.G. (1965). Identification of Mineral Grains. Elsevier Pub. Co., Amsterdam.

Jordan, W.M. (1975). An assessment of the water resources of Tasmania from river gauging and rainfall record 1920-1969. Water Res. Surv., Rivers & Water Supply Comm. Tasmania.

Kemp, E. M. (1978). Tertiary climatic evolution and vegetation history in the southeast Indian Ocean region. Palaeogeog. Palaeoclim. Palaeoecol., 24, 169-208.

Keyser, U. (1972). The occurrence of diamonds along the coast between the Orange River estuary and the Port Nolloh Reserve. Geol. Surv. Rep. South Africa Bull., 54.

King, D. (1963). Tin resources of Tasmania. Unpub. Rep. Tasmania Dept. Mines, 32/13, Utah Development Co.

Kirkpatrick, J.B. & Dickinson, K.J.M. (1984). Tasmania 1 : 50 000 Vegetation Map. Forestry Comm., Tasmania.

Klominsky, J. & Groves, D.I. (1970). The contrast in granitic rock types associated with tin and gold mineralization in Australia. Proc. Australas. Inst. Min. Metall., 234, 71-77.

Krauskopf, K.B. (1956). Dissolution and precipitation of silica at low temperatures. Geochim. Cosmochim. Acta, 10, 1-27.

Krol, G.L. (1960). Theories on the genesis of kaksa. Geol. Mijn., 39, 437-443.

Kuzvart, M. & Bohmer, M. (1978). Prospecting and Exploration of Mineral Deposits. Developments in Economic Geology Vol. 8, Elsevier Pub. Co., Amsterdam.

Lampietti, F.J., Davies, W. & Young, D.J. (1968). Prospecting for tin off Tasmania. Min. Mag., 119, 160-169.

Langford-Smith, T. ed. (1978). Silcrete in Australia. University of New England Press, Armidale.

Leaman, D.E. & Symonds, P.A. (1975). Gravity survey of northeastern Tasmania. Pap. Geol. Surv., Tasmania Dept. Mines, 2.

Lishmund, S.R. & Oakes, G.M. (1983). Diamonds, sapphires and Cretaceous/Tertiary diatremes in New South Wales. Quat. Notes Geol. Surv. New South Wales, 53, 23-27.

Luskin, A., Hobday, D.K. & Baillie, P.W. (1989). Boobyalla Sub-basin. In Burrett, C.F. & Martin, E.L. eds. Geology and Mineral Resources of Tasmania. Geol. Soc. Aus. Spec. Pub., 15, 356-358.

Mackie, W. (1923). The principles that regulate the distribution of particles of heavy minerals in sedimentary rocks, as illustrated by the sandstone of the north-east of Scotland. Trans. Edinburgh Geol. Soc., 11, 138-164.

MacNevin, A.A. (1972). Sapphires in the New England district, New South Wales. Rec. Geol. Surv. New South Wales, 14, 19-35.

Macphail, M. (1975). Late Pleistocene environments in Tasmania. Search, 6, 295-300.

Marshall, B. (1968). Joint and fault development in north-east Tasmania. Geol. Mag., 105, 186-187.

McClenaghan, M.P. & Baillie, P.W. (1975). Geological survey explanatory report - Launceston. Geological Atlas 1 : 250 000 series, Tasmania Dept. Mines.

McClenaghan, M.P., Turner, N.J., Baillie, P.W., Brown, A.V., Williams, P.R. & Moore, W.R. (1982). Geology of the Ringarooma-Boobyalla Area. Geol. Surv. Bull., Tasmania Dept. Mines, 61.

McClenaghan, M.P. & Williams, P.R. (1982). Distribution and characterisation of granitoid intrusions in the Blue Tier area. Pap. Geol. Surv., Tasmania Dept. Mines, 4.

McDougall, I. & Leggo, P.J. (1965). Isotopic age determinations on granitic rocks from Tasmania. J. Geol. Soc. Aus., 12, 295-232.

McDougall, I. & Wilkinson, J.F.G. (1967). Potassium-argon dates on some Cainozoic volcanic rocks from northeastern New South Wales. J. Geol. Soc. Aus., 14, 225-233.

McFarlane, M.J. (1983). Laterites. In Goudie, A.S. & Pye, K. eds. Chemical Sediments and Geomorphology. Academic Press, London.

Milner, H.B. (1962). Sedimentary Petrography. Vols. 1 & 2. George Allen & Unwin Ltd., London, 6th ed.

Moore, W.R., Baillie, P.W., Forsyth, S.M. & Hudspeth, J.W. (1984). Boobyalla Sub-basin: a Cretaceous onshore extension of thew southern edge of the Bass Basin. Aus. Petrol. Expl. Assoc. J., 24, 110-117.

Morrison, K.C. (1980). Sedimentology of the Pioneer Placer Deposit. Unpub. B.Sc. Hons. thesis, University of Tasmania.

Morton, A.C. (1985). Heavy minerals in provenance studies. In Zuffa, G.G. ed. Provenance of Arenites. D. Reidel Pub. Co., 249-277.

Mursky, G.A. & Thompson, R.M. (1958). A specific gravity index for minerals. Canadian Miner., 6, 273-287.

Nye, P.B. (1925). The sub-basaltic tin deposits of the Ringarooma valley. Geol. Surv. Bull., Tasmania Dept. Mines, 35.

Nye, P.B. & Blake, J. (1938). The geology and mineral deposits of Tasmania. Geol. Surv. Bull., Tasmania Dept. Mines, 44.

Ollier, C.D. (1978). Silcrete and weathering. In Langford-Smith, T. ed. Silcrete in Australia. University of New England Press, Armidale.

Ollier, C.D. (1979). Evolutionary geomorphology of Australia and Papua New Guinea. Trans. Inst. Brit. Geog. New Series, 4, 516-539.

Ollier, C.D. (1983). Weathering or hydrothermal alteration? Catena, 10, 57-59.

Ollier, C.D. (1988). The regolith in Australia. Earth-Sci. Rev., 25, 355-361.

Osberger, R. (1967). Dating Indonesian cassiterite placers. Min. Mag., 117, 260-261.

Owens, H.B. (1954). Bauxites in Australia. Bull. Bur. Min. Res. Geol. & Geophys. Aus., 24.

Owers, N.F. (1970). Preliminary explanation of Scotia deep lead, Tasmania. Unpub. Rep. Tasmania Dept. Mines, Blue Metals Industries Mining Pty. Ltd.

Pettijohn, F.T. (1941). Persistence of heavy minerals and geologic age. J. Geol., 49, 610-625.

Pryor, W.A. (1958). Dip direction indicator. J. Sed. Pet., 28, 230.

Quilty, P.G. (1972). The biostratigraphy of the Tasmanian marine Tertiary. Pap. Proc. Roy. Soc. Tasmania, 106, 25-44.

Raeburn, C. & Milner, H.B. (1925). Alluvial Prospecting. Thomas Murby & Co., London.

Reid, A.M. & Henderson, Q.J. (1928). Blue Tier tin Field. Geol. Surv. Bull., Tasmania Dept. Mines, 38.

Reid, A.M. & Henderson, Q.J. (1929). Avoca mineral district. Geol. Sur. Bull., Tasmania Dept. Mines, 40.

Reid, I. & Frostick, L.E. (1985). Role of settling, entrainment and dispersive equivalence and interstice trapping in placer formation. J. Geol. Soc. London, 142, 739-746.

Rickards, R.B. & Banks, M.R. (1979). An Early Devonian monograptid from the Mathinna Beds. Alcheringa, 3, 307-311.

Rittenhouse, G. (1943). The transportation and deposition of heavy minerals. Geol. Soc. Amer. Bull., 54, 1725-1780.

Robinson, V.A. (1974). Geological history of the Bass Basin. Aus. Petrol. Expl. Assoc. J., 14, 45-49.

Rubey, W.W. (1933). The size-distribution of heavy minerals within a water-laid sandstone. J. Sed. Pet., 3, 3-29.

Saks, S.E. & Gavshina, A.N. (1976). Stream deposition of cassiterite. Litholoqiya i Poleznye Iskopaemye, 2, 129-134.

Santokh Singh, D. & Bean, J.H. (1968). Some general aspects of tin minerals in Malaysia. Proc. Tech. Conf. on Tin, vol. 2, Int. Tin Coun., 459-478.

Sedmik, E.C.E. (1964). Winnaleah area geophysical surveys, Tasmania 1961-62. Rec. Bur. Min. Res. Geol. & Geophys. Aus., 1964/54.

Shackleton, N.J. (1977). The oxygen isotope record of the Late Pleaistocene. Phil. Trans. Roy. Soc. London B, 280, 169-182.

Shackleton, N.J. & Kennett, J.P. (1975). Palaeotemperature history of the Cenozoic and the initiation of Antarctica glaciation: oxygen and carbon isotope analyses in DSDP sites. In Kennett, J.P., Houtz, R.E., et al. eds. Initial Reports of the Deep Sea Drilling Project Vol. 29. U.S. Government Printing Office, Washington, 743-755.

Shackleton, N.J. & Opdyke, N.D. (1973). Oxygen isotope and palaeomagnetic stratigraphy of equatorial Pacific core V28-238: oxygen isotope temperatures and ice volumes on a 10^5 year and 10^6 year scale. Quat. Res., 3, 39-55.

Solomon, M. (1962). The tectonic history of Tasmania. J. Geol. Soc. Aus., 9, 311-339.

Sprigg, R.C. (1979). Stranded and submerged sea-beach systems of southeast South Australia and the aeolian desert cycle. Sed. Geol., 22, 53-96.

Spry, A. (1962). Igneous activity. J. Geol. Soc. Aus., 9, 255-284.

Standard, J.C. (1973). Endurance drilling programme, South Mount Cameron, Tasmania - end of phase 1. Unpub. Rep. Tasmania Dept. Mines, vols. 1 & 2, Blue Metals Industries Mining Pty. Ltd.

Standard, J.C. (1973a). Results of drilling programme on Scotia tin lead, Tasmania. Unpub. Rep. Tasmania Dept. Mines, 73-967, Blue Metals Industries Mining Pty. Ltd.

Steane, J.D. (1972). Ringarooma, Boobyalla and Great Mussel Roe Rivers. Water Res. Surv. Rep., Rivers & Water Supply Comm. Tasmania, 12.

Steane, J.D. (1983). Ringarooma River - silting by mine tailings. Unpub. Excurs. Field Notes, Annual Meeting Aus. Standing Comm. Soil Conservation.

Stephens, C.G. (1971). Laterite and silcrete in Australia: a study of the genetic relationships of laterite and silcrete and their companion materials, and their collective significance in the formation of the weathered mantle, soils, relief and drainage of the Australia continent. Geoderma, 5, 5-52.

Steveson, B.G. & Taylor, R.G. (1973). Trace element content of some cassiterites from eastern Australia. Proc. Roy. Soc. Queensland, 84, 43-54.

Sutherland, D.G. (1982). The transport and sorting of diamonds by fluvial and marine processes. Econ. Geol., 77, 1613-1620.

Sutherland, D.G. (1985). Geomorphological controls on the distribution of placer deposits. J. Geol. Soc. London, 142, 727-737.

Sutherland, F.L. (1969). A review of the Tasmanian Cainozoic volcanic province. Geol. Soc. Aus. Spec. Pub., 2, 133-144.

Sutherland, F.L. (1971). The question of late Cainozoic uplifts in Tasmania. Search, 2, 431-432.

Sutherland, F.L. (1973). The geological development of the southern shores and islands of Bass Strait. Proc. Roy. Soc. Victoria, 85, 133-144.

Sutherland, F.L. & Hollis, J.D. (1982). Mantle-lower crust petrology from inclusions in basaltic rocks in eastern Australia - an outline. J. Volcan. & Geotherm. Res., 14, 1-29.

Sutherland, F.L. & Kershaw, R.C. (1971). The Cainozoic geology of Flinders Island, Bass Strait. Pap. Proc. Roy. Soc. Tasmania, 105, 131-177.

Sutherland, F.L. & Wellman, P. (1986). Potassium-argon ages of Tertiary volcanic rocks, Tasmania. Pap. Proc. Roy. Soc. Tasmania, 120, 77-86.

Taguchi, S., Harayama, M. & Hayashi, M. (1985). ESR signal of zircon and geologic age. In Ikeya, M. & Miki, T. eds. ESR Dating and Dosimetry. Ionics, Tokyo, 191-196.

Taylor, D. (1986). Some thoughts on the development of the alluvial tinfields of Malay-Thai Peninsula. Bull. Geol. Soc. Malaysia, 19, 375-392.

Taylor, G. & Ruxton, B.P. (1987). A duricrust catena in south-east Australia. Zeitsch. Geomorph. N.F., 31, 385-410.

Taylor, G. & Smith, I.E. (1975). The genesis of sub-basaltic silcretes from the Monaro, New South Wales. J. Geol. Soc. Aus., 22, 377-385.

Taylor, G. & Smith, I.E. (1976). Reply to discussion. J. Geol. Soc. Aus., 23, 115-116.

Taylor, R.G. (1979). Geology of Tin Deposits. Developments in Economic Geology, 11. Elsevier Pub. Co., Amsterdam.

Thom, B.G. (1973). The dilemma of high interstadial sea levels during the last glaciation. In Broad, C., Chorley, R.J., Haggett, P. & Stoddart, D.R. eds. Progress in Geography 5. Edward Arnold, London, 170-245.

Thomas, D.E. (1953). The Blue Tier tin field. Pub. 5th Empire Min. Metall. Cong., 1, 1213-1221.

Toh, E. (1978). Comparison of exploration for alluvial tin and gold. Proc. 11th Commonwealth Min. Metall. Cong., 269-278.

Tourtelot, H.A. (1968). Hydraulic equivalence of grains of quartz and heavier minerals and implications for the study of placers. U.S. Geol. Surv. Prof. Pap., 594F, 1-13.

Townrow, J.A. (1964). A speculation on the Rhaeto-Liassic climate in Tasmania. Pap. Proc. Roy. Soc. Tasmania, 98, 113-118.

Traub, I. & Moh, G.H. (1978). Trace elements in tin ores (with special attention to Asian occurrences). Proc. 3rd Reg. Conf. on Geology & Mineral Resources of Southeast Asia, Bangkok, 361-365.

Tuck, R. (1968). Origin of bedrock values of placer deposits. Econ. Geol., 63, 191-193.

Turner, N.J. (1980). A summary of the geology of north eastern Tasmania. In Abstract, Coal, Tin, Surfical Deposits and Geology of North East Tasmania. Geol. Soc. Aus., 1, 2-6.

Twelvetrees, W.H. (1900). Preliminary report on the deep lead or infra-basaltic stanniferous gravels of the Ringarooma valley near Derby. Rep. Sec. Mines Tasmania, Government Printer 1899-1900, 107-127.

Twelvetrees, W.H. (1916). The Gladstone mineral district. Geol. Surv. Bull., Tasmania Dept. Mines, 25.

Vail, P.R., Mitchum Jr., R.M. & Thompson III, S. (1977). Seismic stratigraphy and global changes of sea level, Part 4: global cycles of relative changes of sea level. In Payton, C.E. ed. Seismic

Stratigraphy - Applications to Hydrocarbon Exploration. Amer. Assoc. Petrol. Geol. Mem., 26, 83-97.

van de Geer, G., Colhoun, E.A. & Bowden, A. (1979). Evidence and problems of interglacial marine deposits in Tasmania. Geol. Mijn., 58, 29-32.

van Overeem, A.J.A. (1960). Geological control of dredging operations on placer deposits in Billiton. Geol. Mijn., 39, 458-463.

Veevers, J.J. ed. (1984). Phanerozoic Earth History of Australia. Oxford Geological Sciences Series No. 2, Clarendon Press, Oxford.

Wass, S.Y. & Irving, A.J. (1976). A Catalogue of Occurrences of Xenoliths and Megacrysts in Volcanic Rocks of Eastern Australia. Aus. Mus., Sydney.

Wellington, H.K. (1982). R818 Core drilling in Ringarooma Bay. Unpub. Rep. Tasmania Dept. Mines.

Wellman, P. (1974). Potassium-argon ages on the Cainozoic volcanic rocks of eastern Victoria, Australia. J. Geol. Soc. Aus., 21, 359-376.

Wellman, P. & McDougall, I. (1974). Cainozoic igneous activity in eastern Australia. Tectonophysics, 23, 49-65.

Wellman, P. & McDougall, I. (1974a). Potassium-argon ages on the Cainozoic volcanic rocks of New South Wales. J. Geol. Soc. Aus., 21, 247-272.

Wey, R. & Siffert, B. (1962). Reactions de la silica monomoleculaire en solution avec lesions Al^{3+} et Mg^{2+}. Genesis et synthese des argiles. Coll. Int. CNRS, 105, 11-23. (Referred to in Millot, G. 1970. Geology of Clays. Springer, Berlin).

Williams, E. (1959). The sedimentary structures of the Upper Scamander sequence and their significance. Pap. Proc. Roy. Soc. Tasmania, 93, 29-32.

Williams, E. (1978). Tasman fold belt system in Tasmania. Tectonophysics, 48, 159-206.

Williamson, P.E., Pigram, C.J., Colwell, J.B., Schorl, A.S., Lockwood, K.L. & Branson, J.C. (1987). Review of stratigraphy, structure, and hydrocarbon potential of Bass Basin, Australia. Amer. Assoc. Petrol. Geol. Bull., 71, 253-280.

Woolnough, W.G. (1927). The chemical criteria of peneplanation. J. Proc. Roy. Soc. New South Wales, 61, 1-53.

Yim, W.W.-S. (1980). Heavy mineral studies of stanniferous deep leads, north-east Tasmania. Rec. Bur. Min. Res. Geol. & Geophys. Aus., 1980/67, 81.

Yim, W.W.-S. (1981). Geochemical investigations on fluvial sediments contaminated by tin-mine tailings, Cornwall, England. Environ. Geol., 3, 245-256.

Yim, W.W.-S. (1984). Liberation studies on tin-bearing sands off north Cornwall, United Kingdom. Mar. Min., 5, 87-99.

Yim, W.W.-S. (1986). Application of the Zeiss TGA 10 particle-size analyzer in the exploration of stanniferous placers. Bull. Geol. Soc. Malaysia, 20, 619-625.

Yim, W.W.-S., Gleadow, A.J.W. & van Moort, J.C. (1985). Fission track dating of alluvial zircons and heavy mineral provenance in northeast Tasmania. J. Geol. Soc. London, 142, 351-356.

Young, R.W. (1978). Silcrete in a humid landscape: The Shoalhaven valley and adjacent coastal plains of southern New South Wales. In Langford-Smith, T. ed. Silcrete in Australia. University of New England Press, Armidale, 195-207.

Young, R.W. (1985). Silcrete distribution in eastern Australia. Zeitsch. Geomorph. N.F., 29, 21-36.

Young, R.W. & McDougall, I. (1982). Basalts and silcretes on the coast near Ulladulla, southern New South Wales. J. Geol. Soc. Aus., 29, 425-430.

Zeller, E.J. (1968). Use of electron spin resonance for measurement of natural radiation damage. In MacDougall, D.J. ed. Thermoluminescence of Geological Materials. Academic Press, London, 271-279.

Zeller, E.J., Levy, P.W. & Mattern, P.L. (1967). Geological dating by electron spin resonance. Proc. Symp. on Radioactive Dating and Low Level Counting, International Atomic Energy Authority, Wien, 531-540.

APPENDIX I

SUMMARY OF OXIDE PERCENTAGES AND STRUCTURAL FORMULAE OF MINERALS OBTAINED BY ELECTRON MICROPROBE ANALYSIS

Key :

a - Total iron reported as FeO
b - Fe^{2+} & Fe^{3+}
Note - All totals given are unadjusted.

(1) CORUNDUM (oxygen number 3)

C1/C3 - Pioneer Mine

Sample ref.	C1	C2	C3
Al_2O_3	99.72	99.52	99.60
FeO^a	-	-	0.27
Na_2O	0.32	-	-
Total	99.66	103.31	101.81
Structural formula			
Al	2.0000	1.9970	1.9970
Fe^b	-	-	0.0040
Na	-	0.0100	-
Total	2.0000	2.0070	2.0013

(2) FELDSPAR (oxygen number 8) - oligoclase

F1/F2 - Le Fevre Road

Sample ref.	F1	F2
SiO_2	62.31	60.25
Al_2O_3	23.02	23.84
CaO	4.16	5.60
Na_2O	7.84	6.98
K_2O	0.95	0.73
Total	98.29	97.21
Structural formula		
Si	2.8007	2.7437
Al	1.2196	1.2796
Ca	0.2004	0.2636
Na	0.6831	0.6164
K	0.0545	0.0425
Total	4.9582	4.9459

(3) GARNET (oxygen number 12) - almandine and spessartine

G1 - Blue Tier Parmeener Supergroup
G2/G3 - Dorset Mine
G4/G6 - Monarch Mine
G7/G13 - Pioneer Mine
G14 - Ringarooma Bay borehole NE646
G15/G17 - Spinel Creek

Sample ref.	G1	G2	G3	G4	G5	G6	G7	G8
SiO_2	36.93	36.08	37.19	36.15	35.70	34.91	36.56	36.28
TiO_2	0.22	-	-	-	-	-	-	-
Al_2O_3	20.84	21.35	21.37	21.18	21.01	21.17	21.59	22.04
FeO^a	19.66	9.19	15.13	35.19	35.13	35.60	12.76	7.67
MnO	23.98	37.25	30.81	7.36	7.52	6.57	28.73	33.67
MgO	0.96	-	-	-	-	0.46	-	-
CaO	0.82	0.68	1.56	0.23	0.23	0.26	-	-
Na_2O	-	-	-	-	-	0.77	0.35	0.34
P_2O_5	0.35	-	-	0.30	0.36	-	-	-
Total	103.75	104.55	106.05	100.42	99.95	101.37	103.13	101.88
Structural formula								
Si	2.9385	2.8888	2.9249	2.9649	2.9485	2.9030	2.9910	2.9670
Al	1.9538	2.0147	1.9806	2.0474	2.0448	2.0750	2.0820	2.1240
Ti	0.0310	-	-	-	-	-	-	-
Fe^b	1.3082	0.6152	0.9950	2.4141	2.4265	2.4760	0.8730	0.5250
Mn	1.6162	2.5266	2.0529	0.5115	0.5260	0.4630	1.9920	2.3310
Mg	0.1133	-	-	-	-	0.0570	-	-
Ca	0.0702	0.0587	0.1314	0.0205	0.0202	0.0230	-	-
Na	-	-	-	-	-	0.1240	0.0570	0.0540
P	0.0234	-	-	0.0212	0.0252	-	-	-
Total	8.0366	8.1040	8.0849	7.9796	7.9912	8.1210	7.9950	8.0010

Sample ref.	G9	G10	G11	G12	G13	G14	G15	G16
SiO_2	36.44	36.41	36.71	36.50	35.07	37.54	35.65	35.99
TiO_2	0.25	-	-	-	-	0.34	-	-
Al_2O_3	22.14	22.18	21.72	21.04	21.35	20.88	20.85	21.21
FeO^a	9.30	3.73	9.92	15.75	5.90	31.40	7.98	5.71
MnO	30.80	37.14	31.17	28.53	39.82	2.28	33.02	32.80
MgO	-	-	-	-	-	1.28	-	-
CaO	0.52	-	-	0.26	-	7.78	4.50	6.99
Na_2O	0.55	0.54	0.47	-	-	-	-	-
P_2O_5	-	-	-	0.35	-	-	-	-
Total	100.74	100.76	101.10	102.44	102.14	101.49	102.01	102.70
Structural formula								
Si	2.9670	2.9700	2.9970	2.9484	2.8716	2.9848	2.8977	2.8882
Al	2.1240	2.1330	2.0900	2.0031	2.0608	1.9563	1,9978	2.0064
Ti	0.0150	-	-	-	-	0.0202	-	-
Fe^b	0.6330	0.2550	0.6780	1.0640	0.4038	2.0879	0.5425	0.3833
Mn	2.1240	2.5650	2.1560	1.9515	2.7620	0.1537	2.2734	2.2296
Mg	-	-	-	-	-	0.1513	-	-
Ca	0.0450	-	-	0.0224	-	0.6624	0.3922	0.6011
Na	0.0870	0.0870	0.0740	-	-	-	-	-
P	-	-	-	0.0242	-	-	-	-
Total	7.9950	8.0100	7.9950	8.0137	8.1210	8.0167	8.1036	8.1071

Sample ref.	G17
SiO_2	36.10
TiO_2	-
Al_2O_3	21.19
FeO^a	5.90
MnO	32.87
MgO	-
CaO	6.84
Na_2O	-

P_2O_5	-
Total	102.89
Structural formula	
Si	2.8926
Ti	-
Al	2.0008
Fe[b]	0.3952
Mn	2.2309
Mg	-
Ca	0.5875
Na	-
P	-
Total	8.1071

(4) Ilmenite (oxygen number 3) - Mg-rich and Mg-poor

I1/I11 - Banca Mine
I12/I18 - Bells Plain Mine
I19/I29 - Blackberries Mine
I30/I31 - Blue Tier Parmeener Supergroup
I32 - Briseis Mine
I33 - Dobson Mine
I34 - Forest Lodge
I35/I40 - Le Fevre Road
I41/I53 - Pioneer Mine
I54/I64 - Schramms Road
I65/I80 - Weld River

Sample ref.	I1	I2	I3	I4	I5	I6	I7	I8
SiO_2	-	-	-	-	-	-	-	-
TiO_2	53.80	53.89	53.68	52.20	51.42	50.55	50.73	51.09
Al_2O_3	0.29	0.23	-	0.28	-	-	-	0.19
Cr_2O_3	-	-	-	-	-	-	-	-
FeO[a]	33.72	36.47	35.55	39.53	34.70	37.87	36.62	33.93
MnO	0.41	0.29	0.41	0.40	0.47	0.30	0.56	0.46
MgO	9.56	7.52	6.04	5.96	7.18	5.34	6.37	6.31
CaO	-	-	-	-	0.43	-	-	-
Na_2O	-	-	-	-	-	-	-	-
P_2O_5	-	-	-	-	-	-	-	-
SO_3	-	-	-	-	-	-	-	-
Cl_2O	-	-	-	-	-	-	-	-
Total	97.79	98.40	95.68	98.37	94.20	94.06	84.28	95.75
Structural formula								
Si	-	-	-	-	-	-	-	-
Al	0.0084	0.0066	-	0.0082	-	-	-	0.0057
Cr	-	-	-	-	-	-	-	-
Ti	0.9770	0.9852	1.0108	0.9710	0.9839	0.9840	0.9791	0.9726
Fe[a]	0.6810	0.7414	0.7444	0.8177	0.7383	0.8197	0.7859	0.7984
Mn	0.0084	0.0061	0.0087	0.0084	0.0101	0.0066	0.0123	0.0098
Mg	0.3441	0.2723	0.2254	0.2196	0.2722	0.2058	0.2436	0.2381
Ca	-	-	-	-	0.0117	-	-	-
Na	-	-	-	-	-	-	-	-
P	-	-	-	-	-	-	-	-
S	-	-	-	-	-	-	-	-
Cl	-	-	-	-	-	-	-	-

Total	2.0188	2.0115	1.9893	2.0250	2.0162	2.0161	2.0209	2.0246
Sample ref.	I9	I10	I11	I12	I13	I14	I15	I16
SiO_2	-	-	-	-	-	-	0.25	-
TiO_2	51.64	51.51	51.07	50.46	49.76	48.49	47.68	48.07
Al_2O_3	-	0.18	0.21	1.02	1.07	0.92	1.20	0.53
Cr_2O_3	-	-	0.24	-	-	-	-	-
FeO^a	33.93	35.97	37.45	37.92	38.86	45.53	45.39	40.80
MnO	0.43	0.46	0.32	0.39	0.46	0.50	0.53	0.24
MgO	8.33	7.63	5.87	9.04	8.94	3.85	4.08	5.27
CaO	-	-	-	-	-	-	-	-
Na_2O	-	-	-	0.84	0.64	0.58	0.72	-
P_2O_5	-	-	-	-	-	-	-	-
SO_3	-	-	-	-	-	-	-	-
Cl_2O	-	-	-	-	-	-	-	-
Total	94.33	95.75	95.16	106.03	106.17	102.35	107.12	94.92
Structural formula								
Si	-	-	-	-	-	-	0.0080	-
Al	-	0.0054	0.0063	0.0290	0.0310	0.0270	0.0470	0.0162
Cr	-	-	0.0048	-	-	-	-	-
Ti	0.9805	0.9714	0.9780	0.9180	0.9090	0.9160	1.2000	0.9396
Fe^b	0.7163	0.7543	0.7975	0.7670	0.7890	0.9570	1.2710	0.8869
Mn	0.0091	0.0098	0.0069	0.0080	0.0100	0.0110	0.0150	0.0054
Mg	0.3136	0.2852	0.2230	0.3260	0.3240	0.1440	0.2030	0.2042
Ca	-	-	-	-	-	-	-	-
Na	-	-	-	0.0390	0.0300	0.0280	0.0470	-
P	-	-	-	-	-	-	-	-
S	-	-	-	-	-	-	-	-
Cl	-	-	-	-	-	-	-	-
Total	2.0196	2.0260	2.0165	2.0872	2.0911	2.0840	2.7914	2.0523
Sample ref.	I17	I18	I19	I20	I21	I22	I23	I24
SiO_2	-	-	0.43	1.13	0.39	-	-	-
TiO_2	48.01	48.12	49.92	60.41	57.04	51.27	51.36	52.18
Al_2O_3	0.59	0.48	0.81	1.01	0.83	0.60	0.57	0.62
Cr_2O_3	-	-	-	-	-	-	-	-
FeO^a	41.76	42.46	42.32	32.50	36.62	41.97	42.11	42.93
MnO	-	0.53	5.01	3.44	3.78	4.98	5.32	3.09
MgO	4.52	3.24	0.87	0.84	0.74	0.72	0.39	0.56
CaO	-	-	-	-	-	-	-	-
Na_2O	-	-	0.64	0.67	0.60	0.46	0.25	0.62
P_2O_5	-	-	-	-	-	-	-	-
SO_3	-	-	-	-	-	-	-	-
Cl_2O	-	-	-	-	-	-	-	-
Total	94.88	94.83	103.99	97.15	100.97	103.18	108.42	108.02
Structural formula								
Si	-	-	0.0110	0.0270	0.0100	-	-	-
Al	0.0182	0.0150	0.0240	0.0280	0.0240	0.0180	0.0170	0.0180
Cr	-	-	-	-	-	-	-	-
Ti	0.9425	0.9522	0.9470	1.0740	1.0420	0.9720	0.9750	0.9850
Fe^b	0.9117	0.9394	0.8930	0.6430	0.7440	0.8850	0.8890	0.9010
Mn	-	0.0118	0.1070	0.0690	0.0780	0.1060	0.1140	0.0660
Mg	0.1760	0.1272	0.0330	0.0300	0.0270	0.0270	0.0150	0.0210
Ca	-	-	-	-	-	-	-	-
Na	-	-	0.0310	0.0310	0.0280	0.0220	0.0120	0.0300

P	-	-	-	-	-	-	-	-
S	-	-	-	-	-	-	-	-
Cl	-	-	-	-	-	-	-	-
Total	2.0484	2.0404	2.0460	1.9005	1.9513	2.0303	2.0221	2.0210

Sample ref.	I25	I26	I27	I28	I29	I30	I31	I32
SiO_2	-	-	-	-	-	0.94	0.82	-
TiO_2	53.73	51.72	53.11	60.61	57.21	34.34	37.45	47.88
Al_2O_3	0.73	0.56	0.71	0.79	0.32	2.40	2.94	0.34
Cr_2O_3	-	-	-	-	-	-	-	-
FeO[a]	40.65	41.67	41.41	33.46	32.07	48.02	44.60	44.65
MnO	3.76	5.29	3.54	3.93	2.87	-	-	0.30
MgO	0.62	0.47	0.68	0.64	-	-	-	3.37
CaO	-	-	-	-	-	-	-	-
Na_2O	0.51	0.29	0.55	0.57	0.32	-	-	-
P_2O_5	-	-	-	-	-	1.52	1.80	-
SO_3	-	-	-	-	-	0.57	0.34	-
Cl_2O	-	-	-	-	-	0.15	0.10	-
Total	105.16	105.92	105.31	98.15	92.80	87.94	88.06	96.54
Structural formula								
Si	-	-	-	-	-	0.0274	0.0234	-
Al	0.0210	0.0170	0.0210	0.0220	0.0098	0.0827	0.0989	0.0105
Cr	-	-	-	-	-	-	-	-
Ti	1.0040	0.9800	0.9960	0.0910	1.1109	0.7562	0.8041	0.9374
Fe[b]	0.8450	0.8780	0.8640	0.6700	0.6924	1.1758	1.0649	0.9721
Mn	0.0790	0.1130	0.0750	0.0800	0.0629	-	-	0.0066
Mg	0.0230	0.0180	0.0250	0.0230	-	-	-	0.1307
Ca	-	-	-	-	-	-	-	-
Na	0.0250	0.0140	0.0260	0.0270	0.0163	-	-	-
P	-	-	-	-	-	0.0376	0.0435	-
S	-	-	-	-	-	0.0117	0.0069	-
Cl	-	-	-	-	-	0.0076	0.0049	-
Total	1.9973	2.0191	2.0067	1.9115	1,8924	2.0990	2.0467	2.0574

Sample ref.	I33	I34	I35	I36	I37	I38	I39	I40
SiO_2	-	-	-	-	-	-	-	-
TiO_2	53.65	53.03	51.43	51.05	51.38	47.99	51.49	51.24
Al_2O_3	0.21	0.23	0.66	0.83	0.78	0.91	0.72	0.81
Cr_2O_3	-	-	-	-	-	-	-	-
FeO[a]	34.57	36.48	43.58	42.33	42.40	46.81	43.13	42.13
MnO	0.46	0.81	0.43	0.50	0.40	0.63	0.34	0.51
MgO	9.22	8.47	3.37	4.49	4.47	3.21	3.94	4.67
CaO	-	-	-	-	-	-	-	-
Na_2O	-	-	0.53	0.79	0.57	0.44	0.39	0.65
P_2O5	-	-	-	-	-	-	-	-
SO_3	-	-	-	-	-	-	-	-
Cl_2O	-	-	-	-	-	-	-	-
Total	98.10	99.02	96.50	97.43	100.73	100.17	99.47	99.42
Structural formula								
Si	-	-	-	-	-	-	-	-
Al	0.0059	0.0064	0.0190	0.0240	0.0230	0.0270	0.0210	0.0240
Cr	-	-	-	-	-	-	-	-
Ti	0.9753	0.9650	0.9600	0.9680	0.9530	0.9120	0.9580	0.9500
Fe[b]	0.6989	0.7383	0.9050	0.8740	0.8740	0.9900	0.8920	0.8680
Mn	0.0095	0.0167	0.0090	0.0110	0.0080	0.0140	0.0070	0.0110

Mg	0.3322	0.3055	0.1250	0.1650	0.1640	0.1210	0.1450	0.1710
Ca	-	-	-	-	-	-	-	-
Na	-	-	0.0250	0.0380	0.0270	0.0220	0.0190	0.0310
P	-	-	-	-	-	-	-	-
S	-	-	-	-	-	-	-	-
Cl	-	-	-	-	-	-	-	-
Total	2.0218	2.0319	2.0430	2.0592	2.0494	2.0851	2.0412	2.0541

Sample ref.	I41	I42	I43	I44	I45	I46	I47	I48
SiO_2	-	-	-	0.43	-	-	-	-
TiO_2	55.40	56.22	58.16	68.29	52.09	50.31	53.72	53.14
Al_2O_3	0.93	1.32	1.14	2.28	0.72	0.81	0.56	0.73
Cr_2O_3	-	-	-	-	-	-	-	-
FeO[a]	39.38	39.87	37.48	24.55	38.05	43.64	38.94	39.02
MnO	0.46	0.58	0.57	2.53	0.55	0.47	0.46	0.50
MgO	3.13	1.65	2.00	0.64	8.16	4.30	6.00	6.13
CaO	-	-	-	-	-	-	-	-
Na_2O	0.70	0.36	0.65	0.88	0.44	0.46	0.31	0.47
P_2O_5	-	-	-	-	-	-	-	-
SO_3	-	-	-	-	-	-	-	-
Cl_2O	-	-	-	-	-	-	-	-
Total	101.08	97.29	95.77	97.23	101.59	102.21	100.14	100.53
Structural formula								
Si	-	-	-	0.0100	-	-	-	-
Al	0.0270	0.0380	0.0320	0.0610	0.0210	0.0240	0.0160	0.0210
Cr	-	-	-	-	-	-	-	-
Ti	1.0110	1.0270	1.0500	1.1680	0.9440	0.9390	0.9770	0.9680
Fe[b]	0.7990	0.8100	0.7530	0.4640	0.7670	0.9060	0.7880	0.7900
Mn	0.0090	0.0120	0.0120	0.0490	0.0110	0.0100	0.0090	0.0100
Mg	0.1130	0.0600	0.0720	0.0210	0.2930	0.1590	0.2170	0.2210
Ca	-	-	-	-	-	-	-	-
Na	0.0330	0.0170	0.0300	0.0380	0.0210	0.0220	0.0150	0.0220
P	-	-	-	-	-	-	-	-
S	-	-	-	-	-	-	-	-
Cl	-	-	-	-	-	-	-	-
Total	1.9921	1.9629	1.9486	1.8111	2.0560	2.0601	2.0219	2.0328

Sample ref.	I49	I50	I51	I52	I53	I54	I55	I56
SiO_2	-	-	-	-	-	-	-	-
TiO_2	52.50	51.65	50.99	51.16	50.74	49.14	49.35	49.22
Al_2O_3	0.91	0.56	0.69	1.05	0.34	-	-	-
Cr_2O_3	0.25	-	-	-	-	-	-	-
FeO[a]	38.03	41.01	43.48	38.21	40.42	42.44	41.58	40.41
MnO	0.41	0.94	0.56	0.46	0.42	5.04	5.91	6.35
MgO	7.54	5.37	3.49	8.77	5.06	-	-	-
CaO	-	-	-	-	-	-	-	-
Na_2O	0.37	0.47	0.78	0.35	-	-	-	-
P_2O_5	-	-	-	-	-	-	-	-
SO_3	-	-	-	-	-	0.25	0.26	-
Cl_2O	-	-	-	-	-	-	-	-
Total	102.67	101.11	100.36	100.84	96.97	96.86	97.10	95.98
Structural formula								
Si	-	-	-	-	-	-	-	-
Al	0.0260	0.0160	0.0200	0.0300	0.0101	-	-	-
Cr	0.0050	-	-	-	-	-	-	-

Ti	0.9510	0.9530	0.9530	0.9270	0.9652	0.9704	0.9715	0.9810
Fe[b]	0.7660	0.8420	0.9040	0.7700	0.8549	0.9321	0.9102	0.8955
Mn	0.0080	0.0200	0.0120	0.0090	0.0089	0.1120	0.1311	0.1426
Mg	0.2710	0.1960	0.1290	0.3150	0.1907	-	-	-
Ca	-	-	-	-	-	-	-	-
Na	0.0170	0.0220	0.0380	0.0160	-	-	-	-
P	-	-	-	-	-	-	-	-
S	-	-	-	-	-	0.0045	0.0047	-
Cl	-	-	-	-	-	-	-	-
Total	2.0428	2.0497	2.0550	2.0666	2.0298	2.0191	2.0175	2.0191

Sample ref.	I57	I58	I59	I60	I61	I62	I63	I64
SiO_2	-	-	-	-	-	-	-	-
TiO_2	48.99	49.60	49.08	49.38	50.01	49.10	49.38	50.54
Al_2O_3	-	-	-	-	-	-	-	-
Cr_2O_3	-	-	-	-	-	-	-	-
FeO[a]	41.85	41.61	42.67	41.93	42.35	41.92	42.05	39.83
MnO	4.77	6.50	5.27	5.83	4.23	5.48	5.23	4.39
MgO	-	-	-	-	-	-	-	-
CaO	-	-	-	-	-	-	-	-
Na_2O	-	-	-	-	-	-	-	-
P_2O_5	-	-	-	-	-	-	-	-
SO_3	-	-	-	-	-	-	-	-
Cl_2O	-	-	-	-	-	-	-	-
Total	95.98	97.72	97.03	97.13	96.59	96.51	96.65	94.77
Structural formula								
Si	-	-	-	-	-	-	-	-
Al	0.36	-	-	-	-	-	-	-
Cr	-	-	-	-	-	-	-	-
Ti	0.9749	0.9739	0.9716	0.9749	0.9879	0.9756	0.9784	1.0087
Fe[b]	0.9262	0.9085	0.9393	0.9206	0.9302	0.9262	0.9265	0.8840
Mn	0.1070	0.1438	0.1176	0.1296	0.0940	0.1227	0.1167	0.0988
Mg	-	-	-	-	-	-	-	-
Ca	-	-	-	-	-	-	-	-
Na	-	-	-	-	-	-	-	-
P	-	-	-	-	-	-	-	-
S	-	-	-	-	-	-	-	-
Cl	-	-	-	-	-	-	-	-
Total	2.0195	2.0262	2.0285	2.0251	2.0122	2.0245	2.0216	1.9914

Sample ref.	I65	I66	I67	I68	I69	I70	I71	I72
SiO_2	-	-	-	-	-	-	-	-
TiO_2	51.79	56.53	51.97	47.44	51.62	46.74	51.23	51.18
Al_2O_3	1.51	0.72	0.60	1.33	0.61	1.43	0.89	1.03
Cr_2O_3	-	-	-	-	-	-	-	-
FeO[a]	42.07	38.00	40.88	44.74	43.39	47.05	37.99	39.40
MnO	0.52	3.75	5.37	0.38	3.37	0.44	0.46	0.46
MgO	3.79	0.59	0.62	5.59	0.56	3.81	8.89	7.44
CaO	-	-	-	-	-	-	-	-
Na_2O	0.32	0.41	0.57	0.53	0.45	0.54	0.55	0.50
P_2O_5	-	-	-	-	-	-	-	-
SO_3	-	-	-	-	-	-	-	-
Cl_2O	-	-	-	-	-	-	-	-
Total	97.37	98.92	103.25	102.08	102.39	100.36	99.97	102.14
Structural formula								

Si	-	-	-	-	-	-	-	-
Al	0.0440	0.0210	0.0180	0.0390	0.0180	0.0420	0.0250	0.0290
Cr	-	-	-	-	-	-	-	-
Ti	0.9570	1.0410	0.9820	0.8900	0.9780	0.8880	0.9280	0.9330
Fe^b	0.8640	0.7780	0.8590	0.9330	0.9140	0.9940	0.7650	0.7990
Mn	0.0110	0.0780	0.1140	0.0080	0.0720	0.0090	0.0090	0.0090
Mg	0.1390	0.0210	0.0230	0.2080	0.0210	0.1440	0.3190	0.2690
Ca	-	-	-	-	-	-	-	-
Na	0.0150	0.0190	0.0280	0.0250	0.0220	0.0260	0.0260	0.0230
P	-	-	-	-	-	-	-	-
S	-	-	-	-	-	-	-	-
Cl	-	-	-	-	-	-	-	-
Total	2.0291	1.9584	2.0234	2.1034	2.0243	2.1039	2.0724	2.0636

Sample ref.	I73	I74	I75	I76	I77	I78	I79	I80
SiO_2	0.21	-	-	-	-	-	-	-
TiO_2	58.76	52.44	51.84	51.28	51.21	52.34	51.99	56.07
Al_2O_3	0.88	0.71	0.70	0.90	1.07	0.56	0.78	0.70
Cr_2O_3	-	-	-	-	-	-	-	-
FeO^a	35.99	40.56	39.78	39.80	38.26	39.56	39.75	36.05
MnO	2.99	0.50	0.63	0.61	0.45	0.42	0.52	6.18
MgO	0.64	5.18	6.67	6.63	8.52	6.67	6.39	0.51
CaO	-	-	-	-	-	-	-	-
Na_2O	0.53	0.61	0.38	0.78	0.50	0.45	0.57	0.50
P_2O_5	-	-	-	-	-	-	-	-
SO_3	-	-	-	-	-	-	-	-
Cl_2O	-	-	-	-	-	-	-	-
Total	101.92	108.20	100.44	106.21	106.56	105.37	107.39	97.53
Structural formula								
Si	0.0050	-	-	-	-	-	-	-
Al	0.0250	0.0200	0.0200	0.0260	0.0310	0.0160	0.0220	0.0200
Cr	-	-	-	-	-	-	-	-
Ti	1.0650	0.9640	0.9480	0.9390	0.9280	0.9560	0.9510	1.0350
Fe^b	0.7260	0.8290	0.8090	0.8110	0.7710	0.8030	0.8090	0.7400
Mn	0.0610	0.0100	0.0130	0.0130	0.0090	0.0090	0.0110	0.1280
Mg	0.0230	0.1890	0.2420	0.2410	0.3060	0.2420	0.2320	0.0180
Ca	-	-	-	-	-	-	-	-
Na	0.0250	0.0290	0.0180	0.0370	0.0230	0.0210	0.0270	0.0240
P	-	-	-	-	-	-	-	-
S	-	-	-	-	-	-	-	-
Cl	-	-	-	-	-	-	-	-
Total	1.9296	2.0408	2.0506	2.0660	2.0682	2.0467	2.0512	1.9664

(5) PYROXENE (oxygen number 6) - augite and enstatite

P1 - Blackberries Mine
P2 - Black Creek
P3/P5 - North George River
P6 - Pioneer Mine inclusion within corundum
P7/P8 - Ringarooma Bay borehole NE872

Sample ref.	P1	P2	P3	P4	P5	P6	P7	P8
SiO_2	47.99	56.30	55.89	55.73	55.00	64.73	55.02	55.72
TiO_2	1.66	-	-	-	-	-	-	-

Al_2O_3	7.20	2.08	3.77	4.41	4.56	1.96	5.16	4.06
Cr_2O_3	0.27	0.66	0.22	0.38	0.70	-	0.47	0.20
FeO^a	5.49	5.10	6.25	6.05	7.88	0.23	6.25	6.14
MgO	13.41	33.64	33.39	33.15	31.05	33.08	33.49	34.11
CaO	21.26	1.72	0.77	0.79	1.75	-	0.71	0.65
Na_2O	0.93	-	-	-	-	-	0.28	-
Total	98.21	99.50	100.29	100.51	100.94	99.09	101.38	100.89
Structural formula								
Si	1.8020	1.9491	1.9216	1.9105	1.9005	2.1290	1.8768	1.9045
Al	0.3188	0.0850	0.1527	0.1783	0.1859	0.0760	0.2074	0.1637
Cr	0.0080	0.0180	0.0060	0.0130	0.0191	-	0.0128	0.0055
Ti	0.0468	-	-	-	-	-	-	-
Fe^b	0.1725	0.1476	0.1797	0.1733	0.2278	0.0060	0.1782	0.1756
Mg	0.7503	1.7358	1.7108	1.6937	1.5990	1.6220	1.7028	1.7378
Ca	0.8555	0.0638	0.0282	0.0291	0.0647	-	0.0259	0.0237
Na	0.0677	-	-	-	-	-	0.0185	-
Total	4.0216	3.9994	3.9991	3.9952	3.9970	3.8330	4.0223	4.0108

(6) RUTILE (oxygen number 2)

R1/R2 - Blue Tier Parmeener Supergroup

Sample ref.	R1	R2
SiO_2	0.88	-
TiO_2	92.11	95.75
Al_2O_3	0.30	-
Cr_2O_3	0.31	0.31
FeO^a	0.97	-
P_2O_5	0.35	-
SO_3	1.16	-
Total	96.07	96.06
Structural formula		
Si	0.0024	-
Al	0.0010	-
Cr	0.0007	0.0068
Ti	1.9050	2.0018
Fe^b	0.0022	-
P	0.0008	-
S	0.0022	-
Total	1.9980	2.0018

(7) SPINEL (oxygen number 4) - hercynite and pleonaste

S1 - Amber Hill Mine
S2/S6 - Bells Plain Mine
S7/S10 - Blackberries Mine
S11/S15 - Delta Mine
S16/S18 - Dobson Mine
S19 - Forest Lodge
S20/S29 - Le Fevre Road
S30/S31 - Monarch Mine
S32/S33 - Musselroe Mine
S34/S43 - North George River
S44/S47 - Pioneer Mine

S48/S53 - Ringarooma Bay borehole NE646
S54 - Ringarooma Bay borehole NE847
S55 - Scotia Mine
S56/S57 - Sextus Creek Mine
S58/S61 - Spinel Creek
S62/S69 - Star Hill Mine
S70/S71 - Weld River

Sample ref.	S1	S2	S3	S4	S5	S6	S7	S8
SiO_2	-	-	-	-	-	-	-	-
TiO_2	0.34	0.48	0.58	0.35	0.43	0.45	0.41	0.45
Al_2O_3	63.78	62.08	60.77	62.95	60.44	60.31	61.50	61.29
Cr_2O_3	-	-	-	-	0.21	-	0.41	-
FeO[a]	16.82	17.65	19.52	16.41	23.06	22.45	18.27	19.68
MgO	20.60	19.20	18.49	20.45	15.35	16.94	19.00	18.06
Na_2O	0.24	0.38	0.36	-	0.45	-	0.41	0.53
Total	101.78	104.87	103.85	100.16	91.69	100.14	99.72	101.17
Structural formula								
Si	-	-	-	-	-	-	-	-
Al	1.8997	1.8980	1.8780	1.9021	1.8950	1.8788	1.8850	1.8900
Cr	-	-	-	-	0.0040	-	0.0080	-
Ti	0.0065	0.0090	0.0110	0.0068	0.0090	0.0089	0.0080	0.0090
Fe[b]	0.3554	0.3830	0.4280	0.3518	0.5130	0.4963	0.3970	0.4300
Mg	0.7760	0.7420	0.7230	0.7813	0.6090	0.6674	0.7370	0.7040
Na	0.0118	0.0190	0.0180	-	0.0230	-	0.0210	0.0270
Total	3.0494	3.0514	3.0586	3.0420	3.0531	3.0515	3.0557	3.0597

Sample ref.	S9	S10	S11	S12	S13	S14	S15	S16
SiO_2	-	-	-	-	-	-	-	0.21
TiO_2	0.70	0.98	0.45	1.10	0.20	0.71	0.48	0.31
Al_2O_3	60.43	57.93	62.48	57.77	64.77	60.48	62.12	64.27
Cr_2O_3	-	-	0.40	-	-	-	0.55	-
FeO[a]	22.43	26.85	18.31	25.27	15.13	21.34	18.78	17.41
MgO	18.40	16.28	20.01	17.44	21.45	18.83	20.24	21.07
Na_2O	0.25	-	-	-	-	-	-	-
Total	102.21	102.04	101.65	101.59	101.56	101.71	102.15	103.26
Structural formula								
Si	-	-	-	-	-	-	-	0.0051
Al	1.8462	1.8132	1.8790	1.8045	1.9151	1.8559	1.8646	1.8881
Cr	-	-	0.0080	-	-	-	0.0110	-
Ti	0.0136	0.0195	0.0087	0.0220	0.0038	0.0138	0.0091	0.0058
Fe[b]	0.4862	0.5964	0.3909	0.5601	0.3174	0.4619	0.3999	0.3629
Mg	0.7109	0.6445	0.7610	0.6891	0.8021	0.7263	0.7682	0.7829
Na	0.0124	-	-	-	-	-	-	-
Total	3.0693	3.0737	3.0476	3.0756	3.0385	3.0580	3.0529	3.0449

Sample ref.	S17	S18	S19	S20	S21	S22	S23	S24
SiO_2	-	-	-	-	-	-	-	-
TiO_2	0.28	0.61	0.99	0.41	0.56	0.80	0.71	-
Al_2O_3	63.84	60.62	58.23	63.33	59.57	57.81	57.38	61.24
Cr_2O_3	-	0.40	-	-	-	0.29	-	-
FeO[a]	17.70	21.34	27.19	16.15	23.19	24.52	25.39	23.67
MgO	20.68	18.53	16.88	19.66	15.80	15.70	15.61	14.49
Na_2O	-	-	-	0.35	0.62	0.73	0.68	0.60

Total	102.51	101.50	103.29	105.41	109.04	105.96	107.55	96.34
Structural formula								
Si	-	-	-	-	-	-	-	-
Al	1.8939	1.8554	1.8021	1.9170	1.8760	1.8370	1.8320	1.9220
Cr	-	0.0082	-	-	-	0.0060	-	-
Ti	0.0053	0.0120	0.0196	0.0080	0.0110	0.0160	0.0150	-
Fe^b	0.3727	0.4633	0.5970	0.3470	0.5180	0.5530	0.5750	0.5270
Mg	0.7758	0.7172	0.6606	0.7530	0.6290	0.6310	0.6300	0.5750
Na	-	-	-	0.0170	0.0320	0.0380	0.0360	0.0310
Total	3.0477	3.0561	3.0792	3.0421	3.0668	3.0812	3.0873	3.0546

Sample ref.	S25	S26	S27	S28	S29	S30	S31	S32
SiO_2	-	-	-	-	-	-	-	-
TiO_2	-	0.41	0.29	0.30	0.97	0.56	0.55	0.63
Al_2O_3	61.77	60.62	60.77	62.19	56.57	61.04	61.13	59.00
Cr_2O_3	0.95	0.24	-	-	-	-	-	-
FeO^b	23.24	23.57	20.73	16.18	26.02	18.95	18.70	22.41
MgO	13.42	14.96	17.17	19.82	16.39	19.96	19.78	16.01
Na_2O	-	-	-	-	-	-	-	0.38
Total	96.45	99.80	98.96	98.49	99.95	100.51	100.16	102.42
Structural formula								
Si	-	-	-	-	-	-	-	-
Al	1.8320	1.9220	1.9370	1.9042	1.8997	1.9103	1.8548	1.8240
Cr	-	-	0.0200	0,0051	-	-	-	-
Fe^b	0.5170	0.5252	0.4597	0.3526	0.5895	0.4107	0.4062	0.4844
Ti	-	0.0081	0.0058	0.0059	0.0198	0.0190	0.0108	0.0122
Mg	0.5320	0.5944	0.6790	0.7699	0.6617	0.7709	0.7657	0.6939
Na	0.0320	-	-	-	-	-	-	0.0190
Total	3.0378	3.0371	3.0442	3.0388	3.0770	3.0568	3.0536	3.0679

Sample ref.	S33	S34	S35	S36	S37	S38	S39	S40
SiO_2	-	-	-	-	-	-	-	-
TiO_2	0.96	0.25	0.57	0.53	0.79	0.80	0.86	0.83
Al_2O_3	59.00	62.62	61.13	61.70	57.94	59.36	58.68	57.08
Cr_2O_3	-	0.31	-	0.33	0.28	-	-	-
FeO^a	24.83	16.43	22.48	20.28	26.58	24.77	24.93	26.04
MgO	17.42	20.26	18.00	19.02	16.23	17.23	17.33	16.09
Na_2O	-	-	-	-	-	-	-	-
Total	102.21	99.88	102.18	101.85	101.83	102.15	101.81	100.05
Structural formula								
Si	-	-	-	-	-	-	-	-
Al	1.8240	1.9000	1.8646	1.8698	1.8163	1.8346	1.8234	1.8191
Cr	-	0.0063	-	0.0066	0.0059	-	-	-
Ti	0.0190	0.0049	0.0111	0.0102	0.0159	0.0158	0.0171	0.0168
Fe^b	0.5447	0.3536	0.4865	0.4361	0.5913	0.5431	0.5496	0.5889
Mg	0.6812	0.7772	0.6944	0.7289	0.6436	0.6733	0.6810	0.6486
Na	-	-	-	-	-	-	-	-
Total	3.0689	3.0419	3.0565	3.0515	3.0729	3.0668	3.0711	3.0735

Sample ref.	S41	S42	S43	S44	S45	S46	S47	S48
SiO_2	-	-	-	-	-	-	-	-
TiO_2	-	0.73	0.73	-	0.36	o.52	0.60	0.35
Al_2O_3	59.87	58.38	57.22	66.54	62.70	60.24	59.23	61.19
Cr_2O_3	0.23	-	-	0.50	-	-	-	0.46

FeO[a]	24.92	23.79	25.22	10.11	16.04	19.79	22.77	18.21
MgO	15.74	17.16	16.04	21.84	20.28	18.86	17.37	19.73
Na_2O	-	-	-	-	-	-	-	-
Total	100.76	100.06	99.21	98.98	99.39	99.41	99.96	99.94
Structural formula								
Si	-	-	-	-	-	-	-	-
Al	1.8764	1.8376	1.8319	1.9700	1.9065	1.8689	1.8548	1.8754
Cr	0.0047	-	-	0.0099	-	-	-	0.0094
Ti	-	0.0146	0.0150	-	0.0070	0.0103	0.0120	0.0069
Fe[b]	0.5542	0.5314	0.5728	0.2124	0.3461	0.4358	0.5058	0.3958
Mg	0.6240	0.6829	0.6493	0.8176	0.7799	0.7402	0.6877	0.7644
Na	-	-	-	-	-	-	-	-
Total	3.0593	3.0665	3.0689	3.0099	3.0396	3.0551	3.0604	3.0510

	S49	S50	S51	S52	S53	S54	S55	S56
SiO_2	-	-	-	-	-	-	-	-
TiO_2	0.44	0.44	0.59	0.89	0.65	0.41	0.83	0.21
Al_2O_3	61.76	60.99	58.75	58.35	58.15	63.18	59.95	65.49
Cr_2O_3	-	-	-	-	-	-	-	0.43
FeO[a]	18.35	21.92	21.84	24.27	25.75	18.06	24.24	14.18
MgO	19.45	17.42	17.96	16.86	15.17	20.25	17.25	21.63
Na_2O	-	-	-	-	-	0.24	-	-
Total	100.00	100.77	99.14	100.37	99.72	102.14	102.27	101.94
Structural formula								
Si	-	-	-	-	-	-	-	-
Al	1.8883	1.8819	1.8490	1.8347	1.8531	1.8871	1.8446	1.9212
Cr	-	-	-	-	-	-	-	0.0085
Ti	0.0086	0.0086	0.0119	0.0179	0.0133	0.0079	0.0163	0.0039
Fe[b]	0.3982	0.4800	0.4877	0.5415	0.5823	0.3827	0.5291	0.2952
Mg	0.7520	0.6799	0.7148	0.6704	0.6113	0.7649	0.6711	0.8025
Na	-	-	-	-	-	0.0117	-	-
Total	3.0471	3.0503	3.0634	3.0646	3.0600	3.0543	3.0612	3.0312

Sample ref.	S57	S58	S59	S60	S61	S62	S63	S64
SiO_2	-	-	-	-	-	-	-	-
TiO_2	0.27	0.70	0.34	0.56	0.46	0.41	0.94	0.50
Al_2O_3	64.87	61.19	62.33	57.91	62.58	60.87	57.01	60.36
Cr_2O_3	-	-	0.37	-	-	-	-	0.60
FeO[a]	15.86	23.88	17.49	26.23	22.78	19.91	25.23	20.08
MgO	21.16	18.02	19.02	14.35	17.54	18.29	16.16	17.99
Na_2O	-	-	0.41	0.60	-	0.52	0.66	0.48
Total	102.17	103.79	99.60	98.78	103.36	100.42	103.08	100.99
Structural formula								
Si	-	-	-	-	-	-	-	-
Al	1.9125	1.8484	1.9020	1.8560	1.8848	1.8800	1.8160	1.8690
Cr	-	-	0.0080	-	-	-	-	0.0120
Ti	0.0052	0.0135	0.0070	0.0110	0.0089	0.0080	0.0190	0.0100
Fe[b]	0.3318	0.5117	0.3790	0.5960	0.4867	0.4360	0.5700	0.4410
Mg	0.7890	0.6885	0.7340	0.5810	0.6680	0.7150	0.6510	0.7040
Na	-	-	0.0210	-	-	0.0260	0.0350	0.0240
Total	3.0384	3.0622	3.0489	3.0765	3.0485	3.0615	3.0905	3.0616

Sample ref.	S65	S66	S67	S68	S69	S70	S71
SiO_2	-	-	-	-	-	-	-

TiO_2	0.63	0.73	0.81	0.79	0.33	0.38	0.49
Al_2O_3	58.90	58.45	57.71	57.99	61.94	61.70	61.31
Cr_2O_3	-	-	-	-	0.79	-	0.22
FeO^a	22.33	23.71	25.68	25.14	17.19	19.26	19.51
MgO	17.49	16.58	15.33	15.44	19.28	18.34	18.16
Na_2O	0.65	0.52	0.47	0.65	0.47	0.33	0.31
Total	101.56	100.61	101.77	104.63	101.15	100.24	104.54
Structural formula							
Si	-	-	-	-	-	-	-
Al	1.8460	1.8430	1.8380	1.8430	1.8900	1.8960	1.8880
Cr	-	-	-	-	0.0160	-	0.0040
Ti	0.0130	0.0150	0.0160	0.0160	0.0060	0.0070	0.0100
Fe^b	0.4960	0.5310	0.5800	0.5670	0.3720	0.4200	0.4260
Mg	0.6930	0.6610	0.6180	0.6200	0.7440	0.7130	0.7070
Na	0.0330	0.0270	0.0250	0.0340	0.0240	0.0170	0.0160
Total	3.0813	3.0770	3.0769	3.0796	3.0523	3.0528	3.0518

(8) CHROME-SPINEL (oxygen number 4)

SC1/SC8 - Banca Mine
SC9/SC10 - Blackberries Mine
SC11 - Delta Mine
SC12/SC14 - Le Fevre Road
SC15 - Lottah
SC16 - New Clifton Mine
SC17 - North George River
SC18/SC19 - Pioneer Mine
SC20/SC22 - Ringarooma Bay borehole NE646
SC23 - Ruby Creek
SC24/SC28 - Sextus Creek Mine
SC29 - Star Hill Mine

Sample ref.	SC1	SC2	SC3	SC4	SC5	SC6	SC7	SC8
SiO_2	-	-	-	1.92	-	-	-	-
TiO_2	0.60	0.37	0.47	0.58	0.46	0.30	-	-
Al_2O_3	35.59	36.88	37.72	35.82	39.66	36.90	56.95	56.99
V_2O_5	-	-	-	-	-	-	-	-
Cr_2O_3	29.72	32.04	28.19	25.18	28.39	27.58	11.22	10.80
FeO^a	19.40	15.11	18.34	15.90	16.64	17.04	10.38	10.97
NiO	-	-	-	-	-	-	-	-
MgO	16.21	17.68	17.38	13.52	17.00	15.37	20.44	19.85
Na_2O	-	-	-	-	-	-	-	-
Total	101.51	102.09	102.10	92.92	102.15	97.20	98.99	98.60
Structural formula								
Si	-	-	-	0.0584	-	-	-	-
Al	1.2030	1.2180	1.2516	1.2857	1.3007	1.2833	1.7532	1.7638
V	-	-	-	-	-	-	-	-
Cr	0.6738	0.7098	0.6274	0.6062	0.6246	0.6434	0.2318	0.2242
Ti	0.0130	0.0078	0.0100	0.0132	0.0097	0.0066	-	-
Fe^b	0.4653	0.3541	0.4318	0.4049	0.3873	0.4206	0.2266	0.2409
Ni	-	-	-	-	-	-	-	-
Mg	0.6932	0.7385	0.7294	0.6138	0.7052	0.6760	0.7957	0.7770
Na	-	-	-	-	-	-	-	-
Total	3.0484	3.0281	3.0503	2.9822	3.0275	3.0299	3.0073	3.0058

Sample ref.	SC9	SC10	SC11	SC14	SC15	SC16	SC17	SC18
SiO_2	-	-	-	-	-	-	-	-
TiO_2	0.61	-	-	0.62	0.28	0.82	0.74	-
Al_2O_3	58.19	56.56	7.04	32.70	62.02	57.25	59.38	59.07
V_2O_5	-	-	-	-	-	-	-	-
Cr_2O_3	1.45	12.64	67.16	34.24	1.06	1.09	1.24	10.80
FeO^a	22.03	10.59	17.22	15.32	16.70	23.57	24.42	11.31
NiO	-	-	-	-	-	-	-	0.39
MgO	17.08	21.25	10.00	17.09	19.86	17.32	16.61	21.45
Na_2O	0.64	-	-	-	-	-	-	-
Total	101.47	101.04	101.42	99.97	99.92	100.06	102.39	103.01
Structural formula								
Si	-	-	-	-	-	-	-	-
Al	1.8290	1.7145	0.2734	1.1200	1.8875	1.8080	1.8327	1.7517
V	-	-	-	-	-	-	-	-
Cr	0.0310	0.2570	1.7493	0.7868	0.0217	0.0232	0.0256	0.2148
Ti	0.0120	-	-	0.0135	0.0055	0.0166	0.0146	-
Fe^b	0.4910	0.2279	0.4744	0.3724	0.3607	0.5281	0.5348	0.2380
Ni	-	-	-	-	-	-	-	0.0079
Mg	0.6790	0.8148	0.4911	0.7403	0.7644	0.6918	0.6484	0.8043
Na	0.0330	-	-	-	-	-	-	-
Total	3.0746	3.0141	2.9883	3.0329	3.0398	3.0677	3.0561	3.0166

Sample ref.	SC17	SC18	SC19	SC20	SC21	SC22	SC23	SC24
SiO_2	-	-	-	-	-	-	-	-
TiO_2	1.19	0.28	0.64	0.52	-	0.47	-	-
Al_2O_3	54.56	60.34	38.13	58.97	57.89	36.04	57.12	32.51
V_2O_5	-	-	-	-	-	0.20	-	-
Cr_2O_3	2.81	1.41	25.41	2.22	10.30	27.46	10.72	36.86
FeO^a	26.95	17.23	18.63	19.57	11.28	19.34	11.20	14.34
NiO	-	-	-	-	-	-	-	-
MgO	16.48	19.52	16.81	19.29	20.85	16.78	20.73	17.59
Na_2O	-	-	0.39	-	-	-	-	-
Total	101.98	98.78	104.40	100.58	100.32	100.28	99.77	101.31
Structural formula								
Si	-	-	-	-	-	-	-	-
Al	1.7229	1.8681	1.2880	1.8194	1.7599	1.2275	1.7490	1.0994
V	-	-	-	-	-	0.0046	-	-
Cr	0.0598	0.0293	0.5760	0.0460	0.2100	0.6274	0.2201	0.8361
Ti	0.0240	0.0055	0.0140	0.0103	-	0.0102	-	-
Fe^b	0.6063	0.3785	0.4470	0.4285	0.2433	0.4676	0.2433	0.3442
Ni	-	-	-	-	-	-	-	-
Mg	0.6610	0.7643	0.7180	0.7526	0.8016	0.7228	0.8029	0.7523
Na	-	-	0.0210	-	-	-	-	-
Total	3.0810	3.0457	3.0647	3.0569	3.0149	3.0599	3.0153	3.0320

Sample ref.	SC25	SC26	SC27	SC28	SC29
SiO_2	-	-	-	-	-
TiO_2	0.22	0.93	0.25	-	0.26
Al_2O_3	45.37	26.49	37.59	39.37	41.35
V_2O_5	-	-	-	-	-
Cr_2O_3	25.14	41.56	33.99	21.08	26.48
FeO^a	11.76	15.36	11.18	11.62	14.54
NiO	-	-	-	0.33	-
MgO	20.26	17.42	19.77	20.97	18.26

Na_2O	-	-	-	-	-
Total	102.75	101.77	102.79	103.37	102.44
Structural formula					
Si	-	-	-	-	-
Al	1.4222	0.9160	1.2139	1.5159	1.3731
V	-	-	-	-	-
Cr	0.5287	0.9641	0.7365	0.4343	0.5699
Ti	0.0044	0.0205	0.0052	-	0.0053
Fe^b	0.2615	0.3769	0.2562	0.2531	0.3335
Ni	-	-	-	0.0069	-
Mg	0.8031	0.7681	0.8077	0.8145	0.7411
Na	-	-	-	-	-
Total	3.0200	3.0393	3.0194	3.0247	3.0230

(9) TITANOMAGNETITE (oxygen number 4) - titanomagnetite and ulvospinel

TM1/TM9 - Le Fevre Road
TM10 - Schramms Road

Sample ref.	TM1	TM2	TM3	TM4	TM5	TM6	TM7	TM8
SiO_2	0.21	0.36	0.46	0.32	-	-	0.30	0.30
TiO_2	14.67	6.15	3.98	15.87	19.70	20.71	9.88	10.46
Al_2O_3	7.25	4.17	4.17	7.07	3.68	3.80	4.82	4.85
FeO^a	74.94	84.79	84.69	73.00	72.76	72.09	82.55	74.60
MnO	0.40	0.77	0.62	0.55	0.52	0.48	0.77	0.80
MgO	2.08	-	0.31	2.23	1.77	2.15	0.95	0.37
CaO	-	-	0.15	0.22	-	-	-	-
Na_2O	-	-	-	-	-	-	0.74	-
Total	99.55	96.24	94.38	99.25	98.42	99.23	100.21	91.39
Structural formula								
Si	0.0092	0.0164	0.0212	0.0126	-	-	0.0120	0.0136
Al	0.3793	0.2211	0.2281	0.3264	0.1735	0.1762	0.2370	0.2584
Ti	0.4896	0.2080	0.1387	0.4676	0.5921	0.6120	0.3100	0.3555
Fe^b	2.7810	3.1903	3.2844	2.3924	2.4325	2.3696	2.8830	2.8186
Mn	0.0151	0.0292	0.0245	0.0183	0.0177	0.0161	0.0270	0.0306
Mg	0.1372	-	0.0215	0.1301	0.1052	0.1260	0.0590	0.0249
Ca	-	-	0.0075	0.0091	-	-	-	-
Na	-	-	-	-	-	-	0.0600	-
Total	3.8114	3.6650	3.7259	3.3565	3.3211	3.2998	3.5886	3.5016

Sample ref.	TM9	TM10
SiO_2	0.48	-
TiO_2	15.24	30.45
Al_2O_3	4.53	2.95
FeO^a	66.85	56.32
MnO	0.55	0.57
MgO	3.09	1.66
CaO	-	-
Na_2O	-	-
Total	90.74	91.95
Structural formula		
Si	0.0208	-
Al	0.2300	0.1378
Ti	0.4936	0.9063

Fe^b	2.4078	1.8640
Mn	0.0200	0.0190
Mg	0.1983	0.0977
Ca	-	-
Na	-	-
Total	3.3705	3.0248

(10) TOURMALINE (oxygen number 29) - schorl

T1/T3 - Blackberries Mine
T4/T7 - Weld River

Sample ref.	T1	T2	T3	T4	T5	T6	T7
SiO_2	39.02	38.77	33.73	40.18	40.67	40.49	41.21
TiO_2	0.84	0.75	0.43	0.55	1.08	1.32	1.27
Al_2O_3	39.04	39.36	33.63	37.54	38.49	36.61	38.45
FeO^a	17.45	17.65	15.26	17.59	12.71	15.34	12.11
MnO	0.38	0.50	0.54	0.31	-	-	-
MgO	0.98	0.67	0.18	1.34	4.13	3.56	4.27
CaO	-	-	-	-	0.62	0.21	0.44
Na_2O	2.29	2.29	1.75	2.48	2.30	2.48	2.25
Total	84.53	84.78	85.52	99.90	99.39	97.13	97.28
Structural formula							
Si	6.7497	6.7497	6.8531	6.9790	6.9090	6.9700	6.9700
Al	7.9967	8.0692	8.0502	7.6870	7.7080	7.4300	7.6650
Ti	0.1087	0.1015	0.0656	0.0720	0.1380	0.1710	0.1610
Fe^b	2.5375	2.5665	2.5930	2.5560	1.8060	2.2090	1.7130
Mn	0.1087	0.0725	0.0947	0.0460	-	-	-
Mg	0.2537	0.1740	0.0558	0.3470	1.0460	0.9130	1.0780
Ca	-	-	-	-	0.1130	0.0380	0.0800
Na	0.7757	0.7757	0.6887	0.8360	0.7570	0.8270	0.7370
Total	18.4510	18.5091	18.4001	18.5234	18.4768	18.5575	18.4045

(11) MISCELLANEOUS

FORSTERITE (oxygen number 4)
Briseis Mine

SiO_2	40.22
FeO^a	10.01
NiO	0.38
MgO	48.50
Total	99.11
Structural formula	
Si	0.9967
Fe^b	0.2075
Ni	0.0075
Mg	1.7916
Total	3.0033

MAGNETITE (oxygen number 3)
Weld River

Al_2O_3	0.94
FeO^a	97.09
MnO	0.70
MgO	0.67
Na_2O	0.60
Total	100.00
Structural formula	
Al	0.0390
Fe^b	2.8650
Mn	0.0210
Mg	0.0350
Na	0.0410
Total	3.0010

This article has been removed for copyright or proprietary reasons.

W. W.-S. Yim, A. J. W. Gleadow, J. C. van Moortt, 1985, Fission track dating of alluvial zircons and heavy mineral provenance in Northeast Tasmania, Journal of the Geological Society, 142, 351-362

APPENDIX III

SIMPLIFIED LOGSHEETS OF SELECTED JETSTREAM BOREHOLES FROM THE SOUTH MOUNT CAMERON BASIN LOCATED IN FIG. 7.17. BASED ON DATA SUPPLIED BY AUSTRALIAN ANGLO-AMERICAN PROSPECTING PROPRIETARY LIMITED

BOREHOLE RRC 2

Surface elevation 148m above mean sea level

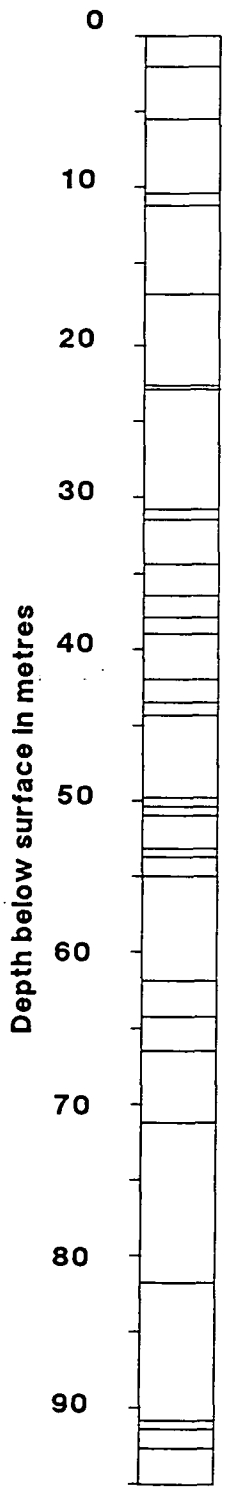

Reddish brown silts and medium to coarse sands
Red clays and sandy clays

Stiff white laminated clays

Silty ochre clays and sandy white clays

Medium to coarse sands

Pyrite-bearing coarse sands and dark brown silts with wood

Stiff brown clays with wood

Coarse sands and dark brown silts with wood

Stiff grey clays with wood

Coarse sands with pyrite nodules

Stiff grey clays with wood
Stiff dark grey clays with wood
Pyrite-bearing fine to medium sands

Pyrite-bearing medium to coarse sands with wood
Stiff grey clays with wood
Fine sands

Stiff dark grey clays with wood

Medium sands with wood
Fine sands and sandy clays
Stiff grey clays and fine sands
Stiff sandy clays. White mottled clays and grey clays
Coarse sands, pyrite nodules and some wood

Stiff grey clays and wood at 60.0m and 61.8m

Coarse sands

Coarse sands and quartz gravels

Pyrite-bearing quartz and sandstone cobbles with fine sands

Gravels with minor sands and clays

Mottled greyish green sandy clays with some gravels

Green clays with minor gravels
Stiff mottled greyish green clays
Dark greenish black rock fragments (?basalt)

BOREHOLE RRC 3

Surface elevation 129m above mean sea level

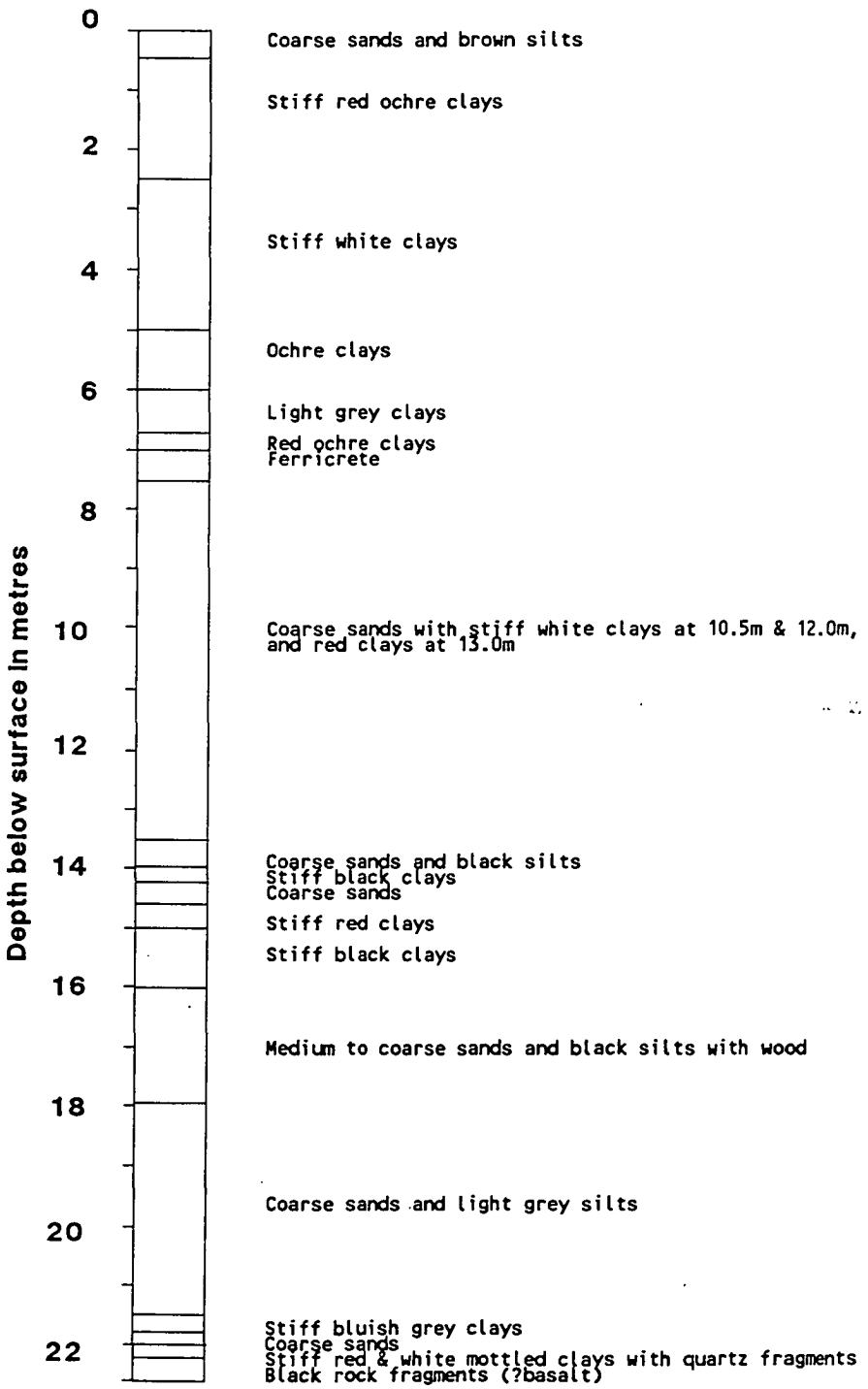

BOREHOLE RRC 5

Surface elevation 148m above mean sea level

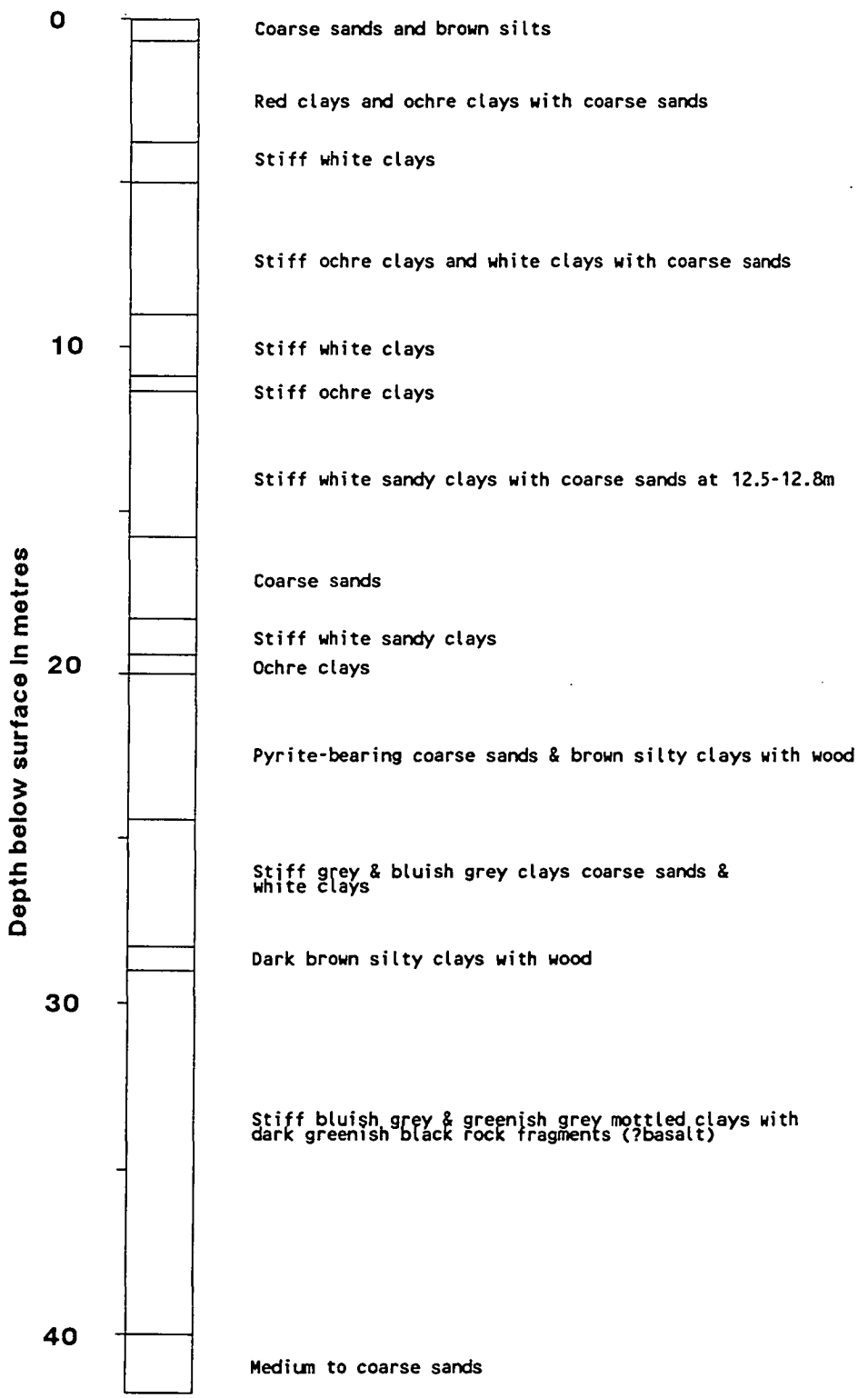

BOREHOLE RRC 16

Surface elevation 8 1m above mean sea level